MECHANISM AND PREVENTION OF ATRIAL FIBRILLATION

EDITED BY: Guowei Li, Deirdre Lane, Tatjana Potpara and Yafei Li
PUBLISHED IN: Frontiers in Cardiovascular Medicine

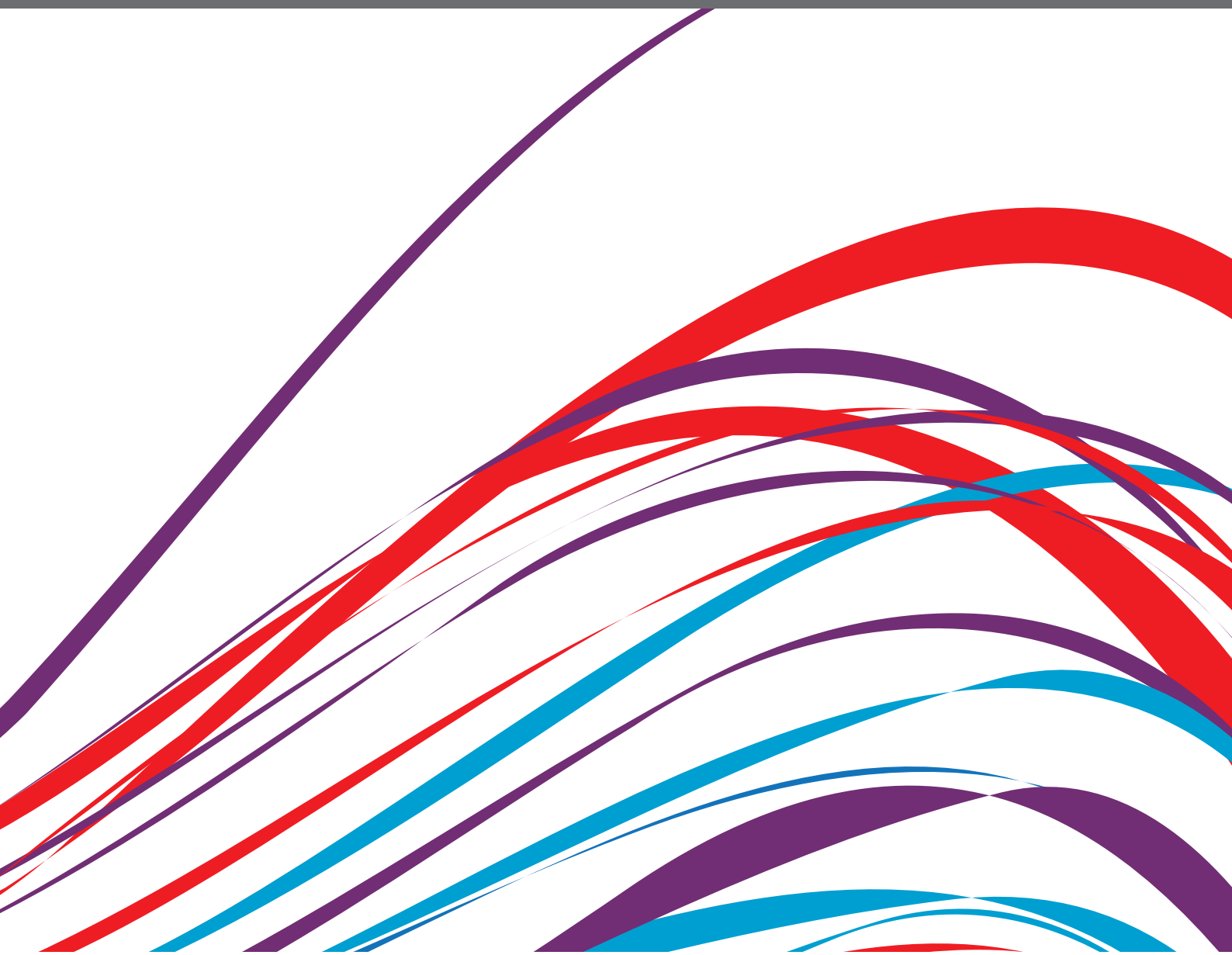

frontiers Research Topics

ISSN 1664-8714
ISBN 978-2-83250-773-5
DOI 10.3389/978-2-83250-773-5

About Frontiers

Frontiers is more than just an open-access publisher of scholarly articles: it is a pioneering approach to the world of academia, radically improving the way scholarly research is managed. The grand vision of Frontiers is a world where all people have an equal opportunity to seek, share and generate knowledge. Frontiers provides immediate and permanent online open access to all its publications, but this alone is not enough to realize our grand goals.

Frontiers Journal Series

The Frontiers Journal Series is a multi-tier and interdisciplinary set of open-access, online journals, promising a paradigm shift from the current review, selection and dissemination processes in academic publishing. All Frontiers journals are driven by researchers for researchers; therefore, they constitute a service to the scholarly community. At the same time, the Frontiers Journal Series operates on a revolutionary invention, the tiered publishing system, initially addressing specific communities of scholars, and gradually climbing up to broader public understanding, thus serving the interests of the lay society, too.

Dedication to Quality

Each Frontiers article is a landmark of the highest quality, thanks to genuinely collaborative interactions between authors and review editors, who include some of the world's best academicians. Research must be certified by peers before entering a stream of knowledge that may eventually reach the public - and shape society; therefore, Frontiers only applies the most rigorous and unbiased reviews.
Frontiers revolutionizes research publishing by freely delivering the most outstanding research, evaluated with no bias from both the academic and social point of view. By applying the most advanced information technologies, Frontiers is catapulting scholarly publishing into a new generation.

What are Frontiers Research Topics?

Frontiers Research Topics are very popular trademarks of the Frontiers Journals Series: they are collections of at least ten articles, all centered on a particular subject. With their unique mix of varied contributions from Original Research to Review Articles, Frontiers Research Topics unify the most influential researchers, the latest key findings and historical advances in a hot research area! Find out more on how to host your own Frontiers Research Topic or contribute to one as an author by contacting the Frontiers Editorial Office: frontiersin.org/about/contact

MECHANISM AND PREVENTION OF ATRIAL FIBRILLATION

Topic Editors:
Guowei Li, Guangdong Second Provincial General Hospital, China
Deirdre Lane, University of Liverpool, United Kingdom
Tatjana Potpara, University of Belgrade, Serbia
Yafei Li, Army Medical University, China

Citation: Li, G., Lane, D., Potpara, T., Li, Y., eds. (2022). Mechanism and Prevention of Atrial Fibrillation. Lausanne: Frontiers Media SA.
doi: 10.3389/978-2-83250-773-5

Table of Contents

frontiers | Frontiers in Cardiovascular Medicine

TYPE Editorial
PUBLISHED 31 October 2022
DOI 10.3389/fcvm.2022.1066542

OPEN ACCESS

EDITED AND REVIEWED BY
Matteo Anselmino,
University of Turin, Italy

*CORRESPONDENCE
Guowei Li
ligw@gd2h.org.cn

SPECIALTY SECTION
This article was submitted to Cardiac Rhythmology, a section of the journal Frontiers in Cardiovascular Medicine

RECEIVED 11 October 2022
ACCEPTED 21 October 2022
PUBLISHED 31 October 2022

CITATION
Li G, Lane DA, Tatjana PS and Li Y (2022) Editorial: Mechanism and prevention of atrial fibrillation. *Front. Cardiovasc. Med.* 9:1066542. doi: 10.3389/fcvm.2022.1066542

Editorial: Mechanism and prevention of atrial fibrillation

Guowei Li[1]*, Deirdre A. Lane[2], Potpara S. Tatjana[3] and Yafei Li[4]

[1]Center for Clinical Epidemiology and Methodology, Guangdong Second Provincial General Hospital, Guangzhou, China, [2]Liverpool Centre for Cardiovascular Science, University of Liverpool and Liverpool Heart and Chest Hospital, Liverpool, United Kingdom, [3]School of Medicine, University of Belgrade, Belgrade, Serbia, [4]Department of Epidemiology, College of Preventive Medicine, Army Medical University (Third Military Medical University), Chongqing, China

KEYWORDS

atrial fibrillation, prevention, mechanism, prediction, basic science

Editorial on the Research Topic
Mechanism and prevention of atrial fibrillation

Introduction

Atrial fibrillation (AF) remains the most common sustained arrhythmia, with an estimated amount of more than 37 million patients globally (1). While AF is substantially related with increased risks of stroke and cardiovascular mortality, the prevention, diagnosis, treatment and management of AF continue to be suboptimal (2). With the emerging high-quality research and advanced progress on AF, this Research Topic aimed to collect state-of-art evidence and provide new insights into the mechanism and prevention of AF. Articles published in this Research Topic reported interesting findings and helped with our further knowledge of AF.

Risk factors in relation to risk of AF

The survey study by Thirumal et al. explored the relationship between duration of lifetime occupational radiation exposure and risk of atrial arrhythmias, based on data from 1,478 cardiologists' responses in the US. They reported a significant association between elevated radiation exposure hours and increased risk of atrial arrhythmias, highlighting the preventive attention required when using fluoroscopy-assisted procedures for cardiologists. Another cohort study of Kim et al. conducted in Korea assessed the existence of diabetes mellitus in relation to stiff left atrial physiology in patients who had AF catheter ablation, by using a propensity score matching technique. Diabetes mellitus was found to significantly associate with increased risk of stiff left atrial physiology, while patients with stiff physiology were related with elevated risk of AF recurrence. A third investigation of Garcia et al., as a multicenter retrospective cohort study, reported that left circumflex artery obstruction was independently associated with

increased risk of AF recurrence in patients who received catheter ablation and had no history of coronary artery disease (CAD), yielding a hazard ratio (HR) of 2.32 [95% confidence interval (CI): 1.36–3.98]. All these observational studies emphasized the clinical management to control the risk of arrhythmias.

There was another study of Musotto et al. depicting the morphological features of the left atrial appendage with thromboembolism risk under the condition of AF. This study demonstrated the active and passive contraction for hemodynamics in the left atrial appendage, and analyzed the hemodynamic role of AF in risk of thromboembolism. Results from this study provided some evidence of the mechanism of increased thromboembolism risk in AF by exploring hemodynamic parameters and anatomical phenotypes.

Prediction of risk of AF

Three interesting studies in this Research Topic investigated prediction of AF. The first assessed the post-operative AF prediction of DNA methylation biomarkers in 221 patients receiving cardiac surgery, with an area under the curve (AUC) of 0.79 in the validation cohort for the prediction model. Findings from this study may provide some support in the combination of epigenomic and clinical information for predicting risk of post-operative AF (Fischer et al.).

Another prospective cohort study of Chen et al. explored the macrophage inflammatory protein-1 alpha (MIP-1α) for its link with left atrial remodeling in patients with AF. The significant relationship between a higher MIP-1α and larger volume of left atrial suggested the potential prediction of MIP-1α regarding the left atrial remodeling in AF.

Ortega-Martorell et al. used data from 18,518 patients admitted to intensive care unit (ICU) to build three prediction model of new episodes of AF: for the overall cohort, for the ventilated patients, and for the non-ventilated patients. The prediction models based on clinical information yielded good performance in predicting new episodes of AF, with an AUC of 0.84, 0.82, and 0.91 for the overall, ventilated and non-ventilated cohorts, respectively.

Basic science in AF mechanism

One bioinformatic study of Ke et al. explored the competing endogenous RNAs (ceRNAs) by building the lncRNA-miRNA-mRNA network in AF, based on data from public databases. They found that based on the ceRNA theory, the network of LOC101928304/miR-490-3p/LRRC2 may be significantly related with AF, which may help deepen the understanding of AF pathogenesis and thus its prevention and treatment.

Wang and Tu summarized the progress of genetic and epigenetic research for ventricular arrhythmias in patients without structural heart disease. Unlike the other studies collected in this Research Topic that focused on atrial arrhythmias, their review generated an evidence map to aid in easy intake of most up-to-date regulatory mechanisms for ventricular arrhythmias including susceptibility genes, lncRNA, DNA methylation, histone modification, genomic imprinting, and 3D genomic architecture.

To summarize, this Research Topic collected interesting and novel research on the mechanism and prevention of AF. Results from these published studies expanded our understanding of pathogenesis, regulation, prevention and management of AF.

Author contributions

GL and YL: conceived and designed the Editorial. GL: drafted the Editorial. DAL, PST, and YL: made revisions and provided support in the Editorial. All authors read and approved the submitted version.

Acknowledgments

We would like to acknowledge all the authors for their contributions to this Research Topic.

Conflict of interest

The authors declare that the research was conducted in the absence of any commercial or financial relationships that could be construed as a potential conflict of interest.

Publisher's note

References

1. Lippi G, Sanchis-Gomar F, Cervellin G. Global epidemiology of atrial fibrillation: an increasing epidemic and public health challenge. *Int J Stroke*. (2021) 16:217–21. doi: 10.1177/1747493019897870

2. Hindricks G, Potpara T, Dagres N, Arbelo E, Bax JJ, Blomström-Lundqvist C, et al. 2020 ESC Guidelines for the diagnosis and management of atrial fibrillation developed in collaboration with the European Association for Cardio-Thoracic Surgery (EACTS): the Task Force for the diagnosis and management of atrial fibrillation of the European Society of Cardiology (ESC) Developed with the special contribution of the European Heart Rhythm Association (EHRA) of the ESC. *Eur Heart J*. (2021) 42:373–498. doi: 10.1093/eurheartj/ehaa612

frontiers in Cardiovascular Medicine

ORIGINAL RESEARCH
published: 09 December 2021
doi: 10.3389/fcvm.2021.784792

Macrophage Inflammatory Protein-1 Alpha, a Potential Biomarker for Predicting Left Atrial Remodeling in Patients With Atrial Fibrillation

Yung-Lung Chen[1,2,3], *Hui-Ting Wang*[4], *Pei-Ting Lin*[1,2], *Jiin-Haur Chuang*[3,5†] and *Ming-Yu Yang*[3,6*†]

[1] Section of Cardiology, Department of Internal Medicine, Kaohsiung Chang Gung Memorial Hospital, Kaohsiung, Taiwan, [2] School of Medicine, College of Medicine, Chang Gung University, Taoyuan, Taiwan, [3] College of Medicine, Graduate Institute of Clinical Medical Sciences, Chang Gung University, Taoyuan, Taiwan, [4] Emergency Department, Kaohsiung Chang Gung Memorial Hospital, Kaohsiung, Taiwan, [5] Division of Pediatric Surgery, Department of Surgery, Kaohsiung Chang Gung Memorial Hospital, Kaohsiung, Taiwan, [6] Department of Otolaryngology, Kaohsiung Chang Gung Memorial Hospital, Kaohsiung, Taiwan

OPEN ACCESS

Edited by:
Guowei Li,
Guangdong Second Provincial General Hospital, China

Reviewed by:
Yumei Xue,
Guangdong Academy of Medical Sciences, China
Göksel Çinier,
Dr. Siyami Ersek Chest Cardiovascular Surgery Training and Research Hospital, Turkey

***Correspondence:**
Ming-Yu Yang
yangmy@mail.cgu.edu.tw

†These authors have contributed equally to this work

Specialty section:
This article was submitted to Cardiac Rhythmology, a section of the journal Frontiers in Cardiovascular Medicine

Received: *28 September 2021*
Accepted: *17 November 2021*
Published: *09 December 2021*

Citation:
Chen Y-L, Wang H-T, Lin P-T, Chuang J-H and Yang M-Y (2021) Macrophage Inflammatory Protein-1 Alpha, a Potential Biomarker for Predicting Left Atrial Remodeling in Patients With Atrial Fibrillation. Front. Cardiovasc. Med. 8:784792. doi: 10.3389/fcvm.2021.784792

Objectives: Left atrial (LA) remodeling itself is an independent risk factor for ischemic stroke and mortality, with or without atrial fibrillation (AF). Macrophage inflammatory protein-1 alpha (MIP-1α) has been reported to be involved in the induction of autoimmune myocarditis and dilated cardiomyopathy. Little is known about whether MIP-1α can be used to predict LA remodeling, especially in patients with AF.

Methods: We prospectively enrolled 78 patients who had received a cardiac implantable electronic device due to sick sinus syndrome in order to define AF accurately. AF was diagnosed clinically before enrollment, according to 12-lead electrocardiography (ECG) and 24-h Holter test in 54 (69%) patients. The serum cytokine levels and the mRNA expression levels of peripheral blood leukocytes were checked and echocardiographic study was performed on the same day within 1 week after the patients were enrolled into the study. The 12-lead ECG and 24-h Holter test were performed on the same day of the patients' enrollment, and the device interrogation was performed every 3 months after enrollment. The enrolled patients were clinically followed up for 1 year.

Results: There was no difference in baseline characteristics, cytokine levels and mRNA expression between patients with and without AF. Larger LA volume was positively correlated with higher levels of MIP-1α ($r = 0.461$, $p \leq 0.001$) and the atrial high-rate episodes (AHREs) burden ($r = 0.593$, $p < 0.001$), and negatively correlated with higher levels of transforming growth factor (TGF)-β1 ($r = -0.271$, $p = 0.047$) and TGF-β3 ($r = -0.279$, $p = 0.041$). The higher AHREs burden and MIP-1α level could predict LA volume independently. The mRNA expression of *RORC* was negatively associated with the MIP-1α level.

Conclusions: This study showed that higher MIP-1α was significantly associated with LA remodeling and may have the potentials to predict LA remodeling in terms of a larger LA volume, and that circadian gene derangement might affect the expression of MIP-1α.

Keywords: atrial fibrillation, macrophage inflammatory protein-1 alpha, *RORC*, atrial high-rate episodes, left atrial remodeling

INTRODUCTION

Atrial fibrillation (AF) is one of the most common cardiac arrhythmias, and it increases the risk of ischemic stroke, systemic embolization, heart failure, and mortality, compared to patients without AF (1). Electrical and structural remodeling play an important role in the pathophysiology of AF development (2). Left atrial (LA) enlargement, an easily-measurable phenomenon, is the default clinical hallmark of structural remodeling that occurs most often in response to LA pressure and volume overload. Changes in LA size, as an index of atrial remodeling, are markers of cardiovascular risk in the general population and also in patients with AF (3–8). There is growing evidence of inflammatory and fibrotic cytokines involvement in the context of both AF occurrence and LA remodeling. Also, it has become clear that inflammation, inflammation-related structural alteration and fibrosis are involved in AF propagation and LA remodeling (9). LA remodeling itself is also an independent risk factor for ischemic stroke and mortality, with or without AF (5). Macrophage-produced cytokines, including interleukin (IL)-l, IL-6, IL-12, and TNF-α, were reported to be associated with atrial fibrosis and AF attacks (10). In addition, several inflammatory and fibrotic cytokines, including IL-1β, IL-6, IL-8, IL-10, tumor necrosis factor (TNF)-α, and transforming growth factor (TGF)-β1, could be used to predict AF occurrence and clinical outcome (10–13). Very few published studies have discussed the predictive biomarkers of LA remodeling in patients with and without AF (9).

Macrophage inflammatory protein-1 alpha (MIP-1α), a kind of chemotactic cytokine secreted by fibroblasts and macrophages, plays a potentially important role in the development of inflammatory responses by recruiting mononuclear cells and modulating cytokine production (14). Increasing evidence suggests that MIP-1α plays a significant role in the etiopathogenesis of cardiovascular disease. A previous study showed that MIP-1α is involved in the induction of autoimmune myocarditis, which is the principal cause of heart failure among young adults and is often a precursor of dilated cardiomyopathy (15). Little is known about whether MIP-1α is associated with LA remodeling and even if it could be used to predict LA remodeling, especially in patients with AF.

NR1D1 and *ROR* regulates BMAL1 transcription through competing with the ROR response elements at the promoter region of BMAL1, which plays an important role in the maintenance of circadian rhythms in mammals (16). Our previous study showed that *NR1D1* and *RORC* are most significantly and negatively correlated with AF burden and LA remodeling (17). Previous studies also showed those inflammatory and fibrotic cytokines, which were associated with atrial fibrosis and AF episodes, were regulated by *BMAL1* or *NR1D1* (10, 18–22). It is reasonable to speculate that these important circadian clock genes may not only regulate core clock gene expression, but also involved in the expression of inflammatory and fibrotic cytokines that might cause atrial remodeling in patients with AF. Therefore, we hypothesized that *NR1D1* and *RORC* may regulate the expression of macrophage-associated cytokines and fibrotic cytokines, which are associated with a significant change in serum expression of MIP-1α and in LA remodeling in patients with AF.

MATERIALS AND METHODS

Patient Enrollment and Study Protocol

The diagnosis and burden of AF is usually under-estimated in clinical practice. To confirm the diagnosis and burden of AF, in terms of atrial high-rate episodes (AHREs), we prospectively enrolled patients who had received permanent pacemaker implantation due to sick sinus syndrome at our institute from August 2018 through June 2020. The detailed protocol was described in our previous paper (17). In brief, patients with autoimmune disease, malignancy, and acute and chronic inflammation status were excluded from the study. We enrolled patients into this study at least 1 month after the implantation of the pacemaker to prevent the enrollment of those with an inflammatory status post-pacemaker implantation, which may have influenced the expression of inflammatory and fibrotic biomarkers. The 12-lead electrocardiography (ECG) and 24-h Holter test were performed on the same day of the patients' enrollment. The peripheral blood sample and echocardiographic study were performed on the same day within 1 week after the patients were enrolled into the study. The patients' peripheral blood samples were collected between 8:00 and 9:00 a.m., and serum from the peripheral blood of patients were used for analysis of cytokines expression and total leukocytes were used for analysis of *NR1D1*, *RORC,* and *BMAL1* expression. The enrolled patients were clinically followed up for 1 year. The patient's clinical characteristics, including age, sex, comorbidities such as a history of AF, and echocardiographic findings were analyzed. The study group is defined as patients with AF before the enrollment. The control group is defined as patients who didn't have any AF episode before the enrollment. The definition of heart failure as a baseline characteristic was based on the diagnosis during the previous hospitalization, which included heart failure with a reduced and preserved ejection fraction.

Definition of AHREs and Measurement of LA Diameter

AF was diagnosed before enrollment by 12-lead ECG or a single-lead ECG recording according to the European Society of Cardiology (ESC) guidelines (1). ECG and 24-h Holter tests of studied patients were reviewed in detail by two electrophysiologists. Cardiac implantable electric device interrogation and reading of intracardiac electrograms stored in the device were also performed by two electrophysiologists every 3 months to confirm the occurrence and duration of AHREs. AHREs were detected by the device automatically and defined as an episode of a fast atrial rate $\geq$180 beats per minute lasting at least 5 min, according to 2016 ESC guideline (23). The stored intracardiac electrograms were evaluated by the electrophysiologist to exclude artifacts and far-field signals. As described in our previous paper (17), the LA diameter was measured perpendicular to the long axis of the LA posterior wall, inner edge to inner edge, at the level of the aortic sinuses,

using a 2-dimensional measure. LA volume was measured using the area-length method using the apical 4- and 2-chamber views at the cardiac cycle of the end-ventricular systolic phase, when the LA is at its maximal size. This study was approved by the Institutional Review Board of Chang Gung Memorial Hospital (IRB number: 201702224B0) and conformed to the guidelines set forth by the Declaration of Helsinki. Written informed consent was obtained from the participants before starting the study.

Measurement of Inflammatory and Fibrotic Cytokines

Cytokine measurement was performed simultaneously using the Bio-Plex pro human cytokine assay kit and Bio-Rad Bio-Plex 200 multiplex array system (Bio-Rad Laboratories, Hercules, CA, USA). IL-1 receptor antagonist (IL-1Ra), IL-1β, IL-6, IL-8, IL-10, IL-12, IL-18, TNF-α, MIP-1α, MIP-1β, TGF-β1, TGF-β2, and TGF-β3 were measured according to the manufacturer's instructions (24). In brief, 50 μL of beads were added to the well and washed 2 times. Then, 50 μL of plasma sample was added and incubated with antibody-coupled beads for 30 min at room temperature. After washing 3 times to remove unbound materials, the beads were incubated with 25 μL biotinylated detection antibodies for 30 min at room temperature. After washing away the unbound biotinylated antibodies 3 times, the beads were incubated with 50 μL streptavidin-PE for 10 min at room temperature. Following removal of excess streptavidin-PE in three washes, the beads were resuspended in 125 μL of assay buffer. Finally, the beads were read on the Bio-Plex suspension array system, and the data were analyzed using Bio-Plex Manager software (Bio-Rad Laboratories).

Real-Time Quantitative Reverse Transcriptase-Polymerase Chain Reaction Analysis (qRT-PCR) of *NR1D1*, *RORC*, and *BMAL1*

Isolation of total peripheral blood leukocytes, RNA extraction, cDNA synthesis, and qRT-PCR were performed as previously described (17). Briefly, the 2 μg RNA input for cDNA synthesis was determined by spectrophotometric OD260 measurement, and cDNA was generated with a High Capacity cDNA Reverse Transcription Kit (Applied Biosystems, Foster City, CA, USA), following the manufacture's protocols. Expression of the *NR1D1* and *RORC* genes was analyzed using the TaqMan system, and all TaqMan Gene Expression Assays were purchased from Applied Biosystems. Expression of the human housekeeping gene, *ACTB (actin beta)*, was used for normalizing *NR1D1* and *RORC* expression in real-time qRT-PCR. Real-time qRT-PCR was performed in an ABI 7500 Fast Real-Time System (Applied Biosystems). The expression levels of the *NR1D1*, *RORC,* and *BMAL1* were normalized to the internal control *ACTB* to obtain the relative threshold cycle (ΔCt).

Statistical Analysis

Quantitative data are reported as percentages, median (interquartile range) or mean ± standard deviation as an appropriate approach. The differences in categorical variables between patients with and without AF were analyzed by chi-square or Fisher's exact test, and the differences in continuous data were compared using Student's *t*-test or the Mann–Whitney *U*-test. The AHREs burden was expressed as the ratio of the total AHREs duration to 3 months, as defined by the device automatically. The differences in the expression in the *NR1D1*, *RORC, and BMAL1* genes between the AF group and the non-AF group using the ΔCt values were analyzed by Student's *t*-test. The folds change in circadian clock genes mRNA expression in patients with and without AF was determined by $2^{-\Delta\Delta Ct}$ calculation. Bivariate correlation analysis was used for variables, including AHREs burden, LA size, and the expression of circadian clock genes (expressed as −ΔCt value) and cytokines. A multiple linear regression model was used to assess the association between dependent variables, LA size, and independent variables, namely age, sex, and cytokines. We used SPSS version 17.0 software (SPSS, Chicago, IL, United States) for all statistical analyses.

RESULTS

Baseline Characteristics and Expression of Cytokines, *NR1D1*, *RORC*, and *BMAL1* Genes of Patients With and Without AF

A total of 78 patients were prospectively enrolled. AF was documented in 54 (69%) patients by ECG, 24-h Holter

TABLE 1 | Baseline characteristics of the 78-subject study population.

Variables	AF ($n = 54$)	No-AF ($n = 24$)	*p*-value
Age	70.3 ± 8.4	70.7 ± 7.8	0.824
Sex (male/female)	30/24	10/14	0.328
Hypertension	28 (51.9%)	13 (54.2%)	1.000
Diabetes mellitus	11 (20.4%)	7 (29.2%)	0.395
Previous stroke	9 (16.7%)	2 (8.3%)	0.487
Heart failure	6 (11.1%)	2 (8.3%)	1.000
Coronary artery disease	9 (16.7%)	4 (16.7%)	1.000
Chronic kidney disease	4 (7.4%)	4 (16.7%)	0.213
CHA2DS2-VASc score	2.8 ± 1.5	2.8 ± 1.4	1.000
AHREs burden (IQR)	8.1 (1–100)	0 (0–0)	<0.001
Ventricular pacing (%)	4.2 (0.3–37.4)	0.5 (0–8.8)	0.089
Echocardiographic data			
LA diameter (mm)	43.7 ± 9.9	39.5 ± 4.6	0.011
LA volume (cm^3)	76 ± 43	56 ± 23	0.038
Aorta (mm)	32.3 ± 4.6	33.0 ± 4.5	0.519
LVEDD (mm)	46.5 ± 8.8	48.1 ± 8.5	0.456
LVESD (mm)	34.2 ± 8.8	31.2 ± 7.8	0.149
LVEF (%)	61.3 ± 10.3	64.7 ± 8.8	0.162
Septal E/e' ratio	14.3 ± 8.7	14.2 ± 9.9	0.958
DT (ms)	210.0 ± 75.8	193.7 ± 46.3	0.307
PAP (mmHg)	26.9 ± 7.7	25.8 ± 7.4	0.605

Data are expressed as means ± standard deviation, median (interquartile range) or % (n) as appropriate. AHREs, atrial high-rate episodes; AF, atrial fibrillation; DT, deceleration time; E/e' ratio, the ratio between early mitral inflow velocity and mitral annular early diastolic velocity; IQR, interquartile range; LA, left atrial; LVEDD, left ventricular end-diastolic dimension; LVEF, left ventricular ejection fraction; LVESD, left ventricular end-systolic dimension; PAP, pulmonary artery pressure.

monitoring and pacemaker interrogation data before enrollment. There were 40 (51%) males, and the average age was 70.4 ± 8.2 years. There was no difference in baseline characteristics, including age, sex, hypertension, diabetes mellitus, stroke, heart failure, coronary artery disease, chronic kidney disease, CHA_2DS_2-VASc score, and echocardiographic parameters, but only in LA diameter, between patients with and without AF (**Table 1**). The AHREs burden was higher in the AF group than in the no-AF groups ($p < 0.001$). There was no difference in the percentage of ventricular pacing between patients with and without AF. The LA diameter was larger in the AF group than in the no-AF groups ($p = 0.011$), and the LA volume was also larger in the AF group than in the no-AF groups ($p = 0.038$). There was no difference in the expression level of the 13 cytokines and in mRNA expression of the *NR1D1*, *RORC,* and *BMAL1* genes between the AF group and the no-AF group (**Figure 1**).

Correlation Between LA Size, AHREs Burden, and Cytokines Level in Patients With and Without AF

Analysis of the correlation between LA Size, AHREs burden and cytokine levels in patients with AF showed there was a strong and positive correlation between larger LA volume and higher AHREs burden in patients with AF ($r = 0.593$, $p < 0.001$). There was also a strong and positive correlation between larger LA volume and MIP-1α level ($r = 0.461$, $p < 0.001$), and a negative correlation between larger LA volume and TGF-β1 level ($r =$

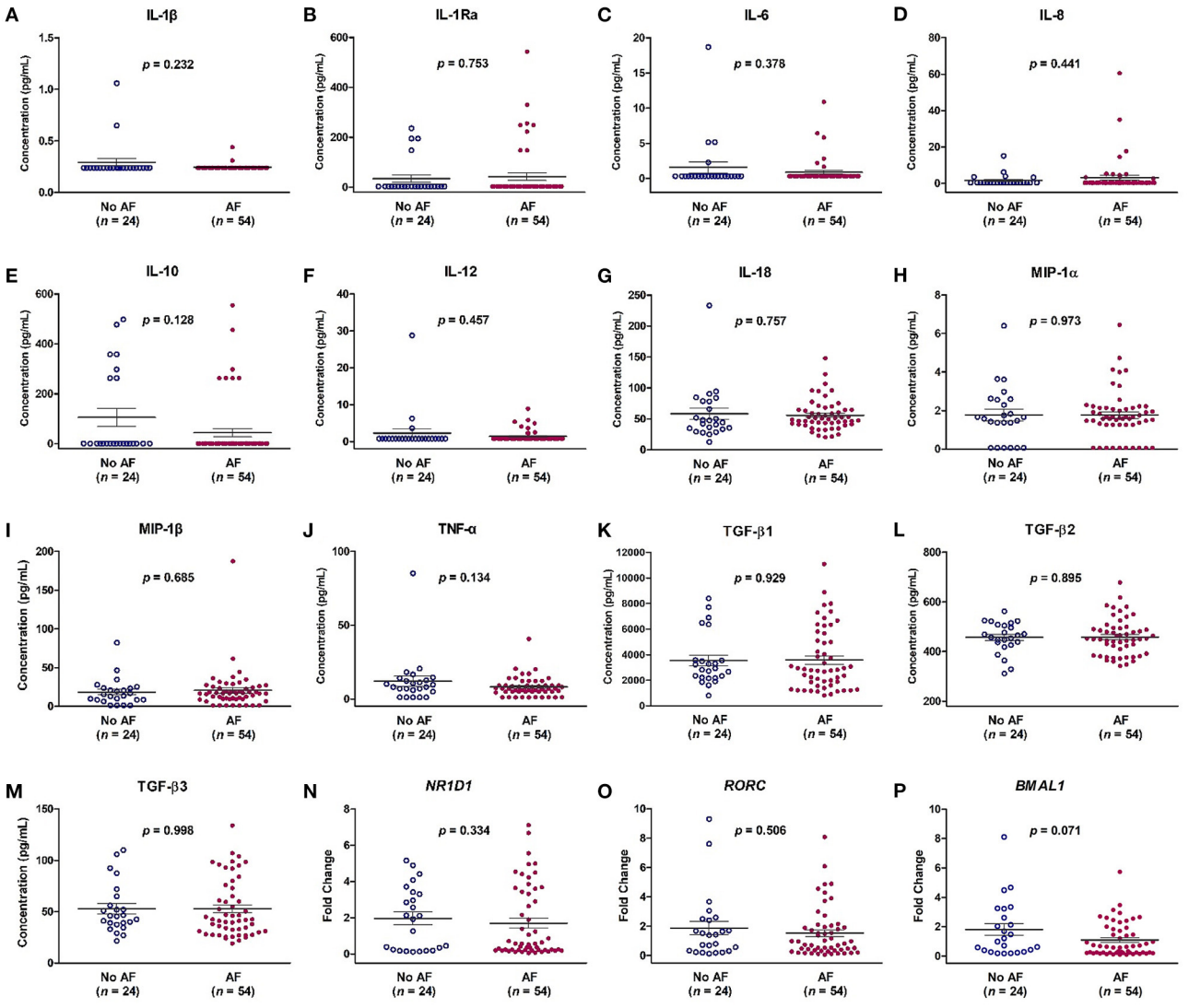

FIGURE 1 | Expression levels of cytokines **(A–M)** and mRNA expression of *NR1D1* **(N)**, *RORC* **(O)**, and *BMAL1* **(P)** in patients with and without atrial fibrillation (AF). The y-axis represents the expression of cytokines or the fold change of the gene expression level in patients with AF compared to patients without AF. The *p*-value analyzed by Student's *t*-test indicates statistical significance as evaluated between patients with ($n = 54$) and without AF ($n = 24$). IL, interleukin; MIP-1α, macrophage inflammatory protein-1 alpha; TGF-β, transforming growth factor beta.

−0.292, p= 0.032) and between large LA volume and TGF-β3 level ($r = -0.279$, $p = 0.041$) in patients with AF. There was no significant correlation between LA volume and levels of other cytokines (all $p > 0.05$) (**Table 2**). The correlation between LA volume and AHREs and between LA volume and cytokines (MIP-1α, TGF-β1, and TGF-β3) is shown in **Figure 2**. With regard to the association between AHREs and cytokine levels, only MIP-1α level was significantly associated with AHREs burden ($r = 0.279$, $p = 0.041$). No other cytokines were significantly associated with AHREs burden. In addition, although the distribution of age, sex, comorbidities and even CHA_2DS_2-VASc scores was the same between patients with and without AF, there was no significant correlation between LA volume and all cytokine levels in those patients without AF (all $p > 0.05$) (**Supplementary Table 1**).

TABLE 2 | Correlation between left atrial (LA) volume and atrial high-rate episodes (AHREs) and between LA volume and cytokines in patients with AF.

Variables	*r*	*p*-value
AHREs	0.593	<0.001
MIP-1α	0.461	<0.001
TGF-β1	−0.292	0.032
TGF-β2	−0.263	0.054
TGF-β3	−0.279	0.041
IL-1β	0.228	0.097
IL-1Ra	0.204	0.139
IL-6	−0.076	0.583
IL-8	0.052	0.710
IL-10	0.002	0.986
IL-12	−0.199	0.149
IL-18	0.120	0.388
MIP-1β	0.240	0.081
TNF-α	0.207	0.133

AHREs, atrial high-rate episodes; IL, interleukin; MIP-1α, macrophage inflammatory protein-1 alpha; TGF-β, transforming growth factor beta.

Multiple Linear Regression Model for Assessment of the Association Between LA Size and Other Variables

Variables including age, sex, AHREs, and the 13 cytokines shown in **Table 2** were used to assess the association with LA size. The results showed AHREs (Standardized β coefficient = 0.506, $p \leq 0.001$) and MIP-1α (Standardized β coefficient = 0.556, $p = 0.014$) were significantly associated with LA size ($r^2 = 0.582$, $p = 0.002$) (**Table 3**). The study population was then stratified according to quartile distribution on the basis of expression levels of MIP-1α. LA size among these subgroups was analyzed, and showed a significant linear trend of the MIP-1α level ($p = 0.005$) (**Table 4**). LA size was significantly larger in

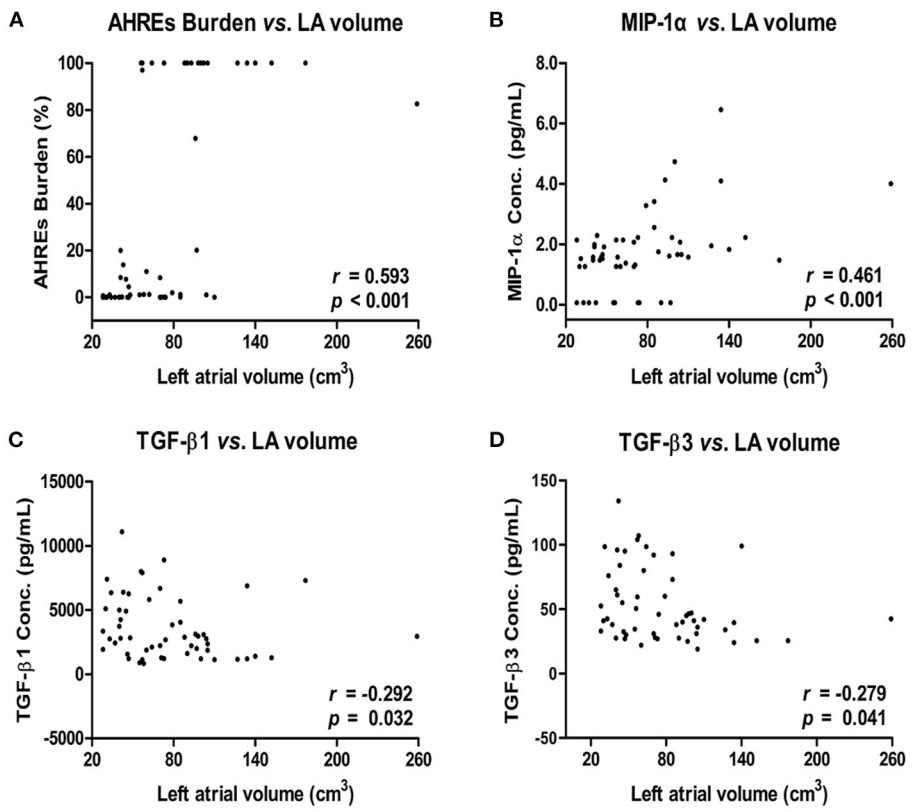

FIGURE 2 | Correlation between left atrial (LA) volume and AHREs burden **(A)** and LA volume and cytokine levels [MIP-1α **(B)**, TGF-β1 **(C)**, and TGF-β3 **(D)**] in patients with AF. The correlation was assessed by bivariate correlation analysis. The *r* and *p*-values indicate the correlation between the expression levels of cytokines and LA volume (expressed as units of cm^3). AHREs, atrial high-rate episodes; MIP-1α, macrophage inflammatory protein-1 alpha; TGF-β, transforming growth factor beta.

those patients with MIP-1α > 2.14 pg/ml (quartile 4 group) than in those patients with MIP-1α < 1.27 pg/ml (quartile 1 group) ($p < 0.01$).

Correlation of MIP-1α and MRNA Expression of *NR1D1*, *RORC,* and *BMAL1* Genes in Patients With AF

Bivariate correlation analysis was used to evaluate the relationship between the mRNA expression of *NR1D1*, *RORC,* and *BMAL1* and the MIP-1α level in patients with AF. There was a negative correlation between *RORC* gene expression and the MIP-1α level ($r^2 = 0.120$, $p = 0.010$), and there was no significant correlation between the mRNA expression of *NRID*1 and *BMAL1* and the MIP-1α level (both $p > 0.05$) (**Figure 3**).

DISCUSSION

There are several important findings in this study. First, LA remodeling in patients with AF was significantly associated with a higher AHREs burden, higher MIP-1α, and lower levels of TGF-β1 and TGF-β3. In contrast, there was no association between LA volume and cytokine levels in patients without AF. Second, among these factors, a higher AHREs burden and higher MIP-1α level could independently predict LA remodeling in patients with AF. Those patients with the highest quartile level of MIP-1α (>2.14 ng/ml) had a larger LA volume than those patients with the lowest quartile level of MIP-1α (<1.27 ng/ml). Third, it is worth noting that mRNA expression of *RORC* only, and not *NR1D1* or *BMAL1*, was significantly

TABLE 3 | Multiple linear regression model predicting left atrial volume.

Variables	Standardized β coefficient	*p*-value
Female sex	−0.018	0.901
Age	0.083	0.579
AHREs	0.506	<0.001
MIP-1α	0.556	0.014
TGF-β1	−0.964	0.164
TGF-β2	−0.241	0.350
TGF-β3	1.008	0.197
IL-1β	−0.023	0.856
IL-1Ra	0.035	0.803
IL-6	0.001	0.997
IL-8	−0.061	0.754
IL-10	−0.072	0.705
IL-12	−0.158	0.303
IL-18	−0.183	0.196
MIP-1β	−0.098	0.516
TNF-α	−0.140	0.641

AHREs, atrial high-rate episodes; IL, interleukin; MIP-1α, macrophage inflammatory protein-1 alpha; TGF-β, transforming growth factor beta.

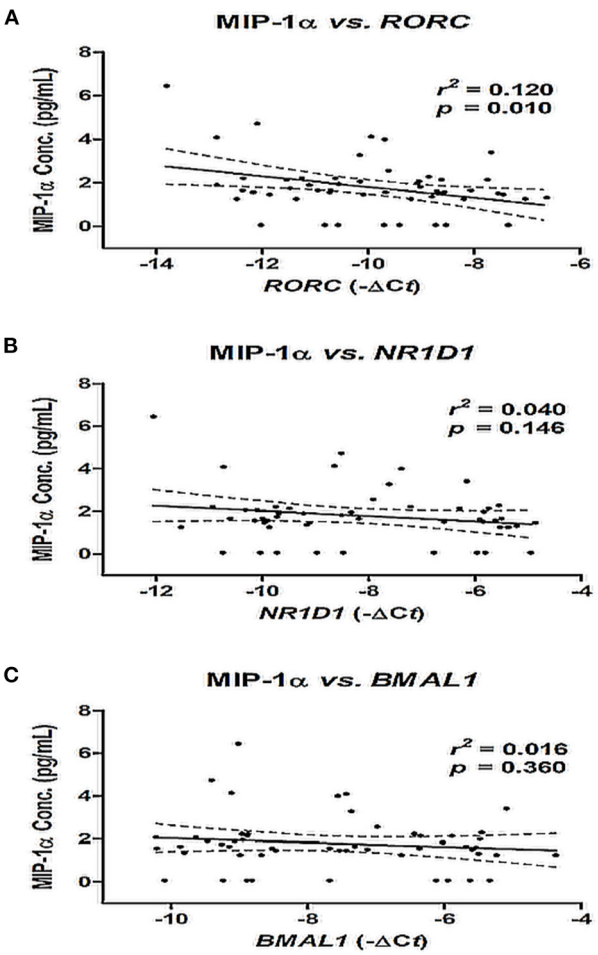

FIGURE 3 | Correlation between MIP-1α level and mRNA expression of *NR1D1* **(A)**, *RORC* **(B)**, and *BMAL1* **(C)** in patients with AF. The correlation was assessed by bivariate correlation analysis. The r^2 and *p*-values indicate the correlation between the MIP-1α level and the mRNA expression of *RORC*, *NR1D1,* and *BMAL1* genes (expressed as −ΔCt value). MIP-1α, macrophage inflammatory protein-1 alpha.

TABLE 4 | Left atrial volume according to quartile distribution on the basis of MIP-1α level.

MIP-1α range (ng/mL)	Quartile 1 (<1.27)	Quartile 2 (1.27–1.64)	Quartile 3 (1.64–2.14)	Quartile 4 (>2.14)	*p*-value for linear trend
LA size (cm^3)	56 ± 22	69 ± 41	78 ± 35	111 ± 55*	0.005

Data are expressed as mean ± standard deviation.
**p < 0.01 vs. quartile 1.*

and negatively correlated with the MIP-1α level in patients with AF.

MIP-1α is well-known for its role in the activation and migration of leukocytes into areas of inflammation. Previous studies showed MIP-1α was associated with left ventricular remodeling, and even could be used to predict the clinical outcome of patients with atherosclerosis, myocardial ischemia, and heart failure (25–28). The results of our study showed that MIP-1α could significantly predict LA remodeling in patients with AF. During the period of atrial injury due to volume or pressure overload and inflammation, cardiac fibroblasts, or resident cardiac macrophages may secrete MIP-1α, which may cause activation and migration of leukocytes into areas of inflammation and participate in the course of repair (29). The latter suggests that MIP-1α may be involved in atrial fibrosis and remodeling in patients with AF. We also found that the AHREs burden and MIP-1α level could be used to predict larger LA size in patients with AF. In those AF patients with potential LA remodeling, more aggressive echocardiography and even cardiac magnetic resonance imaging follow-up may be indicated to evaluate LA remodeling and fibrosis, and this could be used for risk stratification.

Of interest, the influence of MIP-1α on LA remodeling is significant only in the presence of AF, after adjusting for the CHA_2DS_2-VASc score and other demographic data in the present study. Once AF is initiated, the arrhythmia itself causes electrical and structural remodeling, which perpetuates AF and also increases the AF burden (the phenomenon of "AF begets AF"). This may explain both the significant association of higher AHREs burden with LA remodeling and the strong, positive association of MIP-1α level with LA size, and also predict LA remodeling in patients with AF, but not in patients without AF.

TGF-β1 is an important pro-fibrotic biomarker that involves LA fibrosis and remodeling in AF (30). A previous study showed that atrial fibrogenesis is accompanied by a biphasic response of TGF-β1, with an early increase of TGF-β1 in paroxysmal AF patients and a later loss of responsiveness to TGF-β1 in persistent AF (31). The results of our study were in accordance with those of previous studies, in which the TGF-β1 level was negatively correlated with LA size (22, 32). Another study also showed that MIP-1α can induce the expression of TGF-β, and that TGF-β is a potent down-regulator of MIP-1α, which reveals the complex interaction between TGFβ and MIP-1α (33). In our study, we found that MIP-1α rather than TGF-β1 could better predict LA remodeling in AF, after adjusting for age, sex and other cytokines. Future studies are needed to investigate the interaction of MIP-1α and TGF-β1 in the progression of atrial fibrosis and LA remodeling, as well as the role of resident and circulating macrophages and the secreting MIP-1α involved in LA remodeling in patients with AF.

In this study, the expression of *RORC* but not *NR1D1* and *BMAL1* was negatively correlated with the MIP-1α level, and MIP-1α was positively correlated with the AHREs burden and LA remodeling. Taken together, it is possible that circadian clock genes may be helpful in the maintenance of regular cardiac rhythm. The disruption of circadian clock genes expression might affect the expression of MIP-1α, and then lead to the initiation and perpetuation of AF and LA remodeling. Further studies should be conducted to investigate whether disruption of *RORC* would cause an altered expression of MIP-1α and its effect in AF development and LA remodeling.

However, there were two limitations in this study. First, the sample size was too small to evaluate the predictor of LA remodeling and the possible pathophysiologic mechanism. Further larger cohort studies focusing on the causal effects among *RORC*, MIP-1α, and LA remodeling should be performed to confirm the finding. Second, we did not analyze the relationship between medication for AF treatment and its consequent effect on MIP-1α and *RORC* expression, despite the fact that, to date, there are no known drugs used to treat AF that will affect MIP-1α and *RORC*.

CONCLUSIONS

Our study showed that the MIP-1α level was significantly associated with LA remodeling after adjusting for age, sex, and other cytokines and may have the potentials to predict LA remodeling, in terms of increasing LA volume in AF patients. The decreased gene expression of *RORC* was correlated significantly with a higher MIP-1α level and a larger LA size. However, the underlying causal effect between *RORC*, MIP-1α, and LA remodeling should be elucidated in future studies.

DATA AVAILABILITY STATEMENT

The raw data supporting the conclusions of this article will be made available by the authors, without undue reservation.

ETHICS STATEMENT

The studies involving human participants were reviewed and approved by Institutional Review Board of Chang Gung Memorial Hospital. The patients/participants provided their written informed consent to participate in this study.

AUTHOR CONTRIBUTIONS

J-HC and M-YY led in the conception and design of the study, revised the draft of the manuscript, and supervised and validated the clinical work and results. Y-LC collected research data and prepared the draft of the manuscript. H-TW and P-TL performed clinical work and organized the collected data. Y-LC and H-TW performed statistical analysis and drafted the manuscript. All authors have read and agreed to the published version of the manuscript.

FUNDING

This study was supported by grants from the Ministry of Science and Technology of Taiwan (MOST

107-2314-B-182A-151 and MOST 108-2314-B-182A-137) and Chang Gung Memorial Hospital (NMRPG8H0211 and NMRPG8J0251).

ACKNOWLEDGMENTS

We would like to thank Hsin-Yi Chien, Chih-Yun Lin, Nien-Tzu Hsu, and the Biostatistics Center, Kaohsiung Chang Gung Memorial Hospital for their assistance with statistical analysis in this study.

SUPPLEMENTARY MATERIAL

The Supplementary Material for this article can be found online at: https://www.frontiersin.org/articles/10.3389/fcvm.2021.784792/full#supplementary-material

REFERENCES

1. Hindricks G, Potpara T, Dagres N, Arbelo E, Bax JJ, Blomstrom-Lundqvist C, et al. 2020 ESC Guidelines for the diagnosis and management of atrial fibrillation developed in collaboration with the European Association for Cardio-Thoracic Surgery (EACTS): The Task Force for the diagnosis and management of atrial fibrillation of the European Society of Cardiology (ESC) Developed with the special contribution of the European Heart Rhythm Association (EHRA) of the ESC. *Eur Heart J.* (2021) 42:373–498. doi: 10.1093/eurheartj/ehab648
2. Luo X, Yang B, Nattel S. MicroRNAs and atrial fibrillation: mechanisms and translational potential. *Nat Rev Cardiol.* (2015) 12:80–90. doi: 10.1038/nrcardio.2014.178
3. Tsang TS, Barnes ME, Gersh BJ, Takemoto Y, Rosales AG, Bailey KR, et al. Prediction of risk for first age-related cardiovascular events in an elderly population: the incremental value of echocardiography. *J Am Coll Cardiol.* (2003) 42:1199–205. doi: 10.1016/S0735-1097(03)00943-4
4. Pritchett AM, Mahoney DW, Jacobsen SJ, Rodeheffer RJ, Karon BL, Redfield MM. Diastolic dysfunction and left atrial volume: a population-based study. *J Am Coll Cardiol.* (2005) 45:87–92. doi: 10.1016/j.jacc.2004.09.054
5. Hoit BD. Left atrial remodeling: more than just left atrial enlargement. *Circ Cardiovasc Imaging.* (2017) 10:6036. doi: 10.1161/CIRCIMAGING.117.006036
6. McGann C, Akoum N, Patel A, Kholmovski E, Revelo P, Damal K, et al. Atrial fibrillation ablation outcome is predicted by left atrial remodeling on MRI. *Circ Arrhythm Electrophysiol.* (2014) 7:23–30. doi: 10.1161/CIRCEP.113.000689
7. Tekkesin AI, Cinier G, Cakilli Y, Hayiroglu MI, Alper AT. Interatrial block predicts atrial high rate episodes detected by cardiac implantable electronic devices. *J Electrocardiol.* (2017) 50:234–7. doi: 10.1016/j.jelectrocard.2016.09.004
8. Cinier G, Tekkesin AI, Celik TY, Mercan O, Tanboga HI, Gunay MB, et al. Value of interatrial block for the prediction of silent ischemic brain lesions. *J Atr Fibrillation.* (2018) 11:2037. doi: 10.4022/jafib.2037
9. Molina CE, Abu-Taha IH, Wang Q, Rosello-Diez E, Kamler M, Nattel S, et al. Profibrotic, electrical, and calcium-handling remodeling of the atria in heart failure patients with and without atrial fibrillation. *Front Physiol.* (2018) 9:1383. doi: 10.3389/fphys.2018.01383
10. Wu N, Xu B, Xiang Y, Wu L, Zhang Y, Ma X, et al. Association of inflammatory factors with occurrence and recurrence of atrial fibrillation: a meta-analysis. *Int J Cardiol.* (2013) 169:62–72. doi: 10.1016/j.ijcard.2013.08.078
11. Alegret JM, Aragones G, Elosua R, Beltran-Debon R, Hernandez-Aguilera A, Romero-Menor C, et al. The relevance of the association between inflammation and atrial fibrillation. *Eur J Clin Invest.* (2013) 43:324–31. doi: 10.1111/eci.12047
12. Liuba I, Ahlmroth H, Jonasson L, Englund A, Jonsson A, Safstrom K, et al. Source of inflammatory markers in patients with atrial fibrillation. *Europace.* (2008) 10:848–53. doi: 10.1093/europace/eun111
13. Guo Y, Apostalakis S, Blann AD, Lip GY. Plasma CX3CL1 levels and long term outcomes of patients with atrial fibrillation: the West Birmingham Atrial Fibrillation Project. *Cerebrovasc Dis.* (2014) 38:204–11. doi: 10.1159/000365841
14. O'Grady NP, Tropea M, Preas HL 2nd, Reda D, Vandivier RW, Banks SM, et al. Detection of macrophage inflammatory protein (MIP)-1alpha and MIP-1beta during experimental endotoxemia and human sepsis. *J Infect Dis.* (1999) 179:136–41. doi: 10.1086/314559
15. Goser S, Ottl R, Brodner A, Dengler TJ, Torzewski J, Egashira K, et al. Critical role for monocyte chemoattractant protein-1 and macrophage inflammatory protein-1alpha in induction of experimental autoimmune myocarditis and effective anti-monocyte chemoattractant protein-1 gene therapy. *Circulation.* (2005) 112:3400–7. doi: 10.1161/CIRCULATIONAHA.105.572396
16. Crnko S, Du Pre BC, Sluijter JPG, Van Laake LW. Circadian rhythms and the molecular clock in cardiovascular biology and disease. *Nat Rev Cardiol.* (2019) 16:437–47. doi: 10.1038/s41569-019-0167-4
17. Chen YL, Chuang JH, Wang HT, Chen HC, Liu WH, Yang MY. Altered expression of circadian clock genes in patients with atrial fibrillation is associated with atrial high-rate episodes and left atrial remodeling. *Diagnostics.* (2021) 11:90. doi: 10.3390/diagnostics11010090
18. Gibbs JE, Blaikley J, Beesley S, Matthews L, Simpson KD, Boyce SH, et al. The nuclear receptor REV-ERBalpha mediates circadian regulation of innate immunity through selective regulation of inflammatory cytokines. *Proc Natl Acad Sci USA.* (2012) 109:582–7. doi: 10.1073/pnas.1106750109
19. Kitchen GB, Cunningham PS, Poolman TM, Iqbal M, Maidstone R, Baxter M, et al. The clock gene Bmal1 inhibits macrophage motility, phagocytosis, and impairs defense against pneumonia. *Proc Natl Acad Sci USA.* (2020) 117:1543–51. doi: 10.1073/pnas.1915932117
20. Dong C, Gongora R, Sosulski ML, Luo F, Sanchez CG. Regulation of transforming growth factor-beta1 (TGF-beta1)-induced pro-fibrotic activities by circadian clock gene BMAL1. *Respir Res.* (2016) 17:4. doi: 10.1186/s12931-016-0320-0
21. Yeh YH, Kuo CT, Chan TH, Chang GJ Qi XY, Tsai F, et al. Transforming growth factor-beta and oxidative stress mediate tachycardia-induced cellular remodelling in cultured atrial-derived myocytes. *Cardiovasc Res.* (2011) 91:62–70. doi: 10.1093/cvr/cvr041
22. Stanciu AE, Vatasescu RG, Stanciu MM, Serdarevic N, Dorobantu M. The role of pro-fibrotic biomarkers in paroxysmal and persistent atrial fibrillation. *Cytokine.* (2018) 103:63–8. doi: 10.1016/j.cyto.2017.12.026
23. Kirchhof P, Benussi S, Kotecha D, Ahlsson A, Atar D, Casadei B, et al. 2016 ESC Guidelines for the management of atrial fibrillation developed in collaboration with EACTS. *Eur Heart J.* (2016) 37:2893–962. doi: 10.5603/KP.2016.0172
24. Manglani M, Rua R, Hendricksen A, Braunschweig D, Gao Q, Tan W, et al. Method to quantify cytokines and chemokines in mouse brain tissue using Bio-Plex multiplex immunoassays. *Methods.* (2019) 158:22–6. doi: 10.1016/j.ymeth.2019.02.007
25. Aukrust P, Ueland T, Muller F, Andreassen AK, Nordoy I, Aas H, et al. Elevated circulating levels of C-C chemokines in patients with congestive heart failure. *Circulation.* (1998) 97:1136–43. doi: 10.1161/01.CIR.97.12.1136
26. Parissis JT, Adamopoulos S, Venetsanou KF, Mentzikof DG, Karas SM, Kremastinos DT. Serum profiles of C-C chemokines in acute myocardial infarction: possible implication in postinfarction left ventricular remodeling. *J Interferon Cytokine Res.* (2002) 22:223–9. doi: 10.1089/1079990027535 36194
27. de Jager SC, Kraaijeveld AO, Grauss RW, de Jager W, Liem SS, van der Hoeven BL, et al. CCL3 (MIP-1 alpha) levels are elevated during acute coronary

syndromes and show strong prognostic power for future ischemic events. *J Mol Cell Cardiol.* (2008) 45:446–52. doi: 10.1016/j.yjmcc.2008.06.003
28. de Jager SC, Bongaerts BW, Weber M, Kraaijeveld AO, Rousch M, Dimmeler S, et al. Chemokines CCL3/MIP1alpha, CCL5/RANTES and CCL18/PARC are independent risk predictors of short-term mortality in patients with acute coronary syndromes. *PLoS ONE.* (2012) 7:e45804. doi: 10.1371/journal.pone.0045804
29. Van Linthout S, Miteva K, Tschope C. Crosstalk between fibroblasts and inflammatory cells. *Cardiovasc Res.* (2014) 102:258–69. doi: 10.1093/cvr/cvu062
30. Mittal S. Differentiating paroxysmal from persistent atrial fibrillation: long-term electrocardiographic monitoring is mightier than the clinician. *J Am Coll Cardiol.* (2014) 63(25 Pt A):2849–51. doi: 10.1016/j.jacc.2014.04.020
31. Gramley F, Lorenzen J, Koellensperger E, Kettering K, Weiss C, Munzel T. Atrial fibrosis and atrial fibrillation: the role of the TGF-beta1 signaling pathway. *Int J Cardiol.* (2010) 143:405–13. doi: 10.1016/j.ijcard.2009.03.110
32. Behnes M, Hoffmann U, Lang S, Weiss C, Ahmad-Nejad P, Neumaier M, et al. Transforming growth factor beta 1 (TGF-beta 1) in atrial fibrillation and acute congestive heart failure. *Clin Res Cardiol.* (2011) 100:335–42. doi: 10.1007/s00392-010-0248-1
33. Maltman J, Pragnell IB, Graham GJ. Specificity and reciprocity in the interactions between TGF-beta and macrophage inflammatory protein-1 alpha. *J Immunol.* (1996) 156:1566–71.

Conflict of Interest: The authors declare that the research was conducted in the absence of any commercial or financial relationships that could be construed as a potential conflict of interest.

Publisher's Note: All claims expressed in this article are solely those of the authors and do not necessarily represent those of their affiliated organizations, or those of the publisher, the editors and the reviewers. Any product that may be evaluated in this article, or claim that may be made by its manufacturer, is not guaranteed or endorsed by the publisher.

frontiers in Cardiovascular Medicine

ORIGINAL RESEARCH
published: 24 January 2022
doi: 10.3389/fcvm.2022.791156

Construction and Analysis of the lncRNA-miRNA-mRNA Network Based on Competing Endogenous RNA in Atrial Fibrillation

Xiangyu Ke[1†], Junguo Zhang[1,2†], Xin Huang[1], Shuai Li[1], Meifang Leng[3†], Zebing Ye[3] and Guowei Li[1,4*]*

[1] Centre for Clinical Epidemiology and Methodology, Guangdong Second Provincial General Hospital, Guangzhou, China, [2] Department of Epidemiology, School of Public Health, Sun Yat-sen University, Guangzhou, China, [3] Department of Cardiology, Guangdong Second Provincial General Hospital, Guangzhou, China, [4] Department of Health Research Methods, Evidence, and Impact (HEI), McMaster University, Hamilton, ON, Canada

OPEN ACCESS

Edited by:
Daniel M. Johnson, The Open University, United Kingdom

Reviewed by:
Miron Sopic, University of Belgrade, Serbia
Shamone Gore Panter, Cleveland State University, United States

***Correspondence:**
Zebing Ye
jzhzzang@163.com
Guowei Li
lig28@mcmaster.ca

[†]These authors have contributed equally to this work

Specialty section:
This article was submitted to Cardiac Rhythmology, a section of the journal Frontiers in Cardiovascular Medicine

Received: *08 October 2021*
Accepted: *03 January 2022*
Published: *24 January 2022*

Citation:
Ke X, Zhang J, Huang X, Li S, Leng M, Ye Z and Li G (2022) Construction and Analysis of the lncRNA-miRNA-mRNA Network Based on Competing Endogenous RNA in Atrial Fibrillation. Front. Cardiovasc. Med. 9:791156. doi: 10.3389/fcvm.2022.791156

Background: Accumulated studies have revealed that long non-coding RNAs (lncRNAs) play critical roles in human diseases by acting as competing endogenous RNAs (ceRNAs). However, functional roles and regulatory mechanisms of lncRNA-mediated ceRNA in atrial fibrillation (AF) remain unknown. In the present study, we aimed to construct the lncRNA-miRNA-mRNA network based on ceRNA theory in AF by using bioinformatic analyses of public datasets.

Methods: Microarray data sets of GSE115574 and GSE79768 from the Gene Expression Omnibus database were downloaded. Twenty-one AF right atrial appendage (RAA) samples and 22 sinus rhythm (SR) subjects RAA samples were selected for subsequent analyses. After merging all microarray data and adjusting for batch effect, differentially expressed genes were identified. Gene Ontology (GO) categories and Kyoto Encyclopedia of Genes and Genomes (KEGG) pathway enrichment analyses were carried out. A ceRNA network was constructed.

Result: A total of 8 lncRNAs and 43 mRNAs were significantly differentially expressed with fold change >1.5 ($p < 0.05$) in RAA samples of AF patients when compared with SR. GO and KEGG pathway analysis showed that cardiac muscle contraction pathway were involved in AF development. The ceRNA was predicted by co-expressing LOC101928304/ LRRC2 from the constructional network analysis, which was competitively combined with miR-490-3p. The expression of LOC101928304 and LRRC were up-regulated in myocardial tissue of patients with AF, while miR-490-3p was down-regulated.

Conclusion: We constructed the LOC101928304/miR-490-3p/LRRC2 network based on ceRNA theory in AF in the bioinformatic analyses of public datasets. The ceRNA network found from this study may help improve our understanding of lncRNA-mediated ceRNA regulatory mechanisms in the pathogenesis of AF.

Keywords: competing endogenous RNA, long non-coding RNAs, network, atrial fibrillation, bioinformatic analysis

INTRODUCTION

Atrial fibrillation (AF) is the most common sustained arrhythmia characterized by irregular high-frequency excitation and contraction of the atria, and is a major contributor to stroke, heart failure and sudden death (1–3). Approximately 1–2% of the common population suffer from AF, with the prevalence up to over 10% for individuals aged ≥80 years (1, 2, 4, 5). However, there is a lack of effective therapy for AF in general, largely because the pathophysiologic mechanism underlying AF remains unclear. The underlying pathogenesis of AF is multiplex, including electrical remodeling, structural remodeling, Ca^{2+} handling abnormalities and autonomic nervous system changes (6).

Previous studies have identified that non-coding RNAs (ncRNAs) play a critical role in the pathogenesis of AF by regulating core proteins and pivotal pathways (7). Long non-coding RNAs (lncRNAs) are a class of endogenous ncRNAs whose length are >200 nucleotides with no protein-coding potential (8). A number of studies have demonstrated that lncRNAs are involved in multiple biological processes by regulating genes of transcriptional, posttranscriptional, and epigenetic levels (9). Dysregulations of lncRNA expressions and functions have been implicated in the development and progression of many diseases including cancer, neurodegeneration diseases and cardiovascular diseases (10–12).

Competing endogenous RNA (ceRNA) is a novel regulation mechanism in which lncRNA can competitively combine with miRNAs through microRNA response elements (MREs), thus inhibiting gene silencing by isolating miRNAs from messenger RNAs (mRNAs) (13–15). This regulation mechanism has been observed in some cardiovascular diseases. For example, lncRNA PEL was shown to function as a ceRNA to competitively band let-7d and contribute to cardiac fibrosis (16). In addition, lncRNA TNK2-AS1 could regulate ox-LDL-stimulated human aortic smooth muscle cell proliferation and migration by serving as a ceRNA for miR-150-50 to modulate VEGFA and FGF1 expression (17). However, the ceRNA mechanisms related to AF remained largely unclear and required further investigation.

Therefore, in the present study, we aimed to construct the lncRNA-miRNA-mRNA network based on ceRNA theory in AF by using bioinformatic analyses of public datasets. Findings from the ceRNA network may help improve our understanding of lncRNA-mediated ceRNA regulatory mechanisms in the pathogenesis of AF.

MATERIALS AND METHODS

Microarray Datasets of mRNAs and LncRNAs

Two independent human AF gene expression profiles were downloaded from the Gene Expression Omnibus database (GEO, https://www.ncbi.nlm.nih.gov/geo) with accession number of GSE115574 and GSE79768, respectively (**Table 1**). All microarray data were based on GPL570 (Affymetrix Human Genome U133 Plus 2.0 Array). In each data set, only human right atrial appendage (RAA) samples from AF and sinus rhythm (SR) subjects were selected. Finally, a total of 21 AF and 22 SR samples were included for subsequent analyses.

TABLE 1 | The characteristics of datasets in this study.

GSE series	GSE115574	GSE79768
Platform	GPL570	GPL570
Total	30	13
AF	14	7
SR	16	6
Country	Turkey	Taiwan
Contributors	Deniz GC et.al	Tsai F et.al

GSE, gene expression omnibus; AF, atrial fibrillation; SR, sinus rhythm.

Data Pre-processing

Robust multi-array average (RMA) algorithm and log2-transformed were performed for background correction and normalization. The averages of the probe sets of values were calculated as the expression values for the same gene with multiple probe sets. Furthermore, human genome reference hg38 (GRCh38.p13) was utilized to annotate series matrix files to determine transcript biotype and to convert the probe IDs into gene symbols. After merging all microarray data, empirical Bayes frameworks was used to adjust for the batch effects.

Differentially Expressed Genes Analysis

A differential expression analysis on merged GEO series based on paired-sample *t*-tests between AF and SR samples, were performed using "Limma" package of R software. The Benjamini and Hochberg (BH) method was introduced to adjust the raw *P*-values into a false discovery rate to avoid the multi-test problem. The adjust $p < 0.05$ and the gene expression fold change (FC) value ≥1.5 or ≤2/3 ($|\log2\ FC| \geq 0.58$), were set as the thresholds for identifying DEGs including mRNA and LncRNA between the AF and SR sample. Moreover, up-regulated or down-regulated DEGs were visualized as heat map plots.

Functional and Pathway Enrichment Analyses of DEGs Among ceRNA Network

To better understand the biological function and characteristics of DEGs among ceRNA network, Gene Ontology (GO, http://geneontology.org/) (18) and Kyoto Encyclopedia of Genes and Genomes (KEGG, https://www.kegg.jp/) (19) were performed using the "clusterProfiler" package of R software. GO terms and KEGG pathways that met the criterion of adjusted $p < 0.05$ and Q value <0.05, were considered as significantly enriched (18, 19).

ceRNA Network Construction

To constructed LncRNA-miRNA-mRNA networks, first, the differentially expressed LncRNAs and mRNAs with $|\log2\ FC| \geq 0.58$ were selected. The LncRNA-miRNA interactions were predicted by using Mircode (http://www.mircode.org), which provided human miRNA target predictions based on the comprehensive GENCODE gene annotation. Furthermore, predicted miRNAs were utilized to construct miRNA-mRNA

TABLE 2 | The up-regulated and down-regulated differently expressed lncRNAs in merged data.

LncRNA	FC	AveExpr	t	*P* Value	Adjust *P* value	B
Up-regulated						
TRDN-AS1	2.2933	5.0081	5.5285	<0.0001	0.0019	4.9934
UNC5B-AS1	1.9265	5.9359	4.8713	<0.0001	0.0066	3.0102
LINC00702	2.1401	6.1239	3.8955	0.0003	0.0323	0.1999
LOC101928304	1.6665	7.3767	4.8761	<0.0001	0.0066	3.0243
Down-regulated						
LINC00844	0.4813	8.1024	−4.7081	<0.0001	0.0089	2.5262
MUM1L1	0.5764	6.0297	−3.9736	0.0003	0.0286	0.4158
LOC100507477	0.6137	5.6490	−4.9845	<0.0001	0.0057	3.3483
GGTA1P	0.6632	7.7114	−4.8867	<0.0001	0.0065	3.0559

FC, fold change; AveExpr, average expression, defined as average log2-expression level for that gene across all the arrays and channels in the experiment; B, The B-statistic is the log-odds given that the gene is differentially expressed.

interaction using the tools of TargetScan (http://www.targetscan.org/mamm_31/), Mirdb (http://mirdb.org/), MiRTarBase (http://miRTarBase.cuhk.edu.cn/), and MirDIP (http://ophid.utoronto.ca/mirDIP/). The mRNAs predicted by three or above datasets, were used to identify the potential miRNA targets. Since lncRNAs can function as endogenous miRNA sponges and regulate the translation of targeted mRNAs, the expression of lncRNAs and mRNAs should be positively correlated (14). Subsequently, the initial ceRNA network was constructed on the basis of the differentially expressed lncRNAs, predicted miRNAs and mRNAs using the Cytoscape 3.7.2 software (http://cytoscape.org/).

Validation of the Expression of miRNAs Among ceRNA Network

In the ceRNA network, the expression of miRNAs should be negatively correlated with lncRNAs and mRNAs (14). The gene expression profile GSE28954 was downloaded from the GEO database and expression profiling arrays were generated using platform GPL10850 [Agilent-021827 Human miRNA Microarray (V3)]. Additionally, the GSE28954 dataset including 10 RAA sample (4 AF and 6 SR) was used to identify differential expression miRNAs. Any miRNAs were deemed as differentially expressed if adjusted p-values were < 0.05 and fold changes were ≥ 1.5 or $\leq 2/3$. Subsequently, significantly down-regulated miRNAs, up-regulated mRNAs and LncRNAs were used to construct final ceRNA network. Moreover, Funrich software (http://www.funrich.org/) was used to functional enrichment for differential expression miRNAs.

RESULTS

LncRNA and mRNA Expression Profile

Gene expression levels of merged GEO series that have been adjusted for batch effects were standardized; and the results of pre- and post- standardized are showed in **Supplementary Figure 1**. A total of 8 lncRNAs and 43 mRNA were significantly differentially expressed with a fold change >1.5 ($p < 0.05$) in RAA samples of AF patients when compared with SR. The up-and down-regulated differently expressed lncRNAs and mRNAs are listed in **Tables 2**, **3**. Among the 8 lncRNAs, 4 were up-regulated and the remaining were down-regulated. Among the 43 mRNAs, 14 and 39 were up-regulated and down-regulated, respectively. The heat maps of the 8 lncRNAs distinctly separated AF from controls were showed in **Figure 1**.

Functional Enrichment Analyses: GO and KEGG Pathway Analyses

To further investigate the biological functions of the 43 differential expressed mRNA, functional enrichment analyses were performed (**Table 4**). GO enrichment analysis revealed that differential expressed mRNA were enriched in five biological processes (adjusted $p < 0.05$ and Q value < 0.05), but not in the AF associated process. Pathway analyses showed that differential expressed mRNA were enriched in 4 biological processes including bile secretion, cardiac muscle contraction, insulin secretion, protein digestion and absorption. The up-regulated ATP1B4 and down-regulated TRDN were enriched in cardiac muscle contraction (adjusted $p = 0.0360$ and $Q = 0.0278$). Cardiac muscle contraction was found to indicate AF development, which was line with a previous study (20).

Construction of ceRNA Network

Using the Mircode, we obtained 335 miRNAs. Furthermore, we obtained 77019 mRNAs based on the tools of TargetScan, Mirdb, MiRTarBase and MirDIP. By using the Cytoscape, we found that a total of 7 lncRNAs, 91 miRNAs and 28 mRNAs were involved in the lncRNA-miRNA-mRNA network (**Figure 2**). Based on the ceRNA theory (14), the screened lncRNAs and mRNAs were both up-regulated (**Table 5**).

Validation of the Expression of miRNAs Among ceRNA Network

To further validate the ceRNA network of AF, we analyzed miRNA microarrays GSE28954 from the GEO data and results showed that eight differentially expressed miRNAs were identified (**Table 6**). After combining with the findings from

TABLE 3 | The up-regulated and down-regulated differently expressed mRNA in merged data.

mRNA	FC	AveExpr	t	*P* Value	Adjust *P* value	B
Up-regulated						
DNAJA4	1.5251	6.5447	7.2648	<0.0001	0.0001	10.2855
DHRS9	2.3195	8.4284	7.1253	<0.0001	0.0001	9.8654
ANGPTL2	1.5611	6.7732	6.2432	<0.0001	0.0005	7.1793
FRMD3	1.5410	7.8567	5.9835	<0.0001	0.0009	6.3838
CHGB	2.3222	7.9284	5.8236	<0.0001	0.0012	5.8944
LBH	1.7619	7.6184	5.6304	<0.0001	0.0017	5.3041
RPL3L	2.1094	7.2044	5.1515	<0.0001	0.0041	3.8500
COLQ	2.5338	6.1412	5.0006	<0.0001	0.0057	3.3964
COL21A1	1.5923	8.7335	4.7384	<0.0001	0.0089	2.6156
LRRC2	1.6346	6.6767	4.1833	0.0001	0.0212	1.0047
PHLDA1	1.7130	5.5968	4.1370	0.0002	0.0232	0.8736
ATP1B4	1.9225	4.0392	4.1332	0.0002	0.0232	0.8630
RELN	2.3546	7.1304	3.8306	0.0004	0.0358	0.0219
HOGA1	1.6400	5.9306	3.6332	0.0007	0.0469	−0.5107
Down-regulated						
C1orf105	0.4957	6.6784	−4.6479	<0.0001	0.0100	2.3488
G0S2	0.6187	9.3051	−4.6229	<0.0001	0.0105	2.2753
SCARA5	0.6410	7.2144	−4.5603	<0.0001	0.0120	2.0917
TNNI1	0.3292	6.7636	−4.4643	0.0001	0.0140	1.8121
VIT	0.5843	5.1497	−4.4554	0.0001	0.0141	1.7860
BEX2	0.5819	8.2081	−4.3737	0.0001	0.0160	1.5495
PRIMA1	0.6659	6.9603	−4.3647	0.0001	0.0160	1.5236
CACNA2D2	0.6092	7.1702	−4.2543	0.0001	0.0186	1.2069
SFRP5	0.5573	6.3132	−4.2466	0.0001	0.0186	1.1850
SOSTDC1	0.5526	5.3729	−4.2416	0.0001	0.0186	1.1706
SYT13	0.6506	4.9698	−4.2277	0.0001	0.0192	1.1311
TMEM132C	0.6557	6.1435	−4.1234	0.0002	0.0236	0.8353
TMEM176A	0.6291	8.0699	−4.0289	0.0002	0.0266	0.5700
CNTN3	0.5833	6.2783	−4.0121	0.0002	0.0275	0.5232
IRX3	0.6642	7.3042	−3.9392	0.0003	0.0306	0.3206
MFAP4	0.6284	7.9084	−3.8971	0.0003	0.0323	0.2042
KCNN2	0.6305	6.0473	−3.8486	0.0004	0.0349	0.0711
ART3	0.6384	8.6506	−3.8262	0.0004	0.0359	0.0098
SUSD4	0.6213	5.8862	−3.8150	0.0004	0.0362	−0.0208
BCHE	0.6113	6.4957	−3.7419	0.0005	0.0408	−0.2192
CLSTN2	0.6348	5.6674	−3.6521	0.0007	0.0459	−0.4605
CPLX3	0.5812	6.6010	−3.6176	0.0008	0.0485	−0.5522
MGC24103	0.6030	5.3526	−3.9094	0.0003	0.0316	0.2382
REC114	0.6487	4.9716	−5.8065	<0.0001	0.0012	5.8422
TRDN	0.6624	6.5037	−4.9370	<0.0001	0.0061	3.2060
SLC7A11	0.6358	4.7243	−4.8509	<0.0001	0.0069	2.9495
BLM	0.6175	6.1317	−4.8269	<0.0001	0.0073	2.8779

FC, fold change; AveExpr, average expression, defined as average log2-expression level for that gene across all the arrays and channels in the experiment; B, The B-statistic is the log-odds given that the gene is differentially expressed.

Tables 5, **6**, we found that LOC101928304/miR-490-3p/LRRC2 was consistent with the ceRNA mechanism. The expression of LOC101928304 and LRRC2 were up-regulated in myocardial tissue of patients with AF, while miR-490-3p was down-regulated. LOC101928304 was positively correlated with LRRC2 (**Supplementary Figure 2**).

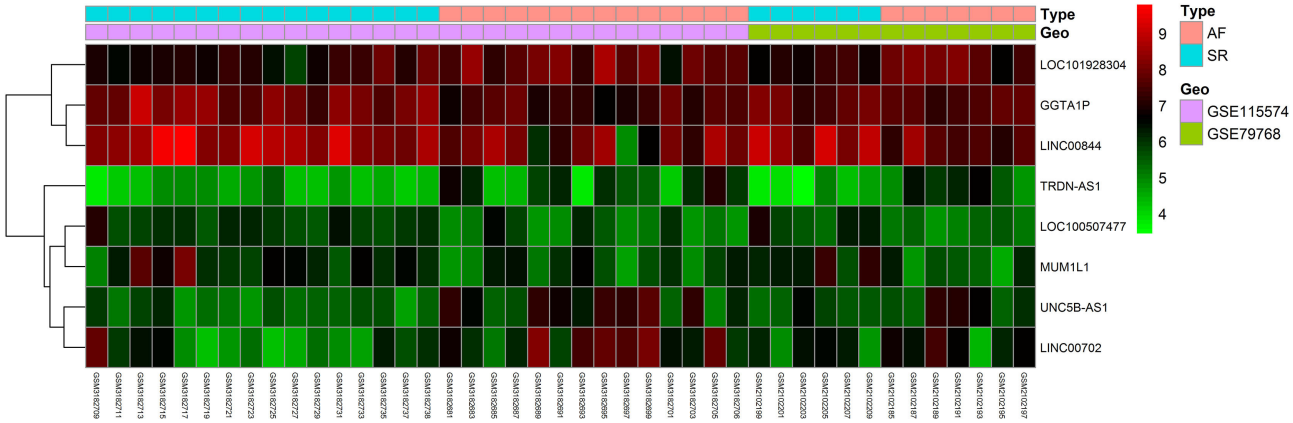

FIGURE 1 | Heatmap of lncRNAs profile comparisons between atrial fibrillation and control. Each row represents a sample and each column represents a single gene. Pink color represents AF samples and blue color presents SR samples. The color scale shows the relative genes expression level in certain slide: green indicates low relative expression levels; red indicates high relative expression levels.

TABLE 4 | Significant enriched GO terms and pathways of differential expressed mRNA.

	Term	Genes	*P* value	Adjust *P* value	Q value
GO terms					
GO:0001941	Postsynaptic membrane organization	RELN/SLC7A11/COLQ	<0.0001	0.0082	0.0057
GO:0043113	Receptor clustering	RELN/SLC7A11/COLQ	<0.0001	0.0107	0.0075
GO:0072578	Neurotransmitter-gated ion channel clustering	RELN/SLC7A11	0.0001	0.0157	0.0110
GO:0050807	Regulation of synapse organization	RELN/SLC7A11/COLQ/ CLSTN2	0.0001	0.0157	0.0110
GO:0050803	Regulation of synapse structure or activity	RELN/SLC7A11/COLQ/ CLSTN2	0.0001	0.0157	0.0110
KEGG pathway					
hsa04976	Bile secretion	ATP1B4/KCNN2	0.0028	0.0360	0.0278
hsa04260	Cardiac muscle contraction	TRDN/ATP1B4	0.0040	0.0360	0.0278
hsa04911	Insulin secretion	ATP1B4/KCNN2	0.0040	0.0360	0.0278
hsa04974	Protein digestion and absorption	COL21A1/ATP1B4	0.0048	0.0360	0.0278

DISCUSSION

In this bioinformatics study, we integrated gene expression profiles of 46 AF samples and 31 SR samples from 2 GEO datasets. We identified 8 lncRNAs and 43 mRNA were significantly differentially expressed with fold change >1.5 ($p < 0.05$). Furthermore, the LOC101928304/miR-490-3p/LRRC2 network based on ceRNA theory was constructed in AF. The expression of LOC101928304 and LRRC2 were up-regulated in myocardial tissue of patients with AF, while miR-490-3p was down-regulated.

Recently, the pathological functions of lncRNAs and miRNAs in cardiovascular disease have been recognized, making them potential candidates as therapeutic targets and biomarkers. However, AF-related lncRNAs and miRNAs still required further research. Recent studies have investigated the expression profiles of lncRNA in AF patients (20–25). For instance, Xu et al. detected the expression levels of lncRNAs in AF in elderly patients, which showed that lncRNAs were closely involved in the pathogenesis of AF (26). Moreover, an increasing number of reports indicate that lncRNAs can regulate protein-coding genes in mammals through the ceRNA network (27), where lncRNAs function as miRNA sponges to upregulate the expression of their targets (28). For instance, Liu et al. identified LINC00964 as a key lncRNA in AF susceptibility- and persistence-associated ceRNA networks (29). By integrating three microarray datasets and construction of a ceRNA network, the study by Wu et al. discovered that HCG11, KRBOX1-AS1, ACBD5 and RAD52 may compete with WEE1 for has-miR-17-5p to affect the development of AF (30). However, given the sparse existing evidence in the literature, the ceRNA mechanisms related to AF remained largely obscure and required further investigation.

Previous studies have found an association between LOC101928304 and cardiovascular diseases. Qiu et al. found that LOC101928304 were related with the functions of blood circulation and heart contraction using high-throughput sequencing of lncRNAs in myocardial tissues collected from patients with dilated cardiomyopathy (DCM) and normal heart donors (31). They also confirmed that LOC101928304 were downregulated in DCM tissues by using real-time PCR (31).

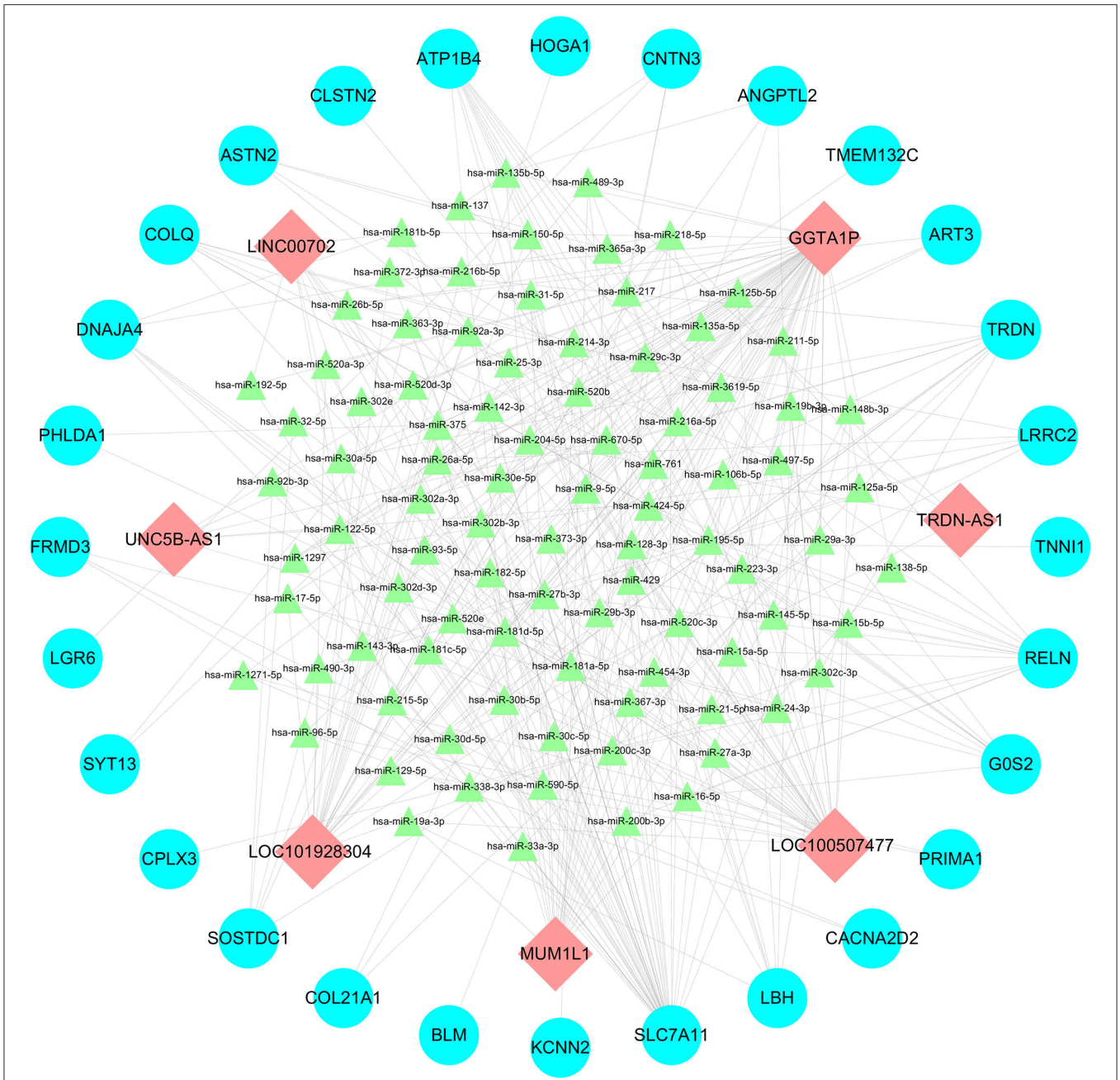

FIGURE 2 | LncRNA-miRNA-mRNA networks between: Red, green, and blue represents lncRNAs, miRNAs and mRNAs, respectively.

Likewise, one study reported that miR-490-3p played a key role in different acute and chronic cardiovascular disease processes (32). Downregulation of miR-490-3p expression in atherosclerosis patients, and miR-490-3p which enhanced cell proliferation and migration of vascular smooth muscle cells and human umbilical vein endothelial cells in atherosclerosis (33, 34). The inhibition of miR-490-3p could promote autophagy to reduce myocardial ischemia reperfusion (IR) injury by upregulating ATG4B (35). Qiang et al. investigated that miR-490-3p was downregulated in patients with chronic heart failure (HF), which might provide novel targets for prevention and treatment of chronic HF (36). Cao et al. revealed that miR-490-3p was down-regulated in AF, which had a potential diagnostic value to distinguish patients with AF from healthy controls (37). First, we constructed the ceRNA network based on lncRNA and mRNA, and predicted the corresponding miRNA. In subsequent verification, we carried out an exploratory analysis because the sample size was limited. Under these circumstances, even if its adjusted $P > 0.05$, we still have reason to believe that miR-490-3p has potential to be part of the ceRNA network that could be

TABLE 5 | The ceRNA network of AF with up-regulated lncRNA and mRNA.

lncRNA	miRNA	mRNA	lncFC	mFC
UNC5B-AS1	hsa-miR-125a-5p	LBH	1.9265	1.7619
UNC5B-AS1	hsa-miR-125b-5p	LBH	1.9265	1.7619
LINC00702	hsa-miR-143-3p	LRRC2	2.1401	1.6346
LINC00702	hsa-miR-181a-5p	PHLDA1	2.1401	1.7130
LOC101928304	hsa-miR-204-5p	ANGPTL2	1.6665	1.5611
LOC101928304	hsa-miR-211-5p	ANGPTL2	1.6665	1.5611
LOC101928304	hsa-miR-214-3p	COLQ	1.6665	2.5338
LOC101928304	hsa-miR-218-5p	RELN	1.6665	2.3546
LINC00702	hsa-miR-27a-3p	RELN	2.1401	2.3546
LINC00702	hsa-miR-27b-3p	RELN	2.1401	2.3546
LOC101928304	hsa-miR-3619-5p	COLQ	1.6665	2.5338
LOC101928304	hsa-miR-375	PHLDA1	1.6665	1.7130
TRDN-AS1	hsa-miR-375	PHLDA1	2.2933	1.7130
LOC101928304	hsa-miR-490-3p	LRRC2	1.6665	1.6346
UNC5B-AS1	hsa-miR-670-5p	LBH	1.9265	1.7619
LOC101928304	hsa-miR-761	COLQ	1.6665	2.5338

lncFC, lncRNA fold change; mFC, mRNA fold change.

TABLE 6 | The differential expression of miRNA in AF patients compared with controls.

miRNA	FC	logFC	AveExpr	t	*P*-Value	adj.P.Val	B
hsa-miR-146b-5p	5.2289	2.3865	0.1283	10.4588	0.0000	0.0005	5.8165
hsa-miR-21-5p	3.3088	1.7263	−0.3083	5.5215	0.0002	0.0608	0.9038
hsa-miR-331-3p	0.6302	−0.6661	−0.0134	−5.0775	0.0005	0.0768	0.2909
hsa-miR-490-3p	0.3849	−1.3774	−0.1368	−4.6268	0.0009	0.0768	−0.3638
hsa-miR-139-5p	0.5946	−0.7500	−0.0444	−4.6021	0.0009	0.0768	−0.4007
hsa-miR-125b-2-3p	0.6196	−0.6906	0.0241	−4.5304	0.0011	0.0768	−0.5080
hsa-miR-143-5p	0.4905	−1.0278	−0.2194	−4.5209	0.0011	0.0768	−0.5223
hsa-miR-128-3p	0.6406	−0.6424	−0.0031	−4.2403	0.0017	0.0930	−0.9502

FC, fold change; Log_2FC, log_2Fold change; AveExpr, average expression, defined as average log2-expression level for that gene across all the arrays and channels in the experiment; B, The B-statistic is the log-odds given that the gene is differentially expressed.

combined with published literature, which should be further verified in subsequent experimental studies. Taken together, our findings were consistent with results from previous studies in that miR-490-3p may participate in the ceRNA network of LOC101928304.

LRRC2 located in chromosome three common eliminated region one, is a member of the leucine-rich repeat-containing family of proteins that have been implicated in various biological pathways. Recently, LRRC2 has been reported to correlate with transcripts associated with cardiac remodeling, thereby playing critical roles in the processes of cardiomyocyte hypertrophy and mitochondrial abundance (38). RNAi-mediated LRRC2 knockdown in a rat-derived cardiomyocyte cell line resulted in enhanced expression of canonical hypertrophic biomarkers as well as increased mitochondrial mass in the context of increased PGC-1α expression (38). LRRC2 partially localized to the mitochondrion and regulated by the mitochondrial master regulator PGC-1α (38). Most notably, mitochondrial dysfunction and cardiomyocyte hypertrophy increase the heterogeneity of atrial electrical conduction, leading to change in atrial structure and potentially facilitating the development of AF (39). The expression of PGC-1α was significantly decreased in AF model of rabbits with rapid pacing, indicating that mitochondrial biosynthesis was impaired in AF (40). LRRC2 may be a mediator of mitochondrial and cardiac function, which involve the PGC-1α-dependent mitochondrial abundance regulation mechanism, thereby ultimately facilitating the development of AF. Nevertheless, a more thorough understanding of LOC101928304/miR-490-3p/LRRC2 pathway in AF is necessary.

Discovering ncRNA-disease associations may help generate diagnostic and therapeutic tools for diseases. However, since uncovering associations via experimental studies are resource and time consuming, bioinformatic analyses for the identification of ncRNAs associated with AF are a helpful approach for preliminary exploration. In our study, we constructed a novel lncRNA-miRNA-mRNA network (LOC101928304/miR-490-3p/LRRC2) based on the ceRNA theory, which may therefore provide insights into the ceRNA regulatory mechanisms in the

pathogenesis of AF. However, our study has some limitations. First, it is difficult to integrate some important factors for analyses, including regions, races and age. Given that the development of AF was caused by numerous environmental and genetic factors, our findings may be influenced by some immeasurable risk factors to an unknown extent. Additionally, specimens were obtained only from within the RAA, whereas AF is predominantly a left atrial disease. KEGG pathway analyses showed that the differently expression lncRNAs were mainly associated with cardiac muscle contraction. The up-regulated ATP1B4 and down-regulated TRDN were enriched in cardiac muscle contraction. Therefore, LOC101928304/miR-490-3p/LRRC2 may be involved in AF through other pathways. Our study may provide some new insights into the AF mechanism based on the bioinformatics analyses; however, the significantly differentially expressed lncRNAs and mRNAs would require experimental investigation of RT-PCR in clinical samples for further validation. In addition, the significantly differentially expressed lncRNAs require experimental investigations using the left atria appendage/pulmonary vein region samples for further validation. Likewise, future experimental research is needed to validate the ceRNA network of LOC101928304/miR-490-3p/LRRC2 in the pathogenesis of AF.

CONCLUSION

The LOC101928304/miR-490-3p/LRRC2 network based on ceRNA theory was constructed in AF in this bioinformatic analysis study. The novel ceRNA network found from this study may help improve our understanding of lncRNA-mediated ceRNA regulatory mechanisms in the pathogenesis of AF.

DATA AVAILABILITY STATEMENT

The datasets presented in this study can be found in online repositories. The names of the repository/repositories and accession number(s) can be found in the article/**Supplementary Material**.

AUTHOR CONTRIBUTIONS

XK, JZ, ZY, and GL were responsible for study conception, design of the study, data acquisition, and analysis and interpretation of results. ML was responsible for data acquisition. ML, XH, and SL took part in the discussion of the paper. XK wrote the manuscript that was reviewed and revised by GL, ZY, ML, XH, and SL. All authors gave approval of the version to be submitted.

FUNDING

This work was supported by the Medical Scientific Research Foundation of Guangdong Province of China (Grant sponsor: GL; Grant no. A2020453), the Science Foundation of Guangdong Second Provincial General Hospital (Grant sponsor: GL; Grant no.YY2018-002), and Doctoral workstation foundation of Guangdong Second Provincial general Hospital (Grant sponsor: XK; Grant no. 2021BSGZ008).

SUPPLEMENTARY MATERIAL

The Supplementary Material for this article can be found online at: https://www.frontiersin.org/articles/10.3389/fcvm.2022.791156/full#supplementary-material

REFERENCES

1. Ahmad Y, Lip GY, Lane DA. Recent developments in understanding epidemiology and risk determinants of atrial fibrillation as a cause of stroke. *Can J Cardiol.* (2013) 29:S4–13. doi: 10.1016/j.cjca.2013.03.009
2. Andrade J, Khairy P, Dobrev D, Nattel S. The clinical profile and pathophysiology of atrial fibrillation: relationships among clinical features, epidemiology, and mechanisms. *Circ Res.* (2014) 114:1453–68. doi: 10.1161/CIRCRESAHA.114.303211
3. Luo X, Yang B, Nattel S. MicroRNAs and atrial fibrillation: mechanisms and translational potential. *Nat Rev Cardiol.* (2015) 12:80–90. doi: 10.1038/nrcardio.2014.178
4. Naccarelli GV, Varker H, Lin J, Schulman KL. Increasing prevalence of atrial fibrillation and flutter in the United States. *Am J Cardio.* (2009) 104:1534–9. doi: 10.1016/j.amjcard.2009.07.022
5. Murphy NF, Simpson CR, Jhund PS, Stewart S, Kirkpatrick M, Chalmers J, et al. A national survey of the prevalence, incidence, primary care burden and treatment of atrial fibrillation in Scotland. *Heart.* (2007) 93:606–12. doi: 10.1136/hrt.2006.107573
6. Nattel S, Harada M. Atrial remodeling and atrial fibrillation: recent advances and translational perspectives. *J Am Coll Cardiol.* (2014) 63:2335–45. doi: 10.1016/j.jacc.2014.02.555
7. Qian C, Li H, Chang D, Wei B, Wang Y. Identification of functional lncRNAs in atrial fibrillation by integrative analysis of the lncRNA-mRNA network based on competing endogenous RNAs hypothesis. *J Cell Physiol.* (2019) 234:11620–30. doi: 10.1002/jcp.27819
8. Liu X, She Y, Wu H, Zhong D, Zhang J. Long non-coding RNA Gas5 regulates proliferation and apoptosis in HCS-2/8 cells and growth plate chondrocytes by controlling FGF1 expression via miR-21 regulation. *J Biomed Sci.* (2018) 25:18. doi: 10.1186/s12929-018-0424-6
9. Kornienko AE, Guenzl PM, Barlow DP, Pauler FM. Gene regulation by the act of long non-coding RNA transcription. *BMC Biol.* (2013) 11:59. doi: 10.1186/1741-7007-11-59
10. Camacho CV, Choudhari R, Gadad SS. Long noncoding RNAs and cancer, an overview. *Steroids.* (2018) 133:93–5. doi: 10.1016/j.steroids.2017.12.012
11. Yu WD, Wang H, He QF, Xu Y, Wang XC. Long noncoding RNAs in cancer-immunity cycle. *J Cell Physiol.* (2018) 233:6518–23. doi: 10.1002/jcp.26568
12. Shi Q, Yang X. Circulating microrna and long noncoding rna as biomarkers of cardiovascular diseases. *J Cell Physiol.* (2016) 231:751–5. doi: 10.1002/jcp.25174
13. Karreth FA, Pandolfi PP. ceRNA cross-talk in cancer: when ce-bling rivalries go awry. *Cancer Discov.* (2013) 3:1113–21. doi: 10.1158/2159-8290.CD-13-0202
14. Tay Y, Rinn J, Pandolfi PP. The multilayered complexity of ceRNA crosstalk and competition. *Nature.* (2014) 505:344–52. doi: 10.1038/nature12986
15. An Y, Furber KL, Ji S. Pseudogenes regulate parental gene expression via ceRNA network. *J Cell Mol Med.* (2017) 21:185–92. doi: 10.1111/jcmm.12952
16. Liang H, Pan Z, Zhao X, Liu L, Sun J, Su X, et al. LncRNA PFL contributes to cardiac fibrosis by acting as a competing endogenous RNA of let-7d. *Theranostics.* (2018) 8:1180–94. doi: 10.7150/thno.20846
17. Cai T, Cui X, Zhang K, Zhang A, Liu B, Mu JJ. LncRNA TNK2-AS1 regulated ox-LDL-stimulated HASMC proliferation and migration via modulating

VEGFA and FGF1 expression by sponging miR-150-5p. *J Cell Mol Med.* (2019) 23:7289–98. doi: 10.1111/jcmm.14575
18. Ashburner M, Ball CA, Blake JA, Botstein D, Butler H, Cherry JM, et al. Gene ontology: tool for the unification of biology. The gene ontology consortium. *Nat Genet.* (2000) 25:25–9. doi: 10.1038/75556
19. Kanehisa M, Sato Y, Furumichi M, Morishima K, Tanabe M. New approach for understanding genome variations in KEGG. *Nucleic Acids Res.* (2019) 47:D590–5. doi: 10.1093/nar/gky962
20. Wu N, Li J, Chen X, Xiang Y, Wu L, Li C, et al. Identification of long non-coding RNA and circular RNA expression profiles in atrial fibrillation. *Heart Lung Circ.* (2020) 29:e157–67. doi: 10.1016/j.hlc.2019.10.018
21. Ruan Z, Sun X, Sheng H, Zhu L. Long non-coding RNA expression profile in atrial fibrillation. *Int J Clin Exp Pathol.* (2015) 8:8402–10.
22. Su Y, Li L, Zhao S, Yue Y, Yang S. The long noncoding RNA expression profiles of paroxysmal atrial fibrillation identified by microarray analysis. *Gene.* (2018) 642:125–34. doi: 10.1016/j.gene.2017.11.025
23. Yu XJ, Zou LH, Jin JH, Xiao F, Li L, Liu N, et al. Long noncoding RNAs and novel inflammatory genes determined by RNA sequencing in human lymphocytes are up-regulated in permanent atrial fibrillation. *Am J Transl Res.* (2017) 9:2314–26.
24. Mei B, Liu H, Yang S, Liang MY, Yue Y, Huang SQ, et al. Long non-coding RNA expression profile in permanent atrial fibrillation patients with rheumatic heart disease. *Eur Rev Med Pharmacol Sci.* (2018) 22:6940–7. doi: 10.26355/eurrev_201810_16165
25. Ruan ZB, Wang F, Gongben BD, Chen GC, Zhu L. Identification of circulating lncRNA expression profiles in patients with atrial fibrillation. *Dis Markers.* (2020) 2020:8872142. doi: 10.1155/2020/8872142
26. Xu Y, Huang R, Gu J, Jiang W. Identification of long non-coding RNAs as novel biomarker and potential therapeutic target for atrial fibrillation in old adults. *Oncotarget.* (2016) 7:10803–11. doi: 10.18632/oncotarget.7514
27. Chu Q, Xu T, Zheng W, Chang R, Zhang L. Long noncoding RNA MARL regulates antiviral responses through suppression miR-122-dependent MAVS downregulation in lower vertebrates. *PLoS Pathog.* (2020) 16:e1008670. doi: 10.1371/journal.ppat.1008670
28. Du Z, Sun T, Hacisuleyman E, Fei T, Wang X, Brown M, et al. Integrative analyses reveal a long noncoding RNA-mediated sponge regulatory network in prostate cancer. *Nat Commun.* (2016) 7:10982. doi: 10.1038/ncomms 10982
29. Liu Y, Liu N, Bai F, Liu Q. Identifying ceRNA networks associated with the susceptibility and persistence of atrial fibrillation through weighted gene co-expression network analysis. *Front Genet.* (2021) 12:653474. doi: 10.3389/fgene.2021.653474
30. Wu J, Deng H, Chen Q, Wu Q, Li X, Jiang S, et al. Comprehensive analysis of differential immunocyte infiltration and potential ceRNA networks involved in the development of atrial fibrillation. *Biomed Res Int.* (2020) 2020:8021208. doi: 10.1155/2020/80 21208
31. Qiu Z, Ye B, Yin L, Chen W, Xu Y, Chen X. Downregulation of AC061961.2, LING01-AS1, and RP11-13E1.5 is associated with dilated cardiomyopathy progression. *J Cell Physiol.* (2019) 234:4460–71. doi: 10.1002/jcp.27247
32. Fan ZX, Yang J. The role of microRNAs in regulating myocardial ischemia reperfusion injury. *Saudi Med J.* (2015) 36:787–93. doi: 10.15537/smj.2015.7.11089
33. Liu Y, Chen Y, Tan L, Zhao H, Xiao N. Linc00299/miR-490-3p/AURKA axis regulates cell growth and migration in atherosclerosis. *Heart Vessels.* (2019) 34:1370–80. doi: 10.1007/s00380-019-01356-7
34. Guo X, Liu Y, Zheng X, Han Y, Cheng J. HOTTIP knockdown inhibits cell proliferation and migration via regulating miR-490-3p/HMGB1 axis and PI3K-AKT signaling pathway in ox-LDL-induced VSMCs. *Life Sci.* (2020) 248:117445. doi: 10.1016/j.lfs.2020.117445
35. Wu Y, Mao Q, Liang X. Targeting the MicroRNA-490-3p-ATG4B-Autophagy axis relieves myocardial injury in ischemia reperfusion. *J Cardiovasc Transl Res.* (2021) 14:173–83. doi: 10.1007/s12265-020-09972-9
36. Qiang L, Hong L, Ningfu W, Huaihong C, Jing W. Expression of miR-126 and miR-508-5p in endothelial progenitor cells is associated with the prognosis of chronic heart failure patients. *Int J Cardiol.* (2013) 168:2082–8. doi: 10.1016/j.ijcard.2013.01.160
37. Cao Y, Cui L. Identifying the key microRNAs implicated in atrial fibrillation. *Anatol J Cardiol.* (2021) 25:429–36. doi: 10.14744/AnatolJCardiol.2020.41625
38. McDermott-Roe C, Leleu M, Rowe GC, Palygin O, Bukowy JD, Kuo J, et al. Transcriptome-wide co-expression analysis identifies LRRC2 as a novel mediator of mitochondrial and cardiac function. *PloS oNE.* (2017) 12:e0170458. doi: 10.1371/journal.pone.0170458
39. Neuberger HR, Schotten U, Verheule S, Eijsbouts S, Blaauw Y, van Hunnik A. Development of a substrate of atrial fibrillation during chronic atrioventricular block in the goat. *Circulation.* (2005) 111:30–7. doi: 10.1161/01.CIR.0000151517.43137.97
40. Dong J, Zhao J, Zhang M, Liu G, Wang X, Liu Y, et al. Beta3-adrenoceptor impairs mitochondrial biogenesis and energy metabolism during rapid atrial pacing-induced atrial fibrillation. *J Cardiovasc Pharmacol Ther.* (2016) 21:114–26. doi: 10.1177/1074248415590440

Conflict of Interest: The authors declare that the research was conducted in the absence of any commercial or financial relationships that could be construed as a potential conflict of interest.

Publisher's Note: All claims expressed in this article are solely those of the authors and do not necessarily represent those of their affiliated organizations, or those of the publisher, the editors and the reviewers. Any product that may be evaluated in this article, or claim that may be made by its manufacturer, is not guaranteed or endorsed by the publisher.

frontiers in Cardiovascular Medicine

ORIGINAL RESEARCH
published: 28 March 2022
doi: 10.3389/fcvm.2022.828478

Diabetes Mellitus Is an Independent Risk Factor for a Stiff Left Atrial Physiology After Catheter Ablation for Atrial Fibrillation

Moon-Hyun Kim, Hee Tae Yu†, Yoon Jung Park, Tae-Hoon Kim, Boyoung Joung, Moon-Hyoung Lee and Hui-Nam Pak†*

Division of Cardiology, Department of Internal Medicine, Yonsei University Health System, Seoul, South Korea

OPEN ACCESS

Edited by:
Tetsuo Sasano, Tokyo Medical and Dental University, Japan

Reviewed by:
Huimin Chu, Ningbo First Hospital, China
Myung-Jin Cha, University of Ulsan, South Korea
Junbeom Park, Ewha Womans Medical Center, South Korea

***Correspondence:**
Hee Tae Yu
heetyu@yuhs.ac

†*These authors share senior authorship*

Specialty section:
This article was submitted to Cardiac Rhythmology, a section of the journal Frontiers in Cardiovascular Medicine

Received: *03 December 2021*
Accepted: *07 March 2022*
Published: *28 March 2022*

Citation:
Kim M-H, Yu HT, Park YJ, Kim T-H, Joung B, Lee M-H and Pak H-N (2022) Diabetes Mellitus Is an Independent Risk Factor for a Stiff Left Atrial Physiology After Catheter Ablation for Atrial Fibrillation. Front. Cardiovasc. Med. 9:828478. doi: 10.3389/fcvm.2022.828478

Background: Scar tissue formation after catheter ablation for atrial fibrillation (AF) may adversely affect the diastolic properties of the left atrium (LA), which can result in a stiff LA physiology in a small proportion of patients. In this study, we aimed to explore the relationship between diabetes mellitus and a stiff LA physiology after AF catheter ablation (AFCA).

Methods: A total of 1,326 patients who underwent de novo AFCA, and baseline and 1-year follow-up echocardiographies were enrolled. After 1:3 propensity score (PS) matching for age, sex, and AF type, we compared 211 patients with DM with 633 patients without DM. A stiff LA physiology was defined as estimated pulmonary arterial pressure increase of >10 mmHg and a right ventricular systolic pressure of >35 mmHg at 1-year follow-up echocardiography. Pulmonary vascular resistance (PVR) was estimated using echocardiographic parameters.

Results: Among the 844 PS-matched patients, a stiff LA physiology was observed in 32 patients (4.1%). The patients with DM showed a higher peak LA pressure ($p < 0.001$) and greater LA wall stress ($p = 0.001$) than did those without. A stiff LA physiology was independently associated with DM [Odds ratio (OR) = 2.39, 95% confidence interval (CI) 1.02-5.59, $p = 0.045$], empirical extra-pulmonary vein LA ablation (OR = 3.14, 95% CI 1.07–9.3, $p = 0.038$) and the ΔPVR (OR = 1.78, 95% CI 1.37–2.31, $p < 0.001$). The ΔPVR was independently associated with DM (β = 0.37, 95% CI 0.06-0.67, $p = 0.020$) and a stiff LA physiology (β = 1.40, 95% CI 0.70–2.10, $p < 0.001$). During the 38.8 ± 29.3months follow-up, the incidence of the clinical recurrence of AF was significantly higher in the patients with a stiff LA physiology than in those without (log rank $p = 0.032$).

Conclusion: A stiff LA physiology was independently associated with DM because of the relatively small decrease in the PVR after AFCA in this population. The patients with a stiff LA physiology had worse rhythm outcomes after AFCA than those without.

Keywords: diabetes mellitus, atrial fibrillation, catheter ablation, pulmonary vascular resistance, stiff left atrium

INTRODUCTION

Atrial fibrillation (AF) is a prevalent arrhythmia that increases morbidity and socioeconomic burden worldwide (1). Currently, AF catheter ablation (AFCA) is an effective rhythm control method for patients with AF (1). Various clinical benefits of AFCA have been reported, including reduced mortality in patients with heart failure (2), reduced risk of stroke and improvements in cognitive function (3).

However, AFCA is a destructive procedure that uses heating or freezing as an energy source (4) and inevitably leads to atrial tissue damage, resulting in necrosis, and scarring. Previous studies have reported that AFCA, particularly extra-pulmonary vein (PV) left atrium (LA) ablation, increases LA stiffness, and worsens post-ablation diastolic function. Repeated catheter ablation has also been reported to increase LA pressure and stiffness compared with the de novo procedure (5). Patients with a higher LA pressure or stiffness or greater wall stress had a higher recurrence rate after AFCA (6). Stiff LA syndrome was first reported as symptomatic pulmonary arterial hypertension caused by a decreased LA function after mitral valve surgery (7). Recently, it has been reported that stiff LA syndrome may develop after extensive AFCA (8). In previous studies, diabetes mellitus (DM) was reported as independent risk factors for stiff LA syndrome (9). To date, there is limited knowledge on the mechanism of stiff LA syndrome after AFCA, and the relationship between stiff LA syndrome and metabolic causes, such as DM, is unknown.

In this study, we applied the term "stiff LA physiology" and used previously reported echocardiographic parameters to define this condition (10). One-year follow-up parameters were used to investigate the incidence and clinical features of a stiff LA physiology in patients who underwent AFCA. The purpose of this study was to explore the association between DM and a stiff LA physiology. We also attempted to elucidate the mechanism of a stiff LA physiology using pulmonary vascular resistance (PVR) derived from echocardiographic findings (11).

MATERIALS AND METHODS

Study Population

The study protocol adhered to the principles of the Declaration of Helsinki and was approved by the institutional review board of the Yonsei University Health System. All patients provided written informed consent for inclusion in the Yonsei AF Ablation Cohort Database. Among 3,777 patients who underwent de novo AFCA in the Yonsei AF Ablation Cohort from September 2009 to October 2020, 1,326 patients who underwent voltage substrate mapping, baseline echocardiography, and 1-year follow-up echocardiography were enrolled in the study. DM was defined as HbA1c $\geq$ 6.5% or taking DM medication before the procedure (12). The study patients were divided into two groups according to the presence of DM via propensity score (PS) matching. After 1:3 PS matching for age, sex, and AF type, we compared 211 patients with DM with 633 patients without DM (**Figure 1**). The exclusion criteria of this study were as follows: (1) permanent AF refractory to electrical cardioversion; (2) AF with rheumatic valvular disease; (3) previous cardiac surgery with concomitant AF surgery or AFCA; (4) unmeasurable voltage map during sinus rhythm owing to frequent re-initiation of AF; and (5) no transthoracic echocardiography at baseline or 1 year later.

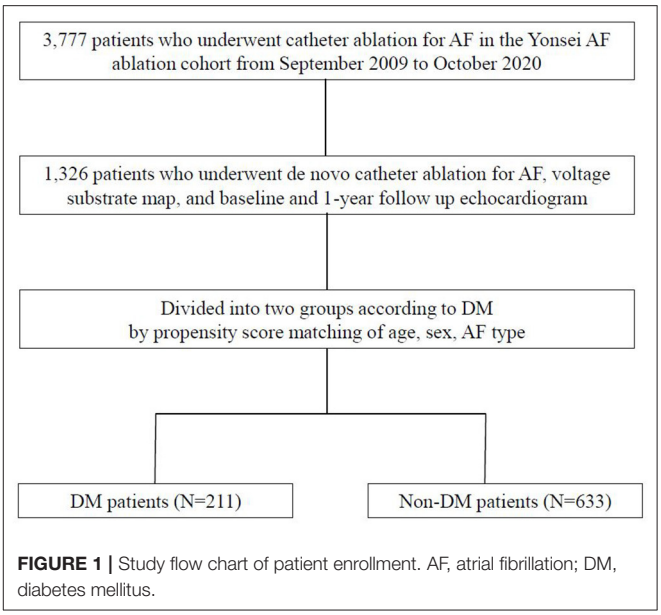

FIGURE 1 | Study flow chart of patient enrollment. AF, atrial fibrillation; DM, diabetes mellitus.

Electrophysiological Mapping and Radiofrequency Catheter Ablation

Three-dimensional (3D) electroanatomical mapping (NavX; St. Jude Medical, Inc., Minnetonka, MN) using a circumferential PV mapping catheter (Lasso; Biosense-Webster Inc., Diamond Bar, CA) through a long sheath (Schwartz left 1; St. Jude Medical, Inc.) was performed. Pulmonary venography was performed after trans-septal punctures using a pigtail catheter. The 3D geometry of both the LA and PV was merged using the NavX system and then generated with 3D spiral computed tomographic (CT) images. Systemic anticoagulation with intravenous heparin was achieved to maintain an activated clotting time of 350-400s during the procedure. An open-irrigated tip catheter (Celsius; Johnson & Johnson Inc., Diamond Bar, CA; NaviStar ThermoCool, Biosense Webster Inc.; ThermoCool SF, Biosense Webster Inc.; ThermoCool SmartTouch, Biosense Webster Inc.; Coolflex, St. Jude Medical, Inc.; 30–35 W; 47°C; FlexAbility, St. Jude Medical, Inc.; and Tacti-Cath, St. Jude Medical, Inc.) was used for AFCA. All patients underwent a de novo procedure involving circumferential PV isolation (CPVI). Most patients (94.8%) received a cavotricuspid isthmus (CTI) block during the procedure unless there was an atrioventricular conduction disease. We conducted an additional linear ablation including a roof line, a posterior inferior line, and an anterior line, especially in the patients with persistent AF. Left lateral isthmus ablation, right atrial ablation, and complex fractionated electrogram ablation were performed in a minority of the patients at the operator's discretion. We defined extra-PV

LA ablation as an additional linear ablation with or without complex fractionated electrogram ablation following CPVI. The procedure ended when there was no immediate recurrence of AF within 10 min after cardioversion with isoproterenol infusion (5–10 mcg/min).

Echocardiographic and Cardiac Computed Tomographic Evaluations

All patients underwent transthoracic echocardiography at baseline and at the 1-year follow-up. The LA diameter, left ventricular (LV) ejection fraction (LVEF), LV mass index (LVMI), peak trans mitral flow velocity (E), and peak septal mitral annular velocity (Em) on tissue Doppler echocardiography were measured in accordance with the American Society of Echocardiography guidelines (13). Retrograde systolic tricuspid flow was obtained from the apical four-chamber view to measure the peak tricuspid pressure drop using continuous-wave Doppler. The LV outflow tract (LVOT) diameter and velocity-time integral (VTI) were measured from the parasternal long axis view and apical three-chamber view using pulsed-wave Doppler. PVR was estimated using the following equation: PVR = pulmonary arterial mean pressure (PAMP) echo–pulmonary capillary wedge pressure (PCWP)/cardiac output (CO) echo (11). PAMP echo was calculated as follows: Pulmonary arterial systolic pressure (PASP) echo × 0.61 + 2 mmHg. PCWP echo was calculated as follows: 1.24 × E/Em + 1.9 mmHg (14). Stroke volume (SV) and CO echo were estimated at the LVOT as follows: SV = (LVOT diameter/2)^2 × LVOT VTI and CO echo = SV × heart rate, respectively (15). These parameters were defined as the PVR-related parameters. The delta value was calculated as follows: delta (Δ) = value at the 1-year follow-up echocardiography–value at the baseline echocardiography.

Three-dimensional spiral CT (64 Channel, Light Speed Volume CT, Philips, Brilliance 63; Amsterdam, the Netherlands) was performed to define the PV anatomy. The 3D spiral CT images of the LA were analyzed using an image processing workstation (Aquarius; TeraRecon, Inc., Foster City, CA).

LA Pressure, LA Wall Thickness, and LAW Stress Measurement

Intracardiac electrograms and hemodynamic measurements were recorded using the Prucka Cardio Lab electrophysiology system (General Electric Medical Systems, Inc., Milwaukee, WI). For catheter access to the LA, a trans-septal puncture approach was used. During AFCA, the LA pressure was measured during sinus rhythm after the trans-septal puncture using a 6-F pigtail catheter (A&A Medical Device, Inc., Gyeonggi-do, Republic of Korea) that was inserted into the LA through a long sheath (Schwartz left 1; St. Jude Medical, Inc.). When the initial rhythm was AF, we measured the LA pressure during sinus rhythm after terminating the AF via internal cardioversion (2–10 J biphasic shocks, Lifepak12; Physiocontrol, Ltd., Redmond, WA), followed by a 3-min waiting period to allow for recovery from atrial stunning from cardioversion (5, 16). We analyzed the peak LA pressure (LAPpeak; v wave), LA nadir pressure (LAPnadir; x wave), and LA mean pressure (LAPmean). These parameters have been defined and calculated in our previous study (17).

We developed a customized software (AMBER, Laonmed Inc., Seoul, Republic of Korea) that measured the LAW thickness by applying Laplace's equation to the cardiac CT images. The LAW thickness was calculated as a numerical streamline connecting the endocardium and epicardium using the Euler method after solving the vector field with Laplace's equation, the partial differential equation in the 3D space (18). Thereafter, the mean LAW thickness was used as a parameter to calculate the LAW-stress. LAW-stress (dyn/cm^2) was calculated using the law of Laplace [s = (P × r)/2 h (s, wall stress; P, pressure; r, radius; h, wall thickness)] (19). The peak LA pressure during sinus rhythm was directly measured during AF, and the LA radius was defined as half of the LA anteroposterior (AP) diameter on transthoracic echocardiography. Therefore, LAW-stress was calculated using the following equation: LAW-stress = (peak LA pressure × LA AP diameter)/(4 × LAW thickness). It was expressed in dyn/cm^2 (1 mmHg = 1,333 dyn/cm^2).

Post-ablation Management and Follow-Up

The patients were instructed to visit the outpatient clinic at 1, 3, 6, and 12 months and then every 6 months thereafter or whenever symptoms occurred after RFCA. Electrocardiography was performed at every visit. Twenty-four-hour Holter monitoring was performed at 3, 6, and 12 months and every 6 months thereafter according to the 2012 Heart Rhythm Society/European Heart Rhythm Association/European Cardiac Arrhythmia Society Expert consensus statement guidelines (20). The patients who experienced symptoms of palpitations underwent Holter/event-monitor examinations to investigate the possibility of arrhythmia recurrence. AF recurrence was defined as any episode of atrial tachycardia (AT) or AF lasting for more than 30s. All electrocardiographic documentations of AF recurrence after a 3-month blanking period were classified as clinical recurrence.

Statistical Analysis

Continuous variables were expressed as means ± standard deviations and compared using Student's *t*-test. Categorical variables were reported as counts (percentages) and compared using the chi-square or Fisher's exact test. Logistic regression analysis was used to investigate the variables related to a stiff LA physiology and DM. Linear regression analysis was used to investigate the variables related to the ΔPVR. The variables with *p*-values of <0.05 in the univariate analysis were selected for the multivariate analysis. Kaplan–Meier analysis with the log-rank test was used to analyze the probability of freedom from AF/AT recurrence after AFCA. Statistical significance was set at *p*-values of <0.05. The Statistical Package for the Social Sciences version 25.0 for Windows (IBM Corp., Armonk, NY) and R software version 3.6.2 (The R Foundation for Statistical Computing, Vienna, Austria) were used for the data analysis.

TABLE 1 | Baseline characteristics according to the presence of DM.

	Before propensity score matching (N = 1,326)			After propensity score matching (N = 844)		
	DM (N = 211)	Non-DM (N = 1,115)	P-value	DM (N = 211)	Non-DM (N = 633)	P-value
Clinical variables						
Age, years	64.2 ± 8.8	58.8 ± 10.8	<0.001	64.2 ± 8.8	64.1 ± 8.7	0.911
Paroxysmal AF, %	121 (57.3)	722 (64.6)	0.051	121 (57.3)	374 (59.1)	0.687
Male, %	147 (69.7)	762 (68.2)	0.687	147 (69.7)	435 (68.7)	0.864
Body mass index, kg/m^2	25.4 ± 3.0	24.8 ± 3.0	<0.001	25.4 ± 3.0	24.8 ± 2.8	<0.001
CHA_2DS_2VASc score	3.5 ± 1.6	1.6 ± 1.4	0.003	3.5 ± 1.6	2.0 ± 1.5	0.013
Congestive heart failure, %	28 (13.3)	169 (15.1)	0.528	28 (13.3)	96 (15.2)	0.575
Hypertension, %	161 (76.3)	471 (42.1)	<0.001	161 (76.3)	320 (50.6)	<0.001
Stroke, %	39 (18.5)	141 (12.6)	0.028	39 (18.5)	90 (14.2)	0.151
Vascular disease, %	56 (26.5)	114 (10.2)	<0.001	56 (26.5)	89 (14.1)	<0.001
3D computed tomography						
LA volume/BSA, mL/m^2	87.1 ± 24.5	87.9 ± 31.1	0.688	87.1 ± 24.5	90.2 ± 24.9	0.125
Pericardial fat volume, mL	125.9 ± 55.7	110.3 ± 53.9	<0.001	125.9 ± 55.7	116.5 ± 54.3	0.035
Catheter ablation						
Ablation time, sec	4991.2 ± 1510.8	4910.2 ± 1645.2	0.508	4991.2 ± 1510.8	4979.8 ± 1632.0	0.929
Fluoroscopic time, min	37.9 ± 13.7	37.7 ± 14.5	0.843	37.9 ± 13.7	36.6 ± 13.6	0.231
Procedure time, min	185.9 ± 46.3	184.8 ± 49.7	0.774	185.9 ± 46.3	185.7 ± 49.5	0.970
Pulmonary vein ablation, %	211 (100.0)	1,118 (100.0)	–	211 (100.0)	633 (100.0)	–
Extra PV LA ablation, %	86 (41.0)	448 (40.1)	0.818	86 (41.0)	241 (38.1)	0.513
CTI, %	199 (94.8)	1,067 (95.6)	0.587	199 (94.8)	615 (97.2)	0.124
LA related parameter						
LA pressure, peak, mmHg	24.9 ± 10.5	22.1 ± 9.6	<0.001	24.9 ± 10.5	21.9 ± 9.5	<0.001
LA voltage	1.4 ± 0.7	1.3 ± 0.7	0.023	1.4 ± 0.7	1.4 ± 0.7	0.797
LA wall thickness	1.9 ± 0.4	2.0 ± 0.3	0.466	1.9 ± 0.4	2.0 ± 0.3	0.074
LA wall stress	193.6 ± 111.5	164.1 ± 95.2	0.001	193.6 ± 111.5	162.0 ± 94.3	0.001

Data are presented as mean ± SD for continuous variables and as proportions for categorical variables. DM, diabetes mellitus; AF, atrial fibrillation; LA, left atrium; BSA, body surface area; CTI, cavo-tricuspid isthmus; PV, pulmonary vein.

RESULTS

Clinical Characteristics of the Patients With DM and a Stiff LA Physiology

1,326 patients were included for analysis and 211 patients were diagnosed with DM (15.9%). The baseline characteristics according to the presence of DM before and after PS matching are shown in **Table 1**. A total of 844 patients (male: 69.0%) PS-matched for age, sex, and AF type had an average age of 64.0 ± 8.7 years, and 58.6% had paroxysmal AF. The patients with DM had more comorbidities, such as hypertension ($p < 0.001$) and vascular disease ($p < 0.001$) than those without DM. The patients with DM showed a higher LA pressure and greater peak ($p < 0.001$) and LAW stress ($p = 0.001$) than did those without. There was no significant difference in performance of extra-PV LA ablation or CTI ablation between the two groups (**Table 1**). Among the 844 patients, a stiff LA physiology was observed in 32 patients (4.1%). The prevalence of DM was higher in the patients with a stiff LA physiology than in those without ($p = 0.037$). The peak LA pressure ($p = 0.010$) and LAW stress ($p = 0.024$) were also higher in the patients with a stiff LA physiology than in those without (**Supplementary Table 1**).

Echocardiographic Characteristics in the Patients With a Stiff LA Physiology and DM

The echocardiographic characteristics according to the presence of a stiff LA physiology are shown in **Table 2**. There was no significant different in the parameters at baseline. At 1-year follow-up echocardiography, the patients with a stiff LA physiology after AFCA showed a larger LA diameter ($p = 0.001$) and higher E/Em ($p = 0.001$) and LVMI ($p = 0.001$) than did those without. Like the echocardiographic findings, there was no significant difference in the PVR-related parameters at baseline. However, at 1-year follow-up, the PAMP ($p < 0.001$) and PCWP ($p = 0.001$) were higher in the patients with a stiff LA physiology than in those without. Moreover, the patients with a stiff LA physiology showed a higher ΔPVR ($p < 0.001$) than did those without (**Figure 2A**).

The echocardiographic characteristics according to the presence of DM are presented in **Supplementary Tables 3**, **4**. While there was no significant difference in the LA diameter, the LVEF, right ventricular systolic pressure (RVSP), and E/Em ($p < 0.001$) were significantly higher in the patients with DM than in those without a baseline. The ΔPVR was also significantly

TABLE 2 | Echocardiographic characteristics according to the presence of a stiff LA physiology.

	Baseline			1-year follow up			Delta value		
	Stiff LA physiology (*N* = 32)	**No stiff LA physiology (*N* = 812)**	***p*-value**	**Stiff LA physiology (*N* = 32)**	**No stiff LA physiology (*N* = 812)**	***p*-value**	**Stiff LA physiology (*N* = 32)**	**No stiff LA physiology (*N* = 812)**	***p*-value**
Echocardiographic findings									
LA diameter, mm	43.5 ± 5.5	42.3 ± 6.0	0.263	42.7 ± 5.1	39.1 ± 5.7	0.001	−0.8 ± 4.5	−3.2 ± 4.7	0.005
LVEF, %	63.1 ± 7.6	62.7 ± 8.6	0.837	66.0 ± 10.7	64.8 ± 7.5	0.368	3.0 ± 7.1	2.0 ± 7.8	0.510
E/Em	12.2 ± 4.6	10.9 ± 4.4	0.085	17.7 ± 10.1	11.2 ± 4.7	0.001	5.3 ± 7.4	0.3 ± 3.9	0.001
RVSP, mmHg	27.8 ± 7.2	27.2 ± 6.9	0.639	44.8 ± 8.4	26.0 ± 6.0	<0.001	17.0 ± 4.3	−0.3 ± 17.6	<0.001
LVMI, g/m^2	98.7 ± 18.2	96.5 ± 23.3	0.619	109.0 ± 23.8	96.1 ± 21.6	0.001	8.0 ± 21.9	−0.3 ± 17.6	0.013
PVR related parameter									
Stroke volume	53.1 ± 17.2	57.8 ± 19.7	0.187	68.7 ± 23.3	61.9 ± 17.6	0.114	15.5 ± 14.5	4.1 ± 21.4	<0.001
Heart rate, bpm	69.3 ± 16.5	66.7 ± 13.0	0.431	67.2 ± 17.7	71.5 ± 10.5	0.243	−0.9 ± 14.1	5.4 ± 13.3	0.079
Cardiac output	3.7 ± 1.2	3.9 ± 1.5	0.562	4.3 ± 1.4	4.4 ± 1.2	0.624	0.9 ± 1.3	0.5 ± 1.5	0.369
PAMP, mmHg	19.0 ± 4.4	18.6 ± 4.2	0.639	29.3 ± 5.1	17.8 ± 3.6	<0.001	10.4 ± 2.6	−0.8 ± 3.9	<0.001
PCWP, mmHg	17.1 ± 5.7	15.4 ± 5.4	0.085	23.9 ± 12.5	15.8 ± 5.8	0.001	6.6 ± 9.2	0.3 ± 4.8	0.001
PVR	0.5 ± 1.5	0.9 ± 1.7	0.303	1.7 ± 3.4	0.4 ± 1.5	0.604	1.1 ± 1.3	−0.5 ± 1.7	<0.001

Data are presented as mean ± SD for continuous variables. LA, left atrium; LVEF, left ventricular ejection fraction; E/Em, the ratio of the early diastolic mitral inflow velocity (E) to the early diastolic mitral annular velocity (Em); RVSP, right ventricular systolic pressure; LVMI, left ventricular mass index; PVR, pulmonary vascular resistance; PAMP, pulmonary artery mean pressure; PCWP, pulmonary capillary wedge pressure.

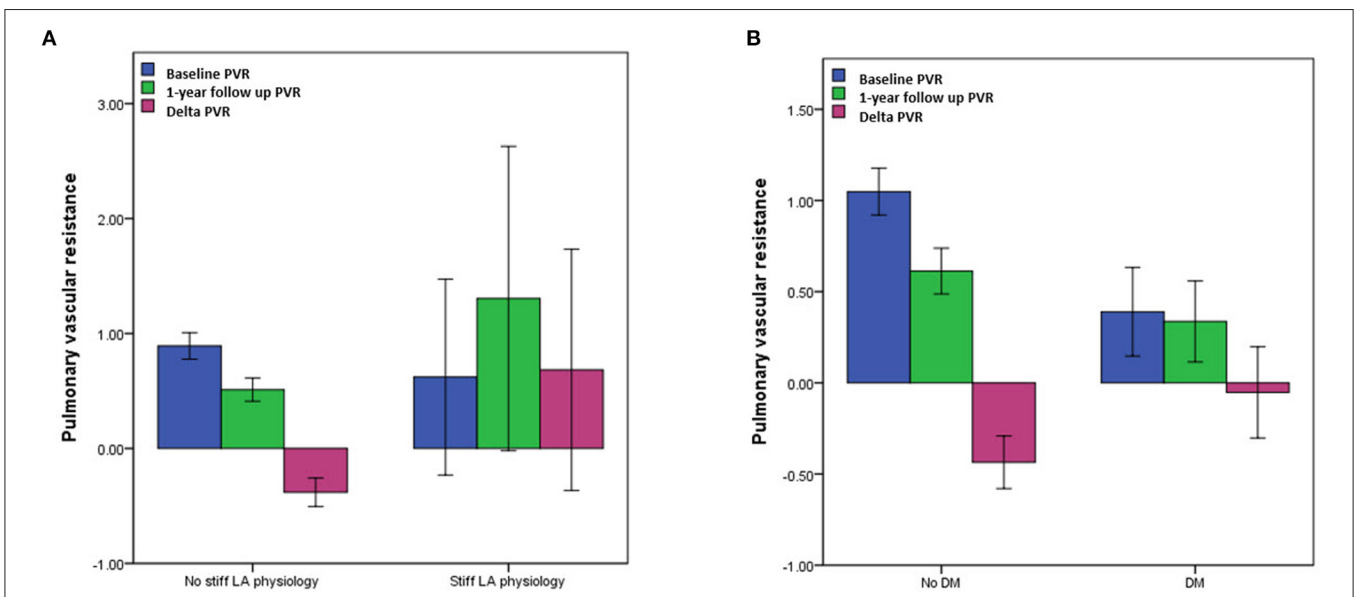

FIGURE 2 | Comparisons of pulmonary vascular resistance (PVR) **(A)** according to the presence of a stiff LA physiology and **(B)** DM. PVR, pulmonary vascular resistance; LA, left atrium; DM, diabetes mellitus.

higher in the patients with DM than in those without ($p = 0.012$) (**Figure 2B**).

Association of a Stiff LA Physiology With DM and the ΔPVR

We investigated the association between a stiff LA physiology and DM using multivariate logistic regression analysis and linear regression analysis. In the adjusted model, a stiff LA physiology was independently associated with DM [OR = 2.39 (1.02–5.59), $p = 0.045$], the pericardial fat volume [OR = 1.01 (1.00–1.02), $p = 0.004$], empirical extra-PV LA ablation [OR = 3.14 (1.07–9.3), $p = 0.038$], and the ΔPVR [OR = 1.78 (1.37–2.31), $p < 0.001$]. We analyzed two multivariate models separately because the 1-year follow-up PVR and ΔPVR had multicollinearity. A stiff LA physiology was also associated with the 1-year follow-up PVR [OR = 1.69 (1.25–2.28), $p = 0.001$] (**Table 3**). To evaluate the contribution of diabetes to stiff LA physiology, an additional multivariate logistic analysis excluding patients of extra PV LA

TABLE 3 | Logistic regression analysis of the stiff LA physiology in the patients.

	Univariate analysis		Multivariate analysis		Multivariate analysis	
	OR (95% CI)	***P*-value**	**OR (95% CI)**	***P*-value**	**OR (95% CI)**	***P*-value**
Age	1.042 (0.999–1.088)	0.058				
Male	0.854 (0.406–1.798)	0.678				
Paroxysmal AF	0.355 (0.169–0.746)	0.006	1.088 (0.378–3.134)	0.876	0.881 (0.302–2.575)	0.817
Body mass index	1.052 (0.935–1.183)	0.397				
Diabetes mellitus	2.122 (1.029–4.374)	0.042	2.935 (1.278–6.742)	0.011	2.386 (1.019–5.587)	0.045
Hypertension	0.969 (0.475–1.975)	0.931				
Congestive heart failure	2.000 (0.877–4.559)	0.099				
Stroke	0.563 (0.169–1.877)	0.350				
Vascular disease	1.945 (0.881–4.296)	0.100				
LA diameter	1.034 (0.975–1.095)	0.263				
LVEF	1.004 (0.963–1.047)	0.837				
E/Em	1.059 (0.992–1.130)	0.087				
LA volume/BSA	1.013 (0.999–1.026)	0.060				
Pericardial fat volume	1.008 (1.002–1.014)	0.007	1.010 (1.003–1.017)	0.006	1.011 (1.003–1.018)	0.004
LA pressure, peak*	1.061 (1.027–1.097)	<0.001				
LA voltage*	0.389 (0.205–0.738)	0.004				
LA wall stress*	1.004 (1.001–1.007)	0.005	1.002 (0.999–1.006)	0.153	1.003 (0.999–1.006)	0.144
Extra PV LA ablation	2.731 (1.316–5.664)	0.007	3.494 (1.190–10.259)	0.023	3.144 (1.067–9.262)	0.038
Extra PV trigger	0.318 (0.043–2.377)	0.264				
Baseline PVR	0.939 (0.757–1.164)	0.564				
1-year follow up PVR	1.395 (1.117–1.742)	0.003	1.689 (1.251–2.281)	0.001		
Delta PVR	1.141 (1.176–1.767)	<0.001			1.782 (1.372–2.314)	<0.001

**LA wall stress was included in the multivariate analysis due to multicollinearity among three variables. Two multivariate models were separately presented because 1-year follow up PVR and delta PVR had a multicollinearity to each other. LA, left atrium; AF, atrial fibrillation; LVEF, left ventricular ejection fraction; E/Em, the ratio of the early diastolic mitral inflow velocity (E) to the early diastolic mitral annular velocity (Em); BSA, body surface area; PV, pulmonary vein; PVR, pulmonary vascular resistance.*

ablation group was performed. As a result, in this subgroup, stiff LA physiology also showed an independent association with 1-year follow-up PVR or ΔPVR (**Supplementary Table 5**). The multivariate linear regression analysis revealed that the ΔPVR was independently associated with DM [β = 0.37 (0.06–0.67), $p = 0.020$], the peak LA pressure [β = −0.02 (-0.03–0.00), $p = 0.034$], and a stiff LA physiology [β = 1.40 (0.70–2.10), $p < 0.001$] in the adjusted model (**Table 4**). The multivariate logistic regression analysis revealed that DM was independently associated with hypertension [OR = 2.25 (1.47–3.43), $p < 0.001$], vascular disease [OR = 1.78 (1.10–2.90), $p = 0.020$], and the ΔPVR [OR = 1.03 (1.01–1.05), $p = 0.001$] in the adjusted model (**Supplementary Table 6**).

Clinical Recurrence of AF After RFCA and a Stiff LA Physiology

During the 38.8 ± 29.3 month follow-up, the incidence of the clinical recurrence of AF was significantly higher in the patients with a stiff LA physiology than in those without (log rank $p = 0.032$) (**Figure 3A**, **Supplementary Table 7**). There was no difference in this incidence between the patients with and without DM (log rank $p = 0.364$) (**Figure 3B**).

DISCUSSION

Our study investigated the association between a stiff LA physiology after AFCA and DM using echocardiographic estimated PVR. We found that a stiff LA physiology was independently associated with DM, the ΔPVR, and empirical extra-PV LA ablation after adjustment for age, sex, and AF type. Compared with the patients without DM, a relatively small decrease in the PVR was observed in the patients with DM after AFCA, which may explain the mechanistic association between DM and a stiff LA physiology. Although the incidence of a stiff LA physiology was low, the clinical recurrence of AF after AFCA was associated with the presence of a stiff LA physiology in our study population.

Stiff LA Physiology After AFCA

Stiff LA syndrome was first described in a patient who developed pulmonary artery hypertension with dyspnea after mitral valve replacement (7). Recently, the concept of stiff LA syndrome has recently been applied to patients who have undergone AFCA. The main clinical findings are dyspnea, congestive heart failure, pulmonary hypertension, and large v waves recorded on PCWP or LA pressure tracings in the absence of marked mitral regurgitation (21). Operators tend to create more ablation

TABLE 4 | Linear regression analysis of the ΔPVR in the patients.

	Univariate analysis		Multivariate analysis	
	B (95% CI)	***P*-value**	**B (95% CI)**	***P*-value**
Age	−0.010 (−0.025–0.004)	0.158		
Male	0.061 (−0.211–0.333)	0.660		
Paroxysmal AF	−0.047 (−0.302–0.207)	0.715		
Body mass index	0.023 (−0.020–0.067)	0.294		
Diabetes mellitus	0.383 (0.096–0.671)	0.009	0.365 (0.057–0.673)	0.020
Hypertension	0.069 (−0.185–0.323)	0.594		
Congestive heart failure	−0.162 (−0.533–0.210)	0.394		
Stroke	0.014 (−0.341–0.369)	0.937		
Vascular disease	−0.036 (−0.366–0.293)	0.829		
LA diameter	−0.017 (−0.038–0.004)	0.122		
LVEF	0.008 (−0.007–0.023)	0.287		
LA volume/BSA	−0.006 (−0.011–0.000)	0.034	−0.005 (−0.011–0.000)	0.057
Pericardial fat volume	0.000 (−0.002–0.003)	0.742		
LA pressure, peak	−0.016 (−0.030–−0.003)	0.018	−0.015 (−0.029–−0.001)	0.034
LA voltage	0.049 (−0.139–0.237)	0.609		
LA wall stress	−0.001 (−0.003–0.000)	0.097		
Stiff LA physiology	1.065 (0.427–1.702)	0.001	1.402 (0.701–2.103)	<0.001
Extra PV LA ablation	0.076 (−0.183–0.335)	0.564		
Extra PV trigger	−0.060 (−0.488–0.367)	0.781		

PVR, pulmonary vascular resistance; AF, atrial fibrillation; LA, left atrium; LVEF, left ventricular ejection fraction; BSA, body surface area; PV, pulmonary vein.

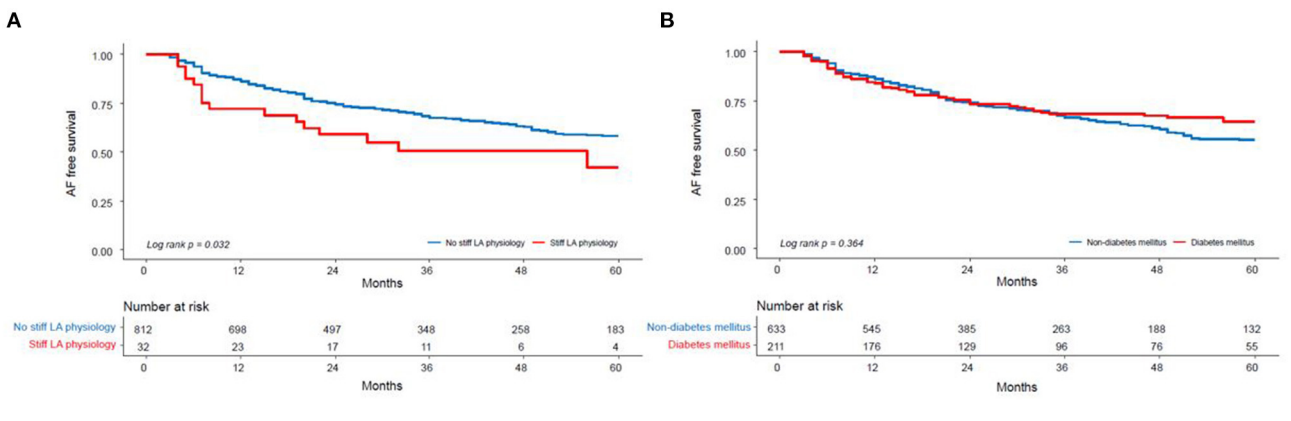

FIGURE 3 | Kaplan–Meier analysis of the clinical recurrence of AF after AFCA **(A)** according to the presence of a stiff LA physiology and **(B)** DM. LA, left atrium; DM, diabetes mellitus.

lesions to reduce the AF recurrence, but extensive ablation lesions usually result in more scar formation in the LA. Moreover, recent clinical trials have revealed no additional benefit of linear ablation or electrogram-guided ablation compared with a CPVI alone (22). In our recent study, extra-PV LA ablation markedly increased the LA pressure and worsened the diastolic function more than CPVI alone; however, there was no difference in the symptoms (5). In addition, we recently conducted a study on a stiff LA physiology defined using the RVSP. Similar to previous findings, DM, a low mean LA voltage, and extra-PV LA ablation were identified as risk factors (4).

Association Between a Stiff LA Physiology and DM

In this study, patients who developed a stiff LA physiology showed an increased PVR after AFCA. There were no differences in the echocardiographic findings or PVR-related parameters at baseline. Among the patients with a stiff LA physiology, the SV increased, while the heart rate decreased after the procedure. There was no difference found in the CO between the two groups. Conversely, the PAMP and PCWP significantly increased in the patients with a stiff LA physiology. In particular, the increase in the PAMP was greater than that in the PCWP,

which resulted in an increase in the PVR. Generally, the LA chamber is characterized by high compliance. It serves an atrial mechanical function through atrial contraction and as a reservoir by maintaining a low LA pressure during atrial relaxation and filling periods (23). Atrial contraction represents a wave in the LA pressure. Subsequent atrial relaxation shows a drop in the x wave, indicating early atrial filling in the PV, followed by an increase in the LA pressure and simultaneous LV contraction. As ventricular contraction continues, the RV also contracts, and the SV enters the LA through the pulmonary circulation and creates a v wave with passive filling (24). In a stiff LA physiology, LA compliance is reduced by atrial scarring and late systole is pronounced, which increases the v wave and PCWP. This can lead to pulmonary vascular remodeling, RV dysfunction, and increased pulmonary artery pressure. Previous studies have reported elevations in the E/Em reflecting diastolic dysfunction in patients with a stiff LA physiology (5). LV diastolic dysfunction increases the pulmonary artery pressure and RVSP and is attributed to a stiff LA physiology.

We found that a stiff LA physiology was independently associated with DM and the ΔPVR, and found an association between DM and the ΔPVR. In the comparison between the patients with and without DM, both groups showed a decrease in PVR after the procedure; however, the decrease in the PVR was smaller in the patients with DM. Regardless of DM, all patients showed a decrease in PVR after AFCA. Among the factors involved in estimated PVR, CO increased, PAMP decreased, and PCWP increased after AFCA. CO is affected by SV and HR, and as previously reported that HR increases in sinus rhythm after AFCA (25). Some studies showed that CO increases after AFCA (26). In addition, we previously reported an observation of increased LA pressure after AFCA (5). For the reasons described above, in the current analysis, it appears that the estimated PVR decreased after the procedure. However, the baseline PVR was significantly lower in the patients with DM, which resulted in a smaller ΔPVR. The reason why the baseline PVR was smaller in the patients with DM is that diastolic dysfunction occurs frequently among them, which increases the E/Em and PCWP (27). DM can lead to LA remodeling due to LA subendocardial fibrosis, oxidative stress, inflammation, and increased renin-angiotensin-aldosterone system activity as well as LV diastolic dysfunction (28). LA remodeling can increase the PCWP and decrease the PVR. Another study found that DM and hyperglycemia decreased pulmonary artery compliance and increased the RV afterload and RV remodeling in patients with pulmonary artery hypertension (29).

Study Limitations

This study had several limitations. First, this was a single-center, observational, retrospective cohort study. Herein, we included highly selective patients who underwent de novo AFCA at a tertiary hospital. The change in the PVI technique was not clearly reflected as it had a long recruitment period of 11 years. Second, the definition of stiff LA syndrome included the patient's symptoms; however, we could not obtain data on the symptoms and thereby used the concept of a stiff LA "physiology" rather than "syndrome." We defined a stiff LA physiology using the RVSP on echocardiography. In previous studies, LA stiffness was evaluated using the peak LA pressure, large v wave pressure, and LA pulse pressure (5, 9, 10). Since there is no gold standard method, LA stiffness was defined using several methods, and the relevant results of each study may be different. Thus, generalization of the results should be considered carefully. Third, the PVR was estimated using the echocardiographic findings. Patients without adequate pre- and post-procedural echocardiographic data were excluded. Potential confounding factors, such as age, comorbidities, medication, heart rate, and rhythm, may also play a role in post-procedural echocardiography. Fourth, we measured the LA pressure during sinus rhythm after cardioversion in the patients with early AF rhythm status. We waited for at least 3 min for the LA pressure to stabilize; however, it was difficult to rule out an effect on the LA after shock. Fifth, since we identified DM before the procedure, data regarding mean blood glucose levels, DM control, and period after diagnosis of DM were not available in this study. Further studies on DM control status including medication use, mean glucose level and stiff LA physiology will be needed. Despite the above limitations, we sought to evaluate the association of DM and a stiff LA physiology after AFCA in the current analysis, and by raising awareness of stiff LA physiology especially in diabetic populations, clinicians can have more attention to treatment options and prognosis for these patients.

CONCLUSION

A stiff LA physiology was independently associated with DM because of the relatively small decrease in the PVR after AFCA in this population. The patients with a stiff LA physiology had worse rhythm outcomes after AFCA than in those without.

DATA AVAILABILITY STATEMENT

The original contributions presented in the study are included in the article/**Supplementary Material**, further inquiries can be directed to the corresponding author.

ETHICS STATEMENT

The studies involving human participants were reviewed and approved by the Institutional Review Board of the Yonsei University Health System. The patients/participants provided their written informed consent to participate in this study. Written informed consent was obtained from the individual(s) for the publication of any potentially identifiable images or data included in this article.

AUTHOR CONTRIBUTIONS

M-HK contributed to the conception and design of the work, interpretation of data, and drafting of the manuscript. HY and H-NP contributed to the conception and design of the work and critical revision of the manuscript. YP, T-HK, BJ, and M-HL contributed to the conception and design of the work and

revision of the manuscript. All authors read and approved the manuscript before its submission.

FUNDING

This work was supported by grants [HI21C0011] from the Ministry of Health and Welfare and a grant [NRF-2020R1A2B5B01001695] from the Basic Science Research Program run by the National Research Foundation of Korea, which is funded by the Ministry of Science, ICT & Future Planning. This study was also supported by a Severance Hospital Research fund for Clinical excellence (SHRC) (C-2021-0019) and a new faculty research seed money grant of Yonsei University College of Medicine for 2021 (2021-32-0043).

SUPPLEMENTARY MATERIAL

The Supplementary Material for this article can be found online at: https://www.frontiersin.org/articles/10.3389/fcvm.2022.828478/full#supplementary-material

REFERENCES

1. Hindricks G, Potpara T, Dagres N, Arbelo E, Bax JJ, Blomstrom-Lundqvist C, et al. 2020 ESC Guidelines for the diagnosis and management of atrial fibrillation developed in collaboration with the European Association for Cardio-Thoracic Surgery (EACTS): the task force for the diagnosis and management of atrial fibrillation of the European society of cardiology (ESC) developed with the special contribution of the European heart rhythm association (EHRA) of the ESC. *Eur Heart J.* (2021) 42:373–498. doi: 10.1093/eurheartj/ehaa612
2. Marrouche NF, Brachmann J, Andresen D, Siebels J, Boersma L, Jordaens L, et al. Catheter ablation for atrial fibrillation with heart failure. *N Engl J Med.* (2018) 378:417–27. doi: 10.1056/NEJMoa1707855
3. Bunch TJ, Crandall BG, Weiss JP, May HT, Bair TL, Osborn JS, et al. Patients treated with catheter ablation for atrial fibrillation have long-term rates of death, stroke, and dementia similar to patients without atrial fibrillation. *J Cardiovasc Electrophysiol.* (2011) 22:839–45. doi: 10.1111/j.1540-8167.2011.02035.x
4. Lee JH, Kwon OS, Yu HT, Kim TH, Uhm JS, Joung B, et al. Risk factors for stiff left atrial physiology 1 year after catheter ablation of atrial fibrillation. *Front Physiol.* (2021) 12:740600. doi: 10.3389/fphys.2021.740600
5. Park JW, Yu HT, Kim TH, Uhm JS, Joung B, Lee MH, et al. Atrial fibrillation catheter ablation increases the left atrial pressure. *Circ Arrhythm Electrophysiol.* (2019) 12:e007073. doi: 10.1161/CIRCEP.118.007073
6. Linhart M, Lewalter T, Mittmann-Braun EL, Karbach NC, Andrie RP, Hammerstingl C, et al. Left atrial pressure as predictor for recurrence of atrial fibrillation after pulmonary vein isolation. *J Interv Card Electrophysiol.* (2013) 38:107–14. doi: 10.1007/s10840-013-9803-9
7. Pilote L, Marpole D, Sniderman A. Stiff left atrial syndrome. *Can J Cardiol.* (1988) 4:255–7.
8. Packer M. Effect of catheter ablation on pre-existing abnormalities of left atrial systolic, diastolic, and neurohormonal functions in patients with chronic heart failure and atrial fibrillation. *Eur Heart J.* (2019) 40:1873–9. doi: 10.1093/eurheartj/ehz284
9. Gibson DN, Di Biase L, Mohanty P, Patel JD, Bai R, Sanchez J, et al. Stiff left atrial syndrome after catheter ablation for atrial fibrillation: clinical characterization, prevalence, and predictors. *Heart Rhythm.* (2011) 8:1364–71. doi: 10.1016/j.hrthm.2011.02.026
10. Witt CM, Fenstad ER, Cha YM, Kane GC, Kushwaha SS, Hodge DO, et al. Increase in pulmonary arterial pressure after atrial fibrillation ablation: incidence and associated findings. *J Interv Card Electrophysiol.* (2014) 40:47–52. doi: 10.1007/s10840-014-9875-1
11. Lindqvist P, Soderberg S, Gonzalez MC, Tossavainen E, Henein MY. Echocardiography based estimation of pulmonary vascular resistance in patients with pulmonary hypertension: a simultaneous doppler echocardiography and cardiac catheterization study. *Eur J Echocardiogr.* (2011) 12:961–6. doi: 10.1093/ejechocard/jer222
12. American Diabetes A. 2. Classification and diagnosis of diabetes: standards of medical care in diabetes-2019. *Diabetes Care.* (2019) 42:S13–28. doi: 10.2337/dc19-S002
13. Mitchell C, Rahko PS, Blauwet LA, Canaday B, Finstuen JA, Foster MC, et al. Guidelines for Performing a comprehensive transthoracic echocardiographic examination in adults: recommendations from the American society of echocardiography. *J Am Soc Echocardiogr.* (2019) 32:1–64. doi: 10.1016/j.echo.2018.06.004
14. Nagueh SF, Middleton KJ, Kopelen HA, Zoghbi WA, Quiñones MA. Doppler tissue imaging: a noninvasive technique for evaluation of left ventricular relaxation and estimation of filling pressures. *J Am Coll Cardiol.* (1997) 30:1527–33. doi: 10.1016/S0735-1097(97)00344-6
15. Blanco P. Rationale for using the velocity-time integral and the minute distance for assessing the stroke volume and cardiac output in point-of-care settings. *Ultrasound J.* (2020) 12:21. doi: 10.1186/s13089-020-00170-x
16. Park J, Joung B, Uhm JS, Young Shim C, Hwang C, Hyoung Lee M, et al. High left atrial pressures are associated with advanced electroanatomical remodeling of left atrium and independent predictors for clinical recurrence of atrial fibrillation after catheter ablation. *Heart Rhythm.* (2014) 11:953–60. doi: 10.1016/j.hrthm.2014.03.009
17. Park J, Yang PS, Kim TH, Uhm JS, Kim JY, Joung B, et al. Low left atrial compliance contributes to the clinical recurrence of atrial fibrillation after catheter ablation in patients with structurally and functionally normal heart. *PLoS ONE.* (2015) 10:e0143853. doi: 10.1371/journal.pone.0143853
18. Kwon O-S, Lee J, Lim S, Park J-W, Han H-J, Yang S-H, et al. Accuracy and clinical feasibility of 3D-myocardial thickness map measured by cardiac computed tomogram. *Int J Arrhyth.* (2020) 21:12. doi: 10.1186/s42444-020-00020-w
19. Wang W, Buehler D, Martland AM, Feng XD, Wang YJ. Left atrial wall tension directly affects the restoration of sinus rhythm after Maze procedure. *Eur J Cardiothorac Surg.* (2011) 40:77–82. doi: 10.1016/j.ejcts.2010.10.022
20. Calkins H, Kuck KH, Cappato R, Brugada J, Camm AJ, Chen SA, et al. 2012 HRS/EHRA/ECAS Expert Consensus Statement on Catheter and Surgical Ablation of Atrial Fibrillation: recommendations for patient selection, procedural techniques, patient management and follow-up, definitions, endpoints, and research trial design. *Europace.* (2012) 14:528–606. doi: 10.1093/europace/eus027
21. Yang Y, Liu Q, Wu Z, Li X, Xiao Y, Tu T, et al. Stiff left atrial syndrome: a complication undergoing radiofrequency catheter ablation for atrial fibrillation. *J Cardiovasc Electrophysiol.* (2016) 27:884–9. doi: 10.1111/jce.12966
22. Verma A, Jiang CY, Betts TR, Chen J, Deisenhofer I, Mantovan R, et al. Approaches to catheter ablation for persistent atrial fibrillation. *N Engl J Med.* (2015) 372:1812–22. doi: 10.1056/NEJMoa1408288
23. Yoon YE, Kim HJ, Kim SA, Kim SH, Park JH, Park KH, et al. Left atrial mechanical function and stiffness in patients with paroxysmal atrial fibrillation. *J Cardiovasc Ultrasound.* (2012) 20:140–5. doi: 10.4250/jcu.2012.20.3.140
24. Reddy YNV, El Sabbagh A, Packer D, Nishimura RA. Evaluation of shortness of breath after atrial fibrillation ablation-Is there a stiff left atrium? *Heart Rhythm.* (2018) 15:930–5. doi: 10.1016/j.hrthm.2018.01.029
25. Yu HT, Kim TH, Uhm JS, Kim JY, Joung B, Lee MH, et al. Prognosis of high sinus heart rate after catheter ablation for atrial fibrillation. *Europace.* (2017) 19:1132–9. doi: 10.1093/europace/euw142
26. Schmidt M, Daccarett M, Brachmann J. Atrial fibrillation ablation in systolic heart failure patients: a promising tool? *Europace.* (2010) 12:1–2. doi: 10.1093/europace/eup397

27. Kadappu KK, Boyd A, Eshoo S, Haluska B, Yeo AE, Marwick TH, et al. Changes in left atrial volume in diabetes mellitus: more than diastolic dysfunction? *Eur Heart J Cardiovasc Imaging.* (2012) 13:1016–23. doi: 10.1093/ehjci/jes084
28. Tadic M, Cuspidi C. The influence of type 2 diabetes on left atrial remodeling. *Clin Cardiol.* (2015) 38:48–55. doi: 10.1002/clc.22334
29. Whitaker ME, Nair V, Sinari S, Dherange PA, Natarajan B, Trutter L, et al. Diabetes Mellitus associates with increased right ventricular afterload and remodeling in pulmonary arterial hypertension. *Am J Med.* (2018) 131:702. doi: 10.1016/j.amjmed.2017.12.046

Conflict of Interest: The authors declare that the research was conducted in the absence of any commercial or financial relationships that could be construed as a potential conflict of interest.

frontiers | Frontiers in Cardiovascular Medicine

ORIGINAL RESEARCH
published: 10 May 2022
doi: 10.3389/fcvm.2022.837725

DNA Methylation-Based Prediction of Post-operative Atrial Fibrillation

Matthew A. Fischer[1], Aman Mahajan[2], Maximilian Cabaj[1], Todd H. Kimball[1], Marco Morselli[3], Elizabeth Soehalim[1], Douglas J. Chapski[1], Dennis Montoya[3], Colin P. Farrell[3], Jennifer Scovotti[1], Claudia T. Bueno[1], Naomi A. Mimila[1], Richard J. Shemin[4], David Elashoff[5,6], Matteo Pellegrini[3], Emma Monte[1] and Thomas M. Vondriska[1,5,7]*

[1] Department of Anesthesiology and Perioperative Medicine, David Geffen School of Medicine at UCLA, Los Angeles, CA, United States, [2] Department of Anesthesiology and Perioperative Medicine, University of Pittsburgh, Pittsburgh, PA, United States, [3] Department of Molecular, Cellular and Developmental Biology, University of California, Los Angeles, Los Angeles, CA, United States, [4] Division of Cardiac Surgery, Department of Surgery, University of California, Los Angeles, Los Angeles, CA, United States, [5] Department of Medicine, University of California, Los Angeles, Los Angeles, CA, United States, [6] Department of Biostatistics, University of California, Los Angeles, Los Angeles, CA, United States, [7] Department of Physiology, University of California, Los Angeles, Los Angeles, CA, United States

OPEN ACCESS

Edited by:
Yafei Li,
Army Medical University, China

Reviewed by:
Mark E. Pepin,
Heidelberg University Hospital, Germany
Francesco Ravaioli,
University of Bologna, Italy
Adam R. Wende,
University of Alabama at Birmingham, United States
Yoga Yuniadi,
National Cardiovascular Center Harapan Kita, Indonesia
Alina Scridon,
George Emil Palade University of Medicine, Pharmacy, Sciences and Technology of Târgu Mureş, Romania
Onne Ronda,
KU Leuven, Belgium

***Correspondence:**
Matthew A. Fischer
mfischer@mednet.ucla.edu

Specialty section:
This article was submitted to Cardiac Rhythmology, a section of the journal Frontiers in Cardiovascular Medicine

Received: *17 December 2021*
Accepted: *17 March 2022*
Published: *10 May 2022*

Citation:
Fischer MA, Mahajan A, Cabaj M, Kimball TH, Morselli M, Soehalim E, Chapski DJ, Montoya D, Farrell CP, Scovotti J, Bueno CT, Mimila NA, Shemin RJ, Elashoff D, Pellegrini M, Monte E and Vondriska TM (2022) DNA Methylation-Based Prediction of Post-operative Atrial Fibrillation. Front. Cardiovasc. Med. 9:837725. doi: 10.3389/fcvm.2022.837725

Background: Atrial fibrillation (AF) is the most common sustained cardiac arrhythmia and post-operative atrial fibrillation (POAF) is a major healthcare burden, contributing to an increased risk of stroke, kidney failure, heart attack and death. Genetic studies have identified associations with AF, but no molecular diagnostic exists to predict POAF based on pre-operative measurements. Such a tool would be of great value for perioperative planning to improve patient care and reduce healthcare costs. In this pilot study of epigenetic precision medicine in the perioperative period, we carried out bisulfite sequencing to measure DNA methylation status in blood collected from patients prior to cardiac surgery to identify biosignatures of POAF.

Methods: We enrolled 221 patients undergoing cardiac surgery in this prospective observational study. DNA methylation measurements were obtained from blood samples drawn from awake patients prior to surgery. After controlling for clinical and methylation covariates, we analyzed DNA methylation loci in the discovery cohort of 110 patients for association with POAF. We also constructed predictive models for POAF using clinical and DNA methylation data. We subsequently performed targeted analyses of a separate cohort of 101 cardiac surgical patients to measure the methylation status solely of significant methylation loci in the discovery cohort.

Results: A total of 47 patients in the discovery cohort (42.7%) and 43 patients in the validation cohort (42.6%) developed POAF. We identified 12 CpGs that were statistically significant in the discovery cohort after correcting for multiple hypothesis testing. Of these sites, 6 were amenable to targeted bisulfite sequencing and chr16:24640902 was statistically significant in the validation cohort. In addition, the methylation POAF prediction model had an AUC of 0.79 in the validation cohort.

Conclusions: We have identified DNA methylation biomarkers that can predict future occurrence of POAF associated with cardiac surgery. This research demonstrates the

use of precision medicine to develop models combining epigenomic and clinical data to predict disease.

Keywords: post-operative atrial fibrillation (POAF), epigenomics, DNA methylation, cardiac surgery, precision medicine

INTRODUCTION

Atrial fibrillation (AF), the most common sustained cardiac arrhythmia, is characterized by rapid, irregular atrial depolarizations that lead to an increased risk of clot formation and subsequent stroke (1). Long-term risks of myocardial ischemia, heart failure and dementia are elevated in patients with AF (2–6). Clinical management of AF involves a combination of pharmacological interventions (such as calcium channel blockers) and interventional techniques (such as radiofrequency ablation) to dampen or eliminate the substrates for arrhythmogenic activity (7).

AF is a frequent arrhythmia after cardiac surgery on cardiopulmonary bypass. Approximately 30–40% of cardiac surgeries are complicated by post-operative atrial fibrillation (POAF), which is associated with greater hospital resource utilization, longer ICU and hospital stays and hence greater healthcare costs (8–10). POAF also significantly elevates the risk for more serious long-term cardiovascular complications including myocardial infarction, cardiac arrest, bleeding, renal failure, stroke and death. For coronary artery bypass grafting (CABG) surgery alone, the Society of Thoracic Surgeons database recorded 161,816 procedures in the United States in 2019, plus thousands more procedures in which mitral or aortic valve replacements were performed alone or concomitant with CABG (11).

DNA methylation frequently occurs on cytosines followed by guanine (CpGs) and has been shown to correlate with gene expression in development and disease (12). DNA methylation has been implicated in diseases such as cancer (13), and recent studies have implicated altered global DNA methylation in cardiovascular disease (14–18). Because it has been shown in the Framingham cohort that DNA methylation in peripheral blood samples is associated with AF in the outpatient setting (19), we sought to find CpGs associated with POAF, a clinically distinct manifestation of AF, after cardiac surgery. It would be useful for mechanistic studies to determine the association of these DNA methylation loci with altered gene expression in left atrial tissue; however, it is not possible to obtain left atrial tissue samples from all patients undergoing cardiac surgical procedures without a separate biopsy of the left atrium, an undue risk to patients who otherwise would not have an incision on the left atrium. In this study, we enroll patients undergoing a variety of cardiac surgical procedures (**Supplementary Table 1**) because these are the patients we care for in the operating room and for which we would like to develop perioperative epigenetic assessment of POAF risk. Thus, we sought to assess the association of DNA methylation in peripheral blood samples with POAF.

While the genetic contribution to AF has been well studied (20), including identification of sequence variation associated with POAF (21), the epigenetic contribution through DNA methylation remains under-explored and represents an appealing target for biomarker discovery based on the following rationale: DNA methylation is relatively stable but not immutable (it can be modified throughout life and thus may serve as a molecular beacon of modifiable risk), and some features of DNA methylation are conserved across tissue types while still exerting cell type specific effects (14, 22, 23). For example, in one study (14) a subset of DNA methylation loci associated with dilated cardiomyopathy in left ventricular myocardial tissue also displayed conserved methylation associated with dilated cardiomyopathy across other tissues, including peripheral blood samples. In the present study, we sought to identify pre-operative epigenomic biomarkers that could be deployed in a precision medicine context to predict a specific and prevalent post-operative complication. We report herein two prediction models combining pre-operative clinical variables and DNA methylation marks that predict POAF in cardiac surgery patients.

MATERIALS AND METHODS

Patient Selection

After institutional review board approval and written informed consent, adult patients scheduled for elective cardiac and aortic surgery on cardiopulmonary bypass were enrolled in this prospective study at the Ronald Reagan Medical Center at the University of California, Los Angeles (UCLA). We chose to enroll patients undergoing a variety of cardiac surgical procedures because this reflects the patient population we care for and for which we would like to implement DNA methylation-based prediction of adverse post-operative outcomes. The cardiac surgical procedures examined in this study are presented in **Supplementary Table 1**. Patients were enrolled consecutively. A detailed questionnaire was performed, which recorded known clinical risk factors for POAF such as age, proposed surgery and history of paroxysmal AF. We excluded patients with any of the following: AF at the time of surgery, pre- or post-operative complete heart block, emergent surgery, a history of congenital heart disease, organ transplantation, systemic inflammatory diseases, endocarditis or having cardiac surgery without cardiopulmonary bypass. These exclusions reflect: (1) clinical scenarios where pre-operative epigenetic profiling would not be possible due to insufficient time before the surgical procedure; (2) patients where manifestation of AF would not be clinically evident; and (3) disease processes that would significantly affect the peripheral leukocyte composition (e.g., endocarditis).

We enrolled 128 patients in the discovery cohort and reduced representation bisulfite sequencing (RRBS) data was obtained from pre-operative whole blood samples from all of

these patients. However, 13 samples were excluded from the discovery cohort analysis based on clinical criteria: 4 patients had permanent AF, 5 patients had perioperative complete heart block, 1 patient died post-operatively, 2 patients had surgery off of cardiopulmonary bypass and 1 patient had endocarditis. Five patients were excluded for poor bisulfite conversion or poor mappability. In the validation cohort, 104 patients were enrolled whose whole blood samples underwent targeted bisulfite sequencing. Three patients were excluded based on clinical criteria: 1 patient had permanent AF, 1 patient had peri-operative complete heart block and 1 patient had surgery off of cardiopulmonary bypass. Several of the clinical exclusions in the discovery and validation cohorts reflect ongoing epigenomic biobanking for analysis of other perioperative complications that are outside the scope of this current study.

Occurrence of Post-operative Atrial Fibrillation

Patients were followed prospectively to assess for occurrence of POAF. POAF is defined herein as any occurrence of AF of at least 30 s duration after completion of surgery until hospital discharge. We defined POAF as a binary event because we would like to identify methylation loci associated with the development of POAF rather than those related to sustained AF of longer duration. Patients in the cardiac intensive care unit had continuous electrocardiogram monitoring with both electronic and clinical diagnosis of AF. In addition, patients transferred out of the ICU are monitored via telemetry until discharge from the hospital. To ensure data validity, the occurrence of POAF was cross-checked with the electronic medical record (EMR) and the Society of Thoracic Surgeons (STS) database, which contains outcome data including occurrence of POAF recorded by the surgical and medical teams prior to discharge.

DNA Methylation Data

Prior to the start of surgery, 6 mL whole blood samples were drawn from an arterial line in awake patients before induction of anesthesia. Blood samples were collected in a Becton Dickinson pink stoppered EDTA containing tube (Franklin Lakes, NJ), which was stored on ice and processed within 1–3 h. An overall schematic of the experimental workflow is shown in **Figure 1**. Genomic DNA was isolated (PureLink Genomic DNA Kit, K1820-01) from whole blood (separately we biobanked buffy coat containing leukocytes and platelets at −80°C), subjected to enzymatic digestion with MspI (NEB, R0106S) and bisulfite converted (EpiTect Fast. DNA Bisulfite Kit, Qiagen, 59824). RRBS library preparation was adapted from previous studies (22, 24) using 200 ng of genomic DNA from each sample. In the discovery cohort, libraries were prepared using Illumina TruSeq kit, size-selected for 330 bp with AMPure XP beads and subjected to 100 bp, single-end sequencing on Illumina HiSeq instruments. BS-Seeker2 (25) was used to align the reads to hg38, allowing for up to 10 mismatches, and methylation was called for CpGs and then processed using MethylKit in R as described in previous publications (22, 24). The RRBS approach measures CpG methylation, expressed as the ratio of methylated sequencing reads to all reads for that CpG. We excluded samples with poor bisulfite conversion or mappability.

For the validation cohort, the DNA methylation status of 12 statistically significant CpGs from the discovery cohort were measured in our validation cohort using targeted bisulfite sequencing. As such, the validation cohort was collected after the discovery cohort was completed and the CpGs of interest were identified after analysis of the discovery cohort. The significant CpGs in the discovery cohort had to be identified before sequencing the validation cohort so that DNA probes could be developed to specifically enrich for those same CpGs in the validation cohort using targeted bisulfite sequencing (26). Targeted bisulfite sequencing is less expensive and achieves a higher read depth for the CpGs of interest compared to whole genome bisulfite sequencing or RRBS. For these reasons, targeted bisulfite sequencing is a more focused implementation within a precision medicine environment. For each patient in the validation cohort, 200 ng samples of genomic DNA underwent library preparation involving unique adaptor ligation and were subsequently pooled to be individually sequenced together. Single stranded DNA was then hybridized with 120 bp biotinylated DNA probes designed and synthesized by Integrated DNA Technologies (Coralville, IA). The primer and probe sequences used for targeted bisulfite sequencing (both for validation of RRBS-derived CpGs and for Framingham Heart Study significant CpGs) are included as a **Supplementary Excel File**. Following biotinylated probe pull down with streptavidin coated magnetic beads, the pooled samples underwent bisulfite conversion, PCR amplification, sequencing and alignment to human reference genome hg38 followed by counting methylated and unmethylated CpGs using BSBolt (27).

Cell Type Deconvolution

To account for the known confounding of cell type composition on DNA methylation analysis (28), we compared a variety of methods for controlling for cell type heterogeneity. Reference-based deconvolution was performed in the discovery cohort using a method described by Orozco et al. (22), which provides cell type composition estimates using DNA methylation sequencing data. In parallel, reference-free deconvolution was performed on whole blood methylation ratio data using RefFreeEWAS (29) and ReFACTor (30) in R. We separately performed parameter optimization for the reference-free methods and determined that both ReFACTor and RefFreeEWAS optimally modeled 4 surrogates for cell type composition in our dataset.

Fluorescence activated cell sorting (FACS) was performed on a subset (n=14) of patients in the discovery cohort for which additional blood samples were available to assess the accuracy of *in silico* cell type estimation. 5 mL of whole blood was drawn from an arterial line prior to induction of anesthesia at the same time as the blood draw for the methylation data. FACS analysis was performed at the UCLA Immunogenetics Clinical Laboratory to determine percent composition of neutrophils, monocytes, B cells, CD4+ T cells, CD8+ T cells, and NK cells.

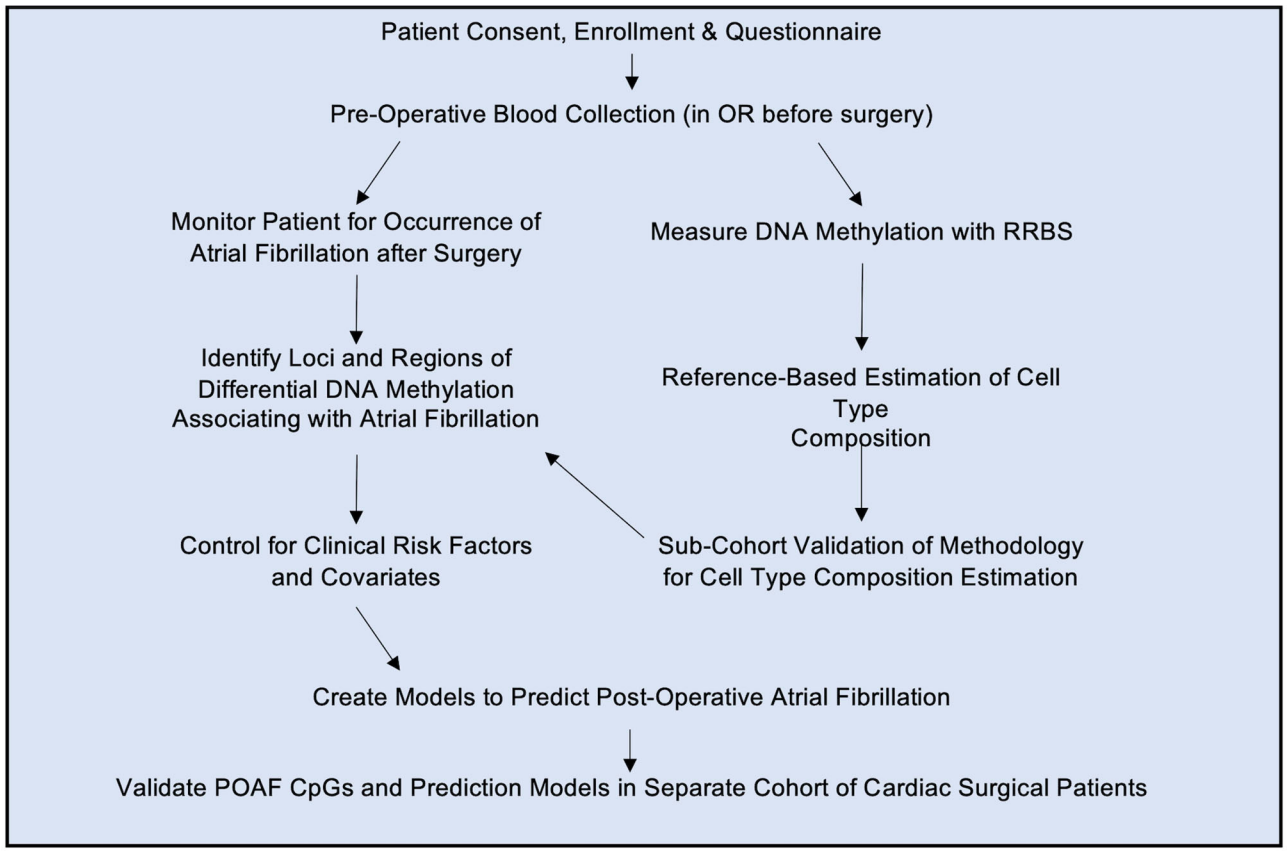

FIGURE 1 | Study Design. Patients giving informed consent were enrolled in the study and a blood sample was drawn in the operating room (OR) prior to surgery. Genomic DNA was isolated from blood and subjected to reduced representation bisulfite sequencing (RRBS). The resulting methylation status was determined as described in the text. Patients were monitored for post-operative atrial fibrillation and differential DNA methylation loci were used to build a model to predict post-operative atrial fibrillation based on pre-operative blood samples. The statistically significant CpGs and predictive model were then analyzed in a separate validation cohort of cardiac surgical patients.

Statistical Analyses

For each sample in the discovery and validation cohorts, we removed from analysis CpGs with $<10\times$ coverage. Additionally, CpGs were removed from the cohort if they were located at SNPs with minor allele frequency >1% in humans (dbSNP build 150 common SNPs: http://hgdownload.cse.ucsc.edu/goldenpath/hg38/database/snp150Common.txt.gz) or not present in at least 50% of the cohort after filtering for coverage.

Using the DSS-general package (31) in R version 4.0.2, beta binomial regression was used to regress bisulfite sequencing count data at the filtered CpGs on POAF status. In this regression analysis, we controlled for established clinical covariates (19, 21, 32) (age, sex, history of paroxysmal AF, body mass index, diabetes, hypertension, congestive heart failure, pulmonary vein isolation, MAZE procedure and cardiopulmonary bypass time) and methylation covariates (19) (smoking status, ethnicity and cell type composition estimates) to identify CpGs meeting a predetermined significance threshold (p-value $< 5 \times 10^{-8}$) for POAF. Patients with more than 2 surgical procedures on cardiopulmonary bypass had a higher incidence of POAF in our cohort so their occurrence was included as a clinical covariate in our analysis. The Manhattan plot in **Figure 2** was generated using the ggmanh (33) package in R. The QQ plot was generated using qqman (34) and gglot2 (35) in R. For the validation cohort, we used DSS-general in R to model differential methylation at CpGs highly significant in our discovery cohort and performed regression analysis to determine the association of each CpG with POAF.

The methylation POAF model was constructed and trained using the percent methylation of 3 of the most significant methylation predictors (chr16:24640902, chr16:33770791, and chr21:44932986) and 3 of the most significant clinical predictors (age, history of paroxysmal AF and more than 1 cardiac surgical procedure) in the discovery cohort. The clinical risk factors for this model were selected by stepwise logistic regression in JMP version 16.0.0 (Cary, NC). The methylation model was trained on the discovery cohort using five-fold cross validation repeated 10 times using the caret package in R. The model was then separately tested on the validation cohort to assess model performance in an independent

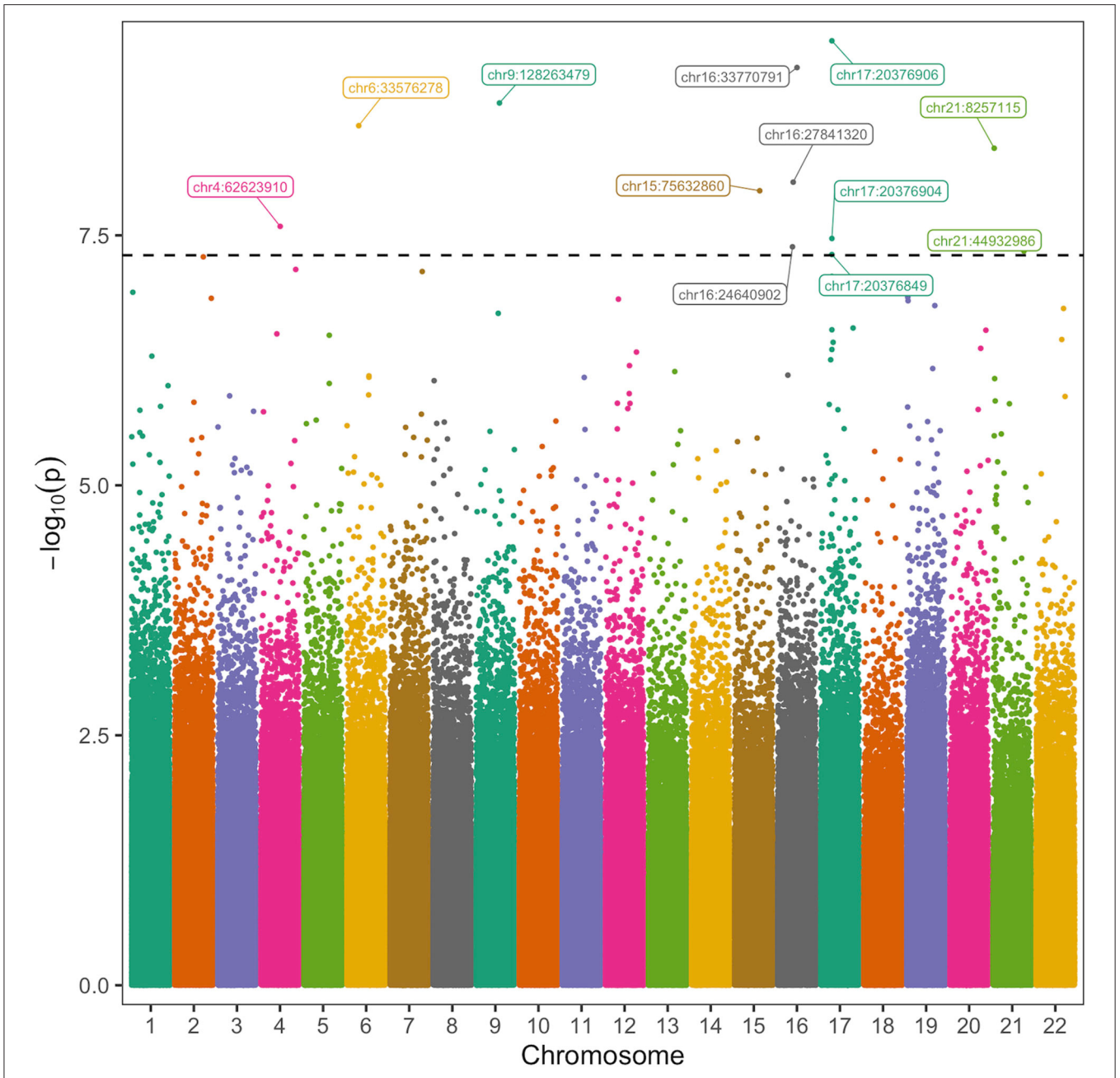

FIGURE 2 | Manhattan Plot of CpGs Associated with Post-operative Atrial Fibrillation. The vertical axis represents the negative log 10 of the *p*-value of each CpG's association with POAF. The horizontal axis represents the chromosome and position of each CpG. Twelve CpGs had significant association with POAF after controlling for known clinical and methylation covariates. The black horizontal dashed line corresponds to a *p*-value of 5×10^{-8}.

set of samples. An additional methylation POAF prediction model was constructed using chr17:20376906, the CpG within the chr17:20376813-20376906 differentially methylated region (DMR) that was most statistically significant in the discovery cohort, and 4 clinical risk factors (age, history of paroxysmal AF, cardiopulmonary bypass time in minutes and more than 1 cardiac surgical procedure) which were chosen using stepwise logistic regression in JMP. Similarly, this additional methylation model was trained on the discovery cohort using five-fold cross validation repeated 10 times using the caret package in R. Determination of the chr17:20376813-20376906 DMR was made using the callDMR function in DSS-general with default parameters.

In a separate analysis, we performed targeted bisulfite sequencing of published significant CpGs associated with outpatient AF in the Framingham cohort (19). We used

the liftOver tool (https://genome.ucsc.edu/cgi-bin/hgLiftOver) to convert hg19 coordinates to hg38 coordinates. We then performed targeted bisulfite sequencing against these loci to determine the methylation status of these CpGs in our validation cohort. We again used DSS-general in R to perform regression analysis to determine the association of each CpG with POAF.

RESULTS

Of the 110 patients analyzed in the discovery cohort, 47 patients developed POAF for an incidence of 42.7%. There were 101 patients analyzed in the validation cohort, 43 of which experienced POAF for a similar incidence of 42.6%. The incidence in both cohorts is similar to other cardiac surgical populations. The characteristics of the 211 patients analyzed in this study are displayed in **Table 1** by cohort. Patients who developed POAF had a longer length of stay with a median difference of an additional 3 days (median of 9 days total vs. 6 days). The difference in length of stay in patients experiencing POAF in all 211 patients was statistically significant (p-value < 0.001) as calculated by the Mann-Whitney U test. The surgical procedures for this patient cohort are displayed in **Supplementary Table 1**. This table shows that patients who had 2 or more surgical procedures (any combination of the following: aortic valve surgery, mitral valve surgery, pulmonic valve surgery, tricuspid valve surgery, CABG surgery, open aortic surgery and myomectomy) on cardiopulmonary bypass had a higher risk of POAF and so this was included as a covariate in our analysis. The racial and ethnic composition of this cohort, another covariate in our analysis, is shown in **Supplementary Table 2**.

Because DNA methylation at some CpGs is cell-type specific, differences in cell type composition is a known source of confounding which can mistakenly attribute differences in cellular composition as biologic differences related to the disease being studied (28). To account for the heterogeneity of cells in human blood, we compared three methods to control for cell type composition, a reference-based method (22) and two reference-free methods [ReFACTor (30) and RefFreeEWAS (29)]. The reference-based method estimates were the most highly correlated with FACS data so therefore we used reference-based estimates of percent cell type composition as covariates in our analysis of the discovery cohort. **Supplementary Table 3** shows the Pearson correlation coefficients between the measured cell type composition and those estimated *in silico* using the reference-based method. The reference-based cell type estimates are statistically significant for neutrophils, monocytes, CD4+ T-cells and NK cells but not B-cells or CD8+ T-cells.

We then analyzed autosomal CpGs in pre-operative blood samples from the discovery cohort for association with POAF while controlling for known clinical and methylation covariates (**Figure 2**). There were 2,557,388 CpGs with 10× coverage in at least 50% of patients in our discovery cohort and an average of 2,151,705 of these CpGs per sample. We identified 12 CpGs with strong association with POAF (**Table 2**). Of these 12 significant CpGs, 7 were within regions of the genome amenable to targeted bisulfite sequencing. CpGs that were not amenable to targeted bisulfite sequencing were within sequences that shared homology with other genomic regions. Six of these CpGs had sequencing data that met sufficient coverage thresholds as defined in the discovery cohort. Of these 6 CpGs, 3 (chr17:20376849, chr17:20376904, and chr17:20376906) are within a differentially methylated region on chromosome 17 and have highly correlated methylation. This DMR, chr17:20376813-20376906, was identified by the callDMR function in DSS using default parameters and contained a total of 12 CpGs in our discovery cohort dataset. In a separate exercise, we used ReFACTor to analyze our data in an unsupervised manner (**Supplementary Table 4**). We performed a beta binomial regression controlling for 4 principal components (as determined

TABLE 1 | Characteristics of patient population.

Characteristic	Discovery		Validation	
	POAF	No POAF	POAF	No POAF
Total Number of Patients	47 (42.7%)	63 (57.3%)	43 (42.6%)	58 (57.4%)
Age, Mean +/– SD	66.8 +/– 8.8	60.1 +/– 15	68.7 +/– 8.6	58.9 +/– 13.3
Female	15 (31.9%)	22 (34.9%)	8 (18.6%)	21 (36.2%)
History of Paroxysmal Atrial Fibrillation	9 (19.1%)	4 (6.3%)	9 (20.9%)	7 (12.1%)
Diabetes Mellitus	12 (25.5%)	16 (25.4%)	14 (32.6%)	18 (31%)
Hypertension	34 (72.3%)	44 (69.8%)	36 (83.7%)	41 (70.7%)
Congestive Heart Failure	18 (38.3%)	14 (22.2%)	15 (34.9%)	16 (27.6%)
Body Mass Index, Mean +/– SD	29.9 +/– 7.5	27.4 +/– 5.2	28.3 +/– 6.5	28.5 +/– 5.9
Current Smoker	2 (4.3%)	6 (9.5%)	1 (2.3%)	1 (1.7%)
Pulmonary Vein Isolation	0 (0%)	2 (3.2%)	1 (2.3%)	1 (1.7%)
MAZE	6 (12.8%)	2 (3.2%)	4 (9.3%)	4 (6.9%)
Two or More Cardiac Surgical Procedures	24 (51.1%)	20 (31.7%)	22 (51.2%)	15 (25.9%)
Cardiopulmonary Bypass Time, Mean +/– SD	156 +/– 56.9	136.7 +/– 52.7	167.7 +/– 64.7	140.7 +/– 60.9

The number and prevalence of clinical risk factors in the discovery and validation cohorts are displayed in this table for patients who experience post-operative atrial fibrillation and for those who do not.

TABLE 2 | CpGs Associated with POAF.

CpG	Methylation	Nearest Gene	Location	Discovery *P*-value	Discovery FDR	Validation *P*-value
chr4:62623910	Hypo	ADGRL3-AS1	Upstream	2.57E-08	8.16E-03	
chr6:33576278	Hyper	BAK1	Intron	2.53E-09	1.61E-03	
chr9:128263479	Hyper	GOLGA2	Intron	1.50E-09	1.27E-03	
chr15:75632860	Hyper	IMP3	Downstream	1.13E-08	4.11E-03	
chr16:24640902	Hyper	TNRC6A	Exon	4.11E-08	1.01E-02	0.026
chr16:27841320	Hyper	GSG1L	Intron	9.28E-09	3.93E-03	
chr16:33770791	Hypo	LOC390705	Upstream	6.63E-10	8.42E-04	0.054
chr17:20376849	Hypo	CCDC144CP	Intron	4.91E-08	1.01E-02	0.226
chr17:20376904	Hypo	CCDC144CP	Intron	3.40E-08	9.59E-03	0.690
chr17:20376906	Hypo	CCDC144CP	Intron	3.58E-10	8.42E-04	0.624
chr21:8257115	Hyper	CBS	Intron	4.25E-09	2.16E-03	
chr21:44932986	Hyper	LINC01547	Exon	4.55E-08	1.01E-02	0.078

Twelve CpGs have p-values $<5 \times 10^{-8}$ in the discovery cohort after controlling for clinical and methylation covariates. The CpG methylation status associated with POAF, nearest gene, CpG location relative to the nearest gene and the statistical significance of these loci in the validation cohort are also listed. The methylation status of six CpGs in the validation cohort were unable to be measured using the targeted bisulfite sequencing approach. One CpG, chr16:24640902, was successfully validated in a separate cohort.

TABLE 3 | Methylation model for post-operative atrial fibrillation.

Model Parameter	Estimate	Standard Error	*P*-value	Odd's Ratio	95% CI
Intercept	−13.363	3.942			
Chr16:24640902, per 10% methylation	10.413	3.415	0.002	2.833	(1.45, 5.53)
Chr16:33770791, per 10% methylation	−4.330	1.952	0.027	0.649	(0.44, 0.95)
Chr21:44932986, per 10% methylation	6.171	2.906	0.034	1.853	(1.05, 3.28)
Age, per 10 years	0.077	0.025	0.002	2.170	(1.33, 3.55)
History of Paroxysmal Atrial Fibrillation	2.636	0.932	0.005	13.953	(2.24, 86.77)
More than 1 Cardiac Surgical Procedure	0.941	0.494	0.057	2.562	(0.97, 6.74)

This model uses 3 CpGs and 3 clinical risk factors to predict POAF. This model was constructed using multivariate regression of pre-operative risk factors to predict post-operative atrial fibrillation. Methylation ratios were used instead of the count data used in the primary analysis. Coefficient estimates, odd's ratios, p-values and 95% CIs reflect the significance of each parameter in the format of this model after five-fold cross validation using only the discovery cohort data. The model was then assessed separately on the independent validation cohort.

by the package's parameter optimization tool) and the clinical risk factors as previously described in our initial analysis. Notably, the most important loci (chr16:24640902 and chr17:20376849-20376906) used in our models are still significant after accounting for these principal components.

Out of the 6 CpGs significant in the discovery cohort that were able to be sequenced in the validation cohort, one, chr16:24640902, was statistically significant in the validation cohort (p-value = 0.026). Chr16:24640902 is within the gene body of TNRC6A, a protein expressed in multiple tissues, including in the left atrium and previously associated with permanent AF (36). The methylation status of chr16:24640902 in patients experiencing POAF and in those that do not is shown in **Supplementary Figure 1**. **Supplementary Table 5** shows the Pearson correlation of CpGs used in the POAF prediction models with cell type estimates calculated *in silico* with the reference-based method for cell type deconvolution. In addition, there is minimal statistical inflation in our analysis with $\lambda = 1.026$ (See QQ plot in **Supplementary Figure 2**).

We created two POAF prediction models using clinical risk factors and methylation data. The methylation POAF model (**Table 3**) was developed using three of the most significant methylation loci and 3 of the most significant clinical risk factors in the discovery cohort. After feature selection in the discovery cohort, the methylation POAF model was trained on discovery cohort data only. The methylation POAF model had an AUC of 0.83 in the discovery cohort and 0.79 in the validation cohort. ROC curves comparing the POAF methylation model performance in the discovery and validation cohorts to published clinical models are shown in **Figure 3**. The AUC of the methylation loci without clinical risk factors was 0.67 in the validation cohort (data not shown). An additional POAF prediction model (**Supplementary Table 6**) uses chr17:20376906, the CpG within the chr17: 20376813-20376906 DMR that was most statistically significant in the discovery cohort, and 4 additional clinical risk factors. This model had an AUC of 0.81 in the discovery cohort and 0.67 in the validation cohort.

We compared the methylation POAF model (**Table 3**) to two clinical risk factor POAF models: the CHA_2DS_2-VASc POAF model (37) and the Vanderbilt Cardiac Surgery Registry clinical-only model (21). CHA_2DS_2-VASc, a tool used to predict the risk of embolic stroke in patients with AF, has been shown to

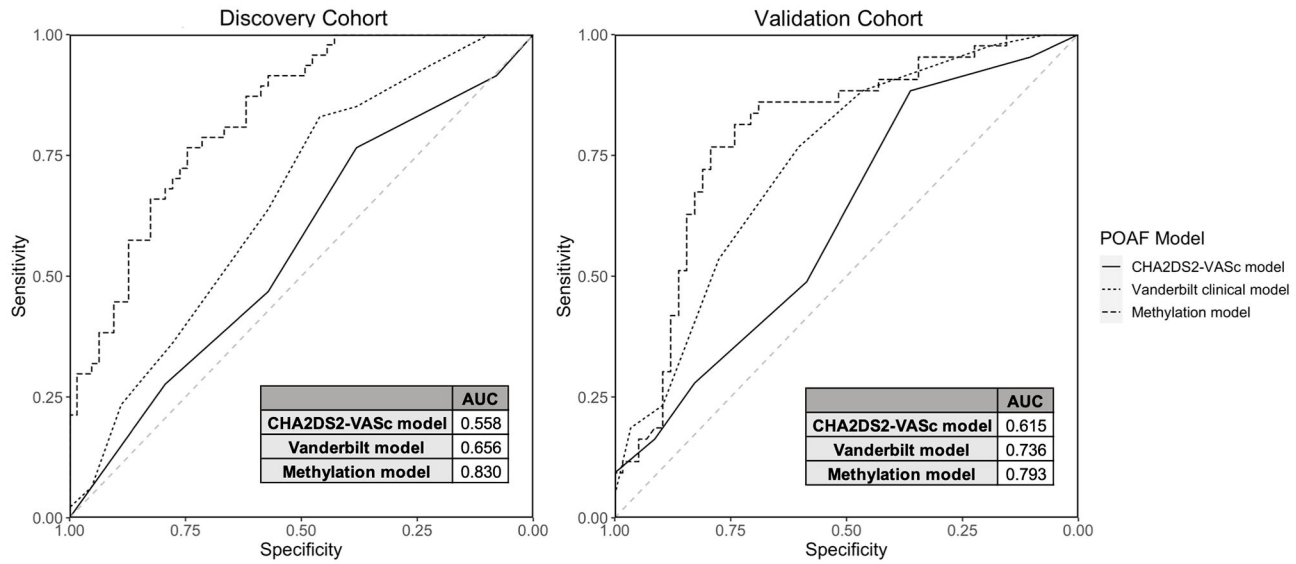

FIGURE 3 | Discovery and Validation Cohort Model Performance. ROC curves and AUCs are shown comparing model performance in the discovery and validation cohorts for the CHA_2DS_2-VASc model, the Vanderbilt Cardiac Surgery Registry clinical-only model and the methylation model (3 CpGs + 3 clinical risk factors).

predict POAF (37) and has a scoring system that is familiar to most clinicians. The Vanderbilt Cardiac Surgery Registry clinical-only model is a validated prediction model that utilizes seven risk factors for POAF prediction. The CHA_2DS_2-VASc model (37) and the Vanderbilt Cardiac Surgery Registry clinical-only model (21) had AUCs of 0.62 and 0.74, respectively, in the validation cohort in our dataset. The methylation POAF model demonstrated a statistically significant improvement in prediction in the validation cohort over the CHA_2DS_2-VASc model with p-value = 0.00535 by DeLong's test. Compared to the Vanderbilt Cardiac Surgery Registry clinical-only model (21), the methylation POAF model showed a statistically significant improvement in the discovery cohort (p-value = 0.00117) but not the validation cohort (p-value = 0.264).

In a separate analysis, we assessed the statistical significance of 21 CpGs previously shown to be associated with AF in the Framingham cohort (**Supplementary Tables 7**, **8**) in our validation cohort. In the validation cohort, the most significant Framingham CpG was cg12739419 (p-value = 0.033) but it was not statistically significant after accounting for multiple hypothesis testing with the Benjamini-Hochberg procedure (38). The CpG cg12739419, which is known to be associated with the AF SNP rs3807989 and the gene CAV1 in the Framingham cohort, demonstrated hypomethylation associated with POAF, consistent with hypomethylation found at this CpG in the Framingham cohort.

DISCUSSION

AF is highly prevalent, ranging from 2.7 to 6.1 million affected individuals in the United States and inflicting a cost of ∼$6 billion per year on the healthcare system (39). As the most common sustained cardiac arrhythmia, AF is associated with increased risk of stroke, thromboembolism, renal failure, and myocardial infarction. Approximately 40% of people diagnosed with AF or heart failure will develop the other condition (39).

POAF in particular exacerbates morbidity and healthcare costs for patients undergoing what are now routine cardiac surgeries in medical centers around the world (8–10). Previous studies have identified genetic (20) and DNA methylation differences (19, 40) that correlate with AF, but no previous work has provided a molecular measurement that can be made in the blood of presurgical patients that will aid prediction of AF prior to its occurrence. The present study provides such information for the setting of POAF, enabling the development of a simple pre-operative blood test that, when combined with common clinical measurements, can guide the physician in managing cardiac surgery patients according to their relative risk. The prospective design of this study is crucial in that it allows for assessment of epigenetic marks as risk factors for future disease—predominantly in patients without a history of AF—rather than sequelae of disease given the dynamic nature of DNA methylation.

We present a methylation POAF model with 3 clinical factors and 3 CpGs that has an AUC of 0.79 in our validation cohort. We compared this novel prediction model to the CHA_2DS_2-VASc POAF model and the Vanderbilt Cardiac Surgery Registry clinical-only model. Though CHA_2DS_2-VASc was developed to determine the risk of embolic stroke in patients with AF, it has been shown to predict POAF (37), is simple to implement and has a scoring system that is familiar to most clinicians. The Vanderbilt Cardiac Surgery Registry clinical-only model is a validated prediction model that utilizes seven risk factors

for POAF prediction (21). The combined clinical and DNA methylation model had higher AUCs than the CHA_2DS_2-VASc model (37) and a leading clinical POAF prediction model (21) which had AUCs of 0.62 and 0.74, respectively, in our validation cohort. The multicenter risk index for atrial fibrillation after cardiac surgery (32) is another important POAF model but was not compared to the methylation model because post-operative risk factors were not a component of the current study.

The methylation POAF model had a statistically significant improvement in prediction over the CHA_2DS_2-VASc model in both the discovery and validation cohorts. The methylation POAF model showed statistically improved prediction compared to the Vanderbilt Cardiac Surgery Registry clinical-only model in the discovery cohort only. This demonstrates that DNA methylation can add predictive value to clinical risk factors, though the extent to which this is possible depends on how well the particular clinical risk factors are represented in the patient population in question. The methylation POAF model's performance in the validation cohort shows clearly improved prediction over the CHA_2DS_2-VASc model, demonstrating an improvement incorporating DNA methylation biomarkers with clinical predictors. Although the goal of this research was to identify DNA methylation biomarkers that would be applicable to patients who present for a variety of elective cardiac surgical procedures, the diversity of cardiac disease within this cohort such as those with different forms of valvular heart disease may limit the application of these models to cardiac surgical populations which may have a relatively higher proportion of isolated coronary artery bypass grafting procedures compared to combined surgical procedures more typical in the University setting.

In this study, we performed targeted bisulfite sequencing of CpGs associated with AF in the Framingham cohort (19). The finding that the Framingham CpGs were not statistically significant in our validation cohort is consistent with the notion that POAF (not measured in the Framingham study) is a clinically distinct manifestation of AF and has risk factors that are unique compared to AF in the outpatient setting (41). In addition, because we utilized RRBS rather than the Infinium HumanMethylation450 BeadChip Array technology used in the Framingham cohort, the sites associated with POAF in this study were not measured in the Framingham cohort dataset and cannot be analyzed to assess their association with AF in the outpatient setting.

The methodology presented in this study could be implemented in a precision medicine environment where an epigenomic risk metric of POAF and other adverse peri-operative outcomes could be determined from a blood draw with other routine pre-operative labs. In particular, epigenomic risk profiles could be of significant value in perioperative risk stratification and planning perioperative care for each patient. Further research is needed to refine prediction models and associations with additional outcomes of interest. The epigenomic profile of each patient could also help assess perioperative risk and guide clinical decision making for patients at risk for POAF and other adverse outcomes. In addition, it could help guide which drugs or treatments patients may respond better to given their own perioperative risks and epigenomic profile. DNA methylation risk loci could also be targeted directly. In a rat model of spontaneous AF, administration of the DNA methylation inhibitor decitabine reduced atrial tachycardia, demonstrating the possibility of targeting DNA methylation for therapeutic effect (42). It will also be informative to evaluate whether these or other epigenomic marks may serve as biomarkers for AF outside of the context of cardiac surgery. With improvements in sequencing technology, patient samples can be pooled to simultaneously undergo targeted bisulfite sequencing for each individual sample at many loci of interest for reduced cost compared to RRBS and whole genome bisulfite sequencing. Targeted bisulfite sequencing costs $25–50 per sample with results available in ∼2 weeks. Targeted bisulfite sequencing would ideally be utilized for patients undergoing surgeries that have a relatively higher risk of adverse outcomes—such as cardiac surgery—and include epigenetic risk factors for multiple adverse outcomes that could be used together for optimal perioperative planning.

Though this is an association study, the prospective study design and utilization of epigenetic risk factors have the potential to identify mechanisms impacting POAF susceptibility with greater granularity than clinical risk factors alone. What are the molecular mechanisms by which the association between DNA methylation and risk of AF is established? DNA methylation in so-called CpG islands is thought to control gene expression by silencing promoters and regulatory regions (43). Gene body methylation, however, is associated with increased transcription (12). The genes nearest to the regions of altered methylation observed in this study (**Table 2**) provide some hints about a potential molecular mechanism acting in cis to regulate the nearest gene. Chr16:24640902, a CpG statistically significant in both the discovery and validation cohorts, is within the gene body of TNRC6A, a protein expressed in many tissues including the left atrium, associated with miRNA-mediated gene silencing (44) and previously associated with permanent AF (36). The significance of micro-RNAs has emerged in the pathophysiology of AF through electrical and structural remodeling (45). The other CpGs in the POAF prediction model have unknown relation to AF. Overall, these sites may reflect molecular mechanisms in the left atrium that create substrates for POAF, which then become activated by the physiologic stress of cardiopulmonary bypass and surgery. Another mechanism by which altered CpG methylation may control gene expression and organ phenotype is through chromatin structure, recently appreciated to be globally remodeled in the setting of heart failure in human cells and animal models (46, 47). Future studies will be required to resolve the molecular mechanisms definitively—however, this study provides a novel set of biomarkers to be explored clinically in larger cohorts for their ability to aid in the prediction of AF, toward the goal of preventing many of the downstream disease sequelae precipitated by this arrhythmia.

DATA AVAILABILITY STATEMENT

The datasets presented in this study can be found in online repositories. The names of the repository/repositories and accession number(s) can be found below: GEO; GSE194156.

ETHICS STATEMENT

The studies involving human participants were reviewed and approved by University of California, Los Angeles. The patients/participants provided their written informed consent to participate in this study.

AUTHOR CONTRIBUTIONS

MF performed bioinformatic, read mapping/alignment and statistical analyses with contributions from DM, DC, and DE. MC, TK, ES, and EM performed experiments including genomic DNA library preparation. MM, CF, and MP performed bisulfite sequencing. JS, NM, and CB obtained patient data. MF and RS recruited patients and performed clinical assessment. MF, AM, and TV conceived of the study which was directed by MF and TV. MF and TV wrote the manuscript. All authors contributed to the article and approved the submitted version.

FUNDING

This project was supported by the UCLA Department of Anesthesiology, the UCLA Cardiovascular Theme and NIH grants UL1TR001881 (UCLA CTSI, PI: Steven Dubinett), HL 105699 (TMV), HL150667 (TMV), HL 115238 (TMV). MF was supported by a Starter Grant from the Society of Cardiovascular Anesthesiologists and a mentored research training grant by the Foundation for Anesthesia Education and Research.

SUPPLEMENTARY MATERIAL

The Supplementary Material for this article can be found online at: https://www.frontiersin.org/articles/10.3389/fcvm.2022.837725/full#supplementary-material

REFERENCES

1. Morin DP, Bernard ML, Madias C, Rogers PA, Thihalolipavan S, Estes NA. The state of the art: atrial fibrillation epidemiology, prevention, and treatment. *Mayo Clin Proc*. (2016) 91:1778–810. doi: 10.1016/j.mayocp.2016.08.022
2. Kalantarian S, Stern TA, Mansour M, Ruskin JN. Cognitive impairment associated with atrial fibrillation: A meta-analysis. *Ann Intern Med*. (2013) 158:338-46. doi: 10.7326/0003-4819-158-5-201303050-00007
3. Lee HY, Yang PS, Kim TH, Uhm JS, Pak HN, Lee MH, et al. Atrial fibrillation and the risk of myocardial infarction: A nation-wide propensity-matched study. *Sci Rep*. (2017) 7:12716. doi: 10.1038/s41598-017-13061-4
4. Owan TE, Hodge DO, Herges RM, Jacobsen SJ, Roger VL, Redfield MM. Trends in prevalence and outcome of heart failure with preserved ejection fraction. *N Engl J Med*. (2006) 355:251-9. doi: 10.1056/NEJMoa052256
5. Bunch TJ. Atrial fibrillation and dementia. *Circulation*. (2020) 142:618–20. doi: 10.1161/circulationaha.120.045866
6. Verma A, Kalman JM, Callans DJ. Treatment of patients with atrial fibrillation and heart failure with reduced ejection fraction. *Circulation*. (2017) 135:1547–63. doi: 10.1161/circulationaha.116.026054
7. Xu J, Luc JG, Phan K. Atrial fibrillation: Review of current treatment strategies. *J Thorac Dis*. (2016) 8:e886–e900. doi: 10.21037/jtd.2016.09.13
8. Greenberg JW, Lancaster TS, Schuessler RB, Melby SJ. Postoperative atrial fibrillation following cardiac surgery: A persistent complication. *Eur J Cardiothorac Surg*. (2017) 52:665–72. doi: 10.1093/ejcts/ezx039
9. D'Agostino RS, Jacobs JP, Badhwar V, Fernandez FG, Paone G, Wormuth DW, et al. The society of thoracic surgeons adult cardiac surgery database: 2018 update on outcomes and quality. *Ann Thorac Surg*. (2018) 105:15–23. doi: 10.1016/j.athoracsur.2017.10.035
10. Ha AC, Mazer CD, Verma S, Yanagawa B, Verma A. Management of postoperative atrial fibrillation after cardiac surgery. *Curr Opin Cardiol*. (2016) 31:183–90. doi: 10.1097/HCO.0000000000000264
11. Bowdish ME, D'Agostino RS, Thourani VH, Schwann TA, Krohn C, Desai N, et al. Sts adult cardiac surgery database: 2021 update on outcomes, quality, and research. *Ann Thorac Surg*. (2021) 111:1770–80. doi: 10.1016/j.athoracsur.2021.03.043
12. Greenberg MVC, Bourc'his D. The diverse roles of dna methylation in mammalian development and disease. *Nat Rev Mol Cell Biol*. (2019) 20:590–607. doi: 10.1038/s41580-019-0159-6
13. Jones PA, Issa JP, Baylin S. Targeting the cancer epigenome for therapy. *Nat Rev Genet*. (2016) 17:630–41. doi: 10.1038/nrg.2016.93
14. Meder B, Haas J, Sedaghat-Hamedani F, Kayvanpour E, Frese K, Lai A, et al. Epigenome-wide association study identifies cardiac gene patterning and a novel class of biomarkers for heart failure. *Circulation*. (2017) 136:1528–44. doi: 10.1161/circulationaha.117.027355
15. Movassagh M, Choy MK, Knowles DA, Cordeddu L, Haider S, Down T, et al. Distinct epigenomic features in end-stage failing human hearts. *Circulation*. (2011) 124:2411–22. doi: 10.1161/CIRCULATIONAHA.111.040071
16. Huan T, Joehanes R, Song C, Peng F, Guo Y, Mendelson M, et al. Genome-wide identification of dna methylation qtls in whole blood highlights pathways for cardiovascular disease. *Nat Commun*. (2019) 10:4267. doi: 10.1038/s41467-019-12228-z
17. Ma J, Rebholz CM, Braun KVE, Reynolds LM, Aslibekyan S, Xia R, et al. Whole blood dna methylation signatures of diet are associated with cardiovascular disease risk factors and all-cause mortality. *Circ Genom Precis Med*. (2020) 13:e002766. doi: 10.1161/circgen.119.002766
18. Agha G, Mendelson MM, Ward-Caviness CK, Joehanes R, Huan T, Gondalia R, et al. Blood leukocyte dna methylation predicts risk of future myocardial infarction and coronary heart disease. *Circulation*. (2019) 140:645–57. doi: 10.1161/circulationaha.118.039357
19. Lin H, Yin X, Xie Z, Lunetta KL, Lubitz SA, Larson MG, et al. Methylome-wide association study of atrial fibrillation in framingham heart study. *Sci Rep*. (2017) 7:40377. doi: 10.1038/srep40377
20. Fatkin D, Santiago CF, Huttner IG, Lubitz SA, Ellinor PT. Genetics of atrial fibrillation: State of the art in 2017. Heart Lung Circ. (2017) 26:894-901. doi: 10.1016/j.hlc.2017.04.008
21. Kolek MJ, Muehlschlegel JD, Bush WS, Parvez B, Murray KT, Stein CM, et al. Genetic and clinical risk prediction model for postoperative atrial fibrillation. *Circ Arrhythm Electrophysiol*. (2015) 8:25–31. doi: 10.1161/circep.114.002300
22. Orozco LD, Farrell C, Hale C, Rubbi L, Rinaldi A, Civelek M, et al. Epigenome-wide association in adipose tissue from the metsim cohort. *Hum Mole Genet*. (2018) 27:2586. doi: 10.1093/hmg/ddy205
23. Orozco LD, Morselli M, Rubbi L, Guo W, Go J, Shi H, et al. Epigenome-wide association of liver methylation patterns and complex metabolic traits in mice. *Cell Metab*. (2015) 21(6):905–17. doi: 10.1016/j.cmet.2015.04.025
24. Chen H, Orozco L, Wang J, Rau CD, Rubbi L, Ren S, et al. DNA methylation indicates susceptibility to isoproterenol-inducd cardiac pathology and is associated with chromatin states. *Circ Res*. (2016) 118:786–97. doi: 10.1161/CIRCRESAHA.115.305298
25. Guo W, Fiziev P, Yan W, Cokus S, Sun X, Zhang MQ, et al. Bs-Seeker2: A versatile aligning pipeline for bisulfite sequencing data. *BMC Genom*. (2013) 14:774. doi: 10.1186/1471-2164-14-774

26. Morselli M, Farrell C, Rubbi L, Fehling HL, Henkhaus R, Pellegrini M. Targeted bisulfite sequencing for biomarker discovery. *Methods*. (2020) 187:13-27. doi: 10.1016/j.ymeth.2020.07.006
27. Farrell C, Thompson M, Tosevska A, Oyetunde A, Pellegrini M. Bisulfite bolt: A bisulfite sequencing analysis platform. *bioRxiv*. (2021). doi: 10.1101/2020.10.06.328559
28. Jaffe AE, Irizarry RA. Accounting for cellular heterogeneity is critical in epigenome-wide association studies. *Genome Biol*. (2014) 15:R31. doi: 10.1186/gb-2014-15-2-r31
29. Houseman EA, Kile ML, Christiani DC, Ince TA, Kelsey KT, Marsit CJ. Reference-free deconvolution of dna methylation data and mediation by cell composition effects. *BMC Bioinform*. (2016) 17:259. doi: 10.1186/s12859-016-1140-4
30. Rahmani E, Zaitlen N, Baran Y, Eng C, Hu D, Galanter J, et al. Sparse pca corrects for cell type heterogeneity in epigenome-wide association studies. *Nat Methods*. (2016) 13:443–5. doi: 10.1038/nmeth.3809
31. Park Y, Wu H. Differential Methylation Analysis For Bs-Seq data under general experimental design. *Bioinformatics*. (2016) 32:1446–53. doi: 10.1093/bioinformatics/btw026
32. Mathew JP, Fontes ML, Tudor IC, Ramsay J, Duke P, Mazer CD, et al. A multicenter risk index for atrial fibrillation after cardiac surgery. *JAMA*. (2004) 291:1720–9. doi: 10.1001/jama.291.14.1720
33. Lee J. Ggmanh: Visualization Tool for Gwas Result. *R package version 0.99.12 ed*. (2022).
34. Turner SD. Qqman: An r package for visualizing gwas results using Q-Q and manhattan plots. *bioRxiv*. (2014). doi: 10.1101/005165
35. Wickham H. *Ggplot2: Elegant Graphics for Data Analysis*. New York, NY: Springer-Verlag (2016).
36. Doñate Puertas R, Jalabert A, Meugnier E, Euthine V, Chevalier P, Rome S. Analysis of the microrna signature in left atrium from patients with valvular heart disease reveals their implications in atrial fibrillation. *PLoS ONE*. (2018) 13:e0196666. doi: 10.1371/journal.pone.0196666
37. Kashani RG, Sareh S, Genovese B, Hershey C, Rezentes C, Shemin R, et al. Predicting postoperative atrial fibrillation using cha2ds2-vasc scores. J Surg Res. (2015) 198:267-72. doi: 10.1016/j.jss.2015.04.047
38. Benjamini Y, Hochberg Y. Controlling the false discovery rate: a practical and powerful approach to multiple testing. *J Royal Statis Soc Ser B*. (1995) 57:289-300.
39. Benjamin EJ, Virani SS, Callaway CW, Chamberlain AM, Chang AR, Cheng S, et al. Heart disease and stroke statistics-2018 update: A report from the american heart association. *Circulation*. (2018) 137:e67–492. doi: 10.1161/CIR.0000000000000558
40. Zhao G, Zhou J, Gao J, Liu Y, Gu S, Zhang X, et al. Genome-wide dna methylation analysis in permanent atrial fibrillation. *Mol Med Rep*. (2017) 16:5505-14. doi: 10.3892/mmr.2017.7221
41. Dobrev D AM, Heijman J, Guichard J, Nattel S. Postoperative atrial fibrillation: Mechanisms, manifestations and management. *Nat Rev Cardiol*. (2019) 16:417-36. doi: 10.1038/s41569-019-0166-5
42. Doñate Puertas R, Meugnier E, Romestaing C, Rey C, Morel E, Lachuer J, et al. Atrial fibrillation is associated with hypermethylation in human left atrium, and treatment with decitabine reduces atrial tachyarrhythmias in spontaneously hypertensive rats. *Transl Res*. (2017) 184:57–67.e5. doi: 10.1016/j.trsl.2017.03.004
43. Jones PA. Functions of DNA methylation: Islands, start sites, gene bodies and beyond. *Nat Rev Genet*. (2012) 13:484–92. doi: 10.1038/nrg3230
44. Nishi K, Nishi A, Nagasawa T, Ui-Tei K. Human Tnrc6a Is an argonaute-navigator protein for microrna-mediated gene silencing in the nucleus. *RNA*. (2013) 19:17–35. doi: 10.1261/rna.034769.112
45. Nattel S, Harada M. Atrial remodeling and atrial fibrillation: Recent advances and translational perspectives. *J Am Coll Cardiol*. (2014) 63:2335–45. doi: 10.1016/j.jacc.2014.02.555
46. Rosa-Garrido M, Chapski DJ, Schmitt AD, Kimball TH, Karbassi E, Monte E, et al. High-resolution mapping of chromatin conformation in cardiac myocytes reveals structural remodeling of the epigenome in heart failure. *Circulation*. (2017) 136:1613–25. doi: 10.1161/CIRCULATIONAHA.117.029430
47. Gilsbach R, Schwaderer M, Preissl S, Grüning BA, Kranzhöfer D, Schneider P, et al. Distinct epigenetic programs regulate cardiac myocyte development and disease in the human heart *in vivo*. *Nat Commun*. (2018) 9:391. doi: 10.1038/s41467-017-02762-z

Conflict of Interest: The authors declare that the research was conducted in the absence of any commercial or financial relationships that could be construed as a potential conflict of interest.

frontiers | Frontiers in Cardiovascular Medicine

ORIGINAL RESEARCH
published: 13 May 2022
doi: 10.3389/fcvm.2022.897709

Development of a Risk Prediction Model for New Episodes of Atrial Fibrillation in Medical-Surgical Critically Ill Patients Using the AmsterdamUMCdb

Sandra Ortega-Martorell[1,2], Mark Pieroni[1,2], Brian W. Johnston[2,3,4], Ivan Olier[1,2] and Ingeborg D. Welters[2,3,4]**

[1] School of Computer Science and Mathematics, Liverpool John Moores University, Liverpool, United Kingdom, [2] Liverpool Centre for Cardiovascular Science, Liverpool, United Kingdom, [3] Institute of Life Course and Medical Sciences, University of Liverpool, Liverpool, United Kingdom, [4] Liverpool University Hospitals NHS Foundation Trust, Liverpool, United Kingdom

OPEN ACCESS

Edited by:
Guowei Li,
Guangdong Second Provincial General Hospital, China

Reviewed by:
Dominique Monlezun,
University of Texas MD Anderson Cancer Center, United States
Bert Vandenberk,
University of Calgary, Canada

***Correspondence:**
Sandra Ortega-Martorell
S.OrtegaMartorell@ljmu.ac.uk
Ingeborg D. Welters
I.Welters@liverpool.ac.uk

Specialty section:
This article was submitted to Cardiac Rhythmology, a section of the journal Frontiers in Cardiovascular Medicine

Received: 16 March 2022
Accepted: 26 April 2022
Published: 13 May 2022

Citation:
Ortega-Martorell S, Pieroni M, Johnston BW, Olier I and Welters ID (2022) Development of a Risk Prediction Model for New Episodes of Atrial Fibrillation in Medical-Surgical Critically Ill Patients Using the AmsterdamUMCdb. Front. Cardiovasc. Med. 9:897709. doi: 10.3389/fcvm.2022.897709

The occurrence of atrial fibrillation (AF) represents clinical deterioration in acutely unwell patients and leads to increased morbidity and mortality. Prediction of the development of AF allows early intervention. Using the AmsterdamUMCdb, clinically relevant variables from patients admitted in sinus rhythm were extracted over the full duration of the ICU stay or until the first recorded AF episode occurred. Multiple logistic regression was performed to identify risk factors for AF. Input variables were automatically selected by a sequential forward search algorithm using cross-validation. We developed three different models: For the overall cohort, for ventilated patients and non-ventilated patients. 16,144 out of 23,106 admissions met the inclusion criteria. 2,374 (12.8%) patients had at least one AF episode during their ICU stay. Univariate analysis revealed that a higher percentage of AF patients were older than 70 years (60% versus 32%) and died in ICU (23.1% versus 7.1%) compared to non-AF patients. Multivariate analysis revealed age to be the dominant risk factor for developing AF with doubling of age leading to a 10-fold increased risk. Our logistic regression models showed excellent performance with AUC.ROC $>$ 0.82 and $>$ 0.91 in ventilated and non-ventilated cohorts, respectively. Increasing age was the dominant risk factor for the development of AF in both ventilated and non-ventilated critically ill patients. In non-ventilated patients, risk for development of AF was significantly higher than in ventilated patients. Further research is warranted to identify the role of ventilatory settings on risk for AF in critical illness and to optimise predictive models.

Keywords: atrial fibrillation, critically ill patients, risk prediction, AmsterdamUMCdb, ICU

INTRODUCTION

Atrial Fibrillation (AF) is the commonest arrhythmia worldwide and increases the risk of stroke and heart failure (1). AF is characterised by irregular atrial electric activity and ventricular response. In the general population diabetes, high blood pressure and coronary artery disease are the main risk factors. AF is also common after major surgery and in patients suffering from acute severe illness, in particular infection (2). Up to 44% of all patients admitted to intensive

care units suffer from incident AF (3–6). Many of these episodes occur in patients without a history of AF. The occurrence of AF in patients admitted with sinus rhythm represents a clinical deterioration in acutely unwell patients and leads to increased morbidity and mortality (7). The onset of AF is often associated with haemodynamic instability and usually requires treatment either with anti-arrhythmic drugs or electric cardioversion to control heart rate and rhythm.

Large repositories of Electronic Health Records have been used to develop risk prediction for AF in the general population using machine learning algorithms. A recent risk prediction model, developed for the general population, the CHARGE-AF (The Cohorts for Heart and Aging Research in Genomic Epidemiology AF) score, predicts an individual's 5-year risk of new AF using clinical variables including age, ethnicity, height, weight, blood pressure, medication and comorbidities (8). Due to the long period covered and the differences in patient population, such models are not suitable for the prediction of AF in acute illness. Previous research on large datasets to explore incidence, risk factors and outcome of AF in acutely unwell patients focused on septic patients and relied on United States databases (9, 10).

In addition, risk factors for developing AF in the general population compared to critically ill patients may vary substantially. Traditional risk factors associated with AF in the community include structural and valvular heart disease, neither of which is clearly related to AF in critical illness (11). In addition, acute factors, rather than pre-existing cardiovascular comorbid conditions, are thought to be associated with increased risk for newly diagnosed AF during critical illness (9). In particular, invasive ventilation or the use of vasoactive drugs and inotropes may trigger episodes of AF in the critical care setting (11) but has no relevance in ambulatory care.

Over the last decade, the use of various modelling techniques for AF has grown exponentially (12) and includes detection as well as prediction of AF. Existing models of risk prediction for AF are based on specific cardiac cohorts (12) and are not easily transferable to critical care, despite the numerous reviews (11, 13–15) which describe the risk factors for AF in sepsis and critical illness. As a consequence, the identification of subsets of critically ill patients at risk of developing AF before its clinical manifestation requires improvement. To date the availability of sophisticated risk prediction models in critical care is limited. The few existing models focus on septic patients only (16) and do not include the large proportion of critically ill patients with non-infectious pathologies. Advanced models for prediction of AF during critical illness, but before its clinical onset, would allow early interventions with a view to preventing serious AF-associated complications, such as haemodynamic instability, stroke and thromboembolic events.

To date models focusing on prediction and detection of AF are mainly based on data from the Medical Information Mart for Intensive Care (MIMIC) III database, which comprises data obtained in a single large tertiary care centre in the United States. So far, European databases have not been used to identify risk factors or to construct prediction models for AF in critical illness. The Amsterdam University Medical Centers Database (AmsterdamUMCdb), endorsed by the European Society of Intensive Care Medicine (ESICM), is the first freely accessible European intensive care unit (ICU) database (17).

Here we present a logistic regression model for the prediction of AF in critical illness using the AmsterdamUMCdb database (18). In addition to static variables, we include time series of vital signs, blood results and ventilatory settings in septic and non-septic patients in this model. We develop different models to predict the first occurrence of AF in patients admitted to critical care in sinus rhythm and to identify factors associated with the occurrence of AF. Furthermore we differentiate between ventilated and non-ventilated patients to account for mechanical ventilation as an established risk factor for development of AF in critical care.

MATERIALS AND METHODS

Data

We used data from the AmsterdamUMCdb, a freely available database, accessible after completing the mandatory training and guaranteeing the involvement of a practising intensivist in the research team to provide domain expertise. The database contains data from a 32-bed mixed surgical-medical academic ICU and a 12-bed high-dependency unit (medium care unit) (18). For patients who developed AF after ICU admission, the timestamp of the first episode of AF, as documented in the database, was used, while for non-AF patients the endpoint was the end of their ICU stay. Variables were extracted until 1 h before the first recorded AF episode for AF patients, whereas for non-AF patients data were analysed for the whole ICU stay. The interval of 1 h between the last data set included and the onset of AF was deliberately chosen because if applied in clinical practice, such a time frame would allow interventions to prevent the onset of the AF episode to be initiated. Variables included demographic data coded in classes (e.g., age, gender, weight and height), vital signs coded continuously (e.g., heart rate, breath rate, temperature, systolic blood pressure, and oxygen saturation), blood results and variables describing the level of respiratory support, such as FiO2 (**Table 1**).

Admissions with more than 35% missing data were excluded from the analysis. In the remaining cases, missing data for numeric variables were imputed with the median of the corresponding variable, and for categorical variables, they were imputed with the mode. Admissions and variables with dynamic features were converted into tabular representations by extracting their means.

Ventilation Status

Patients were considered to have been ventilated if they were explicitly recorded in the database as having been ventilated, i.e., patients that have associated an item in table "processitems" indicating 'Ventilate'. In addition, patients that did not have an explicit record in the "processitems" table of having been ventilated, but had O2 concentration or FiO2 records associated with their admission, were also classified as ventilated. This definition includes patients receiving invasive and non-invasive ventilatory support.

TABLE 1 | Demographics, vital signs, and routine prognostic scores used for modelling.

	AF (*N* = 2374)	Non-AF (*N* = 16144)	P-value
Location			<0.001
MC	150 (6.4%)	3308 (20.5%)	
IC	1837 (78.0%)	11797 (73.3%)	
IC&MC	369 (15.7%)	998 (6.2%)	
Urgency [yes]	826 (34.8%)	4382 (27.1%)	<0.001
Admission year group			0.098
2003–2009	1355 (57.1%)	9504 (58.9%)	
2010–2016	1019 (42.9%)	6640 (41.1%)	
ICU mortality	548 (23.1%)	1151 (7.1%)	<0.001
Gender [male]	861 (36.3%)	5556 (34.4%)	0.077
Age group (years)			<0.001
18–39	52 (2.2%)	2001 (12.4%)	
40–49	71 (3.0%)	1721 (10.7%)	
50–59	239 (10.1%)	2973 (18.4%)	
60–69	586 (24.7%)	4354 (27.0%)	
70–79	911 (38.4%)	3874 (24.0%)	
80+	515 (21.7%)	1221 (7.6%)	
Weight group (kg)			0.437
59–	204 (8.8%)	1214 (7.8%)	
60–69	354 (15.3%)	2513 (16.1%)	
70–79	608 (26.3%)	4309 (27.6%)	
80–89	613 (26.5%)	3980 (25.5%)	
90–99	316 (13.7%)	2134 (13.7%)	
100–109	120 (5.2%)	818 (5.2%)	
110+	98 (4.2%)	627 (4.0%)	
Height group (cm)			0.005
159–	148 (6.5%)	795 (5.2%)	
160–169	597 (26.1%)	3657 (24.0%)	
170–179	855 (37.4%)	6034 (39.7%)	
180–189	592 (25.9%)	3980 (26.2%)	
190+	93 (4.1%)	749 (4.9%)	
Average ALAT (mmol/l)	32.500 (19.312, 66.617)	28.500 (19.000, 53.400)	<0.001
Average Anion Gap (mmHg)	9.172 (7.145, 11.773)	8.333 (6.384, 10.189)	<0.001
Average APTT (mmHg)	44.000 (38.134, 54.000)	38.000 (34.250, 43.333)	<0.001
Average Breath Rate (g/l)	17.664 (14.146, 22.249)	16.909 (14.267, 20.013)	<0.001
Average Ca Ion (g/l)	1.143 (1.096, 1.183)	1.163 (1.127, 1.197)	<0.001
Average Calcium (mmol/l)	2.010 (1.887, 2.130)	2.020 (1.905, 2.143)	0.001
Average CK (mmol/l)	290.536 (131.438, 649.056)	319.367 (175.525, 564.979)	0.005
Average Creatinine (mmol/l)	101.345 (78.000, 148.858)	80.500 (65.000, 101.167)	<0.001
Average CRP (mmol/l)	47.342 (7.000, 126.333)	13.250 (2.600, 60.000)	<0.001
Average Diastolic Blood Pressure (mmHg)	58.327 (53.000, 64.053)	61.939 (56.519, 68.154)	<0.001
Average Glucose (mmol/l)	8.075 (7.200, 9.280)	7.944 (7.028, 8.883)	<0.001
Average Hb (mmol/l)	6.666 (6.112, 7.500)	6.909 (6.300, 7.700)	<0.001
Average Heart Rate (mmol/l)	84.231 (74.097, 96.675)	79.842 (71.300, 89.155)	<0.001
Average Inspiration Min Volume	8.656 (7.375, 10.373)	7.975 (6.950, 9.288)	<0.001
Average Leucos (mmol/l)	12.050 (9.200, 15.800)	11.775 (9.535, 14.533)	0.021
Average Magnesium (mmol/l)	0.897 (0.775, 1.060)	0.877 (0.760, 1.060)	0.001
Average O2 concentration (10^9/l)	45.494 (40.585, 52.297)	40.286 (36.225, 44.070)	<0.001
Average O2 L/min	5.365 (4.000, 8.507)	4.400 (2.800, 5.272)	<0.001
Average O2 saturation (mmol/l)	75.053 (57.562, 88.592)	80.773 (69.538, 92.408)	<0.001
Average Systolic Blood Pressure (mmHg)	118.470 (107.857, 131.436)	126.223 (114.800, 137.886)	<0.001
Average Temperature (°C)	36.620 (35.995, 36.980)	36.713(36.299, 36.998)	<0.001
Average Thrombo (°C)	173.194 (127.856, 236.406)	190.250 (147.000, 248.000)	<0.001
Average Urine CAD (mmol/l)	91.327 (54.037, 132.036)	129.706 (94.270, 175.833)	<0.001
Average PEEP (mmHg)	8.000 (5.487, 10.110)	5.942 (5.000, 8.000)	<0.001
Average pH (l/min)	7.365 (7.317, 7.402)	7.388 (7.360, 7.413)	<0.001
Average Phosphate (mmHg)	1.110 (0.900, 1.378)	1.013 (0.851, 1.191)	<0.001

(Continued)

TABLE 1 | (Continued)

	AF (*N* = 2374)	Non-AF (*N* = 16144)	P-value
Average PO2 (mmHg)	99.188 (84.595, 120.894)	108.220 (92.150, 131.143)	<0.001
Average Potassium (mmHg)	4.154 (3.940, 4.431)	4.100 (3.907, 4.333)	<0.001
Average Prothrombin Time (cmH2O)	1.400 (1.245, 1.680)	1.256 (1.125, 1.395)	<0.001
Average ST segment (mm)	0.213 (0.123, 0.364)	0.250 (0.150, 0.433)	<0.001
Ventilated [yes]	2066 (87.0%)	12303 (76.2%)	<0.001
APACHE II scores [day 1]			
Total cohort	24 (18.5, 30.5)	17 (12.5, 22.5)	<0.001
Ventilated cohort	25.5 (20, 32.5)	19 (14.5, 24.5)	<0.001
Non-ventilated cohort	21 (16, 27.5)	12 (9, 16)	<0.001
SOFA scores [day 1]			
Total cohort	10 (7, 13)	8 (5, 11)	<0.001
Ventilated cohort	12 (9, 14)	9 (6, 11)	<0.001
Non-ventilated cohort	8 (5, 10)	4 (2, 6)	<0.001

Numeric variables are reported with the median and interquartile range (in brackets), while categorical variables are reported with the frequency and proportion (in brackets). The resulting statistical tests (more details in the Methods section) are reported in the fourth column in the form of p-values.
MC: Medium Care; IC: Intensive Care; IC&MC: IC first, then MC; ALAT: Alanine transaminase; ICU: Intensive Care Unit; APTT: activated partial thromboplastin time; CK: creatine kinase; CRP: C-reactive protein; Hb: haemoglobin; urine CAD: urine output; PEEP: positive end-expiratory pressure; APACHE: Acute Physiology And Chronic Health Evaluation; SOFA: Sequential Organ Failure Assessment.

Model Outcome

The outcome to be predicted in this model was the first documented episode of AF in patients admitted to ICU in sinus rhythm. As a previous history of AF is not coded in the AmsterdamUMC database, this outcome does not discriminate between new onset and pre-existing AF.

Univariate Analysis

For univariate analysis, medians and interquartile ranges were calculated for continuous variables and frequencies and proportions for categorical variables. Differences between AF vs. non-AF patients were assessed using Kruskal-Wallis rank sum and Chi-square tests. Acute Physiology And Chronic Health Evaluation II (APACHE II) and Sequential Organ Failure Assessment (SOFA) scores were calculated upon admission to ICU.

Multivariate Analysis

We performed multivariate statistical modelling using logistic regression (LR) to elucidate associations, in the form of odds ratios (OR), between the factors and the occurrence of AF. LR models the outcome probability or risk to be '1' (positive class) as $P(Y = 1) = 1/\left(1 + \exp\left[-\sum_{k=0}^{K} \beta_k X_k\right]\right)$, where $\{\beta_0, ..., \beta_K\}$ are the logarithms of the OR, which are estimated by maximum likelihood (19).

Variable Selection

For the selection of variables, we ensured that for any pair of them that were considered clinically correlated, only one of them was included (usually the one with fewer missing values), e.g., for albumin and calcium, only calcium was selected. Subsequently, pairwise correlations between variables were calculated to verify that the variables included in the study were not highly collinear (above 0.7 using Pearson correlation). Relevant input variables were automatically selected using a sequential forward search algorithm using 3-fold cross-validation. The selection algorithm starts with a baseline model (i.e., all coefficients but the intercept set to zero, $\beta_{k \neq 0} = 0$), and in each step, the variable that most improves the performance on the validation set is added (20).

Model Performance

Nested cross-validation was implemented, with the inner iterations to evaluate the variable selection, and the outer iterations to evaluate the training with the selected set of variables. Model performances were measured using the area under the receiver operator characteristic (AUC) curve. We report AUC means and confidence intervals (CI) for the full patient cohort, and ventilated and non-ventilated patients separately. Due to the class imbalance in the datasets, we also produced precision-recall curves to evaluate the three models developed. Their baselines were determined by the ratio of positives (P) and negatives (N) as y = P / (P + N) (21).

R version 3.6.3 was used for all analyses.

RESULTS

Data Groups

From a total of 23,106 admissions extracted, patients < 18 years of age, multiple admissions and cases with > 35% missing data were excluded, resulting in 18,518 analysable cases, of which 2,374 were patients with AF patients, while 16,144 had no episodes of AF reported (**Figure 1**). A total of 2,066 (87%) of the patients with AF and 12,303 (76.2%) of non-AF patients required ventilation, leaving 308 (23%) AF patients and 3,841 (23.8%) non-AF patients who did not require ventilation.

Univariate statistical comparisons between AF and non-AF groups of patients are displayed in **Table 1**. We found statistically significant group differences (p-value < 0.05) for several vital signs, laboratory results, demographics, and the severity scoring systems. For instance, AF patients were older

than 70 years (60% versus 32%) and died in ICU (23.6% versus 8%) compared to non-AF patients. We also found statistically significant differences between ventilated and non-ventilated patients (p-value < 0.001).

Evaluation of Model Performances

The developed models were able to predict the first occurrence of AF in patients admitted to critical care in sinus rhythm for all the patients in the selection group, and specifically in ventilated and non-ventilated patients, with AUC performances of 0.836 (CI: 0.833–0.838), 0.820 (CI: 0.818–0.823) and 0.912 (CI: 0.883–0.942), respectively. Additionally, the performance of disease severity scores (APACHE II and SOFA) was compared to the developed model (results in **Supplementary Table 2**), which as expected showed that, independently of the data cohort used, our predictive models achieved significantly better performances than severity scores developed for mortality prediction in general. The precision-recall curves for the three models, together with their baselines, are shown in **Figure 2**.

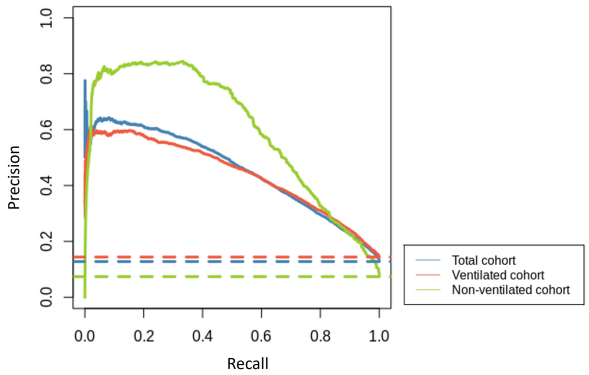

FIGURE 2 | Precision-recall curves for the total cohort (blue), ventilated cohort (red) and non-ventilated cohort (green) are represented with solid lines. Their corresponding baselines are represented with dashed lines.

Explanatory Analysis Using Logistic Regression

The odds ratios (OR) for the total cohort, and the ventilated and non-ventilated patients are presented in **Figure 3**. We identified input variables (factors) either positively or negatively associated with the risk of developing AF in both, ventilated and non-ventilated patients, as well as in the total cohort. Factors positively associated with the development of AF in both ventilated and non-ventilated cohorts include immunoinflammatory markers such as increased average CRP (OR: total = 1.281, ventilated = 1.384, non-ventilated = 1.312) in multivariate analysis, as well as average APTT (OR: total = 1.133, ventilated = 1.150) in the ventilated cohort. Increased oxygen requirements (average O2 concentration, average O2 L/min) and reduced oxygen saturations were associated with the development of AF in both ventilated and non-ventilated patients (average O2 concentration OR: total = 1.334, ventilated = 1.336; average O2 L/min OR: total = 1.287, ventilated = 1.203, non-ventilated = 1.206). Similarly, in ventilated patients, the average PEEP (OR: ventilated = 1.355) was shown to be associated with the development of AF. Across both ventilated and non-ventilated cohorts age appears to be the single most important factor in predicting the development of AF. Patients over 80 years had the greatest risk (with OR: total = 22.909) compared to patients aged 40-49 (OR: total = 1.971). Age was even more significant in the non-ventilated cohort (with OR: non-ventilated = 74.922) in those over 80 years, compared to those aged 40-49 (OR non-ventilated = 2.757). Detailed information of the variables odd ratios and their corresponding 95% confidence intervals can be found in **Table 2**.

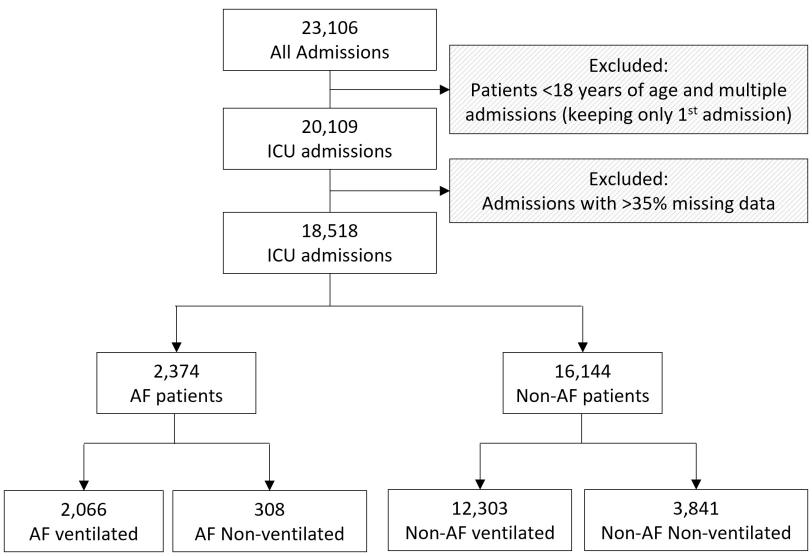

FIGURE 1 | Flowchart of the cohorts analysed including the inclusion and exclusion criteria. ICU: intensive care unit; AF: Atrial Fibrillation.

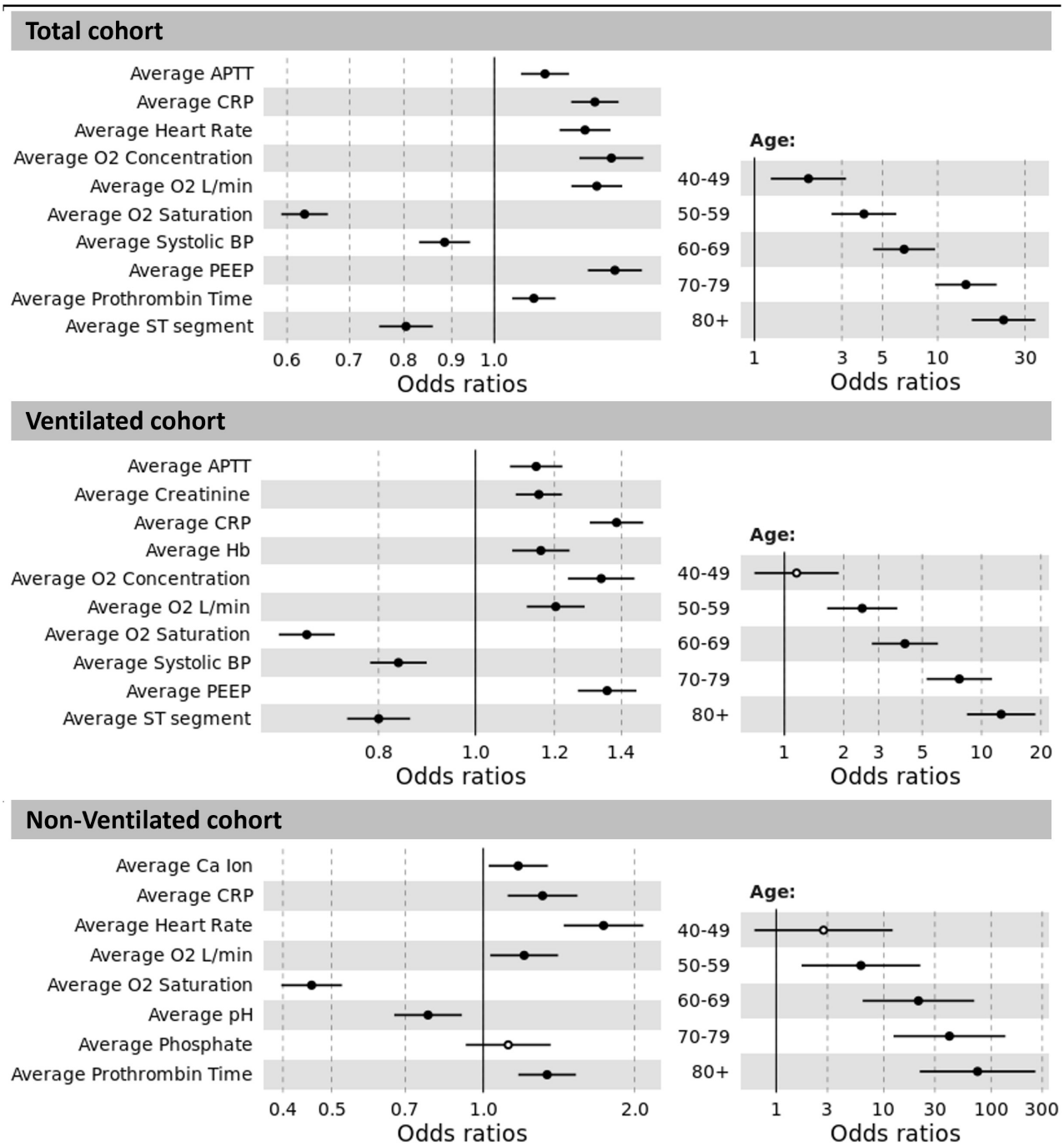

FIGURE 3 | Odds ratios between significant results and prediction of AF for the total cohort, ventilated and non-ventilated cohorts. The non-significant results are displayed as hollow points. Abbreviations: APTT: activated partial thromboplastin time; CRP: C-reactive protein; O2: oxygen; BP: blood pressure; PEEP: positive end-expiratory pressure; Hb: haemoglobin; Ca: calcium.

DISCUSSION

Despite an increasing number of publications about AF in critically ill patients, its precipitants in this population are poorly understood. In this research, we identify modifiable and non-modifiable risk factors to build a logistic regression model for the prediction of a first episode of AF during admission to ICU. We analyse data from the AmsterdamUMCdb, which contains a total of 23,106 ICU admissions. Previous prediction models for AF in critical illness (16) are based on United States databases, include only septic patients (3, 16, 22) or focus on post-cardiac surgery patients (23). Although the risk of developing

TABLE 2 | Detailed information of the variables odd ratios (OR) and their corresponding 95% confidence intervals (CI) for each of the developed models.

Variables per cohort:	OR	95% CI
Total cohort:		
Age group 40–49 years	1.971	[1.229, 3.162]
Age group 50–59 years	3.960	[2.636, 5.950]
Age group 60–69 years	6.565	[4.450, 9.685]
Age group 70–79 years	14.270	[9.696, 21.002]
Age group 80+ years	22.909	[15.363, 34.163]
Average APTT (mmHg)	1.133	[1.068, 1.202]
Average CRP (mmol/l)	1.281	[1.208, 1.358]
Average Heart Rate (mmol/l)	1.250	[1.174, 1.331]
Average O2 concentration (10^9/l)	1.334	[1.233, 1.444]
Average O2 L/min	1.287	[1.209, 1.370]
Average O2 saturation (mmol/l)	0.627	[0.592, 0.663]
Average Systolic Blood Pressure (mmHg)	0.885	[0.831, 0.942]
Average PEEP (mmHg)	1.346	[1.259, 1.438]
Average Prothrombin Time (cmH2O)	1.102	[1.045, 1.163]
Average ST segment (mm)	0.804	[0.753, 0.859]
Ventilated:		
Age group 40–49 years	1.153	[0.706, 1.895]
Age group 50–59 years	2.482	[1.668, 3.791]
Age group 60–69 years	4.086	[2.819, 6.110]
Age group 70–79 years	7.712	[5.345, 11.493]
Age group 80+ years	12.572	[8.549, 19.040]
Average APTT (mmHg)	1.150	[1.083, 1.222]
Average Creatinine (mmol/l)	1.157	[1.097, 1.220]
Average CRP (mmol/l)	1.384	[1.302, 1.472]
Average Hb (mmol/l)	1.163	[1.088, 1.242]
Average O2 concentration (10^9/l)	1.336	[1.239, 1.444]
Average O2 L/min	1.203	[1.126, 1.286]
Average O2 saturation (mmol/l)	0.678	[0.636, 0.723]
Average Systolic Blood Pressure (mmHg)	0.837	[0.784, 0.894]
Average PEEP (mmHg)	1.355	[1.266, 1.449]
Average ST segment (mm)	0.800	[0.743, 0.859]
Non-Ventilated:		
Age group 40–49 years	2.757	[0.624, 12.943]
Age group 50–59 years	6.146	[1.876, 24.884]
Age group 60–69 years	21.090	[7.163, 80.792]
Age group 70–79 years	40.993	[13.907, 157.862]
Age group 80+ years	74.922	[24.268, 298.522]
Average Ca Ion (g/l)	1.174	[0.991, 1.324]
Average CRP (mmol/l)	1.312	[1.116, 1.537]
Average Heart Rate (mmol/l)	1.734	[1.447, 2.086]
Average O2 L/min	1.206	[1.031, 1.407]
Average O2 saturation (mmol/l)	0.456	[0.396, 0.523]
Average pH (l/min)	0.777	[0.665, 0.907]
Average Phosphate (mmHg)	1.121	[0.921, 1.359]
Average Prothrombin Time (cmH2O)	1.340	[1.177, 1.534]

AF is highest in septic patients (3), prediction models for the occurrence of AF in general medical-surgical ICU populations are lacking. McMillan (24) used data from the first 8 h of ICU admission to predict subsequent AF. This approach will miss the significant proportion of critically ill patients who develop episodes of AF before ICU admission to the Emergency Department (25) or early during their ICU stay (26).

In this research, we calculate the means of time series of vital signs, laboratory results and respiratory data to build an LR model for the development of the first episode of AF in patients admitted to ICU with documented sinus rhythm. Depending on ventilation status, our model achieved very good to excellent performance measures with an AUC of 0.82 in ventilated and 0.912 in non-ventilated cohorts. The precision-recall curves (**Figure 2**) also support this assessment, showing that all models clearly distinguish themselves from a random classifier, indicated by their corresponding horizontal baseline. Furthermore, our models displayed good performance at predicting the small class (AF).

Since the occurrence of AF in critical illness is associated with disease severity, we used established critical care risk scores, such as APACHE II or SOFA, calculated on admission to ICU, for comparison. Our model performed significantly better in all cohorts. This may be partly explained by the limited number of variables included in the conventional risk prediction scores APACHE II and SOFA. Furthermore, the use of time series may improve model performance as dynamic changes are considered. In conclusion, while well established for mortality prediction, APACHE II and SOFA on admission are not suitable to predict AF in ICU and more specific scores are needed to identify patients at risk before the clinical onset of this arrhythmia which has repeatedly been associated with higher mortality (27, 28).

We have identified increasing age as the most important predictor of the development of AF in our analysis. Advancing age has been known as a risk factor for AF in the general population for several decades (29). Within the critical care settings, most studies investigating risk factors for AF, focus on septic patients (4, 22, 30). Despite a high level of evidence, a previous meta-analysis showed only a weak association between advanced age and AF in sepsis (22). In contrast, a scoping review (5) and a recent meta-analysis identified increasing age as the dominant risk factor in the general critical care population (13). Our model supports the role of increasing age as the principal risk factor for the occurrence of AF in critical illness: As age doubles, the risk of developing AF increases on average 10-fold. Previous work suggested that ageing in the cardiovascular system, and in particular, structural changes within the atria are major factors in the development of AF in the general population (31, 32). Bosch et al. (11) postulated that inflammation and infection can trigger accelerated cardiac structural and electrical remodelling during critical illness (11). We included CRP as a routine inflammatory marker available in the AmsterdamUMCdb in our model, and could demonstrate that higher CRP concentrations were associated with increased risk of AF.

While acute respiratory failure has been recognised as a risk factor for AF in several studies (3, 15), it remains unknown if the need for intermittent positive pressure ventilation (IPPV) is associated with a different risk profile. Clinically, the need for invasive ventilation is associated with more severe respiratory failure. Hence modelling ventilated versus non-ventilated patients separately allows prediction of AF in respiratory failure of different severity. The application of

positive pressure to the airway leads to pronounced changes in intrathoracic pressure and decreases volume return to the right heart. As a consequence, left ventricular preload also decreases due to lower pulmonary venous return (33). A recent observational study in patients after cardiac surgery found a significant impact between the occurrence of AF and invasive respiratory support (34), supporting the concept that ventilated patients may exhibit a different risk profile compared to non-ventilated patients. We therefore developed three different models for risk prediction of the development of AF in a non-ventilated, a ventilated and in an undifferentiated full cohort. We also observed an impact of ventilatory settings, as higher O2 requirements and higher PEEP were associated with an increased odds ratio for the development of AF. All three models identified age as the strongest risk factor, however, in non-ventilated patients increasing age was associated with a 7-fold higher OR compared to ventilated patients. With advancing age, the severity of respiratory failure, the increased sympathomimetic activity in unsedated patients, and a lower cardiovascular tolerance to inflammation and fluid shifts, are amongst the factors which may contribute to the different weighting of risk factors depending on ventilation status.

Our study has several limitations. We performed internal cross-validation, but external validation of our model is required for generalisability across different ICU databases and before clinical implementation can be pursued. Additionally, missing data were imputed with the median/mode, which is a simple and computationally rapid approach. Alternatively, missing data imputation methods such as regression-based imputation or multiple imputation by chained equations (MICE) could be considered.

Our model was built to predict new episodes of AF in patients admitted to critical care in sinus rhythm. Insufficient information was available in the database regarding the previous medical history of paroxysmal or pre-existing AF. Thus, our model cannot predict new-onset AF, as patients with a known diagnosis of AF may also present in sinus rhythm on admission and develop episodes of AF later in their stay. Finally, in addition to the requirement for models differentiating between ventilation modes, further targeted models for individual ICU subpopulations are required, e.g., patients with sepsis, as they may display a different risk profile.

Within the AmsterdamUMC database, several variables are presented as ranges only, e.g., age, weight and height. This limits the analyses that can be performed. For example, it was impossible to calculate Body Mass Index, which is why weight and height had to be considered as separate variables in our model.

In addition to the requirement for specific models for mechanically ventilated patients, further targeted models for individual ICU subpopulations such as septic patients are required, as they may display a different risk profile.

CONCLUSION

We present a logistic regression model for risk prediction of new episodes of AF in critical illness using the AmsterdamUMCdb database. Our model demonstrates very good performance in ventilated patients and excellent performance in non-ventilated patients. Further work is required to exploit the potential that different ML methods to model risk prediction for new episodes of AF in various cohorts of critically ill patients.

DATA AVAILABILITY STATEMENT

Publicly available datasets were analyzed in this study. This data can be found here: https://amsterdammedicaldatascience.nl/#amsterdamumcd.

ETHICS STATEMENT

Ethical review and approval was not required for the study on human participants in accordance with the local legislation and institutional requirements. Written informed consent for participation was not required for this study in accordance with the national legislation and the institutional requirements.

AUTHOR CONTRIBUTIONS

SO-M and MP extracted and prepared the data. SO-M, IO, and MP conducted the analysis and evaluated the results. IW and BJ provided the clinical expertise and wrote the first draft of the manuscript. All authors were involved in the study design, the selection of relevant variables from the dataset, contributed to the writing, reviewing and editing, and approved the final manuscript.

FUNDING

This research was partially supported by a Ph.D. scholarship of the Faculty of Engineering and Technology, LJMU.

ACKNOWLEDGMENTS

We acknowledge the 3rd Critical Care Datathon organised by the European Society of Intensive Care Medicine (ESICM), as well as their organisers (particularly Ari Ercole, Patrick Thoral, and Paul Elbers), who provided an opportunity for the understanding and exploitation of the AmsterdamUMC database. We are thankful to Martina Zubac, who calculated the disease severity scores (APACHE II and SOFA) used for comparison in this research. We are also grateful to Lama Nazer for the early discussions during the ESICM Datathon.

SUPPLEMENTARY MATERIAL

The Supplementary Material for this article can be found online at: https://www.frontiersin.org/articles/10.3389/fcvm.2022.897709/full#supplementary-material

REFERENCES

1. Lip GYH, Fauchier L, Freedman SB, van Gelder I, Natale A, Gianni C, et al. Atrial fibrillation. *Nat Rev Dis Primers.* (2016) 2:1–26. doi: 10.1038/nrdp.2016.16
2. Chebbout R, Heywood EG, Drake TM, Wild JRL, Lee J, Wilson M, et al. A systematic review of the incidence of and risk factors for postoperative atrial fibrillation following general surgery. *Anaesthesia.* (2018) 73:490–8. doi: 10.1111/ANAE.14118
3. Klein Klouwenberg PMC, Frencken JF, Kuipers S, Ong DSY, Peelen LM, van Vught LA, et al. Incidence, predictors, and outcomes of new-onset atrial fibrillation in critically Ill patients with sepsis. A cohort study. *Am J Respir Crit Care Med.* (2017) 195:205–11. doi: 10.1164/RCCM.201603-0618OC
4. Meierhenrich R, Steinhilber E, Eggermann C, Weiss M, Voglic S, Bögelein D, et al. Incidence and prognostic impact of new-onset atrial fibrillation in patients with septic shock: a prospective observational study. *Crit Care.* (2010) 14:R108. doi: 10.1186/CC9057
5. Wetterslev M, Haase N, Hassager C, Belley-Cote EP, McIntyre WF, An Y, et al. New-onset atrial fibrillation in adult critically ill patients: a scoping review. *Intensive Care Med.* (2019) 45:928–38. doi: 10.1007/S00134-019-05633-X
6. Johnston BW, Chean CS, Duarte R, Hill R, Blackwood B, McAuley DF, et al. Management of new onset atrial fibrillation in critically unwell adult patients: a systematic review and narrative synthesis. *Br J Anaesth.* (2021) 128:759–71. doi: 10.1016/J.BJA.2021.11.016
7. Chen AY, Sokol SS, Kress JP, Lat I. New-onset atrial fibrillation is an independent predictor of mortality in medical intensive care unit patients. *Ann Pharmacother.* (2015) 49:523–7. doi: 10.1177/1060028015574726
8. Alonso A, Krijthe BP, Aspelund T, Stepas KA, Pencina MJ, Moser CB, et al. Simple risk model predicts incidence of atrial fibrillation in a racially and geographically diverse population: the CHARGE-AF consortium. *J Am Heart Assoc.* (2013) 2:e000102. doi: 10.1161/JAHA.112.000102
9. Walkey AJ, Greiner MA, Heckbert SR, Jensen PN, Piccini JP, Sinner MF, et al. Atrial fibrillation among medicare beneficiaries hospitalized with sepsis: incidence and risk factors. *Am Heart J.* (2013) 165:949. doi: 10.1016/J.AHJ.2013.03.020
10. Ding EY, Albuquerque D, Winter M, Binici S, Piche J, Bashar SK, et al. Novel method of atrial fibrillation case identification and burden estimation using the MIMIC-III electronic health data set. *J Intens Care Med.* (2019) 34:851–7. doi: 10.1177/0885066619866172
11. Bosch NA, Cimini J, Walkey AJ. Atrial fibrillation in the ICU. *Chest.* (2018) 154:1424. doi: 10.1016/J.CHEST.2018.03.040
12. Olier I, Ortega-Martorell S, Pieroni M, Lip GYH. How machine learning is impacting research in atrial fibrillation: implications for risk prediction and future management. *Cardiovasc Res.* (2021) 117:1700–17. doi: 10.1093/CVR/CVAB169
13. Wu Z, Fang J, Wang Y, Chen F. Prevalence, outcomes, and risk factors of new-onset atrial fibrillation in critically Ill patients. *Int Heart J.* (2020) 61:476–85. doi: 10.1536/IHJ.19-511
14. Bedford JP, Harford M, Petrinic T, Young JD, Watkinson PJ. Risk factors for new-onset atrial fibrillation on the general adult ICU: a systematic review. *J Crit Care.* (2019) 53:169–75. doi: 10.1016/J.JCRC.2019.06.015
15. Moss TJ, Calland JF, Enfield KB, Gomez-Manjarres DC, Ruminski C, Dimarco JP, et al. New-onset atrial fibrillation in the critically Ill. *Crit Care Med.* (2017) 45:790–7. doi: 10.1097/CCM.0000000000002325
16. Bashar SK, Ding EY, Walkey AJ, McManus DD, Chon KH. Atrial fibrillation prediction from critically Ill sepsis patients. *Biosensors.* (2021) 11:269. doi: 10.3390/BIOS11080269
17. Thoral P, Peppink J, Driessen R, Sijbrands E, Kompanje E, Kaplan L, et al. Sharing ICU patient data responsibly under the society of critical care medicine/European society of intensive care medicine joint data science collaboration: the Amsterdam university medical centers database (AmsterdamUMCdb) example. *Crit Care Med.* (2021) 49:E563–77. doi: 10.1097/CCM.0000000000004916
18. Thoral PJ, Fornasa M, de Bruin DP, Tonutti M, Hovenkamp H, Driessen RH, et al. Explainable machine learning on AmsterdamUMCdb for ICU discharge decision support: uniting intensivists and data scientists. *Crit Care Explor.* (2021) 3:e0529. doi: 10.1097/CCE.0000000000000529
19. Hosmer D. *Applied Logistic Regression*. Hoboken, NJ: Wiley (2013).
20. Kohavi R, John GH. Wrappers for feature subset selection. *Artif Intell.* (1997) 97:273–324. doi: 10.1016/S0004-3702(97)00043-X
21. Saito T, Rehmsmeier M. The precision-recall plot is more informative than the ROC plot when evaluating binary classifiers on imbalanced datasets. *PLoS One.* (2015) 10:e0118432. doi: 10.1371/JOURNAL.PONE.0118432
22. Kuipers S, Klouwenberg KMCK, Cremer OL. Incidence, risk factors and outcomes of new-onset atrial fibrillation in patients with sepsis: a systematic review. *Crit Care.* (2014) 18:1–9. doi: 10.1186/S13054-014-0688-5/TABLES/4
23. Mariscalco G, Biancari F, Zanobini M, Cottini M, Piffaretti G, Saccocci M, et al. Bedside tool for predicting the risk of postoperative atrial fibrillation after cardiac surgery: the POAF score. *J Am Heart Assoc.* (2014) 3:e000752. doi: 10.1161/JAHA.113.000752
24. Mcmillan S, Rubinfeld I, Syed Z. Predicting atrial fibrillation from intensive care unit numeric data. *Comput Cardiol.* (2012) 39:213–6.
25. Scheuermeyer FX, Norena M, Innes G, Grunau B, Christenson J, Grafstein E, et al. Decision aid for early identification of acute underlying illness in emergency department patients with atrial fibrillation or flutter. *CJEM.* (2020) 22:301–8. doi: 10.1017/CEM.2019.454
26. Fernando SM, Mathew R, Hibbert B, Rochwerg B, Munshi L, Walkey AJ, et al. New-onset atrial fibrillation and associated outcomes and resource use among critically ill adults – a multicenter retrospective cohort study. *Crit Care.* (2020) 24:1–10. doi: 10.1186/S13054-020-2730-0/TABLES/5
27. Qian J, Kuang L, Chen F, Liu X, Che L. Prognosis and management of new-onset atrial fibrillation in critically ill patients. *BMC Cardiovasc Disord.* (2021) 21:231. doi: 10.1186/S12872-021-02039-W/FIGURES/3
28. Shaver CM, Chen W, Janz DR, May AK, Darbar D, Bernard GR, et al. Atrial fibrillation is an independent predictor of mortality in critically Ill patients. *Crit Care Med.* (2015) 43:2104–11. doi: 10.1097/CCM.0000000000001166
29. Benjamin EJ, Levy D, Vaziri SM, D'agostino RB, Belanger AJ, Wolf PA. Independent risk factors for atrial fibrillation in a population-based cohort: the Framingham heart study. *JAMA.* (1994) 271:840–4. doi: 10.1001/JAMA.1994.03510350050036
30. Aibar J, Schulman S. New-onset atrial fibrillation in sepsis: a narrative review. *Semin Thromb Hemost.* (2021) 47:18–25. doi: 10.1055/S-0040-1714400
31. Nattel S, Harada M. Atrial remodeling and atrial fibrillation: recent advances and translational perspectives. *J Am Coll Cardiol.* (2014) 63:2335–45. doi: 10.1016/J.JACC.2014.02.555
32. Chen Q, Yi Z, Cheng J. Atrial fibrillation in aging population. *Aging Med (Milton).* (2018) 1:67–74. doi: 10.1002/AGM2.12015
33. Luecke T, Pelosi P. Clinical review: positive end-expiratory pressure and cardiac output. *Crit Care.* (2005) 9:607–21. doi: 10.1186/CC3877
34. Schnaubelt S, Stajic A, Koller L, Hofer F, Kazem N, Hammer A, et al. The impact of invasive respiratory support on the development of postoperative atrial fibrillation following cardiac surgery. *J Clin Anesth.* (2021) 72:110309. doi: 10.1016/J.JCLINANE.2021.110309

Conflict of Interest: The authors declare that the research was conducted in the absence of any commercial or financial relationships that could be construed as a potential conflict of interest.

frontiers | Frontiers in Cardiovascular Medicine

ORIGINAL RESEARCH
published: 30 May 2022
doi: 10.3389/fcvm.2022.863939

The Inverse Correlation Between the Duration of Lifetime Occupational Radiation Exposure and the Prevalence of Atrial Arrhythmia

Rithika Thirumal[1,2†], Catherine Vanchiere[2,3†], Ruchi Bhandari[4†], Sania Jiwani[5], Ronald Horswell[6], San Chu[6], Surbhi Chamaria[7], Pavan Katikaneni[2,8], Marjan Boerma[9], Rakesh Gopinathannair[10], Brian Olshansky[11], Steven Bailey[2,5,8] and Paari Dominic[2,8]*

[1] Department of Internal Medicine, University of Cincinnati, Cincinnati, OH, United States, [2] School of Medicine, Louisiana State University Health Sciences Center, Shreveport, LA, United States, [3] Department of Internal Medicine, Temple University, Philadelphia, PA, United States, [4] Department of Epidemiology and Biostatistics, West Virginia University, Morgantown, WV, United States, [5] Department of Internal Medicine, Louisiana State University Health Sciences Center, Shreveport, LA, United States, [6] Pennington Biomedical Research Center, Louisiana State University, Baton Rouge, LA, United States, [7] Mercy Hospital, Fort Smith, AK, United States, [8] Center for Cardiovascular Diseases and Sciences, Louisiana State University Health Sciences Center, Shreveport, LA, United States, [9] Department of Pharmaceutical Sciences, University of Arkansas Medical Center, Little Rock, AK, United States, [10] Department of Cardiology, Kansas City Heart Rhythm Institute, Overland Park, KS, United States, [11] Department of Medicine, University of Iowa Hospitals and Clinics, Iowa City, IA, United States

Objective: Advancements in fluoroscopy-assisted procedures have increased radiation exposure among cardiologists. Radiation has been linked to cardiovascular complications but its effect on cardiac rhythm, specifically, is underexplored.

Methods: Demographic, social, occupational, and medical history information was collected from board-certified cardiologists via an electronic survey. Bivariate and multivariable logistic regression analyses were performed to assess the risk of atrial arrhythmias (AA).

Results: We received 1,478 responses (8.8% response rate) from cardiologists, of whom 85.4% were male, and 66.1% were ≤65 years of age. Approximately 36% were interventional cardiologists and 16% were electrophysiologists. Cardiologists > 50 years of age, with > 10,000 hours (h) of radiation exposure, had a significantly lower prevalence of AA vs. those with ≤10,000 h (11.1% vs. 16.7%, $p = 0.019$). A multivariable logistic regression was performed and among cardiologists > 50 years of age, exposure to > 10,000 radiation hours was significantly associated with a lower likelihood of AA, after adjusting for age, sex, diabetes mellitus, hypertension, and obstructive sleep apnea (adjusted OR 0.57; 95% CI 0.38–0.85, $p = 0.007$). The traditional risk factors for AA (age, sex, hypertension, diabetes mellitus, and obstructive sleep apnea) correlated positively with AA in our data set. Cataracts, a well-established complication of radiation exposure, were more prevalent in those exposed to > 10,000 h of radiation vs. those exposed to ≤10,000 h of radiation, validating the dependent (AA) and independent variables (radiation exposure), respectively.

OPEN ACCESS

Edited by:
Guowei Li,
Guangdong Second Provincial General Hospital, China

Reviewed by:
Dimitrios Vrachatis, National and Kapodistrian University of Athens, Greece
Andrea Di Cori, Pisana University Hospital, Italy
Pedro Silva Cunha, Hospital de Santa Marta, Portugal

****Correspondence:***
Paari Dominic
paari.dominic@lsuhs.edu

† These authors have contributed equally to this work

Specialty section:
This article was submitted to Cardiac Rhythmology, a section of the journal Frontiers in Cardiovascular Medicine

Received: *27 January 2022*
Accepted: *28 March 2022*
Published: *30 May 2022*

Citation:
Thirumal R, Vanchiere C, Bhandari R, Jiwani S, Horswell R, Chu S, Chamaria S, Katikaneni P, Boerma M, Gopinathannair R, Olshansky B, Bailey S and Dominic P (2022) The Inverse Correlation Between the Duration of Lifetime Occupational Radiation Exposure and the Prevalence of Atrial Arrhythmia. Front. Cardiovasc. Med. 9:863939. doi: 10.3389/fcvm.2022.863939

Conclusion: AA prevalence may be inversely associated with radiation exposure in Cardiologists based on self-reported data on diagnosis and radiation hours. Large-scale prospective studies are needed to validate these findings.

Keywords: atrial arrhythmia, fluoroscopy, radiation, interventional cardiologists, electrophysiologists, invasive cardiology

INTRODUCTION

The field of cardiology has made remarkable progress in the past 30 years in the development of percutaneous therapies. These new catheterization procedures have lead to increased radiation exposure among cardiologists which has become an area of concern (1). Fluoroscopic procedures are a source of medical occupation related radiation exposure and, with cardiac procedures becoming more intricate, radiation exposure has increased, further amplifying the need to investigate the impact of occupational radiation exposure (2–4).

Atrial tachycardia (AT), atrial flutter (Afl), and atrial fibrillation (AF) are a continuum of atrial arrhythmias (AA) that lead to atrial remodeling and increased risk of thromboembolism (5, 6). Atrial fibrillation (AF) is a common clinical arrhythmia that increases the risk of stroke, heart failure, and other cardiac complications (7, 8). Many risk factors have been established for AA, including hypertension (HTN), diabetes mellitus (DM), obstructive sleep apnea (OSA), coronary artery disease (CAD), and advanced age. Recently, high dose radiation therapy, as seen in cancer patients, has been associated with an increased incidence of AF. This may be due to oxidative DNA damage leading to cardiac inflammation and fibrosis, both of which are risk factors for AF (7, 9–11). Ironically, while ablative radiation with stereotactic body radiation therapy can be therapeutically useful for patients with ventricular arrythmias, exposure to longitudinal low-dose radiation can be detrimental to the operators (12, 13).

Although cardiologists are not exposed to high acute doses of radiation, their longitudinal exposure to low doses is cause for concern, particularly as the arrhythmogenic effects of this exposure are still unclear. Studies have surveyed invasive cardiologists to assess a variety of occupational hazards, including orthopedic and ophthalmologic complications, but the impact of occupational radiation exposure on the prevalence of AA is still unexplored in this cohort (11, 14, 15).

In this study, we examined the impact of cumulative low-dose radiation exposure on cardiovascular health and, more specifically, the risk of AA among cardiologists exposed to procedural radiation. We hypothesize that increased radiation exposure is associated with a higher prevalence of AA. The results of this study can help guide future research and increase awareness of the impact of radiation exposure in the field of invasive cardiology.

METHODS

An electronic survey was distributed to 16,790 board-certified cardiologists (∼42% were interventional cardiologists or electrophysiologists) who were members of the American College of Cardiology, the Society of Cardiovascular Angiography and Interventions, or the Heart Rhythm Society (16). Along with the survey link (**Supplementary Material 1**), the participants received a brief description of the study and a consent letter that outlined the potential risks involved with participation in the study. Participants were also asked to distribute the survey to colleagues in their practices and/or institutions to maximize the number of potential responses. As the initial step, participants were informed that continuing to the survey serves as their consent for study participation; no written consent was obtained. Participants completed a brief survey collecting information regarding elements of their demographic, social, occupational, and medical health histories. No identifiers were obtained during data collection. Follow-up email reminders were sent over a period of 4 months to maximize the number of responses (**Supplementary Figure 1**). All de-identified survey submissions were included in the analysis. The research reported in this article was approved by the Louisiana State University institutional review board and adheres to institutional guidelines.

Statistical Analysis

For this study, the outcome variable, AA, was defined as one or more of the following: frequent premature atrial contractions, AT, AFL, and AF. The diagnosis of AA was self-reported, included symptomatic and asymptomatic clinical diagnosis and were not restricted to any particular mode of diagnosis. The key predictor variable, total hours of radiation exposure, was calculated by multiplying "approximate hours of occupational radiation exposure per week" by 52 and "years of occupational radiation exposure."

We compared the likelihood of AA among cardiologists with significant radiation exposure to minimally radiated cardiologists, and, in the process, determined the impact of occupational radiation exposure on cardiovascular health. Frequencies and percentages are presented for the following groups: (1) prevalence of comorbidities among those with and without AA $>$ 50 years of age; (2) demographic, social, and occupational characteristics among those with 10,000 h or less of radiation exposure versus greater than 10,000 h; (3) prevalence of comorbidities among those with 10,000 h or less of radiation exposure versus greater than 10,000 h; (4) demographic, social, and occupational characteristics among all cardiologists vs. those with AA; (5) prevalence of AA based on procedure performed. Each of these groups was compared with Chi-square test or Fisher's exact test when expected cell count was $<$ 5. Bivariate and multivariable logistic regression analyses were conducted to determine the association of AA with key demographic factors, comorbidities and total hours of radiation exposure. Results were

considered statistically significant at $p < 0.05$. All analyses were conducted in SPSS version 27.0 (17).

RESULTS

Characteristics of Respondents

The survey was completed by 1,478 cardiologists (8.8% response rate); ∼10% response rate among interventional cardiologists and electrophysiologists and 7% response rate among other subspecialties (16). The respondents were predominately male (86.1%) and white/Caucasian (79.0%). The median age was 56–60 years; two-thirds were ≥65 years of age (**Supplementary Table 1**). Interventional cardiologists constituted 35.6% of the respondents and 16.4% were electrophysiologists (**Figure 1A**). A chest/abdomen protective lead attire (vest or apron) was always worn by 73.3% of invasive cardiologists (interventional cardiologists and electrophysiologists). As outlined in **Supplementary Table 2** and **Figure 1B**, the procedures most performed by the survey participants were angiography (45.1%), percutaneous coronary interventions (44.1%), coronary thrombectomy (35.4%), and pacemaker/defibrillator placement (33.6%). Pulsed fluoroscopy was the primary imaging modality, used by 44.2% of the respondents who used imaging, compared to 19.7 and 9.3% who used low and high dose cineangiography, respectively. Among their social habits, 74.7% of all participants consumed alcohol and 2.2% were current tobacco users. Various co-morbidities were observed among respondents (**Supplementary Table 3**), including AA (11.1%), cancer (11.3%), cataracts (18.1%), carotid artery disease (1.4%), CAD (8.7%), DM (5.5%), dyslipidemia (27.1%), HTN (30.4%), OSA (8.0%), and stroke/transient ischemic attack (TIA) (2.5%).

Radiation Exposure and AA

Aligning with the objective of the study, a focused analysis regarding the risk of AA was performed. Among the respondents, 9.2% had AF, 3.3% had frequent premature atrial contractions, 2.6% had Afl, and 1.6% had AT, leading to an AA prevalence of 11.1% among our participants. AA was significantly more prevalent among men than women (15.7 vs 5.4%, $p = 0.004$) and in those ≥65 years of age vs. those < 65 years of age (21.4 vs. 8.7%, $p < 0.001$). The likelihood of AA was significantly lower among cardiologists performing any of the following procedures: atherectomy, electrophysiologic studies, irregular rhythm ablations, and pacemaker/defibrillator lead extractions (**Supplementary Table 2**, **Figure 1B**). There was an approximately two-fold increase in AA prevalence in the presence of the following risk factors: DM (23.2% AA in those with DM vs. 10.4% AA in those without DM, $p < 0.001$), CAD (34.9% vs 8.8%, $p < 0.001$), HTN (16.0% vs 8.9%, $p < 0.001$), and OSA (26.3% vs 9.8%, $p < 0.001$). To determine the association between radiation exposure and the risk of AA, we first examined the distribution of respondents with AA stratified by age groups, as a function of hours of exposure to radiation. We found a clear separation of the number of respondents reporting AA around 10,000 h of exposure (**Figure 2A**). As most cardiologists <50 years of age had <10,000 h of exposure to radiation, and the conditions being evaluated generally increase with age, we focused on cardiologists >50 years of age. To validate the threshold of 10,000 h of exposure to radiation to study its relationship to AA, another well-established, rarely disputed consequence of occupational radiation exposure among cardiologists, namely cataracts, was initially investigated. **Figure 2B** shows the increased manifestation of cataracts with age and with increasing hours of exposure to radiation. A multivariable regression analysis showed that apart from age, >10,000 h of radiation exposure was an independent risk factor for the likelihood of cataracts (adjusted OR 1.72; 95% CI 1.24–2.37, $p = 0.001$), in agreement with historical data. Based on this, further investigations regarding the influence of radiation exposure on the cardiovascular health of cardiologists was focused on the 1,033 participants who were >50 years of age (**Supplementary Figure 1**).

Baseline Characteristics of Cardiologists > 50 Years of Age Based on Exposure Hours

Compared to those with low radiation exposure (≤10,000 h), those with high radiation exposure (> 10,000 h) were more likely to be male (93.4% males in high exposure group vs. 86.7% in low exposure group, $p = 0.005$) and were more likely to be interventional cardiologists/electrophysiologists rather than another sub-specialty (79.4 vs. 20.6%, $p < 0.001$, **Table 1**). Cardiologists with high radiation exposure were significantly more likely to perform the procedures outlined in **Table 1**. Alcohol consumption and tobacco use were similar in the two groups. Approximately 43% of cardiologists in the low radiation exposure group did not have any type of occupational radiation exposure. Most cardiologists' institutions monitor radiation exposure (71.2% cardiologists) via dosimetry; among these, only 3.6% of cardiologists had crossed their institution's threshold (4.6% in low exposure vs. 2.6% in high exposure, $p = 0.15$). Almost all of the cardiologists (99.1%) with high radiation exposure wore lead attire covering the thoracic/abdominal area (vest or apron); 12.3 and 3.7% wore protective attire covering the head and shins, respectively; and 87.5% of high radiation exposed cardiologists used a front shield during procedures.

Risk of AA in Cardiologists > 50 Years of Age Based on Total Hours of Radiation Exposure

Among cardiologists >50 years of age, the difference in the risk of AA based on specific procedures was not significant. However, when categorized by subspecialty, electrophysiologists and interventional cardiologists combined had a significantly lower prevalence of AA compared to other types of cardiologists (10.5 vs. 18.5%, $p < 0.001$). The effects of traditional risk factors on the prevalence of AA were assessed in cardiologists and found to be similar to those in the general population. There was an increased prevalence of DM, CAD, congestive heart failure (CHF), OSA, and valvular heart disease in cardiologists with AA compared to those without AA (**Supplementary Table 3**).

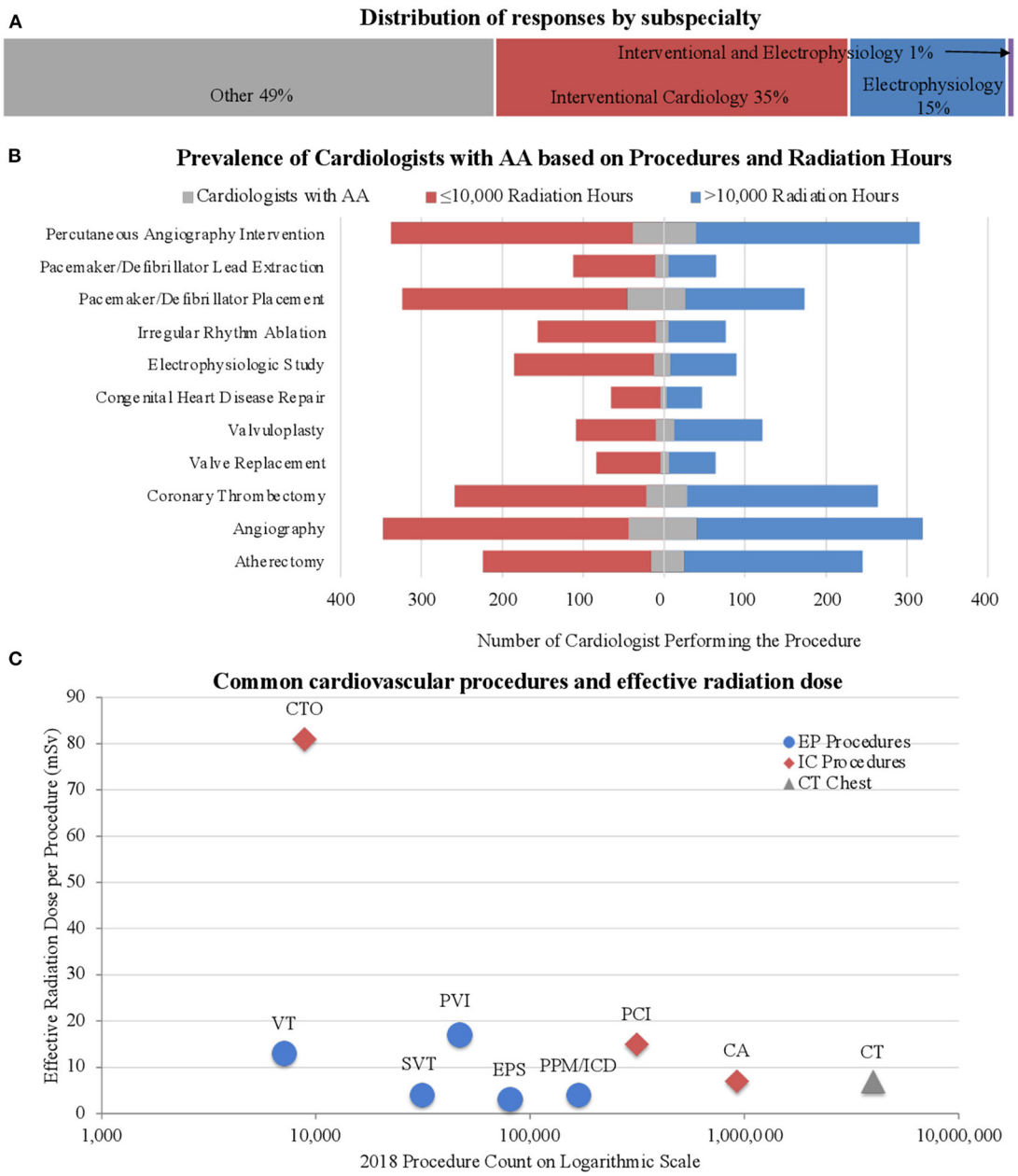

FIGURE 1 | Subspecialty and procedural distribution. **(A)** Distribution of responses based on subspecialty. Approximately half the respondents were invasive cardiologists. **(B)** Prevalence of AA among cardiologists based on type of procedure. Note the increased occurrence of AA among those with lower radiation exposure, especially in those performing pacemaker/defibrillator placement. **(C)** The number of procedures performed in the United States was collected from the 2018 CMS Part B National Summary Data File (18). The effective dose of radiation per procedure was determined through a review of the literature (19, 20). Our survey participants reported procedure frequencies consistent with those found nationwide from the 2018 data as described. The chest CT is depicted as a reference value. CTO, Chronic Total Occlusion; VT, VT ablation; SVT, SVT ablation; PVI, Pulmonary vein Isolation; EPS, EP Study; PPM/ICD, Pacemaker and ICD Placement; PCI, Percutaneous Coronary Intervention; CA, Coronary Angiography; CT, Chest CT (Reference).

A significant decrease in AA was observed among cardiologists with high radiation exposure compared to those with low radiation exposure (11.1 vs. 16.7%, $p = 0.019$, **Table 2**). Apart from cataracts, which were more prevalent in those with high radiation exposure (30.9 vs. 23%, $p = 0.007$), other medical conditions, many of which are risk factors for AA, were equally distributed in the two groups, including cancer (15.3% in low exposure vs. 14.6% in high exposure, $p = 0.766$), CAD (13.6 vs. 10.3%, $p = 0.132$), DM (7.6 vs. 6.9%, $p = 0.683$), HTN (38.0 vs. 41.1%, $p = 0.326$), and OSA (9.7 vs. 11.7%, $p = 0.326$), indicating that these co-morbidities did not play a significant role in the difference in prevalence of AA in the low and high radiation exposure groups.

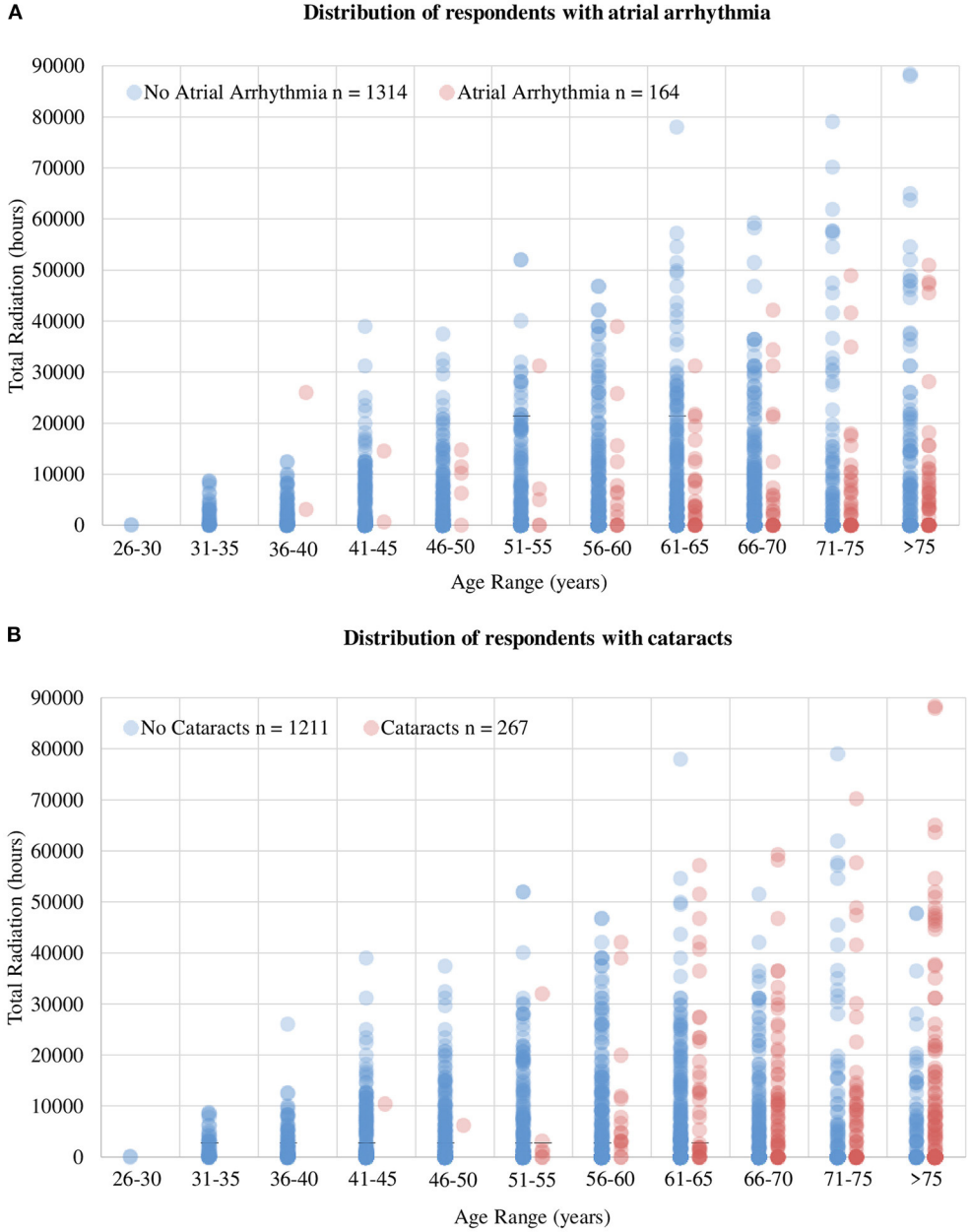

FIGURE 2 | Distribution of respondents with AA and cataracts. **(A)** Total number of radiation hours per age group in cardiologists reporting AA and those without AA. It exhibits a clear delineation of number of cases of AA around 10,000 h of radiation and 50 years of age, leading to the thresholds used to stratify response during analysis. **(B)** The influence of age and total radiation hours on the prevalence of cataracts. The influence of increasing age on the prevalence of cataracts is evident but more importantly, note the increased prevalence of cataracts with increasing total hours of radiation, indicating the accuracy of the dataset collected as well as validating the selection of 10,000 radiation hours as the threshold to delineate exposure groups.

A multivariable logistic regression was performed to identify the risk factors and protective factors of AA (**Table 3**) adjusting for age, sex, race, DM, HTN, and OSA. Apart from confirming the traditional risk factors of AA such as age, sex, and OSA, results also showed that exposure to >10,000 h of radiation was an independent protective factor against the risk of AA (adjusted OR 0.57; 95% CI 0.38–0.85, $p = 0.007$). The role played by personal radiation exposure, such as that received during CT scans and X-rays for personal healthcare, was also accounted for. There was a significantly lower prevalence of personal radiation exposure in the high occupational exposure group compared to low exposure group (81.6 vs. 88.2%, $p = 0.002$). As expected, there was a significantly higher prevalence of stroke/TIA in the setting of AA compared to without AA (5.9 vs. 2.8%, $p = 0.049$) but there was no significant difference of stroke/TIA among cardiologists based on hours

TABLE 1 | Demographics, social, and occupational history based on hours of radiation exposure.

		# of Cardiologists with ≤10,000 h (%) $n = 648$*	# of Cardiologists with > 10,000 h (%) $n = 350$*	p-value†
Demographic characteristics				
Sex	Male	560 (86.7%)	325 (93.4%)	0.005
	Female	84 (13.0%)	22 (6.3%)	
Age	≥ 66 years	309 (47.7%)	160 (45.7%)	0.552
	51–65 years	339 (52.3)	190 (54.3)	
Race	White/Caucasian	568 (88.2%)	304 (87.6%)	0.453
	Black/African American	11 (1.7%)	3 (0.9%)	
	Other	65 (10.1%)	40 (11.5%)	
Ethnicity	Hispanic	15 (2.6%)	12 (3.6%)	0.355
Social history				
Hx of alcohol use		519 (80.6%)	279 (80.2%)	0.874
Hx of alcohol abuse		46 (7.2%)	14 (4.1%)	0.051
Hx of tobacco use	Present, current	12 (1.9%)	9 (2.6%)	0.750
	Absent, quit	578 (90.3%)	311 (89.4%)	
	Absent, never	50 (7.8%)	28 (8.0%)	
Occupational history				
Type of cardiologist	EP and interventional cardiology	194 (29.9%)	278 (79.4%)	<0.001
	Other	454 (70.1%)	72 (20.6%)	
Type of procedure	Atherectomy	90 (13.9%)	204 (58.3%)	<0.001
	Angioplasty	189 (29.2%)	272 (77.7%)	<0.001
	Coronary thrombectomy	120 (18.5%)	223 (63.7%)	<0.001
	Transcatheter valve replacement	20 (3.1%)	41 (11.7%)	<0.001
	Valvuloplasty	41 (6.3%)	93 (26.6%)	<0.001
	Congenital heart disease repair	27 (4.2%)	34 (9.7%)	<0.001
	Electrophysiologic study	97 (15.0%)	71 (20.3%)	0.032
	Irregular rhythm ablation	72 (11.1%)	58 (16.6%)	0.014
	Pacemaker/defibrillator placement	201 (31.0%)	148 (42.3%)	<0.001
	Pacemaker/defibrillator lead Extraction	51 (7.9%)	53 (15.1%)	<0.001
	Percutaneous angiographic intervention	180 (27.8%)	271 (77.4%)	<0.001
Imaging most used	Pulsed fluoroscopy	209 (32.4%)	209 (60.2%)	<0.001
	Low-frame cineangiography	93 (14.4%)	92 (26.5%)	
	High-frame cineangiography	66 (10.2%)	46 (13.3%)	
	None	277 (42.9%)	0 (0.0%)	
Dosimetry threshold	Crossed	17 (4.6%)	9 (2.6%)	0.150
	Never crossed	352 (95.4%)	338 (97.4%)	
Protective attire	Head cap	41 (6.3%)	43 (12.3%)	0.001
	Shin shields	5 (0.8%)	13 (3.7%)	0.001
	Front shield	287 (77.4%)	302 (87.5%)	<0.001
	Vest or apron	368 (56.8%)	347 (99.1%)	<0.001

*Sample number may vary due to exclusion of respondents electing to not answer.
†Chi-squared test, $p < 0.05$ is considered significant.

of radiation (3.1% in low exposure vs. 3.1% in high exposure, $p = 0.961$).

DISCUSSION

Occupational radiation exposure in cardiologists may be associated with various complications. A few of these are well established, e.g., orthopedic complications and cataracts, while others are actively being investigated, e.g., infertility, but its effects on AA have not been previously explored (21). Historically, high-dose radiation (5,000 mSv) and moderate-dose radiation exposure (>500 mSv) were thought to have significant cardiovascular effects, such as stroke and heart disease; however, the degree of cardiovascular risk associated with lower doses (<500 mSv) is currently unknown (22–24). Invasive cardiologists, i.e., those exposed to chronic high levels of occupational radiation exposure, such as interventional cardiologists and electrophysiologists, are a unique population

TABLE 2 | Prevalence of medical conditions based on hours of radiation.

	≤10,000 h prevalence (%) $n = 648$[a]	> 10,000 h prevalence (%) $n = 350$[a]	p-value[b]
Medical condition			
Atrial arrhythmia	108 (16.7%)	39 (11.1%)	0.019
Aortic atherosclerosis	23 (3.5%)	14 (4.0%)	0.719
Cancer	99 (15.3%)	51 (14.6%)	0.766
Cardiomyopathy	6 (0.9%)	5 (1.4%)	0.530
Carotid artery disease	14 (2.2%)	6 (1.7%)	0.631
Cataracts	149 (23.0%)	108 (30.9%)	0.007
Chronic obstructive pulmonary disease	7 (1.1%)	5 (1.4%)	0.762
Congestive heart failure	10 (1.5%)	1 (0.3%)	0.109
Coronary artery disease	88 (13.6%)	36 (10.3%)	0.132
Dermatitis	20 (3.1%)	16 (4.6%)	0.230
Diabetes mellitus	49 (7.6%)	24 (6.9%)	0.683
Dyslipidemia	215 (33.2%)	119 (34.0%)	0.793
Hypertension	246 (38.0%)	144 (41.1%)	0.326
Infertility	12 (1.9%)	8 (2.3%)	0.641
Ischemic heart disease	35 (5.4%)	14 (4.0%)	0.328
Myocarditis	3 (0.5%)	0 (0.0%)	0.556
Obstructive sleep apnea	63 (9.7%)	41 (11.7%)	0.326
Peripheral vascular disease	7 (1.1%)	4 (1.1%)	1.000
Pulmonary fibrosis	4 (0.6%)	0 (0.0%)	0.304
Pulmonary hypertension	2 (0.3%)	1 (0.3%)	1.000
Stroke/transient ischemic attack	20 (3.1%)	11 (3.1%)	0.961
Thyroid disease	51 (7.9%)	21 (6.0%)	0.276
Valvular heart disease	26 (4.0%)	15 (4.3%)	0.836

[a]*Sample number may vary due to exclusion of respondents electing to not answer.*
[b]*Chi-squared test, $p < 0.05$ is considered significant.*

TABLE 3 | Odds of atrial arrhythmia in cardiologists.

	Unadjusted OR (95% CI)[a]	p-value[b]	Adjusted OR (95% CI)[a]	p-value[b]
Atrial arrhythmia (>50 years)				
Age	1.53 (1.36–1.72)	<0.001	1.49 (1.32–1.69)	<0.001
Sex	3.29 (1.41–7.58)	0.006	2.44 (1.20–5.81)	0.043
Race (Black/African American)	0.72 (0.16–3.17)	0.665	1.50 (0.32–7.04)	0.605
Diabetes mellitus	2.02 (1.15–3.54)	0.014	1.20 (0.65–2.21)	0.568
Hypertension	1.38 (0.97–1.95)	0.070	0.92 (0.63–1.35)	0.662
Obstructive sleep apnea	2.53 (1.60–4.02)	<0.001	2.04 (1.23–3.37)	0.006
>10,000 radiation hours	0.63 (0.42–0.93)	0.020	0.57 (0.38–0.86)	0.007

[a]*Odds ratio with 95% confidence interval.*
[b]*$p < 0.05$ is considered significant.*

with consistent longitudinal exposure to low doses of radiation limited to the periphery. Although they are not exposed to the direct X-ray beam, invasive cardiologists receive radiation from the scatter, which can vary extremely, ranging from 0.04 to 38 μSv per procedure (25). Over the course of an interventional cardiologist's career, he or she is exposed to 50–200 mSv of ionizing radiation, which is equivalent to 2,500–10,000 chest X-rays (9, 12, 14, 15, 26). Newer techniques focus on minimizing, or even eliminating radiation use but these protocols are not widespread (27, 28). Most procedures still require some degree of radiation exposure. Using information gathered from the literature review (29), **Figure 1C** demonstrates the degree of radiation exposure based on the type of procedures performed and the number of each procedure performed per year. The number of each type of procedure performed nationwide is similar to those performed by our survey participants, providing additional validation of an accurate random sampling.

This study noted a self-reported lower prevalence of AA in cardiologists >50 years of age with >10,000 h of radiation exposure compared to cardiologists >50 years of age with ≤10,000 h of radiation exposure. Electrophysiologists and interventional cardiologists combined had a significantly lower prevalence of AA compared to other types of cardiologists (10.5 vs. 18.5%, $p < 0.001$). A multivariable regression analysis was performed to adjust for well-established risk factors of AA such as age, sex, OSA, HTN and DM, and >10,000 h of radiation was statistically less likely to be associated with AA when compared to ≤10,000 h of radiation. Well established risk factors of AA, such as age, male sex, HTN, DM, OSA, were still found to be significant risk factors within our data set in univariate analysis, internally validating our dependent variable (AA). In addition, the most studied and widely accepted consequence of occupational radiation exposure, cataracts, was significantly more prevalent among those with high radiation exposure compared to those with low radiation exposure, validating the independent variable (radiation exposure) as well. The prevalence of co-morbidities such as CAD, HTN, DM, and OSA were not significantly different between the low and high radiation exposure groups, further solidifying the evidence that the difference in likelihood of AA is dependent on a secondary factor, possibly their occupational radiation exposure. Given the design of this study, these findings should be interpreted with caution, however, it lays the foundation for further investigation.

The general benefits of low-dose radiation have been studied before but the specifics of the mechanism by which low doses of radiation might be protective against AA is limited and most likely multifactorial. A few theories can provide a possible

explanation for this paradoxical finding, all of which may vary in significance.

Systemic inflammatory mechanisms have been implicated in the initiation and progression of arrhythmias, especially AF (30–32). Inflammation causes variation in membrane potential and ion channel disturbances, leading to cardiac fibrosis, which is a prominent substrate for arrhythmias (30, 31). Several controlled studies have shown increased levels of inflammatory markers in patients with AF compared to those in sinus rhythm (30, 31, 33). Low doses of ionizing radiation have anti-inflammatory effects through various mechanisms at the molecular level (34–38). These mechanisms may depress inflammation in cardiac tissue leading to a decrease in the likelihood of AA among cardiologists exposed to increased cumulative levels of low-dose radiation. However, prior studies were mostly performed with a single dose of radiation. Future studies should identify whether low doses of radiation experienced over a prolonged period have similar consequences of inflammation.

A recent mechanism implicated in AA progression, especially in AF, is DNA damage induced metabolic remodeling of cardiac tissue (39). Considering this finding, the cytogenetic adaptive response can elucidate the benefits of low-dose radiation in protection against DNA damage (40–43). In fact, multiple studies have shown the ability of low-dose radiation to stimulate DNA repair mechanisms, including in interventional cardiologists (29, 43).

The protective effect of radiation may be augmented or confounded by the lifestyle of the invasive cardiologists, since they are among the most physically active members of the profession, at least in the workplace. Most invasive cardiology procedures require protective attire and long hours of standing, which, by itself, may improve physical fitness. To prepare for the increased physical demands of the profession, it may be expected that invasive cardiologists are a healthcare population conscious of their physical fitness. Unfortunately, the physical fitness of the cardiologists was not assessed in the survey, and the literature is limited as well. Further study is required to determine the lifestyle variability among different types of cardiologists and its effect on their cardiovascular health.

LIMITATIONS

The self-reported survey-based method of data collection is a major limitation; however, the fact that the population under investigation comprised board-certified health professionals, whose job it is to diagnose community members with the exact same conditions included in the survey, partially compensates for the self-reported format of this study. The alignment of risk factors of AA determined from this dataset with well-established risk factors provides additional confirmation regarding the accuracy of the dataset. Moreover, having cardiologists serve as both the low and high radiation exposure groups accounts for unknown confounding variables associated with the profession that cannot be adjusted by statistical analysis. An 8.8% response rate introduces the concern for selection bias and there is a high chance of responders and non-responders varying in subspeciality, level of experience and radiation exposure, and prevalence of AA due to personal interest in the study which need to be considered. However, the subspeciality response rate is similar in the responders compared to non-responders. Radiation exposure in this survey was measured in lifetime hours rather than actual dosage which is seldom tracked by physicians themselves. Over the years, there have been significant advancement in radiation protection so "lifetime radiation hours" may vary from "true radiation exposure hours" based on a cardiologist's years of practice. Nevertheless, the positive correlation of this measure with the risk of cataracts in this study population validates the methodology.

The cross-sectional de-identified nature of this study does not allow for follow-up with the participants to deduce the timeline of cataracts or AA as it pertains to the course of their radiation exposure. In addition, the amount of radiation exposure per procedure varies based on the institutional setting, the level of training, and the quality of or adherence to protective apparel. Physicians at academic institutions and fellows-in-training endure more radiation than their experienced, non-teaching counterparts, which should be considered when interpreting this data. Further study is merited to account for these intrinsic shortcomings (14).

CONCLUSION

In this survey-based study of board-certified cardiologists, increased hours of radiation exposure was associated with decreased prevalence of AA, independent of conventional risk factors. This is a hypothesis generating study and a variety of theories can explain these paradoxical findings. Further long-term investigation is warranted in a larger and more detailed population to properly identify the factors that modify the risk of AA in cardiologists.

DATA AVAILABILITY STATEMENT

The raw data supporting the conclusions of this article will be made available by the authors, without undue reservation.

ETHICS STATEMENT

The studies involving human participants were reviewed and approved by Louisiana State University Health Sciences Center Shreveport Institutional Review Board. Written informed consent for participation was not required for this study in accordance with the national legislation and the institutional requirements.

AUTHOR CONTRIBUTIONS

PD devised the study objective, study design, and the survey along with RT, CV, and SJ. Survey questions were revised based on critical input from SCha, SChu, RH, MB, PK, and SB. PD served as the principal investigator. RB performed the statistical analysis and aided in

interpretation of the results. Acquisition and interpretation of data was performed by all authors. The manuscript was written by RT, CV, RB, and PD. Critical revision of the manuscript for important intellectual content was provided by SCha, SChu, RH, MB, PK, RG, BO, and SB. All authors contributed to the article and approved the submitted version.

FUNDING

This study was funded by an institutional grant, for which C.G. Kevil is the institution's PI.

ACKNOWLEDGMENTS

We appreciate Angela Bennett for her assistance in acquiring Institutional Review Board (IRB) Approval and Georgia Morgan for editing this manuscript. We thank all participating cardiologists for their dedication to research and, more importantly, their communities.

SUPPLEMENTARY MATERIAL

The Supplementary Material for this article can be found online at: https://www.frontiersin.org/articles/10.3389/fcvm.2022.863939/full#supplementary-material

Supplemental Material 1 | Cardiovascular health of cardiologists.

Supplemental Figure 1 | Graphical representation of participant recruitment to final study cohort. Participants were recruited through three professional cardiovascular societies. There was an 8.8% response rate among those who received the survey, of which, 1,033 participants were included in the final study (>50 years of age). Interventional cardiologists and electrophysiologists predominately had >10,000 h of radiation exposure while all other specialties predominately had ≤10,000 h of radiation exposure.

Supplemental Table 1 | Prevalence of atrial arrhythmia in cardiologists based on characteristics (all respondents sample).

Supplemental Table 2 | Prevalence of atrial arrhythmia in cardiologists performing each procedure.

Supplemental Table 3 | Prevalence of comorbidity in cardiologists based on presence of atrial arrhythmia ($n = 1{,}033$).

Supplemental Table 4 | Prevalence of atrial arrhythmia in cardiologists based on characteristics (>50 years of age respondents sample).

REFERENCES

1. Alsaddique AA. Impact of advances in invasive cardiology on cardiac surgery. *Open Cardiovasc Med J.* (2009) 3:21–5. doi: 10.2174/1874192400903010021
2. United Nations Scientific Committee on the Effects of Atomic Radiation. *Sources and Effects of Ionizing Radiation. UNSCEAR 2008 Report to the General Assembly, 63rd Session.* Supplement No. 46. Volume 1, Annex A, 21-220 (2008). Available online at: https://www.unscear.org/unscear/en/publications/2008_1.html (accessed November 27, 2020).
3. Sun Z, AbAziz A, Yusof AK. Radiation-induced noncancer risks in interventional cardiology: optimisation of procedures and staff and patient dose reduction. *Biomed Res Int.* (2013) 2013:976962. doi: 10.1155/2013/976962
4. Mohammadi M, Danaee L, Alizadeh E. Reduction of radiation risk to interventional cardiologists and patients during angiography and coronary angioplasty. *J Tehran Heart Cent.* (2017) 12:101–6. Retrieved from: https://jthc.tums.ac.ir/index.php/jthc
5. Vadmann H, Nielsen PB, Hjortshøj SP, Riahi S, Rasmussen LH, Lip GY, et al. Atrial flutter and thromboembolic risk: a systematic review. *Heart.* (2015) 101:1446–55. doi: 10.1136/heartjnl-2015-307550
6. Al Ghamdi B, Hassan W. Atrial remodeling and atrial fibrillation: mechanistic interactions and clinical implications. *J Atr Fibrillation.* (2009) 2:125. doi: 10.4022/jafib.125
7. Morillo CA, Banerjee A, Perel P, Wood D, Jouven X. Atrial fibrillation: the current epidemic. *J Geriatr Cardiol.* (2017) 14:195–203. doi: 10.11909/j.issn.1671-5411.2017.03.011
8. Lippi G, Sanchis-Gomar F, Cervellin G. Global epidemiology of atrial fibrillation: an increasing epidemic and public health challenge. *Int J Stroke.* (2021) 16:217–21. doi: 10.1177/1747493019897870
9. Vaidya V, Liang J, Sio T, Cha S, Nkomo V, Melduni R, et al. Atrial fibrillation after thoracic radiotherapy for cancer: examining differences in clinical characteristics at time of diagnosis compared with the general population. *J Am Coll Cardiol.* 2015;65(10_Supplement):A318. doi: 10.1016/S0735-1097(15)60318-7
10. Lentz R, Chalazan B, Kolek M, Farber-Eger E, Wells Q, Moslehi J, et al. Radiation therapy is not associated with incident atrial fibrillation in patients with thoracic cancer. *Circulation.* (2015) 132:A17218. doi: 10.1161/circ.132.suppl_3.17218
11. Chambers CE. Occupational health risks in interventional cardiology. *J Am Coll Cardiol Intv.* (2015) 8:628–630. doi: 10.1016/j.jcin.2015.01.015
12. Zhang DM, Navara R, Yin T, Szymanski J, Goldsztejn U, Kenkel C, et al. Cardiac radiotherapy induces electrical conduction reprogramming in the absence of transmural fibrosis. *Nat Commun.* (2021) 12:5558. doi: 10.1038/s41467-021-25730-0
13. Cuculich PS, Schill MR, Kashani R, Mutic S, Lang A, Cooper D, et al. Noninvasive cardiac radiation for ablation of ventricular tachycardia. *N Engl J Med.* (2017) 377:2325–36. doi: 10.1056/NEJMoa1613773
14. Abbott JD. Controlling radiation exposure in interventional cardiology. *Circ Cardiovasc Interv.* (2014) 7:425–8. doi: 10.1161/CIRCINTERVENTIONS.114.001815
15. Picano E, Vano E, Domenici L, Bottai M, Thierry-Chef I. Cancer and non-cancer brain and eye effects of chronic low-dose ionizing radiation exposure. *BMC Cancer.* (2012) 12:157. doi: 10.1186/1471-2407-12-157
16. Narang A, Sinha SS, Rajagopalan B, Ijioma NN, Jayaram N, Kithcart AP, et al. The supply and demand of the cardiovascular workforce: striking the right balance. *J Am Coll Cardiol.* (2016) 68:1680–9. doi: 10.1016/j.jacc.2016.06.070
17. IBM Corp. *Released 2020. IBM SPSS Statistics for Windows, Version 27.0.* Armonk, NY: IBM Corp (2020).
18. U.S. Centers for Medicare & Medicaid Services. *Part B National Summary Data File.* (2018). Availalbe online at: ttps://www.cms.gov/Research-Statistics-Data-and-Systems/Downloadable-Public-Use-Files/Part-B-National-Summary-Data-File/Overview
19. Padmanabhan D, Shankar S, Chandrashekharaiah A, Deshpande S. Strategies to reduce radiation exposure in electrophysiology and interventional cardiology. *US Cardiol Rev.* (2019) 13:117–22. doi: 10.15420/usc.2019.21.2
20. Picano E, Vano E. The radiation issue in cardiology: The time for action is now. *Cardiovasc Ultrasound.* (2011) 9:35. doi: 10.1186/1476-7120-9-35
21. Sarkozy A, De Potter T, Heidbuchel H, Ernst S, Kosiuk J, Vano E, et al. Occupational radiation exposure in the electrophysiology laboratory with a focus on personnel with reproductive potential and during pregnancy: a European Heart Rhythm Association (EHRA) consensus document endorsed by the Heart Rhythm Society (HRS). Erratum in: Europace. 2018;20(4):574. *Europace.* (2017) 19:1909–1922. doi: 10.1093/europace/eux252
22. Schultz-Hector S, Trott KR. Radiation-induced cardiovascular diseases: is the epidemiologic evidence compatible with the radiobiologic data? *Int J Radiat Oncol Biol Phys.* (2007) 67:10–8. doi: 10.1016/j.ijrobp.2006.08.071

23. Kreuzer M, Auvinen A, Cardis E, Hall J, Jourdain JR, Laurier D, et al. Low-dose ionising radiation and cardiovascular diseases—strategies for molecular epidemiological studies in Europe. *Mutat Res Rev Mutat Res.* (2015) 764:90–100. doi: 10.1016/j.mrrev.2015.03.002
24. Kamiya K, Ozasa K, Akiba S, Niwa O, Kodama K, Takamura N, et al. Long-term effects of radiation exposure on health. *Lancet.* (2015) 386:469–78. doi: 10.1016/S0140-6736(15)61167-9
25. Gori T, Münzel T. Biological effects of low-dose radiation: of harm and hormesis. *Eur Heart J.* (2012) 33:292–5. doi: 10.1093/eurheartj/ehr288
26. Moreira LA, Silva EN, Ribeiro ML, Martins Wde A. Cardiovascular effects of radiotherapy on the patient with cancer. *Rev Assoc Med Bras.* (2016) 62:192–6. doi: 10.1590/1806-9282.62.02.192
27. Di Cori A, Zucchelli G, Faggioni L, Segreti L, De Lucia R, Barletta V, et al. Role of pre-procedural CT imaging on catheter ablation in patients with atrial fibrillation: procedural outcomes and radiological exposure. *J Interv Card Electrophysiol.* (2021) 60:477–84. doi: 10.1007/s10840-020-00764-4
28. Di Cori A, Zucchelli G, Segreti L, Barletta V, Viani S, Paperini L, et al. Predictors of zero X ray procedures in supraventricular arrhythmias ablation. *Int J Cardiovasc Imaging.* (2020) 36:1599–607. doi: 10.1007/s10554-020-01884-8
29. Russo GL, Tedesco I, Russo M, Cioppa A, Andreassi MG, Picano E. Cellular adaptive response to chronic radiation exposure in interventional cardiologists. *Eur Heart J.* (2012) 33:408–14. doi: 10.1093/eurheartj/ehr263
30. Boos CJ, Anderson RA, Lip GY. Is atrial fibrillation an inflammatory disorder? *Eur Heart J.* (2006) 27:136–49. doi: 10.1093/eurheartj/ehi645
31. Vonderlin N, Siebermair J, Kaya E, Köhler M, Rassaf T, Wakili R. Critical inflammatory mechanisms underlying arrhythmias. *Herz.* (2019) 44:121–9. doi: 10.1007/s00059-019-4788-5
32. Nakamura Y, Nakamura K, Fukushima-Kusano K, Ohta K, Matsubara H, Hamuro T, et al. Tissue factor expression in atrial endothelia associated with nonvalvular atrial fibrillation: possible involvement in intracardiac thrombogenesis. *Thromb Res.* (2003) 111:137–42. doi: 10.1016/s0049-3848(03)00405-5
33. Hu YF, Chen YJ, Lin YJ, Chen SA. Inflammation and the pathogenesis of atrial fibrillation. *Nat Rev Cardiol.* (2015) 12:230–43. doi: 10.1038/nrcardio.2015.2
34. Arenas M, Gil F, Gironella M, Hernández V, Biete A, Piqué JM, et al. Time course of anti-inflammatory effect of low-dose radiotherapy: correlation with TGF-beta(1) expression. *Radiother Oncol.* (2008) 86:399–406. doi: 10.1016/j.radonc.2007.10.032
35. Rodionova N, Ganzha O, Makovetska L, Druzhyna M, Muzalov I, Mikhailenko V. Effect of low dose ionising radiation and nitric oxide on the state of animal blood system. *Probl Radiac Med Radiobiol.* (2013) 18:366–72. Retrieved from: http://radiationproblems.org.ua/abstract17_248.html
36. Rödel F, Schaller U, Schultze-Mosgau S, Beuscher HU, Keilholz L, Herrmann M, et al. The induction of TGF-beta(1) and NF-kappaB parallels a biphasic time course of leukocyte/endothelial cell adhesion following low-dose X-irradiation. *Strahlenther Onkol.* (2004) 180:194–200. doi: 10.1007/s00066-004-1237-y
37. Hildebrandt G, Maggiorella L, Rödel F, Rödel V, Willis D, Trott KR. Mononuclear cell adhesion and cell adhesion molecule liberation after X-irradiation of activated endothelial cells in vitro. *Int J Radiat Biol.* (2002) 78:315–25. doi: 10.1080/09553000110106027
38. Gaipl US, Meister S, Lödermann B, Rödel F, Fietkau R, Herrmann M, et al. Activation-induced cell death and total Akt content of granulocytes show a biphasic course after low-dose radiation. *Autoimmunity.* (2009) 42:340–2. doi: 10.1080/08916930902831233
39. Ramos KS, Brundel BJJM, DNA. Damage, an innocent bystander in atrial fibrillation and other cardiovascular diseases? *Front Cardiovasc Med.* (2020) 7:67. doi: 10.3389/fcvm.2020.00067
40. Liu SZ. Cancer control related to stimulation of immunity by low-dose radiation. *Dose Response.* (2006) 5:39–47. doi: 10.2203/dose-response.06-108.Liu
41. Liu SZ. Biological effects of low level exposures to ionizing radiation: theory and practice. *Hum Exp Toxicol.* (2010) 29:275–81. doi: 10.1177/0960327109363967
42. Jin S, Jiang H, Cai L. New understanding of the low-dose radiation-induced hormesis. *Radiat Med Prot.* (2020) 1:2–6. doi: 10.1016/j.radmp.2020.01.004
43. Liu SZ, Liu WH, Sun JB. Radiation hormesis: its expression in the immune system. *Health Phys.* (1987) 52:579–83. doi: 10.1097/00004032-198705000-00008

Conflict of Interest: The authors declare that the research was conducted in the absence of any commercial or financial relationships that could be construed as a potential conflict of interest.

frontiers | Frontiers in Cardiovascular Medicine

REVIEW
published: 15 June 2022
doi: 10.3389/fcvm.2022.891399

The Genetics and Epigenetics of Ventricular Arrhythmias in Patients Without Structural Heart Disease

*Mengru Wang and Xin Tu**

Key Laboratory of Molecular Biophysics of the Ministry of Education, Center for Human Genome Research, College of Life Science and Technology, Huazhong University of Science and Technology, Wuhan, China

Ventricular arrhythmia without structural heart disease is an arrhythmic disorder that occurs in structurally normal heart and no transient or reversible arrhythmia factors, such as electrolyte disorders and myocardial ischemia. Ventricular arrhythmias without structural heart disease can be induced by multiple factors, including genetics and environment, which involve different genetic and epigenetic regulation. Familial genetic analysis reveals that cardiac ion-channel disorder and dysfunctional calcium handling are two major causes of this type of heart disease. Genome-wide association studies have identified some genetic susceptibility loci associated with ventricular tachycardia and ventricular fibrillation, yet relatively few loci associated with no structural heart disease. The effects of epigenetics on the ventricular arrhythmias susceptibility genes, involving non-coding RNAs, DNA methylation and other regulatory mechanisms, are gradually being revealed. This article aims to review the knowledge of ventricular arrhythmia without structural heart disease in genetics, and summarizes the current state of epigenetic regulation.

Keywords: gene, pathogenesis, non-structural ventricular arrhythmias with genome, ventricular arrhythmias, non-structural heart disease

OPEN ACCESS

Edited by:
Guowei Li,
Guangdong Second Provincial General Hospital, China

Reviewed by:
Thomas M. Vondriska,
University of California, Los Angeles, United States
Bastiaan J. Boukens,
University of Amsterdam, Netherlands

***Correspondence:**
Xin Tu
xtu@hust.edu.cn

Specialty section:
This article was submitted to Cardiac Rhythmology, a section of the journal Frontiers in Cardiovascular Medicine

Received: *07 March 2022*
Accepted: *25 May 2022*
Published: *15 June 2022*

Citation:
Wang M and Tu X (2022) The Genetics and Epigenetics of Ventricular Arrhythmias in Patients Without Structural Heart Disease. Front. Cardiovasc. Med. 9:891399. doi: 10.3389/fcvm.2022.891399

INTRODUCTION

The vast majority of ventricular arrhythmias occurs in structurally diseased hearts, however, a proportion of patients with ventricular tachycardia is free of cardiac structure alterations (1). Ventricular arrhythmias without structural heart disease mainly includes monomorphic ventricular tachycardia classified by location of origin, polymorphic ventricular tachycardia dominated by primary hereditary arrhythmia syndrome, and ventricular fibrillation, i.e., Brugada syndrome (BrS), congenital long QT syndrome (LQTS), short QT syndrome (SQTS), catecholaminergic polymorphic ventricular tachycardia (CPVT) (2, 3). The clinical presentations vary, including palpitations, vertigo, syncope, seizure-like activity and sudden cardiac death. There is no obvious cardiac structural change in patients without structural heart disease, but it may also be due to the lack of detection of pathological changes in the existing technology or focal lesions in the heart. Especially in BrS, structural abnormality has also become one of the pathogenesis, however, due to the restrictions on the acquisition of human samples, structural detection is mostly carried out in patients with severe symptoms. The prominent role of genetics in the pathogenesis of the disease remains of interest (4, 5). With the development of detection technology, we may gain a greater understanding of the mechanisms involved in this disease.

The heart has a set of well-established electrical conduction systems, and the tissues and cells coordinate with each other to make the heart contract and relax in an orderly way, and pump blood

to all parts of the body. The action potential (AP) of human ventricular myocytes is composed of depolarization and repolarization, and is subdivided into five stages, 0 and 1, 2, 3, 4 (6). The flow balance of potassium, sodium, calcium and other ions is essential for the normal beating of the heart. Cardiomyocyte depolarization induced by electrotonic coupling between adjacent cardiomyocytes drives phase 0 initiation, the sodium channel is activated, the sodium ion enters the membrane rapidly, resulting in depolarization (phase 0) (7). Subsequently, Majority of sodium channels are rapidly inactivated and L-type calcium channels are activated. At the same time, the repolarization current generated by potassium channels and Na^+/Ca^{2+} exchangers, namely the instantaneous outward potassium current (Ito) and outward I_{NCX} reduce the membrane potential (phase 1) (8). the sodium current of slowly inactivated sodium channels, mostly inactive calcium channels current ($I_{Ca,L}$) and the sodium-potassium exchanger current operating in forward mode reach a balance with delayed rectifier potassium current (I_K), forming a plateau phase on ECG (phase 2). While the action potential occurs, the influx of calcium ions triggers a further release of calcium ions from the sarcoplasmic reticulum, resulting in intracellular concentration transient elevation, causing muscle contraction, namely cardiac excitation-contraction (E-C) coupling (9). Subsequently, the calcium ion channel is gradually inactivated. The ion current at this time is mainly the outward current of I_K and I_{K1}, and the more negative the intramembrane potential, the more rapid efflux of the potassium ion, which leads to the acceleration of the repolarization until the repolarization is completed (phase 3). The potential is stable at the resting potential level, and the ion pump pumps out the ions pumped into the cell during the action potential. The Na^+/ K^+ pump can pump the Na^+ in the cell out of the cell and pump K^+ into the cell at the same time. Intracellular Ca^{2+} is transported extracellular via the Na^+/ Ca^{2+} exchanger and the Ca^{2+} pump (phase 4) (10). The abnormality caused by the mutation of ion channel protein coding gene will cause the disorder of electrical signal.

Triggered activity, abnormal automaticity, and re-entry are the three mechanisms of ventricular arrhythmias, in ventricular arrhythmias without structural heart disease, usually due to trigger activity (3). Triggered activity that occurs in phase 2 and early phase 3 is called early afterdepolarization (EAD), in late phase 3 and phase 4 are called delayed after-depolarization (DAD) (11), The trigger activity is generated by the membrane depolarisation induced by the I_{NCX} and/or Ica,l (12, 13). Automaticity refers to the spontaneous depolarization of phase 4 membrane potential of the cells with pacemaking function, and the action potential is generated after reaching the threshold potential. Abnormal automaticity is attributed to decreased I_{K1} and/or enhanced I_f (mainly slow inward sodium current, causing automatic membrane depolarization) (14). Once I_{K1} is inhibited, the membrane potential cannot reach the resting potential, which may lead to the generation of abnormal inward currents, such as I_f, causing abnormal automaticity. Re-entry refers to a cardiac impulse that repeatedly runs and activates the cardiac muscle surrounding around the center of anatomical or functional disorders, usually the pathogenesis of structural ventricular arrhythmias, but specific arrhythmias induced by EAD (Torsades de Pointes in LQTS) or DAD (bidirectional ventricular tachycardia in CPVT) may be caused by re-entry involving fascicles of the Purkinje system (3).

In respect to etiology, ventricular arrhythmias in patients without structural heart disease are mostly due to ion channel disorders, including various inherited arrhythmia syndromes and ventricular arrhythmias caused by unknown causes. Besides genetic studies in classical, the effects of epigenetics on ventricular arrhythmias are also being explored, which makes this part that is not yet understood gradually revealed. We searched the PubMed database using the terms "idiopathic ventricular arrhythmias", "genetics", "epigenetics", and "DNA methylation" up to 2021 for articles on ventricular arrhythmias and present the genetics and epigenetics of ventricular arrhythmias in non-structural heart disease in this review. **Table 1** is a brief description.

GENETIC FACTORS OF VENTRICULAR ARRHYTHMIAS WITHOUT STRUCTURAL HEART DISEASE

The advancement of genetic technology has brought a deeper understanding of the genetic factors of the disease. It is a common Mendelian genetic phenomenon that a rare variant of a single gene has a significant impact on protein function and causes disease. However, the incomplete penetrance in the family and the frequency of pathogenic mutations in the normal population have begun to make people think that disease is not only caused by the mutation of a certain gene locus, but that the cumulative pattern of multi-site interaction can also cause the occurrence of disease. Here, we discussed the single-gene and multi-gene factors that cause ventricular arrhythmias and summarized the single gene factors in **Table 2**.

Monogenic Factors

Sodium Ion Channels

Mutations in the gene encoding voltage-gated sodium channels can disrupt sodium channels, cause abnormal sodium current flow and trigger ventricular arrhythmias, due to the significant role of voltage-gated sodium channels in action potentials (15). Alterations in sodium current can cause several types of cardiac disease, including LQTS, BrS, isolated (progressive) conduction defect, atrial fibrillation, sick sinus syndrome, dilated cardiomyopathy and multifocal ectopic premature Purkinje-related complexes (15). In ventricular arrhythmias without structural heart disease, enhanced sodium currents are usually associated with LQTS, whereas diminished sodium currents are associated with BrS (15, 83). Several sodium channel-related pathogenic genes have been identified in ventricular arrhythmias without structural heart disease, including SCN5A, SCN1B, SCN2B, SCN3B, SCN4B, GPD1L, RANGRF, SCN10A, among which SCN5A is the most reported (**Table 2**). SCN5A encodes $Na_v1.5$, which is the alpha subunit of voltage-gated sodium channels. As the main functional subunit of sodium ion channels, it provides activity for the channel. $Na_v1.5$ is responsible for the

TABLE 1 | A brief description of the genetics and epigenetics of ventricular arrhythmias in non-structural heart disease.

	Causative factor	Description	References
Genetics	Monogenic factors	Among the monogenic causative factors, mutations in the sodium channel-encoding gene SCN5A, the potassium channel-encoding genes KCNQ1 and KCNH2, and the calcium channel-encoding gene RYR2 cause the majority of ventricular arrhythmias, while some cases are caused by rare variants in other ion channel and structural genes. In addition, the role of somatic mutations has been identified.	(15–18)
	Polygenic factors	The importance of polygenic factors for ventricular arrhythmias is highlighted by the heterogeneity of causative genes across patients with ventricular arrhythmias and the impact of the accumulation of mutations in multiple genes on the severity of the clinical phenotype. The concept of genetic modifier has been proposed and a recent GWAS analysis validated the link between cumulative mutational effects and the BRS clinical phenotype.	(19–22)
Epigenetics	Non-coding RNA	The research on ventricular arrhythmias without structural heart disease mainly focuses on the regulation of miRNAs on the transcription of genes encoding ion channels such as SCN5A and SCN1B. Circular RNA may serve as a marker for disease progression.	(23–25)
	DNA methylation	DNA methylation usually plays a repressive role in gene transcription. For example, SCN5A promoter hypermethylation levels enhance SCN5A expression in cardiac tissue. In addition, it plays an important regulatory role in gene imprinting.	(26, 27)
	Histone modifications	Histone modifications in the heart have mostly been studied for methylation and acetylation, which are linked to gene transcriptional activation or repression and may play a role in the formation of transmural electrophysiological gradients in the ventricle.	(28–30)
	Genomic imprinting	The methylation level of the long non-coding RNA KCNQ1OT1, which is related to a prolonged QTC interval, affects the expression of the imprinted gene KCNQ1 and may contribute to female predominance and transmission distortion in LQTS.	(31–33)
	Three-dimensional (3D) genome architecture	The ordered chromatin spatial structure allows interactions between functional elements within the topological domains to regulate gene transcription, such as the interaction of enhancers with promoters. The 3D genome architecture study offers a fresh look at the link between SNPs and ventricular arrhythmias discovered by GWAS.	(34–37)

influx of sodium ions and plays a major role during membrane depolarization, as well as the sodium current in the repolarization and refractory period. SCN5A Mutation can be divided into gain-of-function and loss-of-function mutation, leading to an increase or decrease in sodium ion influx and an acceleration or delay in channel inactivation, responsible for about 5–10% of LQTS patients and ∼30% of patients with BrS, respectively (15, 16).

In addition to Nav1.5 that directly affects sodium currents, some proteins can achieve indirect regulation of sodium currents by modulating Nv1.5, have been associated with BrS and LQTS. although their clinical relevance may be limited. SCN1B, SCN2B, and SCN3B encode voltage-gated sodium channel β subunits. Mutations can decrease $Na_v1.5$ cell surface expression and reduce sodium current, leading to BrS (38, 39, 41). SCN4B also encodes sodium channel β subunit, can cause LQTS in a minority of cases. Consistent with the molecular/electrophysiological phenotype previously displayed by LQTS, compared to wild type, the mutation L179F of SCN4B leads to an increase of late sodium current (42). GPD1L is SCN5A regulatory proteins, links redox state to cardiac excitability by PKC-dependent phosphorylation of the sodium channel (84). The GPD1L A280V mutation reduces SCN5A membrane expression, decreases inward Na^+ current, leading to BrS (43). RANGRF (MOG1) is a co-factor of $Na_v1.5$, which plays a potential role in the regulation of $Na_v1.5$ expressions and trafficking. The dominant-negative mutations in RANGRF can disrupt the transport of $Na_v1.5$ to the membrane, resulting in a reduction of I_{Na} and causing clinical manifestations of BrS. Silencing RANGRF can reduce I_{Na} density, in addition, replacing E83D, D148Q, R150Q, and S151Q could disrupt the interaction of RANGRF with $Na_v1.5$ and significantly impair the trafficking of $Na_v1.5$ to the cell surface, indicating that RANGRF may play an important role in the expression of $Na_v1.5$ channel on the cell surface (44, 45). SCN10A encodes $Na_v1.8$, a voltage-gated sodium channel like $Na_v1.5$. Both SCN10A and SCN5A are located on chromosome 3p22.2. Co-expression of SCN10A-WT and SCN5A can increase sodium channel current, while SCN10A mutants (R14L and R1268Q) can cause loss of $Na_v1.5$ current function, which may be the genetic basis of BrS caused by SCN10A. However, most of the mutations associated with SCN10A are not rare variants, are relatively frequent in the population (46).

Potassium Ion Channels

The potassium ion currents associated with ventricular arrhythmias include transient outward potassium current (I_{to}), delayed rectifier potassium current (I_K), inward rectifier K^+ current (I_{K1}), and hyperpolarization-activated currents (I_h). Dysfunction of potassium ion channels can also cause changes in ion balance, causing arrhythmia (**Table 2**).

Hyperpolarization-activated cyclic nucleotide–gated (HCN) channels are responsible for pacing current in neurons and cardiomyocytes, in which HCN4 encode a member of the hyperpolarization-activated cyclic nucleotide–gated (HCN) channels showing slow activation and inactivation kinetics and

TABLE 2 | Genes associated with ventricular arrhythmias in non-structural heart disease.

Gene	Protein (UniProtKB)	Aliases	Functional effect	Symptom	Frequency, %	References
Sodium channel-related genes						
SCN5A	Sodium channel protein type 5 subunit alpha	Nav1.5/LQT3/VF1	$I_{Na}\uparrow$	LQTS	5–10%	(15)
			$I_{Na}\downarrow$	BrS	20–25%	(15)
SCN1B	Sodium channel subunit beta-1		$I_{Na}\downarrow$	BrS	Rare	(38)
SCN2B	Sodium channel subunit beta-2		$I_{Na}\downarrow$	BrS	Rare	(39, 40)
SCN3B	Sodium channel subunit beta-3		$I_{Na}\downarrow$	BrS	Rare	(41)
SCN4B	Sodium channel subunit beta-4	LQT10	$I_{Na}\uparrow$	LQTS	Rare	(42)
GPD1L	Glycerol-3-phosphate dehydrogenase 1-like protein	GPD1-L	$I_{Na}\downarrow$	BrS	Rare	(43)
RANGRF	Ran guanine nucleotide release factor	RANGNRF/MOG1	$I_{Na}\downarrow$	BrS	Rare	(44, 45)
SCN10A	Sodium channel protein type 10 subunit alpha	Nav1.8	$I_{Na}\downarrow$	BrS	∼10%	(46)
Potassium channel-related genes						
Hyperpolarization-activated cyclic nucleotide–gated (HCN) channels						
HCN4	Potassium/sodium hyperpolarization-activated cyclic nucleotide-gated channel 4		$I_f\downarrow$	IVT	Rare	(47)
transient outward potassium current channels						
KCND3	Potassium voltage-gated channel subfamily D member 3	Kv4.3	$I_{to}\uparrow$	BrS	Rare	(48)
KCNE3	Potassium voltage-gated channel subfamily E member 3	MiRP2/HOKPP	$I_{to}\uparrow$	BrS	Rare	(49)
KCNE5	Potassium voltage-gated channel subfamily E regulatory beta subunit 5	MiRP4	$I_{to}\uparrow$	BrS	Rare	(50)
Slowly activating delayed rectifier potassium current channels						
KCNQ1	Potassium voltage-gated channel subfamily KQT member 1	KVLQT1/Kv7.1/LQT1	$I_{Kr}\downarrow$	LQTS	30–35%	(51)
			$I_{Kr}\uparrow$	SQTS	Unknown	(52)
KCNE1	Potassium voltage-gated channel subfamily E member 1	MinK 2/LQT5	$I_{Kr}\downarrow$	LQTS	Rare	(53)
Rapidly activating delayed rectifier potassium current channels						
KCNH2	Potassium voltage-gated channel subfamily H member 2	HERG/Kv11.1/ERG-1/LQT2	$I_{Kr}\downarrow$	LQTS	25–30%	(54)
			$I_{Kr}\uparrow$	SQTS	Unknown	(55)
KCNE2	Potassium voltage-gated channel subfamily E member 2	MiRP1/LQT6	$I_{Kr}\downarrow$	LQTS	Rare	(56)
Inwardly rectifying potassium (Kir) channels						
Inwardly rectifying potassium channels						
KCNJ2	Inward rectifier potassium channel 2	Kir2.1/LQT7	$I_{K1}\uparrow$	SQTS	Unknown	(57)
			$I_{K1}\downarrow$	LQTS	Rare	(58)
G protein-coupled, inwardly rectifying potassium channels						
KCNJ5	G protein-activated inward rectifier potassium channel 4	Kir3.4/GIRK4/LQT13	$I_{KACh}\downarrow$	LQTS	Rare	(59)
ATP-sensitive potassium channels						
KCNJ8	ATP-sensitive inward rectifier potassium channel 8	Kir6.1	$I_{K-ATP}\uparrow$	BrS	Rare	(60)
ABCC9	ATP-binding cassette sub-family C member 9	SUR2	$I_{K-ATP}\uparrow$	BrS	Rare	(61)
Calcium channel-related genes						
CACNA1C	Voltage-dependent L-type calcium channel subunit alpha-1C	Cav1.2/LQT8	$I_{Ca,L}\uparrow$	LQTS	1–2%	(62)
			$I_{Ca,L}\downarrow$	BrS	1–2%	(63)

(Continued)

TABLE 2 | Continued

Gene	Protein (UniProtKB)	Aliases	Functional effect	Symptom	Frequency, %	References
CACNB2	Voltage-dependent L-type calcium channel subunit beta-2	CACNLB2	$I_{Ca,L}$↓	BrS	1–2%	(63)
CACNA2D1	Voltage-dependent calcium channel subunit alpha-2/delta-1	CACNL2A	$I_{Ca,L}$↓	BrS	Rare	(64)
RYR2	Ryanodine receptor 2	ARVC2/ARVD2	Aberrant calcium handling	CPVT	55–60%	(65)
			Aberrant calcium handling	IVF	Rare	(66)
CASQ2	Calsequestrin-2		Aberrant calcium handling	CPVT	<5%	(67)
TRDN	Triadin	TDN/TRISK/CPVT5	Aberrant calcium handling	CPVT	1–2%	(68)
			$I_{Ca,L}$↑	LQTS	1–2%	(69)
CALM1∼3	Calmodulin-1∼3	CaMI/CaMII/CaMIII	$I_{Ca,L}$↑	LQTS	Rare	(70)
			Aberrant calcium handling	CPVT	Rare	(70)
Other related genes						
SNTA1	Alpha-1-syntrophin	LQT12/SNT1	I_{Na}↑	LQTS	Rare	(71)
SLMAP	Sarcolemmal membrane-associated protein	SLAP	I_{Na}↓	BrS	Rare	(72)
PKP2	Plakophilin-2	ARVD9	I_{Na}↓	BrS	Rare	(73)
ANK2	Ankyrin-2	LQT4	Abnormal coordination of multiple functionally related ion channels and transporters	LQTS	Rare	(74)
CAV3	Caveolin-3		I_{Na}↑$I_{Ca,L}$↑I_K↓I_{to}↓	LQTS	Rare	(75)
TECRL	Trans-2,3-enoyl-CoA reductase-like	TERL	Aberrant calcium handling	Mixed phenotype of CPVT and LQTS	Rare	(76)
SLC4A3	Anion exchange protein 3	AE3/SLC2C	Phi↑	SQTS	Unknown	(77)
TRPM4	Transient receptor potential cation channel subfamily M member 4		uncertain	BrS, LQTS	Rare	(78)
Genes specific to IVF						
DPP6	Dipeptidyl aminopeptidase-like protein 6	DPPX/DPP VI/VF2	I_{to}↑	IVF	Unknown	(79)
IRX3	Iroquois-class homeodomain protein IRX-3	IRX-1/IRXB1	I_{Na}↓	IVF	Unknown	(80)
Somatic mutation genes						
GNAI2	Guanine nucleotide-binding protein G(i) subunit alpha-2	GNAI2B/GIP	cAMP↑	RVOT-VT	Rare	(18)
ADORA1	Adenosine receptor A1	A1AR	unknown	RVOT-VT	Rare	(81)
GNAS	Guanine nucleotide-binding protein G(s) subunit alpha isoforms short	GNAS1/NESP	$I_{Ca,L}$↑	RVOT-VT	Rare	(82)

BrS, Brugada syndrome; LQTS, long QT syndrome; SQTS, short QT syndrome; CPVT, catecholaminergic polymorphic ventricular tachycardia; IVF, idiopathic ventricular fibrillation; IVT, idiopathic ventricular tachycardia; RVOT-VT, right ventricular outflow tract ventricular tachycardia; ↑, increased and/ or enhanced; ↓, decreased and/ or weakened.

is the highest expressed isotype in sinoatrial node (SAN) muscle cells, necessary for cardiac pacing (85). HCN4 gene mutation was detected in patients with idiopathic ventricular arrhythmias, which resulted in the decrease of pacemaker (I_f) current (85, 86).

The repolarization of the ventricles is spatially heterogeneous, largely dependent on the gradient of potassium current, especially I_{to} (87). Under normal circumstances, the density of I_{to} in the epicardium is higher than the endocardium and the initial repolarization of the epicardium is earlier than the endocardium, generating a transmural voltage gradient that plays an important role in synchronizing repolarization (87). Gain of function of I_{to} is related to BrS. I_{to} channel is composed of α subunit and β subunit, with the α subunit $K_v4.3$ encoded by KCND3, and the negatively regulated β-subunit MiRP2 encoded by KCNE3. It is a voltage-gated, calcium-independent potassium (K_v) current that can be quickly activated and inactivated, mainly responsible for the initial repolarization phase of the cardiac action potential (88), KCND3 mutations are known to cause BrS. The mutation KCND3 Arg431His (c.1292G>A) detected in BrS patients does not affect the mRNA and total protein expression level of $K_v4.3$, but increase the membrane protein expression of $K_v4.3$ and up-regulate the transient outward potassium current (48). Besides, at the same time, KCNE3 mutation may be the basis of the development of BrS. The co-transfection of the KCNE3 gain-of-function mutation R99H with KCND3 causes a significantly increased current intensity compared to WT KCNE3+KCND3 (49). Actually, the KCNE family encodes five isotypes in the human genome. In addition to KCNE3, KCND3 can be assembled with multiple KCNE subunits, of which KCNE5 can regulate I_{to}, showing a correlation with BrS and idiopathic ventricular fibrillation (50). KCNE5 is located on the X chromosome and when coexpressed with KCND3, the brugada-associated KCNE5 mutations upregulate I_{to} compared to the wild type (50).

There are two types of delayed rectifier K^+ current, slowly activating delayed rectifier K^+ current (I_{Ks}) and rapidly activating delayed rectifier K^+ current (I_{Kr}). Its enhancement is related to SQTS, whereas weakening is related to LQTS (89). The outward K^+ current of I_{Ks} channel is one of the main repolarizing potassium currents in the human heart, which helps to terminate cardiac action potential. The channel is composed of the pore-forming α subunit encoded by KCNQ1 (also known as $K_v7.1$ or K_vLQT1) and the β subunit encoded by KCNE1 (90, 91). Cardiac KCNQ1/KCNE1 channel mutations are the most common cause of inherited long-QT syndromes (92). Loss-of-function mutations of KCNQ1 decrease I_{Ks} current density, leading to LQTS, and there are also mutations that are gain-of-function mutations increase I_{Ks}, leading to SQTS (93, 94). Mutations in KCNE1 gene cause reduced I_{Ks} current density, manifested as loss of function, which can lead to LQTS (53). However, a recent study has indicated that QTc Interval Prolongation (>460 ms) was not observed in most people carrying KCNE1 loss-of-function mutations (95). The rapidly activating delayed rectifier potassium channel is encoded by KCNH2 and KCNE2, which produces only a small outward current during membrane depolarization, however, after the membrane is repolarized, the channel quickly recovers from the inactivation state to the open state, producing a recovery current before the slow channel deactivation. KCNH2 gene encodes the pore-forming α subunit of voltage-gated K^+ channel $K_v11.1$, commonly referred to as Herg. Approximately 90% of LQT- associated KCNH2 mutations reduced I_{Kr} by reducing $K_v11.1$, responsible for 25–30% of LQTS cases channel synthesis or trafficking (54). Gain-of-function mutations are the genetic basis of SQTS, which increase the repolarization current activated in the early stages of AP, resulting in a shortening of the action potential and the QT interval (55). KCNE2 encodes MiRP1, an auxiliary beta-subunit. Compared with the wild-type channel, the mutant HERG/MiRP1 (V65M) channel detected in LQTS patients has a shorter current inactivation time, which may reduce the I_{Kr} current density of cardiomyocytes, weakening the cardiomyocytes' ability to repolarize sudden membrane depolarization (56). It has also been reported that overexpression of wild-type KCNE2 can rescue the phenotype caused by KCNH2 mutation, facilitating the transport of $K_v11.1$ channel protein and cell surface expression, significantly increasing the mutation current (96).

Inwardly rectifying potassium (Kir) channels allow potassium ions to move more easily into rather than out of the cell. The inwardly rectifying potassium channels gene associated with ventricular arrhythmia has KCNJ2, KCNJ5, KCNJ8, and ABCC9 (**Table 2**). I_{K1} plays an important role in stabilizing the resting membrane potential, regulating excitability and causing the final repolarization of atrial and ventricular action potential. Like delayed rectifier potassium channel, its enhancement is related to SQTS and reduction is related to LQTS, while ATP-sensitive potassium channel current (I_{K-ATP}) enhancement will lead to BrS. One of the molecular basis is Kir2.1, which is coded by KCNJ2. Gain-of-function KCNJ2 mutations have been found in SQTS patients, resulting in increased I_{K1}, accelerated ventricular repolarization and shortened QT interval (57, 97). There are also reports in the literature that loss-of-function mutations can cause LQTS (58). Mutations in the Inwardly rectifying potassium channels Kir2.1 encoded by KCNJ2 causing loss of function are associated with a rare clinical phenotype called Andersen-Tawil syndrome (ATS), which contains pleomorphic ventricular tachycardia (98). KCNJ5 encodes Kir3.4, a subunit of the voltage-gated potassium channel, which is controlled by G proteins and combination with Kir3.1, responsible for acetylcholine-activated potassium channel current (I_{KACh}) (59). The KCNJ5 mutation results in defects in channel trafficking and a reduction in the I_{KACh}, which is considered to be the pathogenic gene of LQTS (59). ATP-sensitive potassium channel (K_{ATP}) is one kind of inwardly rectifying channel composed of the pore forming subunits and the regulatory subunits. Kir6.1 encoded by KCNJ8 and SUR2 encoded by ABCC9 are both subunits of ATP-sensitive potassium channels (99). KCNJ8 mutation can reduce the sensitivity of K_{ATP} channels to ATP, resulting in enhanced I_{K-ATP} function, which may lead to BrS (60, 100). Gain-of-function mutation of ABCC9 has also been reported as a possible pathogenic site for BrS, however, the relevance of pathogenic requires further confirmation (61).

Calcium Ion Channels

Voltage-gated L-type calcium channel (LTCC) is the main channel mediating influx of calcium ions into cells in repolarization stage, and in addition, NCX, an ion transport

protein, can mediate the exchange cycle of sodium ions and calcium ions with a coupling ratio of 3:1 (101). Calcium entering the cell through these two distinct mechanisms triggers the release of calcium from the sarcoplasmic reticulum. Voltage-gated L-type calcium channel consists of four subunits α1 subunit, auxiliary β subunit, α2δ subunit, and γ subunit. The four subunits of voltage-gated L-type calcium channels which are, respectively, coded by CACNA1C or CACNA1D, CACNB2, CACNA2D, and CACNG (102, 103). Among them, the mutant genes that have been reported to cause ventricular arrhythmia are CACNA1C, CACNB2, CACNA2D (**Table 2**). CACNA1C encodes $Ca_v1.2$ pore-forming α1 subunit. In general, the enhancement of $I_{Ca,L}$ is related to LQTS, on the contrary causes BrS. Timothy syndrome (TS), which manifests as severe LQTS and multiorgan dysfunction, is mainly caused by gain-of-function mutations located in CACNA1C alternative splicing exon 8 which leads to almost complete loss of voltage-related channel inactivation, resulting in maintained inward Ca^{2+} current, and prolonged Ca^{2+} current that delay cardiomyocyte repolarization (104–106). A few cases are caused by mutations within exon 9 and exon 38 of CACNA1C (107, 108). Gain-of-function mutations in CACNA1C at positions other than exon 8 can cause LQTS with non-Timothy syndrome symptoms (62, 109). The phenotype caused by the loss-of-function mutations of the cardiac L-type calcium channel α1 and β2b subunits is similar to calcium channel blockers, leading to reduced $I_{Ca,L}$, resulting in BrS (63, 110, 111). Subsequent studies identified CACNA2D1 as a novel BrS/SQTS susceptibility gene (64, 112). In addition, it is also reported that KCNE2 can affect $I_{Ca,L}$ by regulating $Ca_v1.2$ (113).

The main function of the sarcoplasmic reticulum (SR) is to store calcium in striated muscle. The genes involved in the release of calcium from the sarcoplasmic reticulum are RYR2, CASQ2, TRDN, CALM1, CALM2, and CALM3, which are pathogenic genes of CPVT (**Table 2**) (65, 114). Among them, TRDN, CALM1, CALM2, CALM3 mutations can also cause LQTS. RYR2 encodes ryanodine receptors (RyR2), responsible for the rapid release of calcium ions from the sarcoplasmic/endoplasmic reticulum (SR/ER) into the cytoplasm. RYR2 mutations may be either loss or gain of function and this may be related with different clinical phenotypes. Approximately 60% of patients with CPVT carry RYR2 mutations, and the main pathogenic mechanism of gain-of-function mutations is increased spontaneous RyR2 opening and pathological calcium release during diastole (17, 65, 115). The RyR2 mutation associated with idiopathic ventricular fibrillation confirmed as a loss-of-function mutation exhibiting Ca^{2+} release deficiency (66). However, a recent study identified a loss-of-function mutation D3291V, which markedly reduced luminal Ca^{2+} sensitivity, and blunted response to adrenergic stimulation, also exhibiting a CPVT phenotype (116). The relationship between gain-of-function or loss-of-function and the clinical phenotype still needs to be elucidated (117). The calsequestrin encoded by CASQ2 is a calcium-binding protein that regulates the amount of calcium released from the SR during excitation-contraction coupling by buffering the calcium in the SR (118, 119). Triadin (TRD) encoded by TRDN is located on the sarcoplasmic reticulum, forms a complex with ryanodine receptors, calsequestrin and junctin, regulating the storage and release of calcium ions (120). Triadn anchors calsequestrin to junctional SR membrane and stabilizes the structure of Ca 2+ release units (121). TRDN deficiency leads to significantly reduced protein levels of RyR2, calsequestrin, and junctin, impaired coupling efficiency between LTCC and RyR2, reduced SR calcium release and calcium-dependent inactivation of LTCC, resulting in defective cardiac excitation-contraction coupling (121, 122). Similarly, Triadin mutations are thought to result in reduced protein levels, which in turnincreased calcium currents and prolonged cardiac action potentials, and increased spontaneous calcium release events caused by cellular and SR calcium overload, which is the basis of TRDN mutation leading to CPVT and LQTS (69, 123). CALM1∼3 encodes Calmodulin, which is Ca^{2+} sensor, signal-transducing protein. Calmodulin binds to RyR2 and LTCC, plays a key role in the calcium-dependent inactivation of the L-type calcium channel $Ca_v1.2$ and the timely closure of the myocardial sarcoplasmic reticulum calcium release channel RyR2. Calcium binding to calmodulin inactivates the LTCC channel, namely calcium-dependent inactivation (124). The mutations associated with LQTS are mainly due to weakening of the combination of calmodulin and calcium, completely eliminating the calcium-dependent inactivation. On the other hand, the binding of calmodulin to RyR2 can inhibit the release of calcium from SR during diastole. Mutations associated with CPVT mainly lead to dysregulation of RyR2 calcium release (70, 125).

Others

The protein encoded by SNTA1 is a component of the $Na_v1.5$ channel macromolecular complex, interacting with the pore-forming α subunit (126). Gain-of-function SNTA1 mutations can affect $Na_v1.5$ gating kinetics, leading to the LQTS phenotype (71). SLMAP encodes the sarcolemmal associated protein located in T-tubules and sarcoplasmic reticulum. SLMAP mutation may cause BrS by regulating the intracellular transport of $Na_v1.5$ channel (72). PKP2 encodes Plakophilin-2, a desmosomal protein. Loss and/or changes in the Plakophlin-2 structure in the heart desmosomes can impair the interaction between myocardial cells and cause myocardial rupture, especially in response to mechanical stress (127). Mutations in PKP2 have been associated with BrS, and the deletion of PKP2 can lead to a decrease in sodium current and $Na_v1.5$ at the site of cell contact (73). Ankyrins bind to spectrins, connects the plasma membrane with the actin cytoskeleton, maintains mechanical strength and regulates the excitability of various cells. The ankyrin family contains three members: ankyrin-R, ankyrin-B and ankyrin-G, are encoded by ANK1, ANK2 and ANK3, respectively (128). Loss-of-function mutation (E1425G) in ankyrin-B (also known as ankyrin 2) can lead to dominant long QT arrhythmia (74, 129). CAV3 encodes a scaffold protein for the cavern in cardiomyocytes and participates in the separation of ion channels. CAV3 mutations are related to LQTS, which can prolong repolarization times by enhancing the late sodium current, enhancing the peak value of L-type calcium current, slowing down deactivation, reducing delayed rectifier potassium current and transient outward potassium current

(75). TECRL (TERL) is an oxidoreductase enzyme localized to the endoplasmic reticulum. Patients with TECRL pathogenic variants manifest a specialized mixed phenotype of CPVT and LQTS, which is an autosomal recessive disease. Functional experiments have shown that homozygous pathogenic variants can lead to reduced levels of RYR2 and CASQ2 proteins, and reduced calcium storage of sarcoplasmic reticulum and aberrant calcium handling (76).

SLC4A3 (AE3) is an electroneutral Cl^-/HCO_3^- exchanger (130). Studies have found that reducing intracellular pH (PHi) could prolong QT interval; the regulation of chloride ion conductance in cardiomyocytes can also change action potential duration. In zebrafish, SLC4A3 mutations can lead to transport defects, reduce Cl,HCO3-exchange over the cell membrane, increase pHi and reduce the QT duration, which may be another development mechanism of SQTS (77). The protein encoded by TRPM4 is a transmembrane N-glycosylated ion channel, a non-selective channel activated by intracellular calcium, permeable to monovalent cations. At present, Trpm4 mutations have been detected in both BrS and LQTS cohort. Miraculously, gain-and loss-of-function variants of TRPM4 channels can cause similar phenotypes (78).

Idiopathic ventricular fibrillation is an exclusive disease that requires excluding the presence of the ventricular fibrillation substrate and specific diseases, including structural heart disease and primary arrhythmia syndrome (131). At present, most genes related to idiopathic ventricular fibrillation overlap with the pathogenic genes of hereditary ventricular arrhythmias, such as CALM1∼3, RYR2, TRDN, CACNA1C, SCN5A, KCNE5 (50, 125, 132–137). However, there are also specific causative genes in the idiopathic ventricular fibrillation (138). A single-pass type II membrane protein DPP6 can promote the cell surface expression of potassium channel KCND2 and regulate its activity and gating characteristics (139–141). Haplotype analysis in both familial and sporadic cases indicated the relevance of DPP6 with idiopathic ventricular fibrillation (133, 142). Furthermore, a DPP6 mutation was detected in idiopathic ventricular fibrillation patients, which disturbs the efflux of potassium ion (79). In addition, mutations of transcription factor IRX3, specifically expressed in His bundle, have also been reported to cause idiopathic ventricular fibrillation by down-regulating SCN5A and connexin-40 mRNA (80). Although several diagnostic approaches have been proposed and pathogenic mechanisms discussed, it is far from enough for studies of idiopathic ventricular fibrillation (143). This situation may change with the development of diagnostic techniques for structural heart disease and the discovery of potential pathogenic mechanisms.

Somatic Mutations

Besides the above germline mutations, i.e., mutations carried by all cells, the effect of somatic mutations, i.e., mutations carried by only some somatic cells, on the occurrence of ventricular arrhythmias is also being investigated. Idiopathic right ventricular outflow tract ventricular tachycardia (RVOT-VT) is the most common form of ventricular arrhythmias in patients without structural heart disease. GNAI2 (f200l) and A1AR (R296C) mutations were detected in biopsy samples collected from the origin of ventricular tachycardia in patients with adenosine insensitive RVOT tachycardia, but not in remote myocardium (18, 81). GNAI2 (F200L) increases intracellular cAMP concentrations and inhibited the inhibition of cAMP by adenosine, the effect of another mutation is unclear (81). Another study identified a cardiac somatic mutation (W234R) in GNAS (Gs-alpha, stimulatory G protein alpha-subunit) in endomyocardial biopsy samples from the origin of tachycardia in RVOT-VT patient, which was not detected in right ventricular apex biopsy samples. The mutation impairs GTP hydrolysis and increased basal intracellular cAMP levels, increasing the basal inward calcium current, and silico modeling show delayed afterdepolarizations and triggered activity (82).

Polygenic Factors

In the process of screening disease-causing genes, we often tend to pay more attention to single-gene factors, emphasizing that a gene mutation corresponds to a clinical phenotype. However, molecular genetics is developing from single-gene research to multi-gene research. The same gene mutation can give rise to multiple distinct phenotypes. The SCN5A mutation detected in a Dutch family causes two phenotypes: LQTS and BrS (144). Mutations that have been reported to be pathogenic may appear no overt phenotype when they exist in other families or individuals, in the same pedigree, mostly display incomplete clinical penetrance (145, 146). It is more common that the same phenotype is caused by a mutation in different genes, in fact, it can also be caused by the accumulation of mutations in multiple different genes, and may affect the severity of the disease. For example, the interaction between KCND3 and SCN5A, $Na_v1.5$ and $K_v4.3$ channels regulates each other's functions through trafficking and gating mechanisms (147). When screening the LQTS susceptibility gene in a Caucasian family with syncope and slightly prolonged QT interval, it was found that there is R800L mutation in SCN5A and A261V mutation in SNTA1. Family members with both mutations have the strongest clinical Phenotype (19). In a GWAS study, two significant association signals were detected in Scn10a locus (rs10428132) and near the HEY2 gene (rs9388451) in patients with BrS, and an additional signal rs11708996 was identified in SCN5A, three common variations present an unexpectedly cumulative effect on disease susceptibility. The association signal of SCN5A-SCN10A indicate that genetic polymorphisms regulating cardiac conduction also affects the susceptibility to arrhythmia (20). In addition, the concept of genetic modifiers also indicates the cooperation between multiple genes. KCNQ1 mutation A341V carriers exhibit inconsistent QT intervals, and AKAP9, encoding a scaffolding protein, variants has been shown to alter the QTc interval of the population and the risk and severity of cardiac events (21, 148). A GWAS study conducted in China investigated the relationship between the NOS1AP gene rs12143842 variant and idiopathic ventricular tachycardia. The results showed that the minor T allele of the rs12143842 SNP was significantly associated with the reduced risk of idiopathic ventricular tachycardia in the Northern Chinese cohort, indicating that SNPs can affect the susceptibility to ventricular tachycardia (149). Consistently, a recent GWAS study with polygenic risk score

analysis in BrS patients confirmed the association of mutation accumulation effects with traits (22).

EPIGENETIC FACTORS OF VENTRICULAR ARRHYTHMIAS WITHOUT STRUCTURAL HEART DISEASE

There are still a large number of cases of hereditary ventricular arrhythmias in which the causative gene has not been detected. For example, in BrS, approximately 20 pathogenic genes have been reported, but comprehensive single gene factors and polygenic factors still account for 60–80% of the causes unknown. In addition to fever, exercise, illness, and other factors, epigenetic factors have gradually attracted attention (150–152). Genetic research on diseases mainly focuses on the primary structure of DNA, i.e., when the DNA sequence changes, causing alterations in gene transcription and translation. Unlike genetics, epigenetics studies the molecules and mechanisms that maintain the state of selectable gene activity states without changing the DNA sequence and has mainly been studied in the fields of non-coding RNA expression, DNA methylation, histone modifications, genomic imprinting, and three-dimensional genome architecture (**Table 1**) (153).

Non-coding RNA

Non-coding RNA refers to RNA that does not encode protein, which is transcribed from the genome and does not translate into protein, but performs biological functions at the RNA level, including microRNA, circular RNA, small nuclear RNA, long non-coding RNA, etc.

MicroRNA (miRNA) is a class of conservative non-coding small RNA, primarily involved in the regulation of post-transcriptional level that can cause target mRNA degradation or repress translation by specific base pairing with target mRNA, thereby affecting the expression of target mRNA. MiR-19b has been reported to be established as a potential candidate for human LQTS, with impaired repolarization of miR-19b-deficient zebrafish, significantly prolonged action potential, showing severe bradycardia and susceptibility to arrhythmias and cardiomyopathy. MiR-19b targets multiple ion channel-related genes. SCN1B acts as the β subunit of $Na_v1.5$, directly regulated by miR-19b and is upregulated upon its loss, possibly leading to prolonged action potential duration by increasing late sodium current. Upon miR-19b reduction, both KCNE4 and KCNE1 are significantly upregulated, which may be due to the impaired cardiac repolarization caused by the inhibition of KCNQ1, resulting in reduced potassium currents, which leads to the prolongation of AP and bradycardia. In addition, the downregulation of the expression of KCNA4, KCND3, SCN12B and CACNA1C indirectly regulated by mir-19b was detected, in which KCNA4 and KCND3 mediate the I_{to}. The notch decreased during early repolarization due to damaged I_{to}, which may explain the increased potential observed in stage 1 of the miR-19b-deficient heart. However, the presence of I_{to} in zebrafish hearts remains controversial. Further, miR-19b reduction can significantly rescue the heterozygous zebrafishes with SQTS phenotype (23).

miRNA can exist stably in a variety of body fluids, known as circulating miRNA. Circulating miRNA levels are associated with multiple diseases, and the expression profile differences significantly between normal people and disease patients, which may be a new class of disease markers. In pediatric patients without organic heart disease, miR-133 plasma levels were increased in children with ventricular tachycardia as compared with healthy controls (24). Circulating miRNA studies in patients with idiopathic ventricular tachycardia and arrhythmogenic cardiomyopathy showed that the plasma levels of miRNA-320 in idiopathic ventricular tachycardia patients were significantly higher than those in ACM patients, which may help to distinguish idiopathic ventricular tachycardia and arrhythmogenic cardiomyopathy (154). MiRNA mostly combines with the UTR region of the coding gene to regulate gene expression, so the sequence of UTR regions is of great significance for controlling the expression of ion channel genes. In fact, there have been reported mutation detection in the SCN5A UTR region and biological predictions of the combined miRNA (25, 155). Variations were also detected in the UTR region of SCN1B, but the miRNAs that may bind to SCN1B were not described in detail (156). Scientists have also tried to screen the genetic mutations of miRNA in LQTS patients to explain the cause of LQTS, but the mutation sites found failed to explain the cause of the disease in the cohort (157).

It is known that KCNH2 encoding $K_v11.1$, which is a subunit of rapid-acting inward rectifying potassium channel, actually KCNH2 intron 9 is splicing inefficient in human heart, only 1/3 of the precursor mRNA is processed into functional $K_v11.1a$ isomers and 2/3 into C-terminal truncated non-functional $K_v11.1a$-USO isomers. The initial step of the splicing process involves the recognition of the 5' splice site by U1 small nuclear ribonucleoprotein. This recognition is mediated by complementary base pairing between the 5' splice site and U1 SnRNA (the RNA component of U1 small ribonucleoprotein) (158). A KCNH2 IVS9-2delA mutation was found in a large LQTS family that resulted in the switching of functional $K_v11.1a$ isoform to the non-functional $K_v11.1a$-USO isoform (159). The extent of complementarity between the 5' splice site and U1 snRNA is an important determinant of splicing efficiency. Modifying the sequence of U1 snRNA can increase its complementarity to the 5' splice site of KCNH2 intron 9, significantly improve the splicing efficiency of the intron 9, increase the expression of the functional $K_v11.1a$ isoforms, and thereby increase the $K_v11.1$ current (158).

DNA Methylation

DNA methylation refers to the process where organisms transfer methyl groups to specific bases with S-adenosylmethionine as the methyl donor under DNA methyltransferase. DNA methylation is regulated at transcription levels and mainly plays an inhibitory role. The common SCN5A polymorphism H558R (rs1805124), a genetic modifier of BRS, can improve the electrocardiographic features and clinical phenotype of SCN5A mutation carriers by repairing abnormal channel gating kinetics and membrane

trafficking and improving sodium channel activity in mutant channels (160–164). In fact, studies have shown that the SCN5A polymorphism H558R can reduce the methylation level of the SCN5A promoter, increase the expression level of SCN5A in the heart tissue, and prevent the occurrence of ventricular fibrillation (26). The G allele of H558R has been linked to QTc interval prolongation, which corresponds to its function (165, 166).

DNA methylation can also play a role in gene imprinting by forming differentially methylated regions (DMRs) on genomes of different parental origins to regulate gene expression (167). For example, there is a differential methylation region within the KCNQ1 locus (KvDMR1), which regulates multiple genes, including KCNQ1, long non-coding RNA KCNQ1OT1, and CDKN1C (27). Since both KCNQ1OT1 and KCNQ1 associated with LQTS are imprinted genes, this part is detailed in the genomic imprinting section.

Histone Modifications

Nucleosome is the basic unit of chromatin composed of histones and DNA wrapped around histones. Modifications of nucleosomes control DNA packaging and regulate the entry of the transcription factor into the DNA. There are at least 15 functional histone modifications that can occur in cells, with histone methylation and demethylation, as well as acetylation and deacetylation, being the most commonly studied modifications in the heart (168).

Histone methylation can be associated with transcriptional activation or repression, while histone acetylation is usually associated with transcriptional activation (169, 170). The active trimethylation of histone H3 at lysine 4 (H3K4me3) mark plays a pivotal role in cell homeostasis in fully differentiated tissues. Decreased h3k4me3 reduces gene expression of KCHIP2, the β-subunit of the I_{to} channel, and attenuates I_{to} and sodium current, prolonging the action potential duration and resulting in increased $I_{Ca,L}$ and enhanced cardiac contractile function (28, 29). KCHIP2 is heterogeneously expressed in the human and mouse ventricular walls, and although there have been no cases of association of KCHIP2 mutations with cardiac disease, functional studies have shown that the gene defect alters repolarization gradients, eliminates fast I_{to}, and increases the susceptibility of murine ventricular cells to ventricular tachycardia (30).

HEY2 is a BrS susceptibility gene, which can not only affect the expression of SCN5A and the formation of the cardiac conduction system but also regulate the expression of transmural potassium channels such as Kcnip2 and KCND2, altering the peak and density of I_{to} and I_{Na} and affecting transmural electrophysiological gradients (20). Studies have shown that H3K4me3 and active H3K27ac (histone H3 acetylated lysine 27) can regulate the ventricular differential transcription of the HEY2 gene by binding to the promoter or enhancer of HEY2, affecting ventricular myocyte depolarization and repolarization (168).

Genomic Imprinting

Genomic imprinting refers to the phenomenon that gene expression has parental selectivity in tissues or cells, and only a specific parental allele is expressed, and the other parental allele are not expressed or rarely expressed. Paternal genes are not expressed as paternal imprinting, and maternal imprinting is the same (171). The KCNQ1 gene, which is an imprinted gene, exists in clusters with other imprinted genes, called imprinted domains. Imprinted domains are regulated by shared regulatory elements (long non-coding RNA and DMR) (171). KCNQ1OT1 is a long non-coding RNA located in the KCNQ1 locus, with a promoter located within the KvDMR1. Affected by differential methylation of the promoter region this gene only expresses the paternal allele, while the maternal allele is silent (172). Unlike KCNQ1OT1, KCNQ1 is biallelic expression in adult tissues and fetal heart, although it shows maternal expression in other fetal tissues and the coding of paternal gene is repressed (27). The main reason is that KCNQ1OT1 can regulate the spatiotemporal expression of KCNQ1 by coordinating chromatin conformation changes and histone modifications. which makes LQTS caused by KCNQ1 mutation not show obvious maternal predisposition, but an autosomal dominant manner (173, 174). Even so, there are still reports that LQTS exhibits female predominance and transmission distortion, i.e., the LQTS allele is more maternally than paternally derived, especially in patients with LQTS due to KCNQ1 mutations, which may be associated with genomic imprinting (31, 32). A study investigating the methylation state of KCNQ1OT1 in a group of patients with symptomatic QTc prolongation found that the rs11023840 AA genotype of KCNQ1OT1 increased the methylation level of KCNQ1OT1 promoter, which was associated with prolonged QTc interval, supporting the role of differential methylation/imprinting of KCNQ1OT1 in symptomatic prolonged QTc risk (33). However, another study showed that different degrees of potassium channel dysfunction caused by variations in different parental origins may also lead to transmission distortion (175). Although inconclusive, there is no doubt that genetic imprinting plays an important role in the pathogenesis of LQTS.

Arsenic trioxide (As2O3, ATO) is a reagent for the treatment of acute promyelocytic leukemia with adverse effects, including the induction of LQTS. Studies have shown that ATO induces a decrease in the transcription level of long non-coding RNA KCNQ1OT1 in the KCNQ1 locus, while KCNQ1OT1 silencing can inhibit the expression of KCNQ1, thus prolonging action potential duration *in vitro* and causing LQTS *in vivo* (176). It has also been reported that miRNA is also involved in ATO-induced QT prolongation, with ATO-induced miR-133 and miR-1 dysregulation acting as the basis of As2O3-induced cardiac electrical disorder. In guinea pigs, ERG protein expression was inhibited by miR-133 while the expression of Kir2.1 channel protein was downregulated by miR-1, resulting in the decrease of rapidly activating delayed rectifier potassium current and inward rectifier potassium current, thereby inducing the prolongation of QT (177).

Three-Dimensional Genome Architecture

With the development of chromosome conformation capture technologies and fluorescence *in situ* hybridization imaging technologies, the role of 3D genome architecture in gene regulation has gradually emerged (178, 179). The genomic DNA in the nucleus is folded into an ordered chromatin spatial

structure that allows elements with a long linear distance can also interact, such as the loop structure formed between enhancer and promoter (180). Among them, CTCF and cohesin complexes assemble three-dimensional chromatin loops in the genome and play a crucial role in regulating the transcriptional patterns of genes (181, 182). CTCF and cohesins are abundantly enriched at topological domain boundaries and localize to CTCF sites, limiting the interaction of functional elements within topological domains (34, 183). Although the association of CTCF binding site variants with ventricular arrhythmias in non-structural heart disease has not been reported, however, CTCF knockout has been reported to cause disorder in the expression of RYR2, KCND2/KCNQ1/SCN5A/CACNB1 and other genes in the ventricle, leads to heart failure, suggesting an association with ventricular arrhythmias (35, 36). Besides, DNA sequence changes that affect the formation of the normal 3D structure of the genome have also been confirmed to be involved in the occurrence and development of the disease (184). Studies have shown that the enhancer (ENHA) in SCN10A interacts with SCN5A promoter, which is necessary for the expression of SCN5A *in vivo* (185). The major allele G of the common variant locus rs6801957 in SCN10A located within this enhancer region establishes a conserved T-box transcription factor binding site to promote enhancer activity, while the risk allele significantly reduces the expression of SCN5A (186). This largely explains the association of this variant site with QRS prolongation in the GWAS study and common variants in SCN10A with BrS (20, 187). In turn, the results of GWAS can also guide the discovery of functional element regions within the loci (188, 189). The analysis of common variants associated with LQTS in the KCNH2 locus identified a conserved cardiac cis-acting element that acts as enhancer and regulates KCNH2 expression through physical proximity to the KCNH2 promoter (37). In fact, GWAS studies have identified a large number of SNPs associated with heart disease, however, the mechanisms of most of the SNPs involved in the occurrence of the disease have not been revealed (190). Marking of regulatory element regions such as enhancers of known disease-causing genes can characterize some variants of unknown significance and provide a theoretical basis for deciphering genetic variation (191). In conclusion, studies of 3D genome architecture provide a new perspective for us to understand the potential mechanism between these SNPs and diseases, as well as a better understanding of the pathogenic mechanism of diseases.

SUMMARY

This article summarizes the genetic and epigenetic factors of ventricular arrhythmia in patients without structural heart disease and introduces the genes that may cause ventricular arrhythmias and their possible pathogenic mechanisms. However, there are still a large number of cases of ventricular arrhythmias without structural heart disease whose causes have not been clarified. Further research and exploration are needed, and the development of high-throughput patch clamping and other related technologies will undoubtedly play an important role. In addition, emerging disciplines such as optogenetics are also developing steadily, which will drive us to have a deeper understanding of the pathogenesis of ventricular arrhythmias.

AUTHOR CONTRIBUTIONS

XT: conceptualization, writing, and supervision. MW: data curation and writing. Both authors contributed to the article and approved the submitted version.

REFERENCES

1. Ortmans S, Daval C, Aguilar M, Compagno P, Cadrin-Tourigny J, Dyrda K, et al. Pharmacotherapy in inherited and acquired ventricular arrhythmia in structurally normal adult hearts. *Expert Opin Pharmacother.* (2019) 20:2101–14. doi: 10.1080/14656566.2019.1669561
2. Prystowsky EN, Padanilam BJ, Joshi S, Fogel RI. Ventricular arrhythmias in the absence of structural heart disease. *J Am Coll Cardiol.* (2012) 59:1733–44. doi: 10.1016/j.jacc.2012.01.036
3. Killu AM, Stevenson WG. Ventricular tachycardia in the absence of structural heart disease. *Heart.* (2019) 105:645–56. doi: 10.1136/heartjnl-2017-311590
4. Nademanee K, Veerakul G, Nogami A, Lou Q, Hocini M, Coronel R, et al. Mechanism of the effects of sodium channel blockade on the arrhythmogenic substrate of Brugada syndrome. *Heart Rhythm.* (2022) 19:407–16. doi: 10.1016/j.hrthm.2021.10.031
5. Nademanee K, Tei C. Two faces of brugada syndrome: electrical and structural diseases. *JACC Clin Electrophysiol.* (2020) 6:1364–6. doi: 10.1016/j.jacep.2020.07.006
6. Liu J, Laksman Z, Backx PH. The electrophysiological development of cardiomyocytes. *Adv Drug Deliv Rev.* (2016) 96:253–73. doi: 10.1016/j.addr.2015.12.023
7. Rivaud MR, Delmar M, Remme CA. Heritable arrhythmia syndromes associated with abnormal cardiac sodium channel function: ionic and non-ionic mechanisms. *Cardiovasc Res.* (2020) 116:1557–70. doi: 10.1093/cvr/cvaa082
8. Jeyaraj D, Ashwath M, Rosenbaum DS. Pathophysiology and clinical implications of cardiac memory. *Pacing Clin Electrophysiol.* (2010) 33:346–52. doi: 10.1111/j.1540-8159.2009.02630.x
9. Eisner DA, Caldwell JL, Kistamas K, Trafford AW. Calcium and excitation-contraction coupling in the heart. *Circ Res.* (2017) 121:181–95. doi: 10.1161/CIRCRESAHA.117.310230
10. Monteiro LM, Vasques-Novoa F, Ferreira L, Pinto-do-O P, Nascimento DS. Restoring heart function and electrical integrity: closing the circuit. *NPJ Regen Med.* (2017) 2:9. doi: 10.1038/s41536-017-0015-2
11. Brandao KO, Tabel VA, Atsma DE, Mummery CL, Davis RP. Human pluripotent stem cell models of cardiac disease: from mechanisms to therapies. *Dis Model Mech.* (2017) 10:1039–59. doi: 10.1242/dmm.030320
12. Blaustein MP, Lederer WJ. Sodium/calcium exchange: its physiological implications. *Physiol Rev.* (1999) 79:763–854. doi: 10.1152/physrev.1999.79.3.763
13. Fozzard HA. Afterdepolarizations and triggered activity. *Basic Res Cardiol.* (1992) 87 (Suppl. 2):105–13. doi: 10.1007/978-3-642-72477-0_10
14. DiFrancesco D. A brief history of pacemaking. *Front Physiol.* (2019) 10:1599. doi: 10.3389/fphys.2019.01599
15. Wilde A, Amin AS. Clinical spectrum of SCN5A mutations: long QT syndrome, brugada syndrome, and cardiomyopathy. *JACC Clin Electrophysiol.* (2018) 4:569–79. doi: 10.1016/j.jacep.2018.03.006
16. Kapplinger JD, Tester DJ, Salisbury BA, Carr JL, Harris-Kerr C, Pollevick GD, et al. Spectrum and prevalence of mutations from the first 2,500 consecutive unrelated patients referred for the FAMILION long QT syndrome genetic test. *Heart Rhythm.* (2009) 6:1297–303. doi: 10.1016/j.hrthm.2009.05.021

17. Medeiros-Domingo A, Bhuiyan ZA, Tester DJ, Hofman N, Bikker H, van Tintelen JP, et al. The RYR2-encoded ryanodine receptor/calcium release channel in patients diagnosed previously with either catecholaminergic polymorphic ventricular tachycardia or genotype negative, exercise-induced long QT syndrome: a comprehensive open reading frame mutational analysis. *J Am Coll Cardiol.* (2009) 54:2065–74. doi: 10.1016/j.jacc.2009.08.022
18. Lerman BB, Dong B, Stein KM, Markowitz SM, Linden J, Catanzaro DF. Right ventricular outflow tract tachycardia due to a somatic cell mutation in G protein subunitalphai2. *J Clin Invest.* (1998) 101:2862–8. doi: 10.1172/JCI1582
19. Hu RM, Tan BH, Orland KM, Valdivia CR, Peterson A, Pu J, et al. Digenic inheritance novel mutations in SCN5a and SNTA1 increase late I(Na) contributing to LQT syndrome. *Am J Physiol Heart Circ Physiol.* (2013) 304:H994–1001. doi: 10.1152/ajpheart.00705.2012
20. Bezzina CR, Barc J, Mizusawa Y, Remme CA, Gourraud JB, Simonet F, et al. Common variants at SCN5A-SCN10A and HEY2 are associated with Brugada syndrome, a rare disease with high risk of sudden cardiac death. *Nat Genet.* (2013) 45:1044–9. doi: 10.1038/ng.2712
21. de Villiers CP, van der Merwe L, Crotti L, Goosen A, George AJ, Schwartz PJ, et al. AKAP9 is a genetic modifier of congenital long-QT syndrome type 1. *Circ Cardiovasc Genet.* (2014) 7:599–606. doi: 10.1161/CIRCGENETICS.113.000580
22. Barc J, Tadros R, Glinge C, Chiang DY, Jouni M, Simonet F, et al. Genome-wide association analyses identify new Brugada syndrome risk loci and highlight a new mechanism of sodium channel regulation in disease susceptibility. *Nat Genet.* (2022) 54:232–9. doi: 10.1038/s41588-021-01007-6
23. Benz A, Kossack M, Auth D, Seyler C, Zitron E, Juergensen L, et al. MiR-19b regulates ventricular action potential duration in zebrafish. *Sci Rep.* (2016) 6:36033. doi: 10.1038/srep36033
24. Sun L, Sun S, Zeng S, Li Y, Pan W, Zhang Z. Expression of circulating microRNA-1 and microRNA-133 in pediatric patients with tachycardia. *Mol Med Rep.* (2015) 11:4039–46. doi: 10.3892/mmr.2015.3246
25. Daimi H, Khelil AH, Neji A, Ben HK, Maaoui S, Aranega A, et al. Role of SCN5A coding and non-coding sequences in Brugada syndrome onset: what's behind the scenes? *Biomed J.* (2019) 42:252–60. doi: 10.1016/j.bj.2019.03.003
26. Matsumura H, Nakano Y, Ochi H, Onohara Y, Sairaku A, Tokuyama T, et al. H558R, a common SCN5A polymorphism, modifies the clinical phenotype of Brugada syndrome by modulating DNA methylation of SCN5A promoters. *J Biomed Sci.* (2017) 24:91. doi: 10.1186/s12929-017-0397-x
27. Mancini-DiNardo D, Steele SJ, Ingram RS, Tilghman SM. A differentially methylated region within the gene Kcnq1 functions as an imprinted promoter and silencer. *Hum Mol Genet.* (2003) 12:283–94. doi: 10.1093/hmg/ddg024
28. Rosati B, Pan Z, Lypen S, Wang HS, Cohen I, Dixon JE, et al. Regulation of KChIP2 potassium channel beta subunit gene expression underlies the gradient of transient outward current in canine and human ventricle. *J Physiol.* (2001) 533:119–25. doi: 10.1111/j.1469-7793.2001.0119b.x
29. Stein AB, Jones TA, Herron TJ, Patel SR, Day SM, Noujaim SF, et al. Loss of H3K4 methylation destabilizes gene expression patterns and physiological functions in adult murine cardiomyocytes. *J Clin Invest.* (2011) 121:2641–50. doi: 10.1172/JCI44641
30. Kuo HC, Cheng CF, Clark RB, Lin JJ, Lin JL, Hoshijima M, et al. A defect in the Kv channel-interacting protein 2 (KChIP2) gene leads to a complete loss of I(to) and confers susceptibility to ventricular tachycardia. *Cell.* (2001) 107:801–13. doi: 10.1016/S0092-8674(01)00588-8
31. Imboden M, Swan H, Denjoy I, Van Langen IM, Latinen-Forsblom PJ, Napolitano C, et al. Female predominance and transmission distortion in the long-QT syndrome. *N Engl J Med.* (2006) 355:2744–51. doi: 10.1056/NEJMoa042786
32. Lorca R, Junco-Vicente A, Martin-Fernandez M, Pascual I, Aparicio A, Barja N, et al. Clinical implications and gender differences of KCNQ1 p.Gly168Arg pathogenic variant in long QT syndrome. *J Clin Med.* (2020) 9:3846. doi: 10.3390/jcm9123846
33. Coto E, Calvo D, Reguero JR, Moris C, Rubin JM, Diaz-Corte C, et al. Differential methylation of lncRNA KCNQ1OT1 promoter polymorphism was associated with symptomatic cardiac long QT. *Epigenomics-Uk.* (2017) 9:1049–57. doi: 10.2217/epi-2017-0024
34. Dixon JR, Selvaraj S, Yue F, Kim A, Li Y, Shen Y, et al. Topological domains in mammalian genomes identified by analysis of chromatin interactions. *Nature.* (2012) 485:376–80. doi: 10.1038/nature11082
35. Lee DP, Tan W, Anene-Nzelu CG, Lee C, Li PY, Luu T, et al. Robust CTCF-Based chromatin architecture underpins epigenetic changes in the heart failure stress-gene response. *Circulation.* (2019) 139:1937–56. doi: 10.1161/CIRCULATIONAHA.118.036726
36. Rosa-Garrido M, Chapski DJ, Schmitt AD, Kimball TH, Karbassi E, Monte E, et al. High-Resolution mapping of chromatin conformation in cardiac myocytes reveals structural remodeling of the epigenome in heart failure. *Circulation.* (2017) 136:1613–25. doi: 10.1161/CIRCULATIONAHA.117.029430
37. van den Boogaard M, van Weerd JH, Bawazeer AC, Hooijkaas IB, van de Werken H, Tessadori F, et al. Identification and characterization of a transcribed distal enhancer involved in cardiac kcnh2 regulation. *Cell Rep.* (2019) 28:2704–14. doi: 10.1016/j.celrep.2019.08.007
38. Watanabe H, Koopmann TT, Le Scouarnec S, Yang T, Ingram CR, Schott JJ, et al. Sodium channel beta1 subunit mutations associated with Brugada syndrome and cardiac conduction disease in humans. *J Clin Invest.* (2008) 118:2260–8. doi: 10.1172/JCI33891
39. Riuro H, Beltran-Alvarez P, Tarradas A, Selga E, Campuzano O, Verges M, et al. A missense mutation in the sodium channel beta2 subunit reveals SCN2B as a new candidate gene for Brugada syndrome. *Hum Mutat.* (2013) 34:961–6. doi: 10.1002/humu.22328
40. Dulsat G, Palomeras S, Cortada E, Riuro H, Brugada R, Verges M. Trafficking and localisation to the plasma membrane of Nav 1.5 promoted by the beta2 subunit is defective due to a beta2 mutation associated with Brugada syndrome. *Biol Cell.* (2017) 109:273–91. doi: 10.1111/boc.201600085
41. Ishikawa T, Takahashi N, Ohno S, Sakurada H, Nakamura K, On YK, et al. Novel SCN3B mutation associated with brugada syndrome affects intracellular trafficking and function of Nav1.5. *Circ J.* (2013) 77:959–67. doi: 10.1253/circj.CJ-12-0995
42. Medeiros-Domingo A, Kaku T, Tester DJ, Iturralde-Torres P, Itty A, Ye B, et al. SCN4B-encoded sodium channel beta4 subunit in congenital long-QT syndrome. *Circulation.* (2007) 116:134–42. doi: 10.1161/CIRCULATIONAHA.106.659086
43. London B, Michalec M, Mehdi H, Zhu X, Kerchner L, Sanyal S, et al. Mutation in glycerol-3-phosphate dehydrogenase 1 like gene (GPD1-L) decreases cardiac Na+ current and causes inherited arrhythmias. *Circulation.* (2007) 116:2260–8. doi: 10.1161/CIRCULATIONAHA.107.703330
44. Kattygnarath D, Maugenre S, Neyroud N, Balse E, Ichai C, Denjoy I, et al. MOG1: a new susceptibility gene for Brugada syndrome. *Circ Cardiovasc Genet.* (2011) 4:261–8. doi: 10.1161/CIRCGENETICS.110.959130
45. Yu G, Liu Y, Qin J, Wang Z, Hu Y, Wang F, et al. Mechanistic insights into the interaction of the MOG1 protein with the cardiac sodium channel Nav1.5 clarify the molecular basis of Brugada syndrome. *J Biol Chem.* (2018) 293:18207–17. doi: 10.1074/jbc.RA118.003997
46. Hu D, Barajas-Martinez H, Pfeiffer R, Dezi F, Pfeiffer J, Buch T, et al. Mutations in SCN10A are responsible for a large fraction of cases of Brugada syndrome. *J Am Coll Cardiol.* (2014) 64:66–79. doi: 10.1016/j.jacc.2014.04.032
47. Wu X, Jiang X, Li H, Tian P, Zhou Z, Shi S, et al. Expression of HCN4 protein in ventricular outflow tract of rabbit with idiopathic ventricular tachycardia. *Zhonghua Yi Xue Za Zhi.* (2015) 95:3620–4.
48. Li X, Li Z, Wang D, Wang DW, Wang Y. A novel gain-of-function KCND3 variant associated with Brugada syndrome. *Cardiology.* (2020) 145:623–32. doi: 10.1159/000508033
49. Delpon E, Cordeiro JM, Nunez L, Thomsen PE, Guerchicoff A, Pollevick GD, et al. Functional effects of KCNE3 mutation and its role in the development of Brugada syndrome. *Circ Arrhythm Electrophysiol.* (2008) 1:209–18. doi: 10.1161/CIRCEP.107.748103
50. Ohno S, Zankov DP, Ding WG, Itoh H, Makiyama T, Doi T, et al. KCNE5 (KCNE1L) variants are novel modulators of Brugada syndrome and idiopathic ventricular fibrillation. *Circ Arrhythm Electrophysiol.* (2011) 4:352–61. doi: 10.1161/CIRCEP.110.959619
51. Wang Q, Curran ME, Splawski I, Burn TC, Millholland JM, VanRaay TJ, et al. Positional cloning of a novel potassium channel gene: KVLQT1 mutations cause cardiac arrhythmias. *Nat Genet.* (1996) 12:17–23. doi: 10.1038/ng0196-17

52. Bellocq C, van Ginneken AC, Bezzina CR, Alders M, Escande D, Mannens MM, et al. Mutation in the KCNQ1 gene leading to the short QT-interval syndrome. *Circulation.* (2004) 109:2394–7. doi: 10.1161/01.CIR.0000130409.72142.FE
53. Garmany R, Giudicessi JR, Ye D, Zhou W, Tester DJ, Ackerman MJ. Clinical and functional reappraisal of alleged type 5 long QT syndrome: causative genetic variants in the KCNE1-encoded minK beta-subunit. *Heart Rhythm.* (2020) 17:937–44. doi: 10.1016/j.hrthm.2020.02.003
54. Ono M, Burgess DE, Schroder EA, Elayi CS, Anderson CL, January CT, et al. Long QT syndrome type 2: emerging strategies for correcting class 2 KCNH2 (hERG) mutations and identifying new patients. *Biomolecules.* (2020) 10:1144. doi: 10.3390/biom10081144
55. Brugada R, Hong K, Dumaine R, Cordeiro J, Gaita F, Borggrefe M, et al. Sudden death associated with short-QT syndrome linked to mutations in HERG. *Circulation.* (2004) 109:30–5. doi: 10.1161/01.CIR.0000109482.92774.3A
56. Isbrandt D, Friederich P, Solth A, Haverkamp W, Ebneth A, Borggrefe M, et al. Identification and functional characterization of a novel KCNE2 (MiRP1) mutation that alters HERG channel kinetics. *J Mol Med.* (2002) 80:524–32. doi: 10.1007/s00109-002-0364-0
57. Priori SG, Pandit SV, Rivolta I, Berenfeld O, Ronchetti E, Dhamoon A, et al. A novel form of short QT syndrome (SQT3) is caused by a mutation in the KCNJ2 gene. *Circ Res.* (2005) 96:800–7. doi: 10.1161/01.RES.0000162101.76263.8c
58. Fodstad H, Swan H, Auberson M, Gautschi I, Loffing J, Schild L, et al. Loss-of-function mutations of the K(+) channel gene KCNJ2 constitute a rare cause of long QT syndrome. *J Mol Cell Cardiol.* (2004) 37:593–602. doi: 10.1016/j.yjmcc.2004.05.011
59. Wang F, Liu J, Hong L, Liang B, Graff C, Yang Y, et al. The phenotype characteristics of type 13 long QT syndrome with mutation in KCNJ5 (Kir3.4-G387R). *Heart Rhythm.* (2013) 10:1500–6. doi: 10.1016/j.hrthm.2013.07.022
60. Barajas-Martinez H, Hu D, Ferrer T, Onetti CG, Wu Y, Burashnikov E, et al. Molecular genetic and functional association of Brugada and early repolarization syndromes with S422L missense mutation in KCNJ8. *Heart Rhythm.* (2012) 9:548–55. doi: 10.1016/j.hrthm.2011.10.035
61. Hu D, Barajas-Martinez H, Terzic A, Park S, Pfeiffer R, Burashnikov E, et al. ABCC9 is a novel Brugada and early repolarization syndrome susceptibility gene. *Int J Cardiol.* (2014) 171:431–42. doi: 10.1016/j.ijcard.2013.12.084
62. Wemhoner K, Friedrich C, Stallmeyer B, Coffey AJ, Grace A, Zumhagen S, et al. Gain-of-function mutations in the calcium channel CACNA1C (Cav1.2) cause non-syndromic long-QT but not Timothy syndrome. *J Mol Cell Cardiol.* (2015) 80:186–95. doi: 10.1016/j.yjmcc.2015.01.002
63. Di Mauro V, Ceriotti P, Lodola F, Salvarani N, Modica J, Bang ML, et al. Peptide-Based targeting of the L-type calcium channel corrects the loss-of-function phenotype of two novel mutations of the CACNA1 gene associated with Brugada syndrome. *Front Physiol.* (2020) 11:616819. doi: 10.3389/fphys.2020.616819
64. Burashnikov E, Pfeiffer R, Barajas-Martinez H, Delpon E, Hu D, Desai M, et al. Mutations in the cardiac L-type calcium channel associated with inherited J-wave syndromes and sudden cardiac death. *Heart Rhythm.* (2010) 7:1872–82. doi: 10.1016/j.hrthm.2010.08.026
65. Wleklinski MJ, Kannankeril PJ, Knollmann BC. Molecular and tissue mechanisms of catecholaminergic polymorphic ventricular tachycardia. *J Physiol.* (2020) 598:2817–34. doi: 10.1113/JP276757
66. Zhong X, Guo W, Wei J, Tang Y, Liu Y, Zhang JZ, et al. Identification of loss-of-function RyR2 mutations associated with idiopathic ventricular fibrillation and sudden death. *Biosci Rep.* (2021) 41: BSR20210209. doi: 10.1042/BSR20210209
67. Wang Q, Michalak M. Calsequestrin. Structure, function, and evolution. *Cell Calcium.* (2020) 90:102242. doi: 10.1016/j.ceca.2020.102242
68. Roux-Buisson N, Cacheux M, Fourest-Lieuvin A, Fauconnier J, Brocard J, Denjoy I, et al. Absence of triadin, a protein of the calcium release complex, is responsible for cardiac arrhythmia with sudden death in human. *Hum Mol Genet.* (2012) 21:2759–67. doi: 10.1093/hmg/dds104
69. Altmann HM, Tester DJ, Will ML, Middha S, Evans JM, Eckloff BW, et al. Homozygous/Compound heterozygous triadin mutations associated with autosomal-recessive long-QT syndrome and pediatric sudden cardiac arrest: elucidation of the triadin knockout syndrome. *Circulation.* (2015) 131:2051–60. doi: 10.1161/CIRCULATIONAHA.115.015397
70. Kotta MC, Sala L, Ghidoni A, Badone B, Ronchi C, Parati G, et al. Calmodulinopathy: a novel, life-threatening clinical entity affecting the young. *Front Cardiovasc Med.* (2018) 5:175. doi: 10.3389/fcvm.2018.00175
71. Wu G, Ai T, Kim JJ, Mohapatra B, Xi Y, Li Z, et al. Alpha-1-syntrophin mutation and the long-QT syndrome: a disease of sodium channel disruption. *Circ Arrhythm Electrophysiol.* (2008) 1:193–201. doi: 10.1161/CIRCEP.108.769224
72. Ishikawa T, Sato A, Marcou CA, Tester DJ, Ackerman MJ, Crotti L, et al. A novel disease gene for Brugada syndrome: sarcolemmal membrane-associated protein gene mutations impair intracellular trafficking of hNav1.5. *Circ Arrhythm Electrophysiol.* (2012) 5:1098–107. doi: 10.1161/CIRCEP.111.969972
73. Persampieri S, Pilato CA, Sommariva E, Maione AS, Stadiotti I, Ranalletta A, et al. Clinical and molecular data define a diagnosis of arrhythmogenic cardiomyopathy in a carrier of a Brugada-syndrome-associated PKP2 mutation. *Genes.* (2020) 11:571. doi: 10.3390/genes11050571
74. Mohler PJ, Schott JJ, Gramolini AO, Dilly KW, Guatimosim S, DuBell WH, et al. Ankyrin-B mutation causes type 4 long-QT cardiac arrhythmia and sudden cardiac death. *Nature.* (2003) 421:634–9. doi: 10.1038/nature01335
75. Zaza A, Grandi E. Mechanisms of Cav3-associated arrhythmia: protein or microdomain dysfunction? *Int J Cardiol.* (2020) 320:97–9. doi: 10.1016/j.ijcard.2020.06.051
76. Devalla HD, Gelinas R, Aburawi EH, Beqqali A, Goyette P, Freund C, et al. TECRL, a new life-threatening inherited arrhythmia gene associated with overlapping clinical features of both LQTS and CPVT. *Embo Mol Med.* (2016) 8:1390–408. doi: 10.15252/emmm.201505719
77. Thorsen K, Dam VS, Kjaer-Sorensen K, Pedersen LN, Skeberdis VA, Jurevicius J, et al. Loss-of-activity-mutation in the cardiac chloride-bicarbonate exchanger AE3 causes short QT syndrome. *Nat Commun.* (2017) 8:1696. doi: 10.1038/s41467-017-01630-0
78. Amarouch MY, El HJ. Inherited cardiac arrhythmia syndromes: focus on molecular mechanisms underlying TRPM4 channelopathies. *Cardiovasc Ther.* (2020) 2020:6615038. doi: 10.1155/2020/6615038
79. Ding DB, Fan LL, Xiao Z, Huang H, Chen YQ, Guo S, et al. A novel mutation of dipeptidyl aminopeptidase-like protein-6 in a family with suspicious idiopathic ventricular fibrillation. *QJM.* (2018) 111:373–7. doi: 10.1093/qjmed/hcy033
80. Koizumi A, Sasano T, Kimura W, Miyamoto Y, Aiba T, Ishikawa T, et al. Genetic defects in a His-Purkinje system transcription factor, IRX3, cause lethal cardiac arrhythmias. *Eur Heart J.* (2016) 37:1469–75. doi: 10.1093/eurheartj/ehv449
81. Cheung JW, Ip JE, Yarlagadda RK, Liu CF, Thomas G, Xu L, et al. Adenosine-insensitive right ventricular tachycardia: novel variant of idiopathic outflow tract tachycardia. *Heart Rhythm.* (2014) 11:1770–8. doi: 10.1016/j.hrthm.2014.06.014
82. Ip JE, Xu L, Dai J, Steegborn C, Jaffre F, Evans T, et al. Constitutively activating GNAS somatic mutation in right ventricular outflow tract tachycardia. *Circ Arrhythm Electrophysiol.* (2021) 14:e10082. doi: 10.1161/CIRCEP.121.010082
83. Han D, Tan H, Sun C, Li G. Dysfunctional Nav1.5 channels due to SCN5A mutations. *Exp Biol Med.* (2018) 243:852–63. doi: 10.1177/1535370218777972
84. Valdivia CR, Ueda K, Ackerman MJ, Makielski JC. GPD1L links redox state to cardiac excitability by PKC-dependent phosphorylation of the sodium channel SCN5A. *Am J Physiol Heart Circ Physiol.* (2009) 297:H1446–52. doi: 10.1152/ajpheart.00513.2009
85. Biel S, Aquila M, Hertel B, Berthold A, Neumann T, DiFrancesco D, et al. Mutation in S6 domain of HCN4 channel in patient with suspected Brugada syndrome modifies channel function. *Pflugers Arch.* (2016) 468:1663–71. doi: 10.1007/s00424-016-1870-1
86. Ueda K, Hirano Y, Higashiuesato Y, Aizawa Y, Hayashi T, Inagaki N, et al. Role of HCN4 channel in preventing ventricular arrhythmia. *J Hum Genet.* (2009) 54:115–21. doi: 10.1038/jhg.2008.16
87. Niwa N, Nerbonne JM. Molecular determinants of cardiac transient outward potassium current (I(to)) expression and regulation. *J Mol Cell Cardiol.* (2010) 48:12–25. doi: 10.1016/j.yjmcc.2009.07.013

88. Amberg GC, Koh SD, Imaizumi Y, Ohya S, Sanders KM. A-type potassium currents in smooth muscle. *Am J Physiol Cell Physiol.* (2003) 284:C583–95. doi: 10.1152/ajpcell.00301.2002
89. Wu W, Sanguinetti MC. Molecular basis of cardiac delayed rectifier potassium channel function and pharmacology. *Card Electrophysiol Clin.* (2016) 8:275–84. doi: 10.1016/j.ccep.2016.01.002
90. Sanguinetti MC, Curran ME, Zou A, Shen J, Spector PS, Atkinson DL, et al. Coassembly of K(V)LQT1 and minK (IsK) proteins to form cardiac I(Ks) potassium channel. *Nature.* (1996) 384:80–3. doi: 10.1038/384080a0
91. Barhanin J, Lesage F, Guillemare E, Fink M, Lazdunski M, Romey G. K(V)LQT1 and lsK (minK) proteins associate to form the I(Ks) cardiac potassium current. *Nature.* (1996) 384:78–80. doi: 10.1038/384078a0
92. Wallace E, Howard L, Liu M, O'Brien T, Ward D, Shen S, et al. Long QT syndrome: genetics and future perspective. *Pediatr Cardiol.* (2019) 40:1419–30. doi: 10.1007/s00246-019-02151-x
93. Dvir M, Strulovich R, Sachyani D, Ben-Tal CI, Haitin Y, Dessauer C, et al. Long QT mutations at the interface between KCNQ1 helix C and KCNE1 disrupt I(KS) regulation by PKA and PIP(2). *J Cell Sci.* (2014) 127:3943–55. doi: 10.1242/jcs.147033
94. Wu ZJ, Huang Y, Fu YC, Zhao XJ, Zhu C, Zhang Y, et al. Characterization of a Chinese KCNQ1 mutation (R259H) that shortens repolarization and causes short QT syndrome 2. *J Geriatr Cardiol.* (2015) 12:394–401. doi: 10.11909/j.issn.1671-5411.2015.04.002
95. Roberts JD, Asaki SY, Mazzanti A, Bos JM, Tuleta I, Muir AR, et al. An international multicenter evaluation of type 5 long QT syndrome: a low penetrant primary arrhythmic condition. *Circulation.* (2020) 141:429–39. doi: 10.1161/CIRCULATIONAHA.119.043114
96. Liu L, Tian J, Lu C, Chen X, Fu Y, Xu B, et al. Electrophysiological characteristics of the LQT2 syndrome mutation KCNH2-G572S and regulation by accessory protein KCNE2. *Front Physiol.* (2016) 7:650. doi: 10.3389/fphys.2016.00650
97. Adeniran I, El HA, Hancox JC, Zhang H. Proarrhythmia in KCNJ2-linked short QT syndrome: insights from modelling. *Cardiovasc Res.* (2012) 94:66–76. doi: 10.1093/cvr/cvs082
98. Plaster NM, Tawil R, Tristani-Firouzi M, Canun S, Bendahhou S, Tsunoda A, et al. Mutations in Kir2.1 cause the developmental and episodic electrical phenotypes of Andersen's syndrome. *Cell.* (2001) 105:511–9. doi: 10.1016/S0092-8674(01)00342-7
99. Hibino H, Inanobe A, Furutani K, Murakami S, Findlay I, Kurachi Y. Inwardly rectifying potassium channels: their structure, function, and physiological roles. *Physiol Rev.* (2010) 90:291–366. doi: 10.1152/physrev.00021.2009
100. Medeiros-Domingo A, Tan BH, Crotti L, Tester DJ, Eckhardt L, Cuoretti A, et al. Gain-of-function mutation S422L in the KCNJ8-encoded cardiac K(ATP) channel Kir6.1 as a pathogenic substrate for J-wave syndromes. *Heart Rhythm.* (2010) 7:1466–71. doi: 10.1016/j.hrthm.2010.06.016
101. Lariccia V, Piccirillo S, Preziuso A, Amoroso S, Magi S. Cracking the code of sodium/calcium exchanger (NCX) gating: old and new complexities surfacing from the deep web of secondary regulations. *Cell Calcium.* (2020) 87:102169. doi: 10.1016/j.ceca.2020.102169
102. Catterall WA. Signaling complexes of voltage-gated sodium and calcium channels. *Neurosci Lett.* (2010) 486:107–16. doi: 10.1016/j.neulet.2010.08.085
103. Zhang Q, Chen J, Qin Y, Wang J, Zhou L. Mutations in voltage-gated L-type calcium channel: implications in cardiac arrhythmia. *Channels.* (2018) 12:201–18. doi: 10.1080/19336950.2018.1499368
104. Fukuyama M, Wang Q, Kato K, Ohno S, Ding WG, Toyoda F, et al. Long QT syndrome type 8: novel CACNA1C mutations causing QT prolongation and variant phenotypes. *Europace.* (2014) 16:1828–37. doi: 10.1093/europace/euu063
105. Splawski I, Timothy KW, Sharpe LM, Decher N, Kumar P, Bloise R, et al. Ca(V)1.2 calcium channel dysfunction causes a multisystem disorder including arrhythmia and autism. *Cell.* (2004) 119:19–31. doi: 10.1016/j.cell.2004.09.011
106. Splawski I, Timothy KW, Decher N, Kumar P, Sachse FB, Beggs AH, et al. Severe arrhythmia disorder caused by cardiac L-type calcium channel mutations. *Proc Natl Acad Sci USA.* (2005) 102:8089–96, 8086–8. doi: 10.1073/pnas.0502506102
107. Colson C, Mittre H, Busson A, Leenhardt A, Denjoy I, Fressard V, et al. Unusual clinical description of adult with Timothy syndrome, carrier of a new heterozygote mutation of CACNA1C. *Eur J Med Genet.* (2019) 62:103648. doi: 10.1016/j.ejmg.2019.04.005
108. Gillis J, Burashnikov E, Antzelevitch C, Blaser S, Gross G, Turner L, et al. Long QT, syndactyly, joint contractures, stroke and novel CACNA1C mutation: expanding the spectrum of Timothy syndrome. *Am J Med Genet A.* (2012) 158A:182–7. doi: 10.1002/ajmg.a.34355
109. Boczek NJ, Best JM, Tester DJ, Giudicessi JR, Middha S, Evans JM, et al. Exome sequencing and systems biology converge to identify novel mutations in the L-type calcium channel, CACNA1C, linked to autosomal dominant long QT syndrome. *Circ Cardiovasc Genet.* (2013) 6:279–89. doi: 10.1161/CIRCGENETICS.113.000138
110. Antzelevitch C, Pollevick GD, Cordeiro JM, Casis O, Sanguinetti MC, Aizawa Y, et al. Loss-of-function mutations in the cardiac calcium channel underlie a new clinical entity characterized by ST-segment elevation, short QT intervals, and sudden cardiac death. *Circulation.* (2007) 115:442–9. doi: 10.1161/CIRCULATIONAHA.106.668392
111. Cordeiro JM, Marieb M, Pfeiffer R, Calloe K, Burashnikov E, Antzelevitch C. Accelerated inactivation of the L-type calcium current due to a mutation in CACNB2b underlies Brugada syndrome. *J Mol Cell Cardiol.* (2009) 46:695–703. doi: 10.1016/j.yjmcc.2009.01.014
112. Templin C, Ghadri JR, Rougier JS, Baumer A, Kaplan V, Albesa M, et al. Identification of a novel loss-of-function calcium channel gene mutation in short QT syndrome (SQTS6). *Eur Heart J.* (2011) 32:1077–88. doi: 10.1093/eurheartj/ehr076
113. Liu W, Deng J, Wang G, Zhang C, Luo X, Yan D, et al. KCNE2 modulates cardiac L-type Ca(2+) channel. *J Mol Cell Cardiol.* (2014) 72:208–18. doi: 10.1016/j.yjmcc.2014.03.013
114. Baltogiannis GG, Lysitsas DN, di Giovanni G, Ciconte G, Sieira J, Conte G, et al. CPVT: Arrhythmogenesis, therapeutic management, and future perspectives. A brief review of the literature. *Front Cardiovasc Med.* (2019) 6:92. doi: 10.3389/fcvm.2019.00092
115. Priori SG, Napolitano C, Memmi M, Colombi B, Drago F, Gasparini M, et al. Clinical and molecular characterization of patients with catecholaminergic polymorphic ventricular tachycardia. *Circulation.* (2002) 106:69–74. doi: 10.1161/01.CIR.0000020013.73106.D8
116. Blancard M, Touat-Hamici Z, Aguilar-Sanchez Y, Yin L, Vaksmann G, Roux-Buisson N, et al. A type 2 ryanodine receptor variant in the helical domain 2 associated with an impairment of the adrenergic response. *J Pers Med.* (2021) 11:579. doi: 10.3390/jpm11060579
117. Hirose S, Murayama T, Tetsuo N, Hoshiai M, Kise H, Yoshinaga M, et al. Loss-of-function mutations in cardiac ryanodine receptor channel cause various types of arrhythmias including long QT syndrome. *Europace.* (2021) 24:497–510. doi: 10.1093/europace/euab250
118. di Barletta MR, Viatchenko-Karpinski S, Nori A, Memmi M, Terentyev D, Turcato F, et al. Clinical phenotype and functional characterization of CASQ2 mutations associated with catecholaminergic polymorphic ventricular tachycardia. *Circulation.* (2006) 114:1012–9. doi: 10.1161/CIRCULATIONAHA.106.623793
119. Faggioni M, Kryshtal DO, Knollmann BC. Calsequestrin mutations and catecholaminergic polymorphic ventricular tachycardia. *Pediatr Cardiol.* (2012) 33:959–67. doi: 10.1007/s00246-012-0256-1
120. Zhang L, Kelley J, Schmeisser G, Kobayashi YM, Jones LR. Complex formation between junctin, triadin, calsequestrin, and the ryanodine receptor. Proteins of the cardiac junctional sarcoplasmic reticulum membrane. *J Biol Chem.* (1997) 272:23389–97. doi: 10.1074/jbc.272.37.23389
121. Chopra N, Yang T, Asghari P, Moore ED, Huke S, Akin B, et al. Ablation of triadin causes loss of cardiac Ca2+ release units, impaired excitation-contraction coupling, and cardiac arrhythmias. *Proc Natl Acad Sci USA.* (2009) 106:7636–41. doi: 10.1073/pnas.0902919106
122. Rabbani B, Khorgami M, Dalili M, Zamani N, Mahdieh N, Gollob MH. Novel cases of pediatric sudden cardiac death secondary to TRDN mutations presenting as long QT syndrome at rest and catecholaminergic polymorphic ventricular tachycardia during exercise: the TRDN arrhythmia syndrome. *Am J Med Genet a.* (2021) 185:3433–45. doi: 10.1002/ajmg.a.62464
123. Clemens DJ, Tester DJ, Marty I, Ackerman MJ. Phenotype-guided whole genome analysis in a patient with genetically elusive long

QT syndrome yields a novel TRDN-encoded triadin pathogenetic substrate for triadin knockout syndrome and reveals a novel primate-specific cardiac TRDN transcript. *Heart Rhythm.* (2020) 17:1017–24. doi: 10.1016/j.hrthm.2020.01.012

124. Ben-Johny M, Yue DT. Calmodulin regulation (calmodulation) of voltage-gated calcium channels. *J Gen Physiol.* (2014) 143:679–92. doi: 10.1085/jgp.201311153
125. Brohus M, Arsov T, Wallace DA, Jensen HH, Nyegaard M, Crotti L, et al. Infanticide vs. inherited cardiac arrhythmias. *Europace.* (2021) 23:441–50. doi: 10.1093/europace/euaa272
126. Choi JI, Wang C, Thomas MJ, Pitt GS. Alpha1-Syntrophin variant identified in drug-induced long QT syndrome increases late sodium current. *PLoS ONE.* (2016) 11:e152355. doi: 10.1371/journal.pone.0152355
127. Campuzano O, Fernandez-Falgueras A, Iglesias A, Brugada R. Brugada syndrome and PKP2: evidences and uncertainties. *Int J Cardiol.* (2016) 214:403–5. doi: 10.1016/j.ijcard.2016.03.194
128. Li J, Chen K, Zhu R, Zhang M. Structural basis underlying strong interactions between ankyrins and spectrins. *J Mol Biol.* (2020) 432:3838–50. doi: 10.1016/j.jmb.2020.04.023
129. Steinfurt J, Bezzina CR, Biermann J, Staudacher D, Marschall C, Trolese L, et al. Two siblings with early repolarization syndrome: clinical and genetic characterization by whole-exome sequencing. *Europace.* (2021) 23:775–80. doi: 10.1093/europace/euaa357
130. Prasad V, Bodi I, Meyer JW, Wang Y, Ashraf M, Engle SJ, et al. Impaired cardiac contractility in mice lacking both the AE3 Cl-/HCO3- exchanger and the NKCC1 Na+-K+-2Cl- cotransporter: effects on Ca2+ handling and protein phosphatases. *J Biol Chem.* (2008) 283:31303–14. doi: 10.1074/jbc.M803706200
131. Visser M, van der Heijden JF, Doevendans PA, Loh P, Wilde AA, Hassink RJ. Idiopathic ventricular fibrillation: the struggle for definition, diagnosis, and follow-up. *Circ Arrhythm Electrophysiol.* (2016) 9:e003817. doi: 10.1161/CIRCEP.115.003817
132. Marsman RF, Barc J, Beekman L, Alders M, Dooijes D, van den Wijngaard A, et al. A mutation in CALM1 encoding calmodulin in familial idiopathic ventricular fibrillation in childhood and adolescence. *J Am Coll Cardiol.* (2014) 63:259–66. doi: 10.1016/j.jacc.2013.07.091
133. Alders M, Koopmann TT, Christiaans I, Postema PG, Beekman L, Tanck MW, et al. Haplotype-sharing analysis implicates chromosome 7q36 harboring DPP6 in familial idiopathic ventricular fibrillation. *Am J Hum Genet.* (2009) 84:468–76. doi: 10.1016/j.ajhg.2009.02.009
134. Roston TM, Sanatani S, Chen SR. Suppression-of-function mutations in the cardiac ryanodine receptor: emerging evidence for a novel arrhythmia syndrome? *Heart Rhythm.* (2017) 14:108–9. doi: 10.1016/j.hrthm.2016.11.004
135. Walsh MA, Stuart AG, Schlecht HB, James AF, Hancox JC, Newbury-Ecob RA. Compound heterozygous triadin mutation causing cardiac arrest in two siblings. *Pacing Clin Electrophysiol.* (2016) 39:497–501. doi: 10.1111/pace.12813
136. Blancard M, Debbiche A, Kato K, Cardin C, Sabrina G, Gandjbakhch E, et al. An African loss-of-function CACNA1C variant p.T1787M associated with a risk of ventricular fibrillation. *Sci Rep.* (2018) 8:14619. doi: 10.1038/s41598-018-32867-4
137. Akai J, Makita N, Sakurada H, Shirai N, Ueda K, Kitabatake A, et al. A novel SCN5A mutation associated with idiopathic ventricular fibrillation without typical ECG findings of Brugada syndrome. *Febs Lett.* (2000) 479:29–34. doi: 10.1016/S0014-5793(00)01875-5
138. Priori SG, Blomstrom-Lundqvist C, Mazzanti A, Blom N, Borggrefe M, Camm J, et al. 2015 ESC guidelines for the management of patients with ventricular arrhythmias and the prevention of sudden cardiac death: the task force for the management of patients with ventricular arrhythmias and the prevention of sudden cardiac death of the European society of cardiology (ESC) endorsed by: association for European paediatric and congenital cardiology (AEPC). *Europace.* (2015) 17:1601–87. doi: 10.1093/eurheartj/ehv316
139. Jerng HH, Qian Y, Pfaffinger PJ. Modulation of Kv4.2 channel expression and gating by dipeptidyl peptidase 10 (DPP10). *Biophys J.* (2004) 87:2380–96. doi: 10.1529/biophysj.104.042358
140. Seikel E, Trimmer JS. Convergent modulation of Kv4.2 channel alpha subunits by structurally distinct DPPX and KChIP auxiliary subunits. *Biochemistry.* (2009) 48:5721–30. doi: 10.1021/bi802316m
141. Soh H, Goldstein SA. I SA channel complexes include four subunits each of DPP6 and Kv4.2. *J Biol Chem.* (2008) 283:15072–7. doi: 10.1074/jbc.M706964200
142. Ten SJ, Postema PG, Boekholdt SM, Tan HL, van der Heijden JF, de Groot NM, et al. Detailed characterization of familial idiopathic ventricular fibrillation linked to the DPP6 locus. *Heart Rhythm.* (2016) 13:905–12. doi: 10.1016/j.hrthm.2015.12.006
143. Conte G, Giudicessi JR, Ackerman MJ. Idiopathic ventricular fibrillation: the ongoing quest for diagnostic refinement. *Europace.* (2021) 23:4–10. doi: 10.1093/europace/euaa211
144. Bezzina C, Veldkamp MW, van Den Berg MP, Postma AV, Rook MB, Viersma JW, et al. A single Na(+) channel mutation causing both long-QT and Brugada syndromes. *Circ Res.* (1999) 85:1206–13. doi: 10.1161/01.RES.85.12.1206
145. Risgaard B, Jabbari R, Refsgaard L, Holst AG, Haunso S, Sadjadieh A, et al. High prevalence of genetic variants previously associated with Brugada syndrome in new exome data. *Clin Genet.* (2013) 84:489–95. doi: 10.1111/cge.12126
146. Priori SG, Napolitano C, Schwartz PJ. Low penetrance in the long-QT syndrome: clinical impact. *Circulation.* (1999) 99:529–33. doi: 10.1161/01.CIR.99.4.529
147. Clatot J, Neyroud N, Cox R, Souil C, Huang J, Guicheney P, et al. Inter-regulation of kv4.3 and voltage-gated sodium channels underlies predisposition to cardiac and neuronal channelopathies. *Int J Mol Sci.* (2020) 21:5057. doi: 10.3390/ijms21145057
148. Chen L, Kass RS. A-kinase anchoring protein 9 and IKs channel regulation. *J Cardiovasc Pharmacol.* (2011) 58:413–59. doi: 10.1097/FJC.0b013e318232c80c
149. Zhang R, Chen F, Yu H, Gao L, Yin X, Dong Y, et al. The genetic variation rs12143842 in NOS1AP increases idiopathic ventricular tachycardia risk in Chinese Han populations. *Sci Rep.* (2017) 7:8356. doi: 10.1038/s41598-017-08548-z
150. Adler A, Topaz G, Heller K, Zeltser D, Ohayon T, Rozovski U, et al. Fever-induced Brugada pattern: How common is it and what does it mean? *Heart Rhythm.* (2013) 10:1375–82. doi: 10.1016/j.hrthm.2013.07.030
151. Mascia G, Arbelo E, Hernandez-Ojeda J, Solimene F, Brugada R, Brugada J. Brugada syndrome and exercise practice: current knowledge, shortcomings and open questions. *Int J Sports Med.* (2017) 38:573–81. doi: 10.1055/s-0043-107240
152. Iglesias DG, Rubin J, Perez D, Moris C, Calvo D. Insights for stratification of risk in Brugada syndrome. *Eur Cardiol.* (2019) 14:45–9. doi: 10.15420/ecr.2018.31.2
153. Cavalli G, Heard E. Advances in epigenetics link genetics to the environment and disease. *Nature.* (2019) 571:489–99. doi: 10.1038/s41586-019-1411-0
154. Sommariva E, D'Alessandra Y, Farina FM, Casella M, Cattaneo F, Catto V, et al. MiR-320a as a potential novel circulating biomarker of arrhythmogenic CardioMyopathy. *Sci Rep.* (2017) 7:4802. doi: 10.1038/s41598-017-05001-z
155. Kiehne N, Kauferstein S. Mutations in the SCN5A gene: evidence for a link between long QT syndrome and sudden death? *Forensic Sci Int Genet.* (2007) 1:170–4. doi: 10.1016/j.fsigen.2007.01.009
156. Ricci MT, Menegon S, Vatrano S, Mandrile G, Cerrato N, Carvalho P, et al. SCN1B gene variants in Brugada syndrome: a study of 145 SCN5A-negative patients. *Sci Rep.* (2014) 4:6470. doi: 10.1038/srep06470
157. Hedley PL, Carlsen AL, Christiansen KM, Kanters JK, Behr ER, Corfield VA, et al. MicroRNAs in cardiac arrhythmia: DNA sequence variation of MiR-1 and MiR-133A in long QT syndrome. *Scand J Clin Lab Invest.* (2014) 74:485–91. doi: 10.3109/00365513.2014.905696
158. Gong Q, Stump MR, Zhou Z. Upregulation of functional Kv11.1a isoform expression by modified U1 small nuclear RNA. *Gene.* (2018) 641:220–5. doi: 10.1016/j.gene.2017.10.063
159. Gong Q, Stump MR, Deng V, Zhang L, Zhou Z. Identification of Kv11.1 isoform switch as a novel pathogenic mechanism of long-QT syndrome. *Circ Cardiovasc Genet.* (2014) 7:482–90. doi: 10.1161/CIRCGENETICS.114.000586

160. Lizotte E, Junttila MJ, Dube MP, Hong K, Benito B, DE Zutter M, et al. Genetic modulation of brugada syndrome by a common polymorphism. *J Cardiovasc Electrophysiol.* (2009) 20:1137–41. doi: 10.1111/j.1540-8167.2009.01508.x
161. Viswanathan PC, Benson DW, Balser JR. A common SCN5A polymorphism modulates the biophysical effects of an SCN5A mutation. *J Clin Invest.* (2003) 111:341–6. doi: 10.1172/JCI200316879
162. Shinlapawittayatorn K, Du XX, Liu H, Ficker E, Kaufman ES, Deschenes I. A common SCN5A polymorphism modulates the biophysical defects of SCN5A mutations. *Heart Rhythm.* (2011) 8:455–62. doi: 10.1016/j.hrthm.2010.11.034
163. Ye B, Valdivia CR, Ackerman MJ, Makielski JC. A common human SCN5A polymorphism modifies expression of an arrhythmia causing mutation. *Physiol Genomics.* (2003) 12:187–93. doi: 10.1152/physiolgenomics.00117.2002
164. Shinlapawittayatorn K, Dudash LA, Du XX, Heller L, Poelzing S, Ficker E, et al. A novel strategy using cardiac sodium channel polymorphic fragments to rescue trafficking-deficient SCN5A mutations. *Circ Cardiovasc Genet.* (2011) 4:500–9. doi: 10.1161/CIRCGENETICS.111.960633
165. Gouas L, Nicaud V, Berthet M, Forhan A, Tiret L, Balkau B, et al. Association of KCNQ1, KCNE1, KCNH2 and SCN5A polymorphisms with QTc interval length in a healthy population. *Eur J Hum Genet.* (2005) 13:1213–22. doi: 10.1038/sj.ejhg.5201489
166. Tsukakoshi T, Lin L, Murakami T, Shiono J, Izumi I, Horigome H. Persistent QT prolongation in a child with gitelman syndrome and SCN5A H558R polymorphism. *Int Heart J.* (2018) 59:1466–8. doi: 10.1536/ihj.17-686
167. Li X. Genomic imprinting is a parental effect established in mammalian germ cells. *Curr Top Dev Biol.* (2013) 102:35–59. doi: 10.1016/B978-0-12-416024-8.00002-7
168. Jimenez J, Rentschler SL. Transcriptional and epigenetic regulation of cardiac electrophysiology. *Pediatr Cardiol.* (2019) 40:1325–30. doi: 10.1007/s00246-019-02160-w
169. Rao SS, Huntley MH, Durand NC, Stamenova EK, Bochkov ID, Robinson JT, et al. A 3D map of the human genome at kilobase resolution reveals principles of chromatin looping. *Cell.* (2014) 159:1665–80. doi: 10.1016/j.cell.2014.11.021
170. Nothjunge S, Nuhrenberg TG, Gruning BA, Doppler SA, Preissl S, Schwaderer M, et al. DNA methylation signatures follow preformed chromatin compartments in cardiac myocytes. *Nat Commun.* (2017) 8:1667. doi: 10.1038/s41467-017-01724-9
171. Monk D, Mackay D, Eggermann T, Maher ER, Riccio A. Genomic imprinting disorders: lessons on how genome, epigenome and environment interact. *Nat Rev Genet.* (2019) 20:235–48. doi: 10.1038/s41576-018-0092-0
172. Smilinich NJ, Day CD, Fitzpatrick GV, Caldwell GM, Lossie AC, Cooper PR, et al. A maternally methylated CpG island in KvLQT1 is associated with an antisense paternal transcript and loss of imprinting in Beckwith-Wiedemann syndrome. *Proc Natl Acad Sci USA.* (1999) 96:8064–9. doi: 10.1073/pnas.96.14.8064
173. Korostowski L, Raval A, Breuer G, Engel N. Enhancer-driven chromatin interactions during development promote escape from silencing by a long non-coding RNA. *Epigenetics Chromatin.* (2011) 4:21. doi: 10.1186/1756-8935-4-21
174. Singh P, Wu X, Lee DH, Li AX, Rauch TA, Pfeifer GP, et al. Chromosome-wide analysis of parental allele-specific chromatin and DNA methylation. *Mol Cell Biol.* (2011) 31:1757–70. doi: 10.1128/MCB.00961-10
175. Itoh H, Berthet M, Fressart V, Denjoy I, Maugenre S, Klug D, et al. Asymmetry of parental origin in long QT syndrome: Preferential maternal transmission of KCNQ1 variants linked to channel dysfunction. *Eur J Hum Genet.* (2016) 24:1160–6. doi: 10.1038/ejhg.2015.257
176. Jiang Y, Du W, Chu Q, Qin Y, Tuguzbaeva G, Wang H, et al. Downregulation of long non-coding RNA kcnq1ot1: an important mechanism of arsenic trioxide-induced long QT syndrome. *Cell Physiol Biochem.* (2018) 45:192–202. doi: 10.1159/000486357
177. Shan H, Zhang Y, Cai B, Chen X, Fan Y, Yang L, et al. Upregulation of microRNA-1 and microRNA-133 contributes to arsenic-induced cardiac electrical remodeling. *Int J Cardiol.* (2013) 167:2798–805. doi: 10.1016/j.ijcard.2012.07.009
178. Zhang Y, Li G. Advances in technologies for 3D genomics research. *Sci China Life Sci.* (2020) 63:811–24. doi: 10.1007/s11427-019-1704-2
179. Schwarzer W, Abdennur N, Goloborodko A, Pekowska A, Fudenberg G, Loe-Mie Y, et al. Two independent modes of chromatin organization revealed by cohesin removal. *Nature.* (2017) 551:51–6. doi: 10.1038/nature24281
180. Woodcock CL, Ghosh RP. Chromatin higher-order structure and dynamics. *Cold Spring Harb Perspect Biol.* (2010) 2:a596. doi: 10.1101/cshperspect.a000596
181. Stadhouders R, Filion GJ, Graf T. Transcription factors and 3D genome conformation in cell-fate decisions. *Nature.* (2019) 569:345–54. doi: 10.1038/s41586-019-1182-7
182. Seitan VC, Faure AJ, Zhan Y, McCord RP, Lajoie BR, Ing-Simmons E, et al. Cohesin-based chromatin interactions enable regulated gene expression within preexisting architectural compartments. *Genome Res.* (2013) 23:2066–77. doi: 10.1101/gr.161620.113
183. Sofueva S, Yaffe E, Chan WC, Georgopoulou D, Vietri RM, Mira-Bontenbal H, et al. Cohesin-mediated interactions organize chromosomal domain architecture. *Embo J.* (2013) 32:3119–29. doi: 10.1038/emboj.2013.237
184. Ouimette JF, Rougeulle C, Veitia RA. Three-dimensional genome architecture in health and disease. *Clin Genet.* (2019) 95:189–98. doi: 10.1111/cge.13219
185. van den Boogaard M, Smemo S, Burnicka-Turek O, Arnolds DE, van de Werken HJ, Klous P, et al. A common genetic variant within SCN10A modulates cardiac SCN5A expression. *J Clin Invest.* (2014) 124:1844–52. doi: 10.1172/JCI73140
186. van den Boogaard M, Wong LY, Tessadori F, Bakker ML, Dreizehnter LK, Wakker V, et al. Genetic variation in T-box binding element functionally affects SCN5A/SCN10A enhancer. *J Clin Invest.* (2012) 122:2519–30. doi: 10.1172/JCI62613
187. Koopmann TT, Adriaens ME, Moerland PD, Marsman RF, Westerveld ML, Lal S, et al. Genome-wide identification of expression quantitative trait loci (eQTLs) in human heart. *PLoS ONE.* (2014) 9:e97380. doi: 10.1371/journal.pone.0097380
188. van Ouwerkerk AF, Bosada FM, van Duijvenboden K, Hill MC, Montefiori LE, Scholman KT, et al. Identification of atrial fibrillation associated genes and functional non-coding variants. *Nat Commun.* (2019) 10:4755. doi: 10.1038/s41467-019-12721-5
189. Montefiori LE, Sobreira DR, Sakabe NJ, Aneas I, Joslin AC, Hansen GT, et al. A promoter interaction map for cardiovascular disease genetics. *Elife.* (2018) 7:e35788. doi: 10.7554/eLife.35788.103
190. Lahrouchi N, Tadros R, Crotti L, Mizusawa Y, Postema PG, Beekman L, et al. Transethnic genome-wide association study provides insights in the genetic architecture and heritability of long QT syndrome. *Circulation.* (2020) 142:324–38. doi: 10.1161/CIRCULATIONAHA.120.045956
191. Gacita AM, Fullenkamp DE, Ohiri J, Pottinger T, Puckelwartz MJ, Nobrega MA, et al. Genetic variation in enhancers modifies cardiomyopathy gene expression and progression. *Circulation.* (2021) 143:1302–16. doi: 10.1161/CIRCULATIONAHA.120.050432

Conflict of Interest: The authors declare that the research was conducted in the absence of any commercial or financial relationships that could be construed as a potential conflict of interest.

frontiers | Frontiers in Cardiovascular Medicine

ORIGINAL RESEARCH
published: 14 July 2022
doi: 10.3389/fcvm.2022.894187

The Role of Patient-Specific Morphological Features of the Left Atrial Appendage on the Thromboembolic Risk Under Atrial Fibrillation

*Giulio Musotto[1,2], Alessandra Monteleone[1], Danila Vella[1], Sofia Di Leonardo[1], Alessia Viola[1,2], Giuseppe Pitarresi[2], Bernardo Zuccarello[2], Antonio Pantano[2], Andrew Cook[3], Giorgia M. Bosi[4] and Gaetano Burriesci[1,4]**

[1] Bioengineering Unit, Ri.MED Foundation, Palermo, Italy, [2] Department of Engineering, University of Palermo, Palermo, Italy, [3] UCL Institute of Cardiovascular Science and Great Ormond Street Hospital for Children, London, United Kingdom, [4] UCL Mechanical Engineering, University College London, London, United Kingdom

OPEN ACCESS

Edited by:
Guowei Li,
Guangdong Second Provincial General Hospital, China

Reviewed by:
Luca Dede,
Politecnico di Milano, Italy
Andrew James Narracott,
The University of Sheffield, United Kingdom

***Correspondence:**
Gaetano Burriesci
g.burriesci@ucl.ac.uk

Specialty section:
This article was submitted to Cardiac Rhythmology, a section of the journal Frontiers in Cardiovascular Medicine

Received: *11 March 2022*
Accepted: *21 June 2022*
Published: *14 July 2022*

Citation:
Musotto G, Monteleone A, Vella D, Di Leonardo S, Viola A, Pitarresi G, Zuccarello B, Pantano A, Cook A, Bosi GM and Burriesci G (2022) The Role of Patient-Specific Morphological Features of the Left Atrial Appendage on the Thromboembolic Risk Under Atrial Fibrillation. Front. Cardiovasc. Med. 9:894187. doi: 10.3389/fcvm.2022.894187

Background: A large majority of thrombi causing ischemic complications under atrial fibrillation (AF) originate in the left atrial appendage (LAA), an anatomical structure departing from the left atrium, characterized by a large morphological variability between individuals. This work analyses the hemodynamics simulated for different patient-specific models of LAA by means of computational fluid–structure interaction studies, modeling the effect of the changes in contractility and shape resulting from AF.

Methods: Three operating conditions were analyzed: sinus rhythm, acute atrial fibrillation, and chronic atrial fibrillation. These were simulated on four patient-specific LAA morphologies, each associated with one of the main morphological variants identified from the common classification: chicken wing, cactus, windsock, and cauliflower. Active contractility of the wall muscle was calibrated on the basis of clinical evaluations of the filling and emptying volumes, and boundary conditions were imposed on the fluid to replicate physiological and pathological atrial pressures, typical of the various operating conditions.

Results: The LAA volume and shear strain rates were analyzed over time and space for the different models. Globally, under AF conditions, all models were well aligned in terms of shear strain rate values and predicted levels of risk. Regions of low shear rate, typically associated with a higher risk of a clot, appeared to be promoted by sudden bends and focused at the trabecule and the lobes. These become substantially more pronounced and extended with AF, especially under acute conditions.

Conclusion: This work clarifies the role of active and passive contraction on the healthy hemodynamics in the LAA, analyzing the hemodynamic effect of AF that promotes clot formation. The study indicates that local LAA topological features are more directly associated with a thromboembolic risk than the global shape of the appendage, suggesting that more effective classification criteria should be identified.

Keywords: left atrial appendage, fluid–structure interaction, LAA morphology, patient-specific models, atrial fibrillation (AF)

INTRODUCTION

The risk of clot formation, ischemic events, and their neurological consequences (1, 2) increase significantly with the pathological condition of atrial fibrillation (AF), a cardiac arrhythmia characterized by irregular electrical activity due to the presence of multiple trigger points on the atrial surface. Although the pathogenesis is still unknown, a vast majority of intracardiac thrombi detected in patients with AF were observed in the left atrial appendage (LAA) (3). This is an anatomical structure departing from the left atrium (LA), partly leaning on the outer wall of the left ventricle, that in normal conditions contracts actively (4) in phase with the atrium. It is reported to play a role in the pressure regulation of the LA, acting as a decompression chamber during the pressure peak corresponding to the ventricular systole (5) and releasing atrial natriuretic peptide (ANP), which can normalize atrial pressure through the activation of specific receptors (6). The LAA is currently classified into four main morphological variants, commonly identified on the basis of the resembling shape as follows: *chicken wing*, *windsock*, *cactus*, and *cauliflower*. Possible relation between the morphological classification and the thrombo–embolic risk has been widely investigated in the literature (7, 8), and a number of numerical studies have been performed on patient-specific models, aiming at identifying hemodynamic changes produced by AF that can be related to higher clotting (9, 10). In particular, the blood shear strain rate (SSR) is a fluid dynamic parameter that can be easily estimated from computational analyses and is commonly correlated with thromboembolic risk (9, 11–14). In fact, SSR is directly related to blood stagnation, which impairs the balance between procoagulant biochemical species, such as thrombin, and anticoagulants promoting the accumulation of the former and the reduction of the latter (15). Moreover, low shear conditions favor platelet activation, adhesion, and stabilization of platelet aggregates, enhancing platelet–fibrin and platelet–endothelium interactions (16).

Still, the numerical studies available in the literature often model the appendage walls as rigid, thus neglecting the contractility and the alteration of the physiological properties and geometric features produced by persistent AF conditions (10, 17). Other studies have included pathological alterations in terms of contractility and remodeling, clearly indicating that these factors can play a major role in the fluid dynamics in the LAA and its alterations produced by AF (14). However, these were applied to simplified anatomical models. This work analyses four patient-specific geometrical models of LAA, classified according to the four morphological variants (9) by means of computational fluid–structure interaction (FSI) simulations.

The models include the active and passive contractility of the LAA walls in conditions of sinus rhythm and AF conditions and simulate their remodeling expected after persistent AF (18, 19). The aim of the work is to clarify the mechanisms related to AF that promote clot formation, and their potential association with anatomical phenotypes and hemodynamic parameters, which could suggest more effective stratification approaches to the thromboembolic risk.

MATERIALS AND METHODS

Models Design

The left atrium is characterized by very complex flow patterns, which depend on the number, shape, and position of the pulmonary veins; the location and shape of the mitral valve; the LAA orifice; and the pressure and flow conditions acting at the veins and valvular ostium (20, 21). Hence, to isolate the role of the atrial appendage and avoid introducing the effect of the patient-specific features characterizing the surrounding anatomy, only the appendage was modeled and analyzed in this work. This assumption does not produce substantial approximations in the determined flow, especially in the distal regions, where the effect of the atrial flow regime becomes negligible and the presence of fluid stagnation increases the risk of clot formation (9).

During the cardiac cycle, the LAA walls deform under the cyclic mechanical actions exerted by blood, while influencing the hemodynamics as a consequence of its passive movement and active contraction. Hence, a two-way FSI simulation was preferred, where the fluid and structural domains are solved in parallel and converge at each step.

A commercial software Ansys 19.2 was used for the simulations. The structural domain was analyzed using an implicit time integration scheme in the Ansys Transient Structural module, as recommended for static and low-frequency dynamic analyses (22, 23). Despite involving a computationally expensive inversion of the global stiffness matrix, these integration schemes have the advantage of achieving global equilibrium at each iteration. Hence, their solutions are unconditionally stable and accurate also for relatively coarse time steps. The fluid domain is solved by employing the computational fluid dynamic (CFD) package Ansys CFX. This code adopts a vertex-based finite volume method to solve the Navier-Stokes equations in an Eulerian description. This approach is particularly convenient when dealing with unstructured tetrahedral meshes, as it strongly reduces the number of degrees of freedom and computational footprint compared to cell-based solvers (24). Moreover, the position of the control volume centered at the boundaries facilitates the treatment of boundary conditions (25) and their exchange at the interface between the two domains. The structural and fluid dynamics solutions were coupled in a two-way FSI simulation through the System Coupling available in the Ansys workbench, which facilitates the data transfer between individual single-physics solvers (26).

The analyzed LAA geometries were defined starting from patient-specific morphologies used in the work by Bosi et al. (9). These are based on radiological scans (computed tomography scan) that return the blood content internal to the LAA and represent the four typical morphologies of the adult population not affected by AF. A detailed description of the segmentation process is provided in Bosi et al. (9). The considered portion of the LAA included the neck and a portion of the atrium between the proximal part of the LAA and the pulmonary veins (**Figure 1A**). This moves the boundary conditions away from the LAA orifice, allowing the contraction of the whole LAA (including its neck region) and the establishment of higher

freedom to the fluid parameters at the LAA inlet. The obtained morphologies were processed on the open-source *Autodesk* program *MeshMixer*, where they were re-meshed and their imperfections were corrected.

The obtained models were closed with a bulge at the open inlet, obtained from a non-uniform rational basis spline (NURBS) tangent to the wall surface at the orifice. This acted as an open surface for the application of the fluid boundary conditions.

To generate the external surface of the LAA solid structure, the internal wall surface (corresponding to the external blood surface) was first smoothened to remove all discontinuities due to the presence of the trabecule and offset in the external direction by 2.1 mm (see **Figure 1B**). This thickness was selected on the

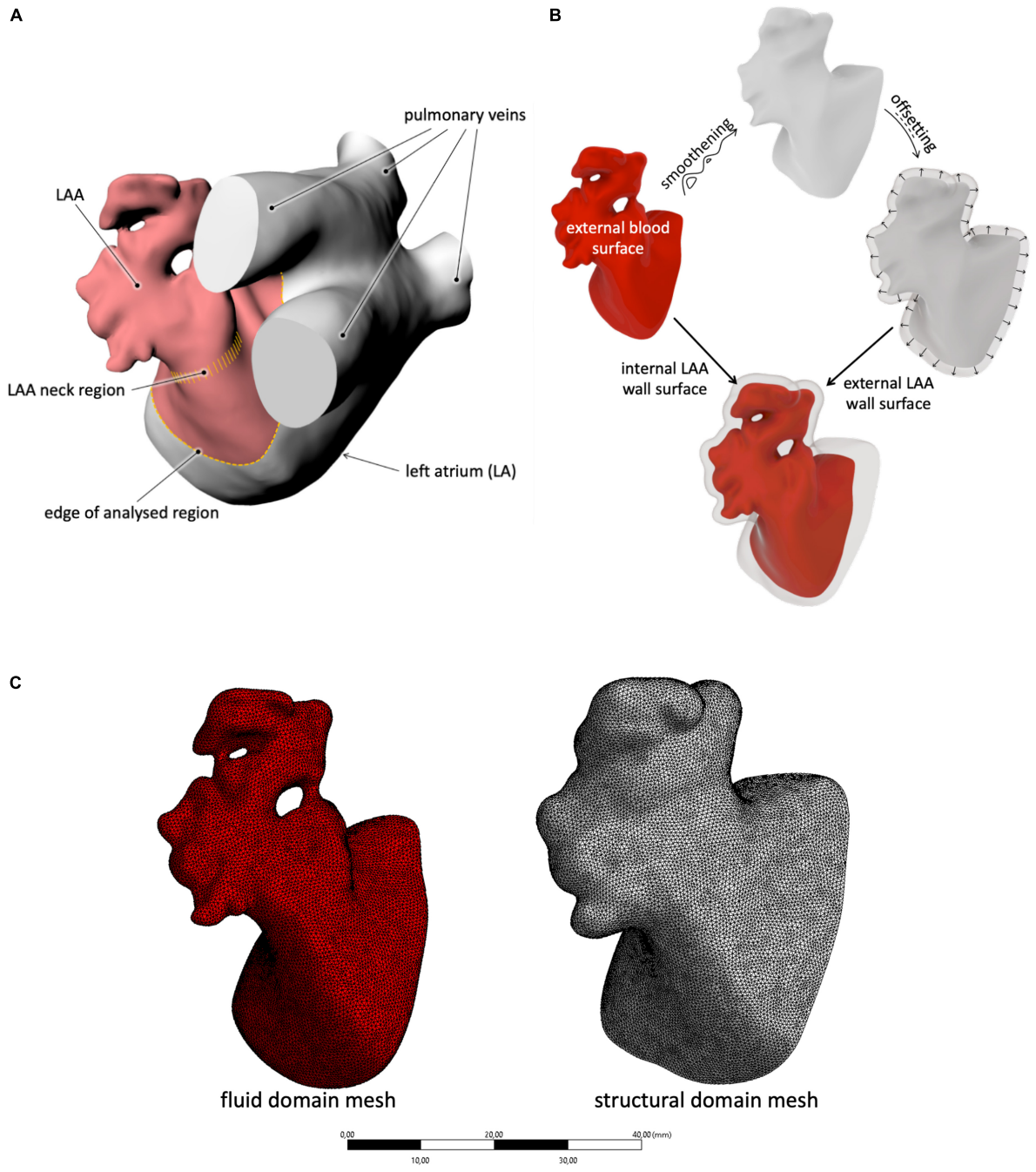

FIGURE 1 | (A) Description of the selection method adopted for the LAA study region; **(B)** schematic procedure used to generate the inner and outer LAA walls, starting from the external blood surface; and **(C)** example of mesh for both the solid and fluid domains with the selected size.

basis of the average wall thickness measured in ovine models (27) and used as an external surface in the construction of the solid part. In particular, the internal and external meshes were transformed into poly surfaces and integrated into a solid volume through the commercial computer-aided design (CAD) software *Rhinoceros 7.0*.

As mentioned above, chronic AF is typically associated with enlargements in the LAA volume. Although the increase of volume associated with this condition is well documented and quantified, no information on the anatomical changes associated with this remodeling is found in the literature. Hence, to verify potential fluid dynamic changes produced by persistent AF, enlarged versions of the four LAA models were created by scaling them up by 150% (28). Despite this being a basic assumption, it is useful to analyze the effect of the LAA size, without introducing other spurious effects.

The CAD models were imported in *ANSYS Workbench* and meshed with quadratic tetrahedral elements for the fluid part and with linear tetrahedral elements for the structural part. The mesh density was selected on the basis of a convergence analysis performed on the *chicken wing* morphology, selected for the setup of all parameters as reported to be the most common, observed in nearly 50% of the patient's population (29). In particular, an average mesh density of 70 element/mm^3 was used for both the structure and the fluid (see **Figure 1C**). The four models are represented in **Figure 2**.

Rheological and Mechanical Properties

Human blood is a concentrated suspension of deformable and aggregable cellular elements in plasma. This can lead to a non-Newtonian shear thinning behavior characterized by thixotropic and viscoelastic properties (30–32). Despite the availability of a number of non-Newtonian models, these are based on steady-state studies (33). Therefore, they are inadequate to describe blood rheology in pulsatile conditions due to the strong time-dependency of the cell aggregation mechanism. Hence, in this work, it was preferred to model the fluid as Newtonian, with a density of 1,062 kg/m^3 and a viscosity of 0.0037 Pa·s, replicating the common physical properties of human blood at large shear rates. The Newtonian behavior is a common assumption that enables direct comparison of the presented work with similar studies in the literature while providing conservative results. In fact, regions, where prolonged stasis is detected, are likely to be even more stagnant under *in vivo* conditions, due to red blood cell aggregation and thrombus formation (34).

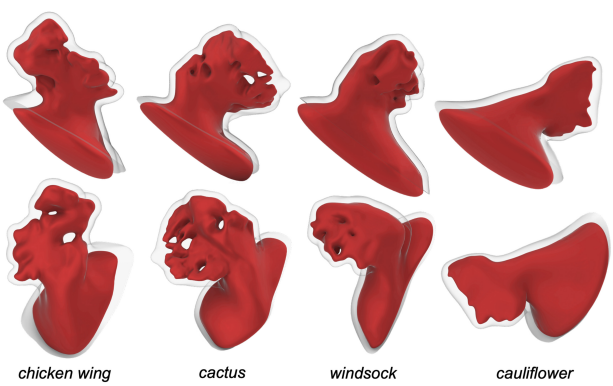

FIGURE 2 | Left atrial appendage CAD models obtained for the four different patient specific shapes, seen from two views.

The tissue of the LAA wall exhibits reduced anisotropy, and the typical non-linearly stiffening constitutive behavior observed in biological soft tissues (27), is characterized by a low-modulus region, a transitional region characterized by a progressive stiffening with strain increases, and a stiff region at larger strains. However, the clinical morphological scans were acquired from pressurized operating hearts, already partially stressed/strained, hence, the wall material was modeled as linear elastic. Anisotropy is reported to be reduced in the wall of the atrium and its appendage (27). Hence, for simplicity, the material was modeled as isotropic. The Young's modulus was set equal to 1.5 MPa, this being the intermediate between that reported for the low and high regions in the left atrium of porcine hearts (35). To account for the material incompressibility, a Poisson's ratio of 0.49 was selected. During LAA contraction, the volume of the appendage is reported to reduce by approximately 60% of its maximum value as a combined effect of the tissue elastic response to the pressure variation and the active contraction of the wall muscle (36). Therefore, a uniformly distributed pressure was imposed at the open surface of the fluid of the *chicken wing* model, replicating the physiological atrial pressure curve obtained from the Wiggers diagram, and the change of volume due to the muscular contractive action was obtained through the setting of a virtual contraction of the structural part. This was achieved by defining orthotropic thermal expansion coefficients of the structural elements. In particular, a local reference system was imposed for each element of the mesh, with the *x-y* plane lying parallel to the inner wall. The coefficient of thermal expansion along the wall thickness (local direction *z*) was defined to maintain volume conservation (for any contraction along the plane there is a corresponding expansion along the thickness), thus mimicking the cardiac muscular behavior. Then, the virtual change of temperature applied to the structure to simulate active contraction was adjusted to replicate clinical evaluations of filling and emptying volumes of the LAA in healthy conditions (36) for the *chicken wing* morphology. In particular, the coefficients of thermal expansion were set equal to 0.05 in the in-plane directions (*x* and *y*) and equal to −0.10 in the out-plane-direction (*z*); and the temperature curve was varied between 0 and 5°C, so as to achieve a relative volume change during the cycle of approximately 60%. For the FSI simulations, the timestep used is 21.5 ms.

In **Figure 3**, a cross-section of the *chicken wing* structural domain model at the maximum expansion and the maximum contraction is represented. The same material parameters were applied to all models.

Boundary Conditions

All nodes of the LAA proximal cross-section were fully constrained. Although this limits the ability of this region to follow a physiological dynamic, the fixed region is in the atrium

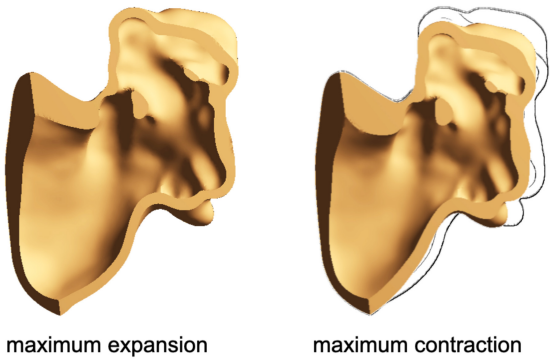

FIGURE 3 | Cross-section of the chicken wing model at the maximum expansion **(left)** and at the maximum contraction **(right)**.

and far from the neck of the LAA, which remains totally free to contract.

For the simulation of sinus rhythm conditions, a uniformly distributed pressure was applied at the open surface of the fluid, based on the physiological atrial pressure described in the Wiggers diagram (37, 38). Then, as described above, a virtual change of temperature was applied to the structure to simulate active contraction (see **Figure 4**).

For the simulation of acute and chronic AF conditions, no active contraction was enforced (by applying a constant virtual temperature equal to 0°C), and the pressure curve applied at the fluid-free surface was modified to account for the lack of atrial contraction (39–42). Hence, the structure only undergoes a passive expansion due to the pressure curve imposed at the opening surface of the fluid. In the case of chronic AF, typically associated with remodeling, the enlarged version of the appendage was used. The simulated heart rate was 70 beats/min, corresponding to a duration of each cycle equal to 860 ms. This is an idealized condition in the case of AF, which was characterized by irregular rhythm and was adopted to allow direct comparison of the results, isolating the effect of the loss of contraction and remodeling. Up to six cardiac cycles were simulated for each morphology, and stabilization of flows was detected for all cases as early as the second cycle.

TABLE 1 | Percentage volume change simulated for all models and all operating conditions.

	Sinus rhythm	AF acute	AF chronic
Chicken wing	56.15%	3.24%	3.30%
Cactus	57.86%	4.10%	4.46%
Windsock	57.43%	2.50%	2.77%
Cauliflower	74.12%	3.84%	3.85%

RESULTS

In total, four different patient-specific models associated with the different morphological classes of the LAA (*chicken wing, cactus*, *windsock,* and *cauliflower*) were analyzed. For each patient-specific morphology, three conditions were analyzed: sinus rhythm, acute AF, and chronic AF, for a total of 12 different numerical simulations.

The volume changes obtained for the different cases are summarized in **Table 1**. The average of the volume variations for the four morphologies in sinus rhythm agrees with the physiological reference value used in the model calibration, as defined by Li et al. (36).

The physical quantities analyzed in the models are the SSR and the peak of velocity at the LAA orifice. As all analyses become periodical after the second cycle, the results were evaluated over the third cardiac cycle. The diagrams in **Figure 5** represent the average wall SSR calculated in the region from the neck of the LAA (smallest orifice cross-section) to its distal end during the cardiac cycle for the four

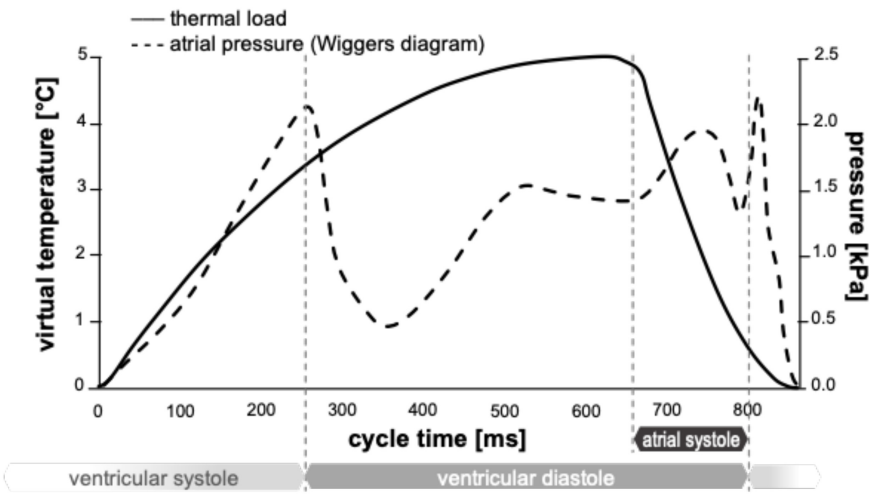

FIGURE 4 | Thermal load (continuous line) and physiological atrial pressure curve (dashed line).

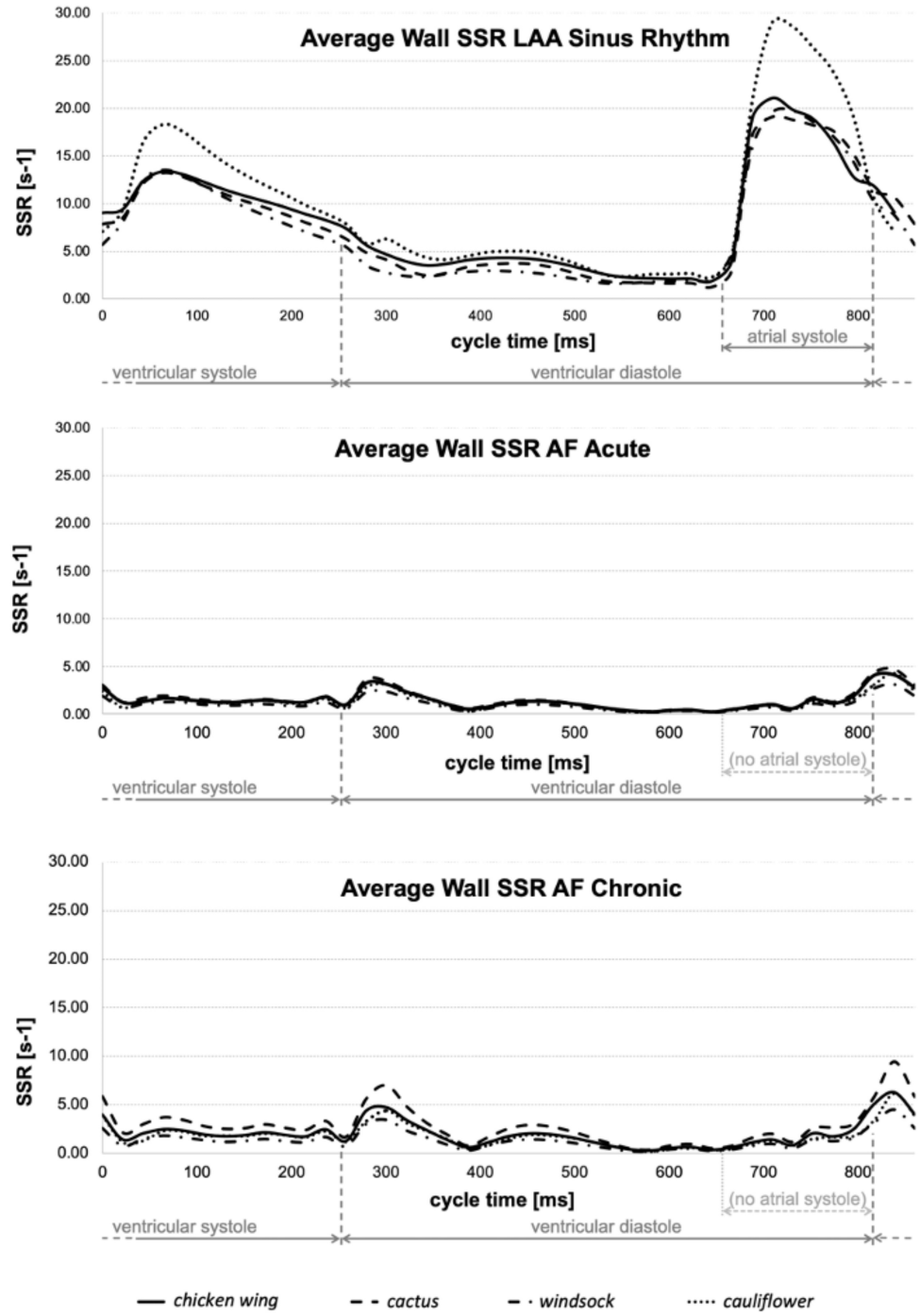

FIGURE 5 | Average wall SSR estimated for all models in sinus rhythm **(top)**, acute AF **(middle)**, and chronic AF **(bottom)** conditions.

appendages in the three different conditions. For clarity, the time in the diagrams is relative to the represented cycle (goes from 0 to 860 ms) rather than to the analysis time (from 1,720 to 2,580 ms).

The color maps in **Figures 6A–C** represent the distribution of wall SSR at the respective peak of the average wall SSR identified from the diagrams in **Figure 5**. To support a more effective visualization of the range of wall SSR, a logarithmic rainbow scale is used in the pictures, with the red color indicating the regions of lowest shear rate where blood clotting is promoted.

To identify regions of the potential risk of thrombosis, the fluid wall that remains exposed for the entire duration of the cycle to SSR values below 10 and 5 s^{-1} are represented in

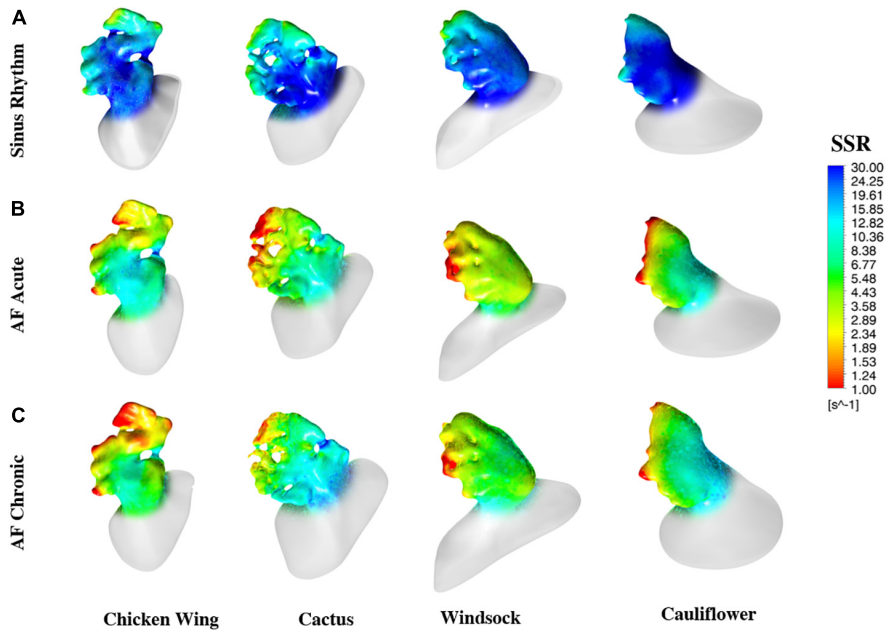

FIGURE 6 | Color maps of the maximum wall SSR at the instant of the cycle when they reach the maximum value, estimated for all models and all operating conditions.

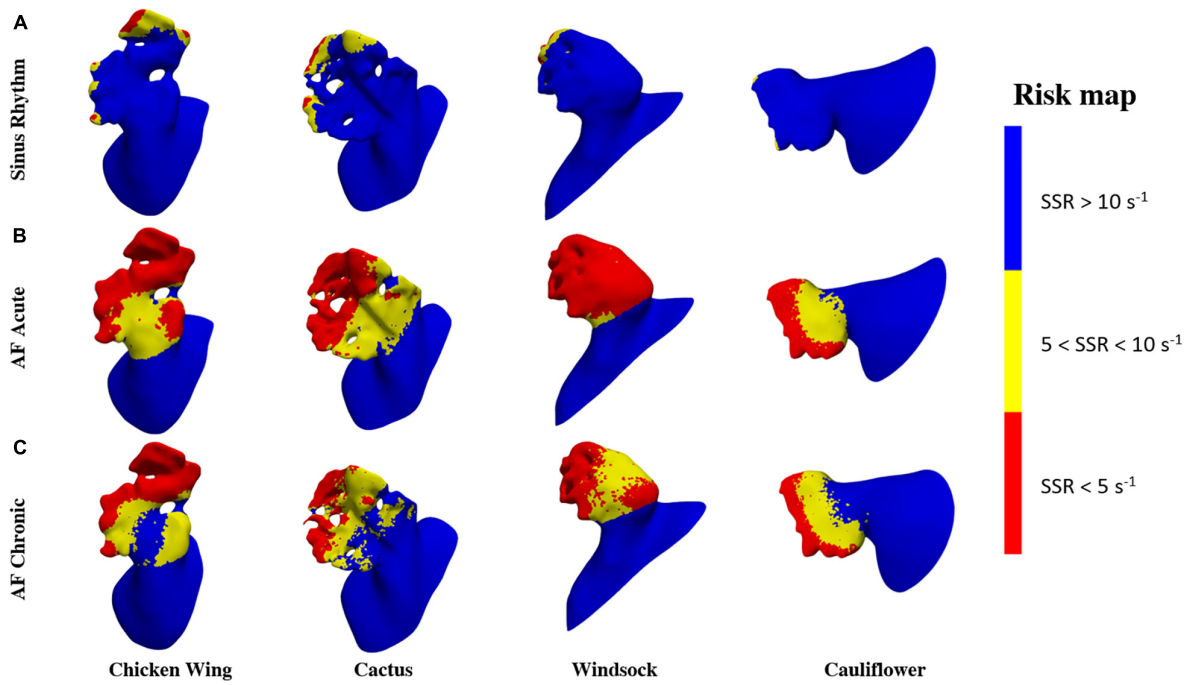

FIGURE 7 | Risk area maps in **(A)** sinus rhythm, **(B)** AF acute, and **(C)** AF chronic.

Figure 7. These thresholds were selected to better identify the regions of low and very low persistent shear rates, where red blood cell aggregation is expected to be more pronounced with a consequent increase in viscosity (in the real case) and clotting (43).

For the different simulations, the percentage of LAA area exposed to SSR values below 10 and 5 s^{-1} for the entire cycle is summarized in **Table 2**.

In the clinical setting, velocity remains the most used parameter for the purposes of a hemodynamic assessment (44).

Hence, the maximum velocity predicted during the cycle at the LAA orifice cross-section for the different simulations was determined and reported in **Table 3**.

DISCUSSION

Although the contraction parameters were set for the *chicken wing* model, under sinus rhythm conditions they produce a very similar percentage of volume changes in all models (about 57%), with the exception of the *cauliflower*, which experienced volume changes of around 30% higher (see **Table 1**). The different behavior of this model could be associated with the fact that it was the only one where the trabecular structure was absent. These may act as tie beams connecting the two main walls defining the appendage chamber, thus reducing the ability of the LAA to modify substantially its shape under the effect of the internal and external loads. These differences are well reflected in the average wall SSR in the LAA region, which is very similar to the *chicken wing, cactus,* and *windsock* models during the whole cardiac cycle, peaking during the active contraction to values around 20 s^{-1} and looks amplified by about 30% for the *cauliflower* (see **Figure 5**, Top).

Under acute and chronic AF conditions, the volume changes reduce dramatically for all cases by over an order of magnitude, with the *cactus* model exhibiting the largest volume change and the *windsock* the lowest, for both acute and chronic conditions (see **Table 1**). Volume variations for the chronic models were expectedly slightly larger, due to the stronger displacements produced by the same pressure acting on larger sections. Interestingly, although the average wall SSR in the LAA region still appears to relate well with the volume change for each condition, it only reduces to about one-fifth of the one predicted in sinus rhythm in the acute case, and to one-third in the chronic case. Globally, the levels of SSR predicted from the models compare well with those indicated in Vella et al. (14), although that study identified higher values observed in the acute conditions than in the enlarged chronic condition. This discrepancy may be because, in Vella et al. (14), LAA wall displacements were imposed, limiting the interplay between the different wall extensions and the elastic expansion and recoil of the structure. This suggests that FSI approaches are more adequate to capture the different factors controlling the phenomenon.

A comparison of the diagrams in **Figure 5** for sinus rhythm and AF conditions indicates that the increase in wall SSR is not just associated with the active contraction producing the atrial systole, but the consequent relaxation phase is equally important, producing an increase in the SSR lasting for the ventricular systole. During this phase, when there is no flow leaving the atrial chamber through the mitral valve, the relaxation of the LAA (a similar effect can be expected for the whole atrial chamber) produces a flow that prevents blood stasis and all potential associated risks.

The color maps of wall SSR distribution (see **Figure 6**) indicate that, in normal conditions, the shear rate reduces at the distal edges and, in particular, after the trabecule and at the lobes. Knees, such as the abrupt bends characterizing the main body of the *chicken wing* and *windsock*, are also associated with some reduction in shear rate. These effects become more pronounced and extended in AF conditions, especially under acute conditions, maintaining the same spatial distribution.

The risk maps in **Figure 7** offer a clearer visualization of the regions where flow conditions promoting blood thickening and clotting are more likely to occur. These risk regions are extremely reduced (less than 5% of the LAA surface is constantly below 5 s^{-1}) and confined at the distal portion of the lobes for the healthy case, but occupy over 55% under acute AF conditions.

This confirms that the active contraction of the LAA plays a clear and marked role in the correct hemodynamics of the region, allowing adequate washing and reducing the risk of clot formation. The maps of risk also show very clearly the crucial role of the lobes (**Figure 7A**) and knees (see yellow regions in **Figure 7B**) in establishing low shear rate regions.

The general behavior appears to be very homogeneous for all models, with the exception of larger volume changes during the cycle and wall SSR predicted for the *cauliflower* in sinus rhythm conditions (this morphology is infrequent, and reported in only about 3% of patients according to Di Biase et al. (29). Under AF conditions, despite the significant morphological differences, all models are well aligned in terms of shear rate values and predicted level of risk.

The association of the LAA morphology with the insurgence of ischemic events is still controversial, with the chicken wing anatomy alternatively identified as the safest one (29, 45) or as the one associated with higher risks (46). Other reports indicate the cauliflower type as a potential predictive risk factor (47, 48). The presented study justifies the incoherency of these findings, diminishing the role of the current morphological classification and attributing more relevance to local topological features, such as the number and depth of lobes, the presence of bends, and the extent of trabeculation. This is supported by a number of clinical studies (48–50) and indicates the need for a new classification, better related

TABLE 2 | Percentage of LAA area exposed to SSR values below 10 and 5 s^{-1} for the entire cycle for the different operating conditions and all models.

	Sinus rhythm		AF acute		AF chronic	
	<5 s^{-1}	<10 s^{-1}	<5 s^{-1}	<10 s^{-1}	<5 s^{-1}	<10 s^{-1}
Chicken Wing	3%	17%	64%	93%	52%	76%
Cactus	3%	11%	55%	93%	33%	63%
Windsock	4%	17%	86%	100%	60%	96%
Cauliflower	0	3%	64%	95%	46%	79%

TABLE 3 | Maximum velocity in sinus rhythm, AF acute, and AF chronic [cm/s].

	Sinus rhythm	AF acute	AF chronic
Chicken Wing	15	2.5	4.6
Cactus	10	2.8	4.4
Windsock	15	2.2	3.5
Cauliflower	20	1.9	4.7

to anatomical characteristics that influence more directly the hemodynamics within the LAA.

Velocities predicted at the orifice were lower than those clinically detected in clinical studies (44). However, direct comparison is not possible, as the velocity measured in patients from echocardiography also includes the motion of the orifice as the effect of atrial motion, which is not taken into consideration in the presented model. It is interesting to observe that, although velocities drop substantially as an effect of AF (**Table 3**), no direct relation between the velocity magnitude and the estimate of the risk can be found. In fact, the orifice velocity depends on the rate of volume variation and the orifice cross-section, so that it is not directly related to the hemodynamics that establishes in the distal portion of the appendage.

The study is based on a number of assumptions and simplifications on the modeled region, the boundary conditions, the material properties, and the rheological characteristics of blood. Although analyzing only the atrial appendage may neglect the effect of the complex fluid dynamics established in the left atrium, the effect of this contribution over the velocities and shear rates estimated on the LAA from previous studies typically dissipates in the first third of the appendage (9, 14). Moreover, the flow patterns in the atrium strongly depend on a number of boundary conditions, such as the pressure at each pulmonary vein or the flow through the mitral valve, whose modeling requires further assumptions and uncertainties. The wall tissue was modeled as linear elastic, with Young's modulus intermediate between that in the low and high rigidity regions in animal tests. Although this choice simplifies the study and avoids substantial alterations of the patient-specific morphologies, the compliance of the atrial wall directly contributes to the component of volume change associated with a passive response to pressure. Hence, its role on the behavior under AF conditions can be relevant. Moreover, it is not known if and how this parameter changes during remodeling. The wall thickness was selected on the basis of animal data and kept constant for all models. The Young's modulus and wall thickness attributed to the LAA structure necessarily have an influence on the passive emptying and filling of the LAA. Lower Young's moduli and thinner walls would increase the fluid pressure contribution compared to the active contraction component. In AF conditions, where the active contraction is missing, modifying these parameters would result in changes in volume variations and SSR values, potentially affecting the evaluation of the thromboembolic risk. Similarly, the passive phases are also directly influenced by the pressure curve imposed at the inlet of the fluid domain, with filling and emptying volumes increasing with the mean and amplitude of the applied pressure load. For what concerns the active phase, the electro-mechanical coupling which characterizes the muscle action was emulated by applying a thermal contraction, following the procedure proposed by Carmody et al. (51). In this case, the thermal response of the material was set to accompany the contraction in a specific direction with dilatation in the orthogonal directions, similar to muscle behavior. Changes in these parameters would alter the effect of the active emptying and the corresponding filling phases. Finally, blood was assumed as Newtonian, thus underestimating the increase of viscosity in the regions of prolonged low shear rate. As mentioned above, this is a conservative assumption, which underestimates the predicted stagnation and clotting potential.

All parameters described above were set on the basis of the available sparse information found in literature and were applied unchanged to all models. This has allowed for the replication, a physiological behavior consistent with clinical observations, providing a better understanding of the phenomena studied. However, the availability of more specific data in healthy and patients with AF about the LAA pressures and dynamics, and the characterization of post-mortem human samples will be essential to increase the reliability of future models.

CONCLUSION

This work analyses four patient-specific LAA anatomies belonging to different morphological types to investigate the mechanisms that promote clot formation in AF conditions. The analysis was performed by means of FSI simulations, modeling the active and passive contractility of the LAA walls in sinus rhythm, and in the/AF condition, also replicating the LAA remodeling typically caused by persistent AF.

The study confirms that the active contractility of the LAA muscular wall is essential in ensuring a physiologically healthy flow, and its impairment caused by AF conditions is the leading factor promoting hemodynamic conditions related to the thromboembolic risk. Hence, FSI models modeling active contraction and the interaction between tissues and pressurized blood are crucial to provide a better insight into the phenomenon.

Most importantly, no major differences were observed between the models in terms of critical flow parameters, indicating that the morphological class is not directly associated with the thromboembolic risk. Still, regions of very low SSR appeared to be concentrated in specific anatomical areas among the various models studied, in particular, in the lobes, after highly trabeculated regions, and in the areas characterized by sudden bends. These observations suggest that a different classification, based on local features rather than on the global gross shape of the LAA, may serve as a better descriptor of thromboembolic risks.

DATA AVAILABILITY STATEMENT

The raw data supporting the conclusions of this article will be made available by the authors, without undue reservation.

ETHICS STATEMENT

This study was carried out in accordance with the recommendations of the South East Research Ethics Research Committee, Ayelsford, Kent, United Kingdom, with written informed consent from all subjects. All subjects gave written informed consent in accordance with the Declaration of Helsinki. The protocol was approved by the South East Research Ethics Research Committee, Ayelsford, Kent, United Kingdom. The

patients/participants provided their written informed consent to participate in this study.

AUTHOR CONTRIBUTIONS

All authors was fully involved in the study and has contributed significantly to the submitted work, in terms of conception and design of the study, analysis and interpretation of the results, and critical review of the manuscript.

FUNDING

This work was supported by the Programme Patto per il Sud Regione Sicilia - FSC 2014/2020 (Project Computational Molecular Design and Screening CHeMISt) PON FSE-FESR Research and Innovation 2014 – 2020 (PON R&I), DDG of MIUR n. 2983 of 05.11.2018, and the Royal Academy of Engineering Fellowship (RF/201920/19/221).

SUPPLEMENTARY MATERIAL

The Supplementary Material for this article can be found online at: https://www.frontiersin.org/articles/10.3389/fcvm.2022.894187/full#supplementary-material

Supplementary Video 1 | A cross-section video of the chicken wing model during a complete cardiac cycle, structural part.

Supplementary Video 2 | A color-maps video of the maximum wall SSR during a complete cardiac cycle, fluid part.

REFERENCES

1. Hagiwara Y, Fujita H, Oh SL, Tan JH, Tan RS, Ciaccio EJ, et al. Computer-aided diagnosis of atrial fibrillation based on ECG signals: a review. *Inf Sci.* (2018) 467:99–114. doi: 10.1016/j.ins.2018.07.063
2. Nattel S. New ideas about atrial fibrillation 50 years on. *Nature.* (2002) 415:219–26. doi: 10.1038/415219a
3. Yaghi S, Song C, Gray WA, Furie KL, Elkind MSV, Kamel H. Left atrial appendage function and stroke risk. *Stroke.* (2015) 46:3554–9. doi: 10.1161/STROKEAHA.115.011273
4. Petty GW, Brown RD, Whisnant JP, Sicks JD, O'Fallon WM, Wiebers DO. Ischemic stroke subtypes. *Stroke.* (1999) 30:2513–6. doi: 10.1161/01.STR.30.12.2513
5. Al-Saady NM, Obel OA, Camm AJ. Left atrial appendage: structure, function, and role in thromboembolism. *Heart.* (1999) 82:547–54. doi: 10.1136/hrt.82.5.547
6. Tabata T. Relationship between left atrial appendage function and plasma concentration of atrial natriuretic peptide. *Eur J Echocardiogr.* (2000) 1:130–7. doi: 10.1053/euje.2000.0019
7. Lane DA, Boos CJ, Lip GYH. Atrial fibrillation (chronic). *BMJ Clin Evid.* (2015) 2015:0217.
8. Yaghi S, Chang AD, Akiki R, Collins S, Novack T, Hemendinger M, et al. The left atrial appendage morphology is associated with embolic stroke subtypes using a simple classification system: a proof of concept study. *J Cardiovasc Comput Tomogr.* (2020) 14:27–33. doi: 10.1016/j.jcct.2019.04.005
9. Bosi GM, Cook A, Rai R, Menezes LJ, Schievano S, Torii R, et al. Computational fluid dynamic analysis of the left atrial appendage to predict thrombosis risk. *Front Cardiovasc Med.* (2018) 5:34. doi: 10.3389/fcvm.2018.00034
10. Masci A, Barone L, Dedè L, Fedele M, Tomasi C, Quarteroni A, et al. The impact of left atrium appendage morphology on stroke risk assessment in atrial fibrillation: a computational fluid dynamics study. *Front Physiol.* (2019) 9:1938. doi: 10.3389/fphys.2018.01938
11. De Sousa DR, Vallecilla C, Chodzynski K, Jerez RC, Malaspinas O, Eker OF, et al. Determination of a shear rate threshold for thrombus formation in intracranial aneurysms. *J Neurointerv Surg.* (2016) 8:853–8. doi: 10.1136/neurintsurg-2015-011737
12. Menichini C, Xu XY. Mathematical modeling of thrombus formation in idealized models of aortic dissection: initial findings and potential applications. *J Math Biol.* (2016) 73:1205–26. doi: 10.1007/s00285-016-0986-4
13. Sarrami-Foroushani A, Lassila T, Hejazi SM, Nagaraja S, Bacon A, Frangi AF. A computational model for prediction of clot platelet content in flow-diverted intracranial aneurysms. *J Biomech.* (2019) 91:7–13. doi: 10.1016/j.jbiomech.2019.04.045
14. Vella D, Monteleone A, Musotto G, Bosi GM, Burriesci G. Effect of the alterations in contractility and morphology produced by atrial fibrillation on the thrombosis potential of the left atrial appendage. *Front Bioeng Biotechnol.* (2021) 9:586041. doi: 10.3389/fbioe.2021.586041
15. Mackman N. New insights into the mechanisms of venous thrombosis. *J Clin Invest.* (2012) 122:2331–6. doi: 10.1172/JCI60229
16. Ouared R, Chopard B, Stahl B, Rüfenacht DA, Yilmaz H, Courbebaisse G. Thrombosis modeling in intracranial aneurysms: a lattice Boltzmann numerical algorithm. *Comput Phys Commun.* (2008) 179:128–31. doi: 10.1016/j.cpc.2008.01.021
17. Dedè L, Menghini F, Quarteroni A. Computational fluid dynamics of blood flow in an idealized left human heart. *Int J Numer Method Biomed Eng.* (2021) 37:e3287. doi: 10.1002/cnm.3287
18. Benra FK, Dohmen HJ, Pei J, Schuster S, Wan B. A comparison of one-way and two-way coupling methods for numerical analysis of fluid-structure interactions. *J Appl Math.* (2011) 2011:456–68. doi: 10.1155/2011/853560
19. Hirschhorn M, Tchantchaleishvili V, Stevens R, Rossano J, Throckmorton A. Fluid–structure interaction modeling in cardiovascular medicine – A systematic review 2017–2019. *Med Eng Phys.* (2020) 78:1–13. doi: 10.1016/j.medengphy.2020.01.008
20. Otani T, Al-Issa A, Pourmorteza A, McVeigh ER, Wada S, Ashikaga HA. Computational framework for personalized blood flow analysis in the human left atrium. *Ann Biomed Eng.* (2016) 44:3284–94. doi: 10.1007/s10439-016-1590-x
21. Vedula V, George R, Younes L, Mittal R. Hemodynamics in the left atrium and its effect on ventricular flow patterns. *J Biomech Eng.* (2015) 137:111003. doi: 10.1115/1.4031487
22. Liu Y. ANSYS and LS-DYNA used for structural analysis. *Int J Comput Aided Eng Technol.* (2008) 1:31–44. doi: 10.1504/IJCAET.2008.021254
23. Yang KH. *'Modal and Transient Dynamic Analysis',. Basic Finite Element Method as Applied to Injury Biomechanics*. Amsterdam: Elsevier (2018). p. 309–82. doi: 10.1016/B978-0-12-809831-8.00008-8
24. Charest MRJ, Canfield TR, Morgan NR, Waltz J, Wohlbier JG. A high-order vertex-based central ENO finite-volume scheme for three-dimensional compressible flows. *Comput Fluids.* (2015) 114:172–92. doi: 10.1016/j.compfluid.2015.03.001
25. Berggren M, Ekström SE, Nordström J. A discontinuous galerkin extension of the vertex-centered edge-based finite volume method. *Commun Comput Phys.* (2009) 5:456–68.
26. Chimakurthi SK, Reuss S, Tooley M, Scampoli SANSYS. Workbench system coupling: a state-of-the-art computational framework for analyzing multiphysics problems. *Eng Comput.* (2018) 34:385–411. doi: 10.1007/s00366-017-0548-4
27. Javani S, Gordon M, Azadani AN. Biomechanical properties and microstructure of heart chambers: a paired comparison study in an ovine model. *Ann Biomed Eng.* (2016) 44:3266–83. doi: 10.1007/s10439-016-1658-7
28. Lacomis JM, Goitein O, Deible C, Moran PL, Mamone G, Madan S, et al. Dynamic multidimensional imaging of the human left atrial appendage. *EP Eur.* (2007) 9:1134–40. doi: 10.1093/europace/eum227

29. Di Biase L, Santangeli P, Anselmino M, Mohanty P, Salvetti I, Gili S, et al. Does the left atrial appendage morphology correlate with the risk of stroke in patients with atrial fibrillation? *J Am Coll Cardiol.* (2012) 60:531–8. doi: 10.1016/j.jacc.2012.04.032
30. Apostolidis AJ, Armstrong MJ, Beris AN. Modeling of human blood rheology in transient shear flows. *J Rheol.* (2015) 59:275–98. doi: 10.1122/1.4904423
31. Chien S. Shear dependence of effective cell volume as a determinant of blood viscosity. *Science.* (1970) 168:977–9. doi: 10.1126/science.168.3934.977
32. Fedosov DA, Pan W, Caswell B, Gompper G, Karniadakis GE. Predicting human blood viscosity in silico. *Proc Natl Acad Sci USA.* (2011) 108:11772–7. doi: 10.1073/pnas.1101210108
33. Yilmaz F, Gundogdu MY. A critical review on blood flow in large arteries; relevance to blood rheology, viscosity models, and physiologic conditions. *Korea-Australia Rheol J.* (2008) 20:197–211.
34. Ducci A, Pirisi F, Tzamtzis S, Burriesci G. Transcatheter aortic valves produce unphysiological flows which may contribute to thromboembolic events: an in-vitro study. *J Biomech.* (2016) 49:4080–9. doi: 10.1016/j.jbiomech.2016.10.050
35. Momtahan N, Poornejad N, Struk JA, Castleton AA, Herrod BJ, Vance BR, et al. Automation of pressure control improves whole porcine heart decellularization. *Tissue Eng Part C Methods.* (2015) 21:1148–61. doi: 10.1089/ten.tec.2014.0709
36. Li CY, Gao BL, Liu XW, Fan QY, Zhang XJ, Liu GC, et al. Quantitative evaluation of the substantially variable morphology and function of the left atrial appendage and its relation with adjacent structures. *PLoS One.* (2015) 10:e0126818. doi: 10.1371/journal.pone.0126818
37. Wiggers CJ, Katz LN. THE CONTOUR OF THE VENTRICULAR VOLUME CURVES UNDER DIFFERENT CONDITIONS. *Am J Physiol Content.* (1922) 58:439–75. doi: 10.1152/ajplegacy.1922.58.3.439
38. Wright BE, Watson GLF, Selfridge NJ. The Wright table of the cardiac cycle: a stand-alone supplement to the Wiggers diagram. *Adv Physiol Educ.* (2020) 44:554–63. doi: 10.1152/advan.00141.2019
39. Fukunami M, Yamada T, Ohmori M, Kumagai K, Umemoto K, Sakai A, et al. Detection of patients at risk for paroxysmal atrial fibrillation during sinus rhythm by P wave-triggered signal-averaged electrocardiogram. *Circulation.* (1991) 83:162–9. doi: 10.1161/01.CIR.83.1.162
40. Steinberg JS, Zelenkofske S, Wong SC, Gelernt M, Sciacca R, Menchavez E. Value of the P-wave signal-averaged ECG for predicting atrial fibrillation after cardiac surgery. *Circulation.* (1993) 88:2618–22. doi: 10.1161/01.CIR.88.6.2618
41. Weng LC, Hall AW, Choi SH, Jurgens SJ, Haessler J, Bihlmeyer NA, et al. Genetic determinants of electrocardiographic P-wave duration and relation to atrial fibrillation. *Circ Genomic Precis Med.* (2020) 13:389–95. doi: 10.1161/CIRCGEN.119.002874
42. Yagishita A, Goya M, Hirao K. Simultaneous recording of the P wave during atrial fibrillation. *Circulation.* (2018) 138:2057–60. doi: 10.1161/CIRCULATIONAHA.118.037198
43. Ranucci M, Laddomada T, Ranucci M, Baryshnikova E. Blood viscosity during coagulation at different shear rates. *Physiol Rep.* (2014) 2:e12065. doi: 10.14814/phy2.12065
44. Fukuda N. Transthoracic Doppler echocardiographic measurement of left atrial appendage blood flow velocity: comparison with transoesophageal measurement. *Eur J Echocardiogr.* (2003) 4:191–5. doi: 10.1016/S1525-2167(02)00166-X
45. Lee JM, Seo J, Uhm J-S, Kim YJ, Lee H-J, Kim J-Y, et al. Why is left atrial appendage morphology related to strokes? An analysis of the flow velocity and orifice size of the left atrial appendage. *J Cardiovasc Electrophysiol.* (2015) 26:922–7. doi: 10.1111/jce.12710
46. Korhonen M, Muuronen A, Arponen O, Mustonen P, Hedman M, Jäkälä P, et al. Left atrial appendage morphology in patients with suspected cardiogenic stroke without known atrial fibrillation. *PLoS One.* (2015) 10:e0118822. doi: 10.1371/journal.pone.0118822
47. Kimura T, Takatsuki S, Inagawa K, Katsumata Y, Nishiyama T, Nishiyama N, et al. Anatomical characteristics of the left atrial appendage in cardiogenic stroke with low CHADS2 scores. *Hear Rhythm.* (2013) 10:921–5. doi: 10.1016/j.hrthm.2013.01.036
48. Khurram IM, Dewire J, Mager M, Maqbool F, Zimmerman SL, Zipunnikov V, et al. Relationship between left atrial appendage morphology and stroke in patients with atrial fibrillation. *Hear Rhythm.* (2013) 10:1843–9. doi: 10.1016/j.hrthm.2013.09.065
49. Yamamoto M, Seo Y, Kawamatsu N, Sato K, Sugano A, Machino-Ohtsuka T, et al. Complex left atrial appendage morphology and left atrial appendage thrombus formation in patients with atrial fibrillation. *Circ Cardiovasc Imaging.* (2014) 7:337–43. doi: 10.1161/CIRCIMAGING.113.001317
50. Koplay M, Erol C, Paksoy Y, Kivrak AS, Özbek S. An investigation of the anatomical variations of left atrial appendage by multidetector computed tomographic coronary angiography. *Eur J Radiol.* (2012) 81:1575–80. doi: 10.1016/j.ejrad.2011.04.060
51. Carmody CJ, Burriesci G, Howard IC, Patterson EA. An approach to the simulation of fluid-structure interaction in the aortic valve. *J Biomech.* (2006) 39:158–69. doi: 10.1016/j.jbiomech.2004.10.038

Conflict of Interest: The authors declare that the research was conducted in the absence of any commercial or financial relationships that could be construed as a potential conflict of interest.

frontiers | Frontiers in Cardiovascular Medicine

TYPE Original Research
PUBLISHED 26 September 2022
DOI 10.3389/fcvm.2022.873135

OPEN ACCESS

EDITED BY
Yafei Li,
Army Medical University, China

REVIEWED BY
Agnieszka Jurek,
Military Institute of Medicine, Poland
Jean-Marc Sellal,
Centre Hospitalier Universitaire de Nancy, France
Deyong Long,
Capital Medical University, China

*CORRESPONDENCE
Rodrigue Garcia
rodrigue_garcia@chu-poitiers.fr

SPECIALTY SECTION
This article was submitted to Cardiac Rhythmology, a section of the journal Frontiers in Cardiovascular Medicine

RECEIVED 10 February 2022
ACCEPTED 05 September 2022
PUBLISHED 26 September 2022

CITATION
Garcia R, Clouard M, Plank F, Degand B, Philibert S, Laurent G, Poupin P, Sakhy S, Gras M, Stühlinger M, Szegedi N, Herczeg S, Simon J, Crijns HJGM, Marijon E, Christiaens L and Guenancia C (2022) Asymptomatic left circumflex artery stenosis is associated with higher arrhythmia recurrence after persistent atrial fibrillation ablation. *Front. Cardiovasc. Med.* 9:873135. doi: 10.3389/fcvm.2022.873135

Asymptomatic left circumflex artery stenosis is associated with higher arrhythmia recurrence after persistent atrial fibrillation ablation

Rodrigue Garcia[1,2]*, Mathilde Clouard[1], Fabian Plank[3], Bruno Degand[1], Séverine Philibert[4], Gabriel Laurent[5], Pierre Poupin[6], Saliman Sakhy[5], Matthieu Gras[1], Markus Stühlinger[3], Nándor Szegedi[7], Szilvia Herczeg[7], Judit Simon[7], Harry J. G. M. Crijns[8], Eloi Marijon[4], Luc Christiaens[1] and Charles Guenancia[5]

[1]Cardiology Department, University Hospital of Poitiers, Poitiers, France, [2]Centre d'Investigation Clinique 1402, University Hospital of Poitiers, Poitiers, France, [3]University Clinic of Internal Medicine III/Cardiology and Angiology, Medical University of Innsbruck, Innsbruck, Austria, [4]Cardiology Department, European Hospital Georges Pompidou, Paris, France, [5]Cardiology Department, University Hospital, Dijon, France, [6]Division of Geriatric Medicine, Tours University Hospital, Tours, France, [7]Heart and Vascular Center, Semmelweis University, Budapest, Hungary, [8]School for Cardiovascular Diseases, Maastricht University Medical Centre, Maastricht, Netherlands

Background: The pathophysiology of persistent atrial fibrillation (AF) remains unclear. While several studies have demonstrated an association between myocardial infarction and atrial fibrillation, the role of stable coronary artery disease (CAD) is still unknown. As a result, we aimed to assess the association between CAD obstruction and AF recurrence after persistent AF ablation in patients with no history of CAD.

Materials and methods: This observational retrospective study included consecutive patients who underwent routine preprocedural cardiac computed tomography (CCT) before persistent AF ablation between September 2015 and June 2018 in 5 European University Hospitals. Exclusion criteria were CAD or coronary revascularization previously known or during follow-up. Obstructive CAD was defined as luminal stenosis $\geq$ 50%.

Results: All in all, 496 patients (mean age 61.8 $\pm$ 10.0 years, 76.2% males) were included. CHA_2DS_2–VASc score was 0 or 1 in 225 (36.3%) patients. Obstructive CAD was present in 86 (17.4%) patients. During the follow-up (24 $\pm$ 19 months), 207 (41.7%) patients had AF recurrence. The recurrence rate was not different between patients with and without obstructive CAD (43.0% vs. 41.5%, respectively; P = 0.79). When considering the location of the stenosis, the recurrence rate was higher in the case of left circumflex obstruction: 56% vs. 32% at 2 years (log-rank $P \leq 0.01$). After Cox multivariate

analysis, circumflex artery obstruction (HR 2.32; 95% CI 1.36–3.98; $P < 0.01$) was independently associated with AF recurrence.

Conclusion: Circumflex artery obstruction detected with CCT was independently associated with 2-fold increase in the risk of AF recurrence after persistent AF ablation. Further research is necessary to evaluate this pathophysiological relationship.

KEYWORDS

atrial fibrillation, ablation, electrophysiology, coronary artery disease, pathophysiology, cardiac computed tomography (CCT), pulmonary vein isolation (PVI)

Introduction

The number of atrial fibrillation (AF) ablation procedures is increasing tremendously worldwide (1, 2). While the mechanisms underlying paroxysmal AF are relatively well-understood, the pathophysiology of persistent AF is complex (3), with atrial substrate and fibrosis playing a crucial role in the genesis and perpetuation of the arrhythmia (4). Myocardial infarction is often associated with AF and may be one of its underlying causes (5–7). Several mechanisms regarding this association have been proposed, including heart failure, inflammation, and atrial ischemia (8–11). Nevertheless, the extent to which asymptomatic coronary artery disease (CAD) may impact AF recurrence after ablation has not been adequately investigated. Up until now, only one single-center study, with a small number of patients and short follow-up, has been published, and no association was found between CAD and arrhythmia recurrence (12).

Preprocedural cardiac computed tomography (CCT) is often performed to assess pulmonary vein anatomy, left atrial dimensions, and to exclude left atrial thrombus before AF catheter ablation (13). Moreover, it is possible to assess the presence of coronary artery stenosis (CAS) at the same time. We consequently hypothesized that coronary stenosis on CCT may be predictive of AF ablation success rate.

The purpose of the current study was to investigate the relation between asymptomatic obstructive CAD and AF recurrence after catheter ablation of persistent AF in a large-scale European multicenter cohort.

Materials and methods

Study population

Consecutive adult patients with symptomatic, drug-refractory persistent AF referred for catheter ablation who underwent preprocedural CCT were screened between September 2015 and June 2018 in 5 European Cardiology Department (the University Hospital of Poitiers, University Hospital of Dijon and European Hospital Georges Pompidou in France, University Hospital of Innsbruck in Austria and Heart and Vascular Center of Semmelweis University in Hungary). Patients with previously known CAD or revascularization during follow-up were excluded. The study was conducted in accordance with the Declaration of Helsinki. All the patients included in this study received an information. According to institutional policy, approval from the Institutional Review Board was not required.

Cardiac computed tomography

Cardiac computed tomography was performed routinely 1–4 weeks prior to AF ablation using standard-of-care, site-specific protocols. The complete heart volume was acquired on a high definition CT scanner within one gantry rotation, allowing a good image quality of the coronary arteries (14, 15). CCT analysis was performed by a single reader blinded to the procedural electrophysiology result. According to the previous study published, the severity of CAD was classified in two categories: obstructive (luminal stenosis $\geq$ 50%) or non-obstructive (absence of CAD or luminal stenosis $<$ 50%) (16). Localization (right coronary, circumflex, and left anterior descending artery) of the lesion was also specified.

Atrial fibrillation ablation

Atrial fibrillation ablation procedures were performed using a cryoballoon ablation catheter (Arctic Front Advance; Medtronic, Inc, Minneapolis, MN, USA) or an open-irrigated radiofrequency ablation catheter (NaviStar, ThermoCool, or ThermoCool SmartTouch; Biosense Webster, Inc, Diamond Bar, CA, USA; Flexability, Tacticath,

TABLE 1 Baseline characteristics.

	Whole population $N = 496$	AF recurrence $N = 207$	No AF recurrence $N = 289$	*P*-value
Age, years	61.8 ± 10.0	62.5 ± 9.5	61.4 ± 10.3	0.24
Male	378 (76.2)	154 (74.4)	224 (77.5)	0.42
Body mass index, kg/m^2	29.0 ± 5.2	29.3 ± 5.4	28.3 ± 5.1	0.33
Hypertension	323 (65.1)	145 (70.0)	178 (61.8)	0.05
Diabetes	69 (13.9)	24 (11.6)	45 (15.6)	0.21
Hypercholesterolemia	230 (46.4)	89 (43.0)	141 (48.8)	0.20
CHA_2DS_2-VASc score				0.91
0–1	225 (36.3)	92 (44.4)	133 (46.0)	
2–3	210 (42.3)	90 (43.5)	120 (41.5)	
≥4	61 (12.3)	25 (12.1)	36 (12.5)	
Left ventricular ejection fraction,%	56.4 ± 11.1	55.0 ± 11.0	57.4 ± 11.1	0.02
Medication				
NOAC	286 (57.7)	114 (55.1)	172 (59.5)	0.32
Vitamin K antagonist	133 (26.8)	64 (30.9)	69 (23.9)	0.08
ß-blockers	327 (65.9)	141 (68.1)	186 (64.4)	0.38
ACEi	139 (28.0)	57 (27.5)	82 (28.4)	0.84
Antiplatelet agents	17 (3.4)	10 (4.8)	7 (2.4)	0.15
Flecainide	34 (6.9)	10 (4.8)	24 (8.3)	0.13
Amiodarone	181 (36.5)	75 (36.2)	106 (36.7)	0.92
AF ablation energy				0.05
Radiofrequency	431 (86.9)	187 (90.3)	244 (84.4)	
Cryoballoon	65 (13.1)	20 (9.7)	45 (15.6)	
AF ablation lesion set				0.18
PVI alone	294 (59.3)	118 (57.0)	176 (60.9)	
PVI + CFAE	70 (14.1)	29 (14.0)	41 (14.2)	
PVI + lines	114 (23.0)	48 (23.2)	66 (22.8)	
PVI + CFAE + lines	18 (3.6)	12 (5.8)	6 (2.1)	

Results are expressed as mean ± SD or number (%). ACEI, angiotensin-converting enzyme inhibitor; AF, atrial fibrillation; CFAE, complex fractionated atrial electrograms; PVI, pulmonary vein isolation; NOAC, novel oral anticoagulants.

Tacticath SE Abbott, Mineapolis, MN, USA) using an electroanatomical mapping system (Carto 3 or EnSite Precision). Briefly, all the patients underwent standard pulmonary vein isolation and electrical isolation was confirmed by a circular multipolar electrode mapping catheter. Additional ablation lesions, such as ablation of complex fractionated atrial electrograms, or mitral, roof, and cavotricuspid lines, were performed at the discretion of the operator.

Endpoints and data collection

The primary objective was to assess the association between obstructive CAD and AF recurrence after persistent AF ablation. Data were collected using an anonymized spread-sheet-based template. Socio-demographic and clinical characteristics were collected at the time of AF ablation. CHA_2DS_2–VASc score was calculated at admission (17). Before AF ablation, all the patients underwent standard two-dimensional transthoracic echocardiography to assess left ventricular ejection fraction, calculated according to the recommendations of the American Society of Echocardiography (18).

Follow-up

Patients were followed up from the time of AF ablation for at least 1 year. All the hospitalization and consultation reports were examined. If necessary, general practitioners and referring cardiologists were contacted to provide previously missing information. Atrial fibrillation recurrences were assessed after a 3-month blanking period (19, 20), and defined as ≥ 1 AF episode recorded during a 12 lead ECG or ≥ 1 AF episode lasting ≥ 30 s documented by Holter monitoring (21). Most of patients had an ECG at 3 months, and a 24-h Holter monitoring at 6, 12, and 24 months.

TABLE 2 Cardiac computed tomography characteristics.

	All population $N = 496$	AF recurrence $N = 207$	No AF recurrence $N = 289$	*P*-value
Left atrial indexed volume, ml/m^2	65.4 ± 23.7	69.3 ± 26.5	62.6 ± 21.1	< 0.01
Obstructive coronary stenosis	86 (17.3)	37 (17.9)	49 (17.0)	0.79
Number of obstructed vessels				0.11
0	410 (82.7)	170 (82.1)	240 (83.0)	
1	54 (10.9)	18 (8.7)	36 (12.5)	
2	24 (4.8)	14 (6.8)	10 (3.5)	
3	8 (1.6)	5 (2.4)	3 (1.0)	

Results are expressed as mean ± SD or number (%). AF, atrial fibrillation.

TABLE 3 Multivariable Cox analysis for AF recurrence after persistent AF ablation.

	Initial model			Final model		
	Hazard ratio	95% CI	*P*-value	Hazard ratio	95% CI	*P*-value
Age, per 1 year increase	1.005	0.989–1.022	0.53			
Body mass index, per 1 kg/m^2 increase	1.035	1.006–1.065	0.02	1.033	1.005–1.062	0.02
Hypertension	1.042	0.748–1.450	0.81			
Diabetes	0.795	0.508–1.244	0.32			
ß-blockers	1.260	0.933–1.701	0.13			
Amiodarone	0.940	0.704–1.255	0.67			
LVEF, per 1% increase	0.996	0.985–1.008	0.53			
LAIV, per 1 ml/m^2 increase	1.011	1.006–1.017	< 0.001	1.012	1.006–1.018	< 0.001
Circumflex artery obstruction	2.322	1.355–3.978	< 0.01	2.154	1.287–3.607	< 0.01
Ablation technique other than PVI combined (ref PVI only)	0.899	0.674–1.198	0.47			

LAIV, left atrial indexed volume; LVEF, left ventricular ejection fraction; PVI, pulmonary vein isolation.

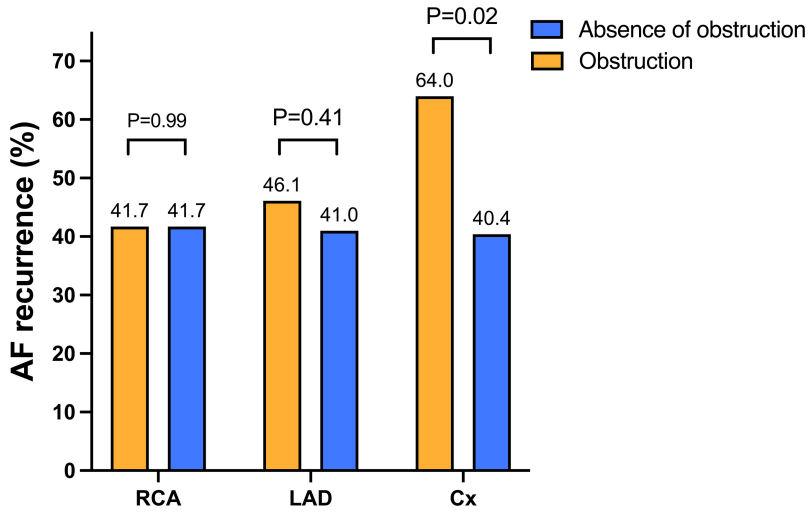

FIGURE 1
Atrial fibrillation recurrence according to the localization of the obstruction. Arrhythmia recurrences did not differ between obstructed and non-obstructed groups regarding the LAD and the RCA. On the contrary, AF recurrences were higher in patients with circumflex artery obstruction compared to patients without circumflex artery obstruction. Abbreviations: AF, atrial fibrillation; Cx, circumflex artery; LAD, left anterior descending; RCA, right coronary artery.

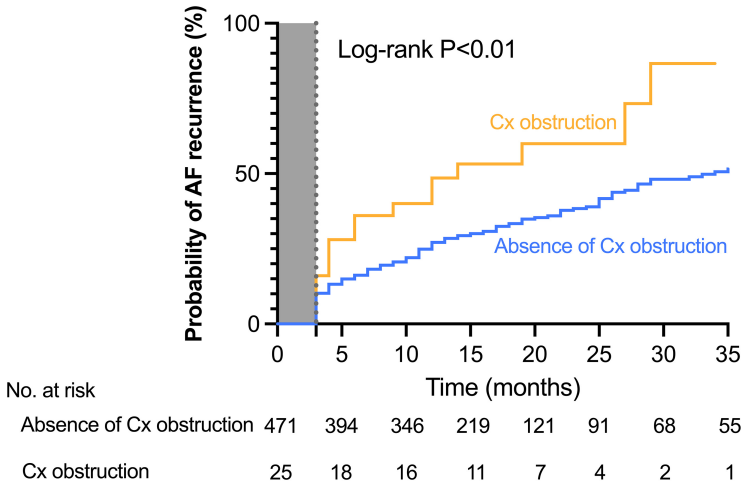

FIGURE 2
Cumulative incidence of atrial fibrillation recurrence in patients with or without circumflex coronary artery obstruction. The Kaplan–Meier estimates of the AF recurrence rate after ablation stratified by the presence or the absence of circumflex obstruction. At 2 years, documented recurrence of AF had occurred in 56.0% (14 of the 25) of patients with circumflex artery obstruction and in 32.1% (151 of the 471) of patients without circumflex artery obstruction (Log-rank hazard ratio [HR], 2.06; 95% confidence interval [CI], 1.02–4.16; $P < 0.01$). Abbreviation: Cx, circumflex artery.

Furthermore, in case of symptoms patients were asked to record an ECG.

Statistical analysis

Continuous variables were expressed as mean and SD or median and interquartile range as appropriate, and categorical variables were reported as numbers and percentages. Comparisons between groups were performed using the Student *t*-tests or the Mann–Whitney *U* tests for continuous variables as appropriate, and χ^2 test for categorical variables. Cumulative incidence curves were built according to the presence or absence of circumflex artery obstruction using the Kaplan–Meier method and compared using a log-rank test. For analysis of the predictive value of circumflex artery obstruction, recurrences during the first 3 months after the ablation procedure (blanking period) were not taken into account (20). Multivariate Cox analysis using an entry procedure was performed on an initial model including factors known to be associated with AF recurrence (age, body mass index, hypertension, diabetes, indexed left atrial volume, left ventricular ejection fraction, ß-blockers, amiodarone, pulmonary vein isolation alone or with additional lesion set, circumflex artery obstruction). Left anterior descending artery and right coronary artery occlusion were forced into the model in order to see if the association between circumflex artery obstruction and AF recurrence changed. Analyses were performed using SPSS 22 (SPSS, Inc., Chicago, IL, USA) and SAS 9.3 (SAS Institute Inc., Cary, NC, USA) statistical software. Two-sided *p*-values of less than 0.05 were considered statistically significant.

Results

Baseline characteristics

Among 652 patients who had preprocedural CCT for persistent AF ablation, 156 (23.9%) were not included because of CAD or coronary revascularization, or impossible coronary assessment due to the quality of the exam. Finally, 496 patients were analyzed. Table 1 illustrates the baseline characteristics of the population. Mean age was 61.8 ± 10.0 years, and 378 (76.2%) patients were men. Mean body mass index was 29.0 ± 5.2 kg/m^2 and 323 (65.1%) had previous hypertension. CHA_2DS_2–VASc score was of 0 or 1 point in 225 (36.6%) patients and 2 or 3 points in 210 (42.3%) patients. Mean left ventricular ejection fraction was 56.4 ± 11.1% and mean left atrial indexed volume was 65.4 ± 23.7 ml/m^2. In the terms of medications, 419 (84.4%) patients were prescribed anticoagulant therapy, 327 (65.9%) ß-blockers, and 181 (36.5%) amiodarone.

Ablation was performed with radiofrequency ablation catheter in 431 (86.9%) patients and with cryoballoon catheter in 65 (13.1%). Among them, 294 (59.3%) had pulmonary vein isolation alone and 202 (40.7%) underwent additional lesion sets.

Prevalence and characteristics of coronary stenosis

Obstructive CAD was present in 86 (17.3%) patients (Table 2). Obstructive CAD was observed in the left anterior

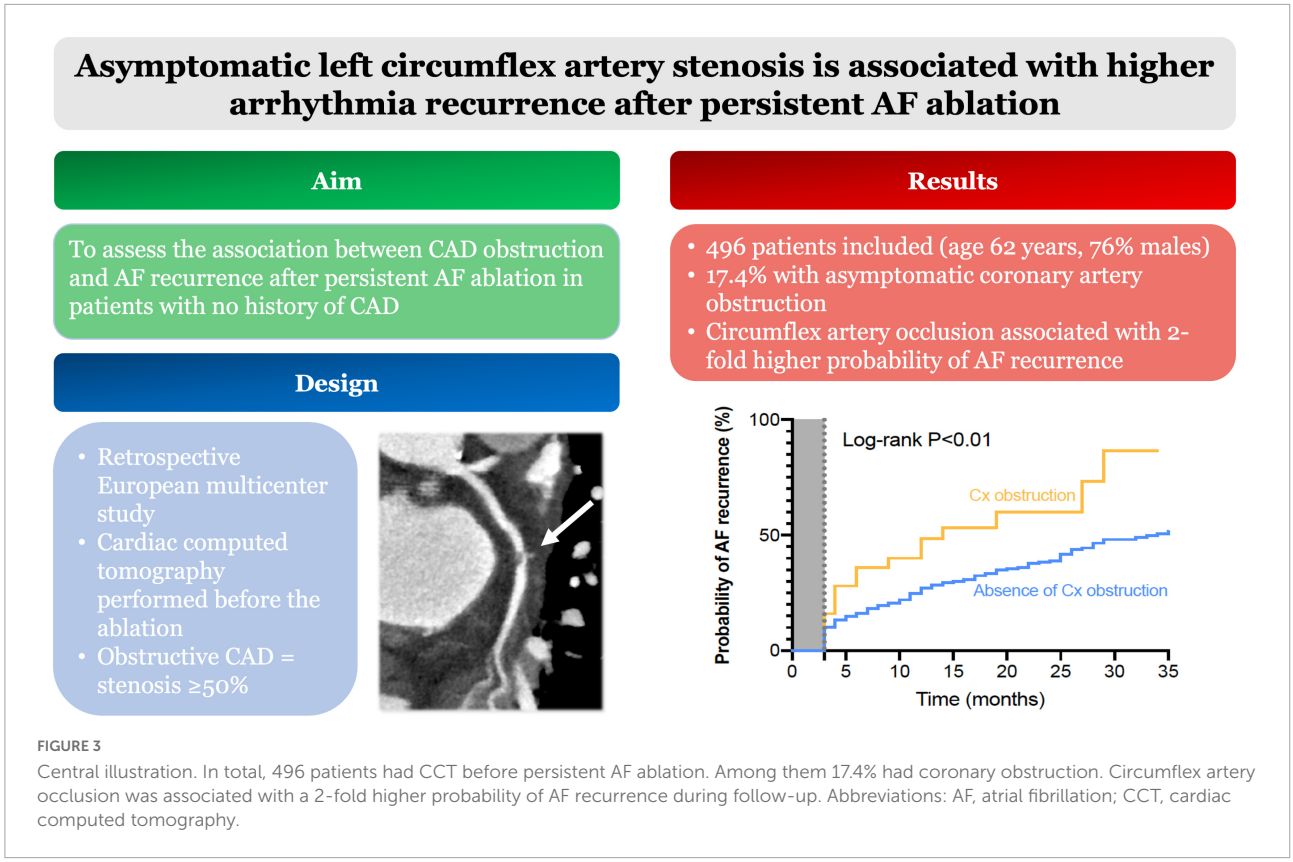

FIGURE 3
Central illustration. In total, 496 patients had CCT before persistent AF ablation. Among them 17.4% had coronary obstruction. Circumflex artery occlusion was associated with a 2-fold higher probability of AF recurrence during follow-up. Abbreviations: AF, atrial fibrillation; CCT, cardiac computed tomography.

descending artery, right coronary artery, and circumflex artery with 76 (15.3%), 24 (4.8%), and 25 (5.0%) patients, respectively.

Recurrence of atrial fibrillation and coronary artery stenosis status

During the mean follow-up of 24 ± 19 months, AF recurrence occurred in 207 (41.7%) patients. AF recurrence rate was not different when considering the number of obstructed coronary arteries: 42.9% in the non-lesion group, 41.1% in the single-vessel lesion group, 41.1% in the 2-vessel lesion group, and 40.8% in the 3-vessel lesion group ($P = 0.98$).

In addition, AF recurrence rate did not differ between patients according to the presence of obstructive CAD [absence of obstructive CAD: 170 (41.5%) patients; obstructive CAD: 37 (43.0%) patients; $P = 0.79$]. When considering the location of the obstruction there was no difference in relation to outcome seen between those with vs. without obstruction in the left anterior descending and right coronary arteries. On the other hand, the recurrence rate was significantly higher in case of circumflex artery obstruction (**Figure 1**). The Kaplan–Meier analysis confirmed a higher risk of AF recurrence in the group in which circumflex artery was stenosed. At 1 year, documented recurrence of AF had occurred in 48.0% (12 out of 25) of patients with circumflex artery obstruction and in 26.1% (123 of the 471) of patients without circumflex artery obstruction. At 2 years, documented recurrence of AF had occurred in 56.0% (14 of the 25) of patients with circumflex artery obstruction and in 32.1% (151 of the 471) of patients without circumflex artery obstruction (Log-rank hazard ratio [HR], 2.06; 95% confidence interval [CI], 1.02 to 4.16; $P < 0.01$) (**Figure 2**). Baseline characteristics of the patients according to circumflex artery obstruction are given in **Supplementary file 1**.

Multivariable Cox regression analysis showed that body mass index (HR 1.04; 95% CI 1.01–1.07 per 1 kg/m^2 increase; $P = 0.02$), left atrial indexed volume (HR 1.01; 95% CI 1.01–1.02 per 1 ml/m^2 increase; $P < 0.001$), and circumflex artery obstruction (HR 2.32; 95% CI 1.36–3.98; $P < 0.01$) were independently associated with AF recurrences at follow-up after persistent AF ablation (**Table 3**). When left anterior descending artery and right coronary artery occlusion were forced in the model, those two variables were not associated with AF recurrence and circumflex artery obstruction was still associated with AF recurrences (HR 2.45; 95% CI 1.37–4.36; $P < 0.01$).

Discussion

In this large-scale international study bringing together 496 patients referred for persistent AF ablation, 5% had obstructive

CAD located on the circumflex artery determined by CCT before ablation (**Figure 3**). This parameter was independently associated with a doubled risk of AF recurrence after ablation, along with of left atrial indexed volume and body mass index.

Prevalence of asymptomatic coronary artery stenosis before atrial fibrillation ablation

Previous studies found prevalence of asymptomatic obstructive CAD ranging from 24 to 41% (16, 22), which was substantially higher than the proportion in our study (17.3%). This difference might be explained by the lower prevalence of cardiovascular risk factors and above all by the higher prevalence of women in our study compared to the one authored by Nucifora et al. Mito's work had also an older population compared to ours.

Association between coronary artery stenosis and atrial fibrillation recurrence

This is the first multicenter study assessing the impact of coronary artery stenosis on AF recurrence after persistent AF ablation. Coronary artery disease might be responsible for AF with several mechanisms: chronic inflammation, heart failure causing atrial stretch, and finally ischemia, all of which are responsible for fibrosis (4, 23–25). In our study, AF recurrence was not significantly different between patients with obstructive CAD and patients without obstructive CAD. These results are in line with a previous study carried out on a limited number of patients with shorter follow-up (12). In order to explore a possible effect of the CAD localization, Kornej et al. tried to determine whether a right coronary stenosis was associated with outcomes after AF ablation but the recurrence rate did not depend on obstruction (26). The present work is the first to evaluate the role of each coronary artery.

Role of circumflex artery in atrial fibrillation recurrences

The anatomy of coronary arteries supplying the left atrium has been described as originating from the first segment of the circumflex artery (27, 28), and Alasady et al. demonstrated that the involvement of the left atrial coronary branch during myocardial infarction was associated with AF onset (29). Moreover, a study on experimental myocardial infarction on swine demonstrated that proximal circumflex artery occlusion involving the left atrial branch was associated with atrial infarction and atrial structural remodeling, characterized by early left atrial dilation, dysfunction, and fibrosis. When proximal circumflex artery occlusion was performed in swine without involving the left atrial branch, only interstitial atrial fibrosis was found with a lesser degree of left atrial dilation or dysfunction, and in cases of left anterior descending occlusion, no atrial fibrosis was found, and there was no left atrial remodeling (24). Taken together, these studies highlight the involvement of the circumflex artery in left atrial vascularization and suggest atrial ischemia and infarction as potential mechanisms of atrial fibrosis and AF. In the present work, only circumflex stenosis, without known clinical infarction, was associated with a higher rate of AF recurrence. These results argue for a regional and targeted, not just global (30), pathophysiological mechanism of atherosclerosis on the perpetuation of atrial fibrillation (31). The other consequence of these findings is that not only symptomatic myocardial infarction, but also silent CAD, is associated with AF recurrence. The mechanism leading to AF recurrence could consequently be silent chronic atrial ischemia related to circumflex coronary stenosis. To shed further light on these results, atrial substrate evaluation through electroanatomical mapping and cardiac magnetic resonance imaging combined with detailed coronary angiography could add new data on the role of the circumflex artery and ischemia in atrial fibrillation.

Limitations

The absence of uniformity in CCT protocols is a methodological limitation. Nevertheless, we were able to highlight the role of circumflex artery stenosis in AF recurrence, which strengthens this result on account of the assessment heterogeneity. Second, the latest classification of coronary artery disease (CAD RAD) was not used in our study because it was not available on all CCT reports (32). However, we have chosen a cutoff (50%) that has already been used in the literature and which reflects a significant rate of CAD (16). In addition, the small number of patients with circumflex artery stenosis (25 patients with LCX obstruction vs. 471 patients without LCX) may have a significant impact on the statistics. Minor change in number recurrence might come to statistic difference. Finally, given the limited CT scan resolution for small artery assessment, we were not able to assess lesions located on the atrial branch of the circumflex artery.

Conclusion

In a large population of patients undergoing persistent AF catheter ablation, this study demonstrates that obstructive stenosis of the circumflex artery defined by pre-procedural

CT scan is independently associated with AF recurrence. Further studies are required to investigate the pathophysiology associated with this finding.

Data availability statement

The raw data supporting the conclusions of this article will be made available by the authors, without undue reservation.

Ethics statement

All patients included in this study received an information letter. According to institutional policy, approval from Institutional Review Board was not required. Written informed consent for participation was not required for this study in accordance with the national legislation and the institutional requirements.

Author contributions

All authors listed have made a substantial, direct, and intellectual contribution to the work, and approved it for publication.

Acknowledgments

We thank Jeffrey Arsham for rereading assistance.

Conflict of interest

The authors declare that the research was conducted in the absence of any commercial or financial relationships that could be construed as a potential conflict of interest.

Publisher's note

All claims expressed in this article are solely those of the authors and do not necessarily represent those of their affiliated organizations, or those of the publisher, the editors and the reviewers. Any product that may be evaluated in this article, or claim that may be made by its manufacturer, is not guaranteed or endorsed by the publisher.

Supplementary material

The Supplementary Material for this article can be found online at: https://www.frontiersin.org/articles/10.3389/fcvm.2022.873135/full#supplementary-material

References

1. Calkins H, Hindricks G, Cappato R, Kim Y-H, Saad EB, Aguinaga L, et al. 2017 HRS/EHRA/ECAS/APHRS/SOLAECE expert consensus statement on catheter and surgical ablation of atrial fibrillation. *Heart Rhythm.* (2017) 14:e275–444.

2. Gandjbakhch, E, Mandel F, Dagher Y, Hidden-Lucet F, Rollin A, Maury P. Incidence, epidemiology, diagnosis and prognosis of atrio-oesophageal fistula following percutaneous catheter ablation: a French nationwide survey. *Europace.* (2020) 23:557–564. doi: 10.1093/europace/euaa278

3. Lee S, Khrestian CM, Sahadevan J, Markowitz A, Waldo AL. New insights into understanding rotor versus focal activation in patients with persistent atrial fibrillation. *JACC Clin Electrophysiol.* (2021) 7:909–19. doi: 10.1016/j.jacep.2020.12.010

4. Marrouche NF, Wilber D, Hindricks G, Jais P, Akoum N, Marchlinski F, et al. Association of atrial tissue fibrosis identified by delayed enhancement MRI and atrial fibrillation catheter ablation: the DECAAF study. *JAMA.* (2014) 311:498–506.

5. Schmitt J, Duray G, Gersh BJ, Hohnloser SH. Atrial fibrillation in acute myocardial infarction: a systematic review of the incidence, clinical features and prognostic implications. *Eur Heart J.* (2009) 30:1038–45.

6. Guenancia C, Toucas C, Fauchier L, Stamboul K, Garnier F, Mouhat B, et al. High rate of recurrence at long-term follow-up after new-onset atrial fibrillation during acute myocardial infarction. *Europace.* (2018) 20:e179–88.

7. Hiraya D, Sato A, Hoshi T, Watabe H, Yoshida K, Komatsu Y, et al. Impact of coronary artery disease and revascularization on recurrence of atrial fibrillation after catheter ablation: importance of ischemia in managing atrial fibrillation. *J Cardiovasc Electrophysiol.* (2019) 30:1491–8. doi: 10.1111/jce.14029

8. Yu-ki I, Kunihiro N, Takeshi K, Stanley N. Atrial fibrillation pathophysiology. *Circulation.* (2011) 124:2264–74.

9. Jason A, Paul K, Dobromir D, Stanley N. The clinical profile and pathophysiology of atrial fibrillation. *Circ Res.* (2014) 114:1453–68.

10. Raphael CE, Heit JA, Reeder GS, Bois MC, Maleszewski JJ, Tilbury RT, et al. Coronary embolus: an underappreciated cause of acute coronary syndromes. *JACC Cardiovasc Interv.* (2018) 11:172–80.

11. Hani S, Katayoun D, Danielle L, Yahye M, Ki L Tack, Stanley N. Atrial ischemia promotes atrial fibrillation in dogs. *Circulation.* (2003) 107:1930–6.

12. den Uijl DW, Boogers MJ, Compier M, Trines SA, Scholte AJHA, Zeppenfeld K, et al. Impact of coronary atherosclerosis on the efficacy of radiofrequency catheter ablation for atrial fibrillation. *Eur Heart J Cardiovasc Imaging.* (2013) 14:247–52.

13. Link Mark S, Michel H, Andrea N. Ablation of atrial fibrillation. *Circulation.* (2016) 134:339–52.

14. Andreini D, Pontone G, Mushtaq S, Conte E, Perchinunno M, Guglielmo M, et al. Atrial fibrillation: diagnostic accuracy of coronary CT angiography performed with a whole-heart 230-μm spatial resolution CT scanner. *Radiology.* (2017) 284:676–84. doi: 10.1148/radiol.2017161779

15. Xu L, Yang L, Fan Z, Yu W, Lv B, Zhang Z. Diagnostic performance of 320-detector CT coronary angiography in patients with atrial fibrillation: preliminary results. *Eur Radiol.* (2011) 21:936–43. doi: 10.1007/s00330-010-1987-0

16. Nucifora G, Schuijf JD, Tops LF, van Werkhoven JM, Kajander S, Jukema JW, et al. Prevalence of coronary artery disease assessed by multislice computed tomography coronary angiography in patients with paroxysmal or persistent atrial fibrillation. *Circ Cardiovasc Imaging.* (2009) 2:100–6.

17. Lip GYH, Nieuwlaat R, Pisters R, Lane DA, Crijns HJGM. Refining clinical risk stratification for predicting stroke and thromboembolism in atrial fibrillation

using a novel risk factor-based approach: the euro heart survey on atrial fibrillation. *Chest*. (2010) 137:263–72. doi: 10.1378/chest.09-1584

18. Gottdiener JS, Bednarz J, Devereux R, Gardin J, Klein A, Manning WJ, et al. American society of echocardiography recommendations for use of echocardiography in clinical trials. *J Am Soc Echocardiogr*. (2004) 17:1086–119.

19. Mansour M, Calkins H, Osorio J, Pollak SJ, Melby D, Marchlinski FE, et al. Persistent atrial fibrillation ablation with contact force-sensing catheter: the prospective multicenter PRECEPT trial. *JACC Clin Electrophysiol.* (2020) 6:958–69. doi: 10.1016/j.jacep.2020.04.024

20. Aryana A, Allen SL, Pujara DK, Bowers MR, O'Neill PG, Yamauchi Y, et al. Concomitant pulmonary vein and posterior wall isolation using cryoballoon with adjunct radiofrequency in persistent atrial fibrillation. *JACC Clin Electrophysiol.* (2021) 7:187–96.

21. Hindricks G, Potpara T, Dagres N, Arbelo E, Bax JJ, Blomström-Lundqvist C, et al. 2020 ESC guidelines for the diagnosis and management of atrial fibrillation developed in collaboration with the European association of cardio-thoracic surgery (EACTS). *Eur Heart J.* (2020) 42:373–498. doi: 10.1093/eurheartj/ehaa612

22. Mito T, Takemoto M, Antoku Y, Masumoto A, Nozoe M, Kinoshita S, et al. Evaluation of coronary artery disease in patients with atrial fibrillation by cardiac computed tomography for catheter ablation: CADAF-CT trial. *Heart Vessels.* (2020) 35:1037–43.

23. De Jong AM, Maass AH, Oberdorf-Maass SU, Van Veldhuisen DJ, Van Gilst WH, Van Gelder IC. Mechanisms of atrial structural changes caused by stretch occurring before and during early atrial fibrillation. *Cardiovasc Res.* (2011) 89:754–65.

24. Aguero J, Galan-Arriola C, Fernandez-Jimenez R, Sanchez-Gonzalez J, Ajmone N, Delgado V, et al. Atrial infarction and ischemic mitral regurgitation contribute to post-MI remodeling of the left atrium. *J Am Coll Cardiol.* (2017) 70:2878–89. doi: 10.1016/j.jacc.2017.10.013

25. Li X, Garcia-Elias A, Benito B, Nattel S. The effects of cardiac stretch on atrial fibroblasts: analysis of the evidence and potential role in atrial fibrillation. *Cardiovasc Res.* (2022) 18:440–460. doi: 10.1093/cvr/cvab035

26. Kornej J, Hindricks G, Arya A, Sommer P, Husser D, Rolf S, et al. Presence and extent of coronary artery disease as predictor for AF recurrences after catheter ablation: the Leipzig heart center AF ablation registry. *Int J Cardiol.* (2015) 181:188–92. doi: 10.1016/j.ijcard.2014.12.039

27. James TN, Burch GE. The atrial coronary arteries in man. *Circulation.* (1958) 17:90–8.

28. Pardo Meo J, Scanavacca M, Sosa E, Correia A, Hachul D, Darrieux F, et al. Atrial coronary arteries in areas involved in atrial fibrillation catheter ablation. *Circ Arrhythm Electrophysiol.* (2010) 3:600–5.

29. Alasady M, Abhayaratna WP, Leong DP, Lim HS, Abed HS, Brooks AG, et al. Coronary artery disease affecting the atrial branches is an independent determinant of atrial fibrillation after myocardial infarction. *Heart Rhythm.* (2011) 8:955–60. doi: 10.1016/j.hrthm.2011.02.016

30. Heeringa J, van der Kuip DAM, Hofman A, Kors JA, van Rooij FJA, Lip GYH, et al. Subclinical atherosclerosis and risk of atrial fibrillation: the rotterdam study. *Arch Intern Med.* (2007) 167:382–7.

31. Aguilar M, Rose RA, Takawale A, Nattel S, Reilly S. New aspects of endocrine control of atrial fibrillation and possibilities for clinical translation. *Cardiovasc Res.* (2021) 117:1645–61. doi: 10.1093/cvr/cvab080

32. Cury RC, Abbara S, Achenbach S, Agatston A, Berman DS, Budoff MJ, et al. CAD-RADSTM: coronary artery disease - reporting and data system: an expert consensus document of the society of cardiovascular computed tomography (SCCT), the American college of radiology (ACR) and the North American society for cardiovascular imaging (NASCI). Endorsed by the American college of cardiology. *J Am Coll Radiol.* (2016) 13:1458.e–66.e.

Advantages of publishing in Frontiers

OPEN ACCESS
Articles are free to read for greatest visibility and readership

FAST PUBLICATION
Around 90 days from submission to decision

HIGH QUALITY PEER-REVIEW
Rigorous, collaborative, and constructive peer-review

TRANSPARENT PEER-REVIEW
Editors and reviewers acknowledged by name on published articles

Frontiers
Avenue du Tribunal-Fédéral 34
1005 Lausanne | Switzerland

Visit us: www.frontiersin.org
Contact us: frontiersin.org/about/contact

REPRODUCIBILITY OF RESEARCH
Support open data and methods to enhance research reproducibility

DIGITAL PUBLISHING
Articles designed for optimal readership across devices

FOLLOW US
@frontiersin

IMPACT METRICS
Advanced article metrics track visibility across digital media

EXTENSIVE PROMOTION
Marketing and promotion of impactful research

LOOP RESEARCH NETWORK
Our network increases your article's readership